

**Models for Percutaneous Absorption –
Influential Parameters and in silico Predictions**

Inaugural-Dissertation

to obtain the academic degree

Doctor rerum naturalium (Dr. rer. nat.)

submitted to the Department of Biology, Chemistry and Pharmacy
of Freie Universität Berlin

by

Katharina Guth

from Landau in der Pfalz

2013

This thesis and all associated experiments were prepared and performed during the years 2009 – 2012. The main part of the work was done in the Laboratory for Biokinetics at the department for Experimental Toxicology and Ecology, BASF SE, Ludwigshafen, Germany and a smaller part at the Center for Chemical Toxicology Research and Pharmacokinetics (CCTRP), College of Veterinary Medicine, North Carolina State University (NCSU) in Raleigh NC, USA under the supervision of

Dr. Eric Fabian, Head of the Laboratory for Biokinetics, department for Experimental Toxicology and Ecology, BASF SE, Ludwigshafen, Germany,

Prof. Jim E. Riviere, DVM, PhD, DSc (hon), Burroughs Wellcome Fund Distinguished Professor of Pharmacology and Director of CCTRP, College of Veterinary Medicine, NCSU in Raleigh NC, USA

and

Prof. Dr. Monika Schäfer-Korting, Head of the department of Pharmacology and Toxicology, Institute for Pharmacy, Freie Universität (FU) Berlin, Germany.

1st Reviewer: Prof. Dr. Monika Schäfer-Korting

Institut für Pharmazie, Pharmakologie und Toxikologie, Freie Universität Berlin

Königin-Luise-Str. 2+4, 14195 Berlin

2nd Reviewer: Prof. Dr. Gerhard Wolber

Institut für Pharmazie, Pharmazeutische Chemie, Freie Universität Berlin

Königin-Luise-Str. 2+4, 14195 Berlin

Date of defence: July 17th, 2013

Acknowledgement

This thesis would have been impossible without the aid and guidance of many people.

First, I would like to express my sincere and deepest gratitude to Prof. Dr. Monika Schäfer-Korting, leader of the Department of Pharmacology and Toxicology, Institute for Pharmacy, FU Berlin, for providing me the opportunity to fulfill my dissertation under her supervision. I want to thank her for excellent and unfailing assistance, valuable comments and constructive advises. My thanks go to her as well as all members of the department for the warm welcome in their group.

I would like to thank Prof. Dr. Gerhard Wolber, Department of Pharmaceutical Chemistry, Institute of Pharmacy, FU Berlin, for his kind acceptance to act as an examiner.

My special thanks go to Dr. Robert Landsiedel, leader of the group Short Term Studies at the Department for Experimental Toxicology and Ecology, BASF SE, Ludwigshafen, for the chance to be part of a challenging research project funded by a leading international company. Thanks for the insights in routine research at a toxicological laboratory and the freedom to develop my own ideas.

My deep thanks to Dr. Eric Fabian, head of the Laboratory for Biokinetics at BASF SE, for fruitful discussions, inspiring ideas and letting me benefit from his broad knowledge. His reflections and way of thinking enriched my work impressively.

I am grateful to Prof. Jim E. Riviere, DVM, PhD, DSc (hon), formerly Burroughs Wellcome Fund Distinguished Professor of Pharmacology and Director of CCTRP, College of Veterinary Medicine, NCSU in Raleigh NC, USA and now Director of the Institute of Computational Comparative Medicine, College of Veterinary Medicine, Kansas State University, Manhattan, KS, USA for welcoming me into his lectures, laboratory and his house to celebrate Thanksgiving with his lovely family. I really enjoyed my time in NC and the possibility to receive a portion of his impressive knowledge.

I am particularly obliged to Jim Brooks, Laboratory Supervisor at CCTRP for being my tutor of in silico modeling and my friend who introduced me to specialties of NC and made me feel at home.

I want to thank Dr. Christine Jaeckh, during my work postdoctoral scientist at BASF SE, for vivid discussions and continuous encouragement.

Further thanks to the Crop Protection division of BASF SE for letting me use dermal absorption and formulation data of several pesticides to build in silico prediction models.

I would like to thank Martina Dammann, statistician at BASF SE, for explaining and discussing statistics with me. Thanks for your patience.

Further thanks to Balint Sinko and Pion Inc., USA, for providing the skin-PAMPA models and the enjoyable collaboration.

I am grateful to my colleagues of the Department for Experimental Toxicology and Ecology, BASF SE, especially to the Laboratory for Pathology for preparation of the histological sections. I also wish to highlight the members of the laboratories for Biokinetics, Applied Alternative Methods, Analytical

Chemistry and Analytical Structure Elucidation. Thanks for the friendly atmosphere, open ears and helping hands.

I want to thank the 'Fachtoxrunde' at BASF SE for enthusiastic discussions about general toxicological topics and my fellow students for all kinds of help ranging from joint laboratory work to critical comments and feedback to presentations. Thanks for your friendship.

My deep thanks to all the people from CCTRP, German Club and the group of Charles Hastings (BASF Corporation, RTP, NC, USA) who supported me and made my time in the US an unforgettable time.

Ganz besonders bedanken möchte ich mich bei meinen Eltern und dem Rest meiner Familie, die immer an mich glauben und mich unterstützen bei allem was ich tue.

Finally, I would like to thank Jochen with all my heart – for everything!

All models are wrong, but some are useful.

George Box (chemist and statistician)

Contents

1	Introduction	1
1.1	Relevance of dermal absorption	1
1.2	Structure and function of human skin	2
1.3	Skin equivalents	7
1.4	Prediction of dermal absorption	10
1.4.1	Experimental models	10
1.4.2	Quantification of dermal absorption using principles of passive diffusion	11
1.4.3	Critical aspects of in vitro experiments	13
1.4.3.1	Experimental influences	13
1.4.3.2	Xenobiotic biotransformation in skin	16
1.4.3.3	Integrity tests	18
1.4.4	In silico prediction models	19
2	Objectives	23
3	Materials and methods	24
3.1	Chemicals, reagents and devices	24
3.2	Test substances	29
3.3	Excised skin samples and skin equivalents	30
3.4	Histological sections	31
3.5	Dermal absorption experiments in vitro	32
3.5.1	Solubility tests	32
3.5.2	Test substance preparation and control analyses	33
3.5.3	Diffusion cell experiments	34
3.5.3.1	Standard experiment (static)	34
3.5.3.2	Standard experiment (flow-through)	35

3.5.3.3	Repeated dosing experiment.....	36
3.5.3.4	Skin integrity testing.....	36
3.5.3.5	Data analyses.....	39
3.5.4	Skin-PAMPA.....	41
3.6	Metabolic activity of skin models.....	42
3.6.1	Subcellular fractions	42
3.6.2	Biotransformation of MCPA-EHE in human skin	43
3.6.2.1	Chemical stability.....	43
3.6.2.2	In vitro biotransformation in human skin S9 fraction	43
3.6.2.3	In vitro biotransformation in human skin during absorption experiments	44
3.6.3	Xenobiotic-metabolizing enzyme activities in skin construct StrataTest®	46
3.7	In silico models for dermal absorption	50
3.7.1	Data mining and calculation of mixture factors.....	50
3.7.2	Abraham-based models containing mixture factor(s).....	52
3.7.3	Substance-based models containing mixture factor(s)	56
3.7.4	Interpretation and application	57
3.8	Statistics.....	57
4	Results.....	59
4.1	Histological sections of skin models	59
4.2	Aspects of dermal absorption experiments in vitro	60
4.2.1	Skin integrity testing	60
4.2.1.1	Binary classification with standard tests	60
4.2.1.2	Correlation of integrity test and absorption results	62
4.2.1.3	Verification of the internal standard approach.....	64
4.2.2	Flow-through versus static experiments	66
4.2.3	Repeated dosing regimen with rat skin	67

4.2.4	Preparation types of human skin ex vivo.....	69
4.2.5	Skin equivalents.....	70
4.2.5.1	StrataTest®	70
4.2.5.2	Skin-PAMPA.....	71
4.2.6	Cross-comparison of various skin models.....	72
4.3	Metabolic activity of skin models.....	75
4.3.1	Biotransformation of MCPA-EHE in human skin	75
4.3.1.1	Chemical stability.....	75
4.3.1.2	In vitro biotransformation in human skin S9 fraction	75
4.3.1.3	In vitro biotransformation in human skin during absorption experiments	76
4.3.2	Xenobiotic-metabolizing enzyme activities in skin construct StrataTest®	78
4.4	In silico models for dermal absorption	79
4.4.1	Abraham-based models containing mixture factor(s).....	80
4.4.2	Substance-based models containing mixture factor(s)	89
5	Discussion	93
5.1	Aspects of dermal absorption experiments in vitro	93
5.1.1	Skin integrity testing	93
5.1.2	Flow-through versus static experiments	98
5.1.3	Repeated dosing regimen with rat skin	98
5.1.4	Preparation types of human skin ex vivo.....	101
5.1.5	Comparison of skin models	103
5.1.6	Relation between AD and maxKp.....	109
5.2	Metabolic activity of skin models.....	110
5.2.1	Biotransformation of MCPA-EHE in human skin	110
5.2.2	Xenobiotic-metabolizing enzyme activities in skin construct StrataTest®	115
5.3	In silico models for dermal absorption	117

5.3.1	Abraham-based models containing mixture factor(s).....	117
5.3.2	Substance-based models containing mixture factor(s)	124
5.3.3	Mechanistic interpretation of the models	126
5.3.4	Applicability domain.....	129
5.3.5	Final remarks	134
6	Conclusion.....	135
7	Summary	137
8	Zusammenfassung.....	140
9	References	143
10	Publications	161
11	Curriculum vitae.....	163
12	Annex.....	165
12.1	Abbreviations	165
12.2	Tables.....	168
12.3	Statement of authorship.....	196

1 Introduction

1.1 Relevance of dermal absorption

The skin – being more than 10 % of the body mass and the largest organ of the human organism – interacts widely with its environment (Walters & Roberts 2002). Although it provides a natural barrier as outlined in chapter 1.2, chemicals may overcome the skin barrier and enter the systemic circulation to a certain extent. Dermal exposure to chemicals occurs from applications in industry, agriculture, pharmaceuticals, cosmetics or household products. Therefore knowledge of dermal absorption is relevant for safety issues as well as for therapeutic aspects. ‘Dermal absorption’ is defined as the global process of uptake of compounds by an organism via the skin. ‘Penetration’ describes the entry of compounds in particular layers, and ‘permeation’ the diffusion from one layer to another or through the entire skin (Schaefer & Redelmeier 1996b).

For pesticides, Article 4 of Regulation 1107/2009 of the European Parliament and Council for placing plant protection products on the market demands the absence of harmful effects on human health, animal health and the environment during application of pesticides (directly) or by residues in food or the environment (indirectly) (The European Parliament & The Council of the European Union 2009). Since dermal exposure is the main route to most pesticides for applicators, field workers and bystanders, dermal uptake must be evaluated by suitable risk assessment and minimized in most cases (Ross et al. 1992; Wolfe 1976). Several models exist to link external exposure with systemic dose. Such ‘internal exposure’ is calculated for different populations, based on classical field application scenarios as well as pulmonary and dermal absorption characteristics (Bundesamt für Verbraucherschutz und Lebensmittelsicherheit (BVL) 2012b; Hoernicke et al. 1998; Krebs et al. 2001; Lundehn et al. 1992; Monteiro-Riviere 2006). To ensure the safety of the applied products on human health, exposure results are compared to toxicologically-derived limit values, for example AOEL (acceptable operator exposure level). Default value for dermal absorption is 10 % for compounds with molecular weight (MW) larger than 500 g/mol and logarithm of octanol/water partition coefficient ($\log P_{ow}$) lower than -1 or higher than 4. For compounds outside these physicochemical properties, the default value is 25 % – if the compound is applied in an undiluted formulation (‘pesticide concentrate’) – or 75 % – if the compound is applied in diluted formulations in concentrations less than 5 % (EFSA Panel on Plant Protection Products and their Residues (PPR) 2012). In contrast to these conservative approaches, more realistic risk assessment is possible based on experimentally obtained information. Several approaches exist to determine dermal uptake as outlined in chapter 1.4.1. In addition to experimental determination, *in silico* models are under evaluation for this purpose. Up to date such models are not regulatory accepted for pesticides, but they may be helpful in early developmental stages. Since many parameters – such as formulation composition and type – influence the extent of dermal absorption (influential parameters are discussed in chapter 1.4.2), EFSA Guidance on dermal absorption demands testing of formulated products including representative dilutions. An extrapolation to other products with the same compound is possible only for closely related formulations (EFSA Panel on Plant Protection Products and their Residues (PPR) 2012). An effective *in silico* model that

addresses the effect of different formulations and allows extrapolation to other formulations is still missing.

Furthermore, knowledge of dermal absorption is also crucial for topically applied pharmaceuticals or cosmetics. For example, based on this knowledge, suitable application scenarios for drugs are developed which lead to therapeutic concentrations at the biological target. Besides dermal application of locally active drugs, this dermal route is also suitable for systemically effective drugs. It is particularly interesting for a compound with a high first-pass-effect in the liver – since it avoids the direct uptake and processing in the liver in comparison to oral administration – and/or a compound with a short elimination half-life – since prolonged application can provide stable blood levels over defined time periods (Cleary 1993; Mutschler et al. 2001).

1.2 Structure and function of human skin

The anatomical structure of the skin is complex and crucial for its various functions. It consists of three layers: epidermis, dermis and hypodermis. The last two layers are pervaded by nerves, blood and lymphatic vessels. Furthermore, different appendages are associated with the skin: hair follicles, sweat ducts, apocrine glands and nails (Walters & Roberts 2002). The generic structure of mammalian skin is depicted in Figure 1.

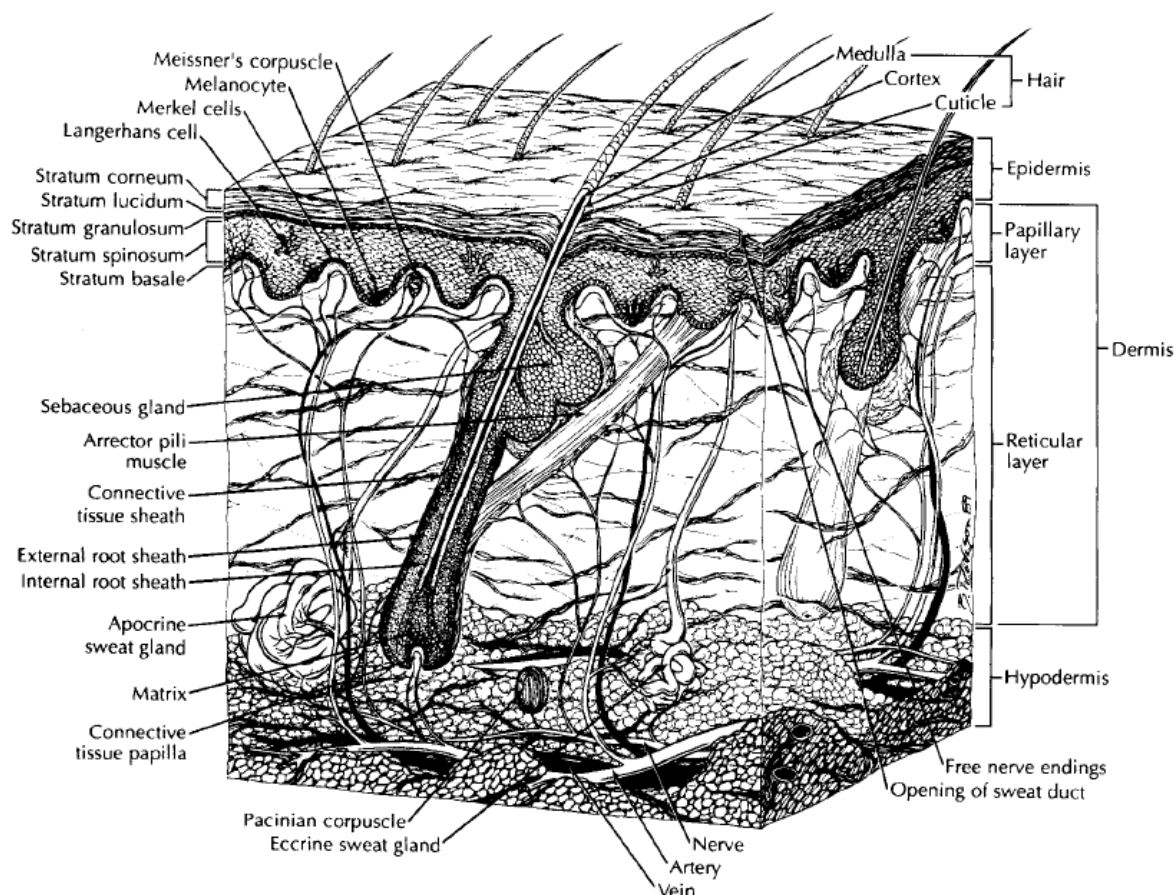


Figure 1: Generic illustration of mammalian skin consisting of three layers (epidermis, dermis, hypodermis) and comprising typical structures like hairs, sweat and sebaceous glands (Monteiro-Riviere 1991). The picture is reprinted with permission.

One of the main functions of the skin is the protection of the organism from environmental perils. For that it acts as a physical barrier against e.g. chemicals, bacteria, fungi and radiation. In addition, physiological defense mechanisms are present. Intruded xenobiotics are confronted with a series of xenobiotic-metabolizing enzymes in the skin tissue, which intend to detoxify the compounds and enhance their excretion, and intruded bacteria are confronted with the immune system of the skin, which intends to eliminate pathogenic germs to avoid infections. The skin is also a major organ for maintaining the homeostasis. Therefore, an epidermal water loss is minimized by the diffusion barrier of the tissue and the body temperature is maintained and regulated via insulation with fatty tissue and hair/fur and by adjustment of sweating and blood flow. Finally, the skin is a sensory organ. With specific receptors it senses environmental influences like heat, cold and pressure (Monteiro-Riviere 2006; Walters & Roberts 2002). A more detailed description of the distinct layers, cell types and their functions is given in the following.

The **epidermis** is a keratinized stratified squamous epithelium without a vascular system. From outside to inside the cell layers are called stratum corneum (SC), stratum lucidum (SL) – which is only present in plantar and palmar skin –, stratum granulosum (SG), stratum spinosum (SS) and stratum basale (SB) as shown schematically in Figure 2. Keratinocytes are the primary cell type in the epidermis, which undergo an orderly pattern of proliferation, differentiation and keratinization from SB to SC where they are finally shed. This process takes about four weeks in human skin and allows the exclusion of formerly penetrated compounds bound to epidermal cells. Shedding of the apical cells is associated with a decreasing number of specialized desmosomes (CD) between the keratinocytes. Other cell types with mainly protective functions in the epidermis are Langerhans cells, Melanocytes and Merkel cells. Langerhans cells are commonly found in the upper SS with dendritic processes up to the SG. As part of the immune system, they phagocytize allergens, migrate after activation to drain lymph nodes, and present antigens on their surface to lymphocytes. Melanocytes are located in the basal layer and produce melanosomes. Transferred to keratinocytes, these pigment-containing granules form a protective cap against ultraviolet radiation over the nucleus and define the color of the skin. Merkel cells are tactile epithelioid cells. They sense mechanical stimuli and induce keratinocyte growth and function as slow adaptive processes (Elias 2005; Monteiro-Riviere et al. 2008; Riviere 2011a; Ryan et al. 2010; Walters & Roberts 2002). Various skin appendages like hairs, sweat ducts and sebaceous glands are specializations of the epidermis, but reach into deeper skin layers. Hair follicles are distributed over the entire skin surface with some exceptions (lips, palms and soles of the feet). Associated with hair follicles are smooth muscles (arrector pili), which cause the hair to stand erect in response to fear or cold, and sebaceous glands that produce sebum. This sebum contains triglycerides, free fatty acids and waxes at pH 5 to lubricate and protect the skin. Eccrine sweat glands produce a solution of electrolytes – mainly sodium chloride – lactate, urea and some amino acids at pH 5, which is directly secreted onto the skin surface for cooling effects. These glands are distributed over the entire body of humans and other anthropoids with few exceptions (e.g. lips and clitoris). In non-primate mammals, these glands were restricted to hairless pads, muzzles and snouts. Apocrine sweat glands are limited to axillary, pubic, areola and perianal regions in humans, but are ubiquitous in other mammals like dogs, cows and sheep. They secrete a 'milk' of proteins, lipoproteins and lipids

into the associated hair follicle. Scents and pheromones present in the secretion probably play roles in sexual and social life (Monteiro-Riviere 2006; Walters & Roberts 2002; Weiner & Hellmann 1960).

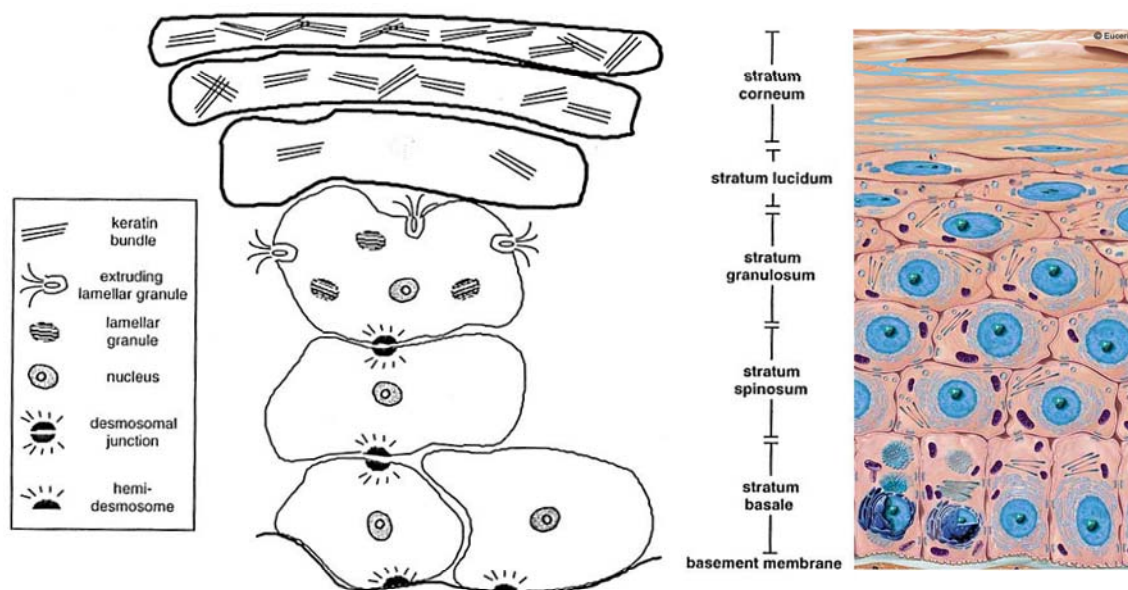


Figure 2: Structure of the epidermis illustrating the differentiation process from basal cells to the completely keratinized cells of the stratum corneum (Beiersdorf Ges mbH & Brand Manager EUCERIN 2009; Walters & Roberts 2002). The picture of differentiating cells is reprinted with permission.

The **SC** or the nonviable epidermis is the outermost layer of the skin and depending on the region of the human body 10 – 20 μm thick. As shown via progressive tape-stripping, the SC provides the main barrier function of the skin (Blank 1953). The function of protecting the organism against invading compounds as well as loss of water is determined by its structure. The SC consists of several layers of completely keratinized flattened cells without nuclei and organelles (corneocytes), which are embedded in a lipid matrix. Therefore, the permeability barrier is provided by dense packaging of keratin bundles inside the cells, the dense packaging of elongated tetrakaidecahedron shaped cells, whose structure extends the extracellular pathway, and finally the lipids filling the extracellular space. The cornified cell envelope (CE), which is tightly connected to the cells, provides a stable, mechanically and chemically resistant scaffold for the aggregation and organization of the extracellular matrix. The inner part of the envelope contains various cross-linked proteins whereby involucrin is covalently connected to the inner plasma membrane and to the outer lipid portion of the envelope. The lipid envelope contains mainly ceramides with a terminal hydroxyl group in the fatty acid moiety, which are connected to the extracellular lipids via hydrophobic interactions (Elias 2005; Hohl 1990; Nemes & Steinert 1999; Walters & Roberts 2002). The predominant compounds in the intercellular space are ceramides (40 – 50 %), cholesterol (20 – 33 %), cholesterol esters (0 – 20 %) and saturated free fatty acids (7 – 13 %). Although it is known, that the amphiphilic ceramides form multiple lipid layers, which withstand a wide range of temperatures, UV radiation, and oxidative processes, and that cholesterol regulates the fluidity of the system, the exact structure and function of the free fatty acids as well as the physical state are still unknown. However, there are hints of coexisting liquid crystalline and gel

phase domains, whereby the gel domain is considered to hinder diffusion of molecules (Norlen 2008; Schurer & Elias 1991; Wertz 2000).

The **SL** consists of several layers of fully-keratinized dense cells devoid of nuclei and organelles. It is translucent and only present in distinct anatomical areas of exceptionally thick skin or hairless regions of the human body like plantar and palmar surfaces (Monteiro-Riviere 2010).

Three to five layers of flattened cells containing irregularly shaped, nonmembrane-bounded keratohyalin granules build the **SG**. Tight junctions (TJ) connect the cells, which were observable as typical 'kissing point' structures. The granules contain precursors of filaggrin and loricrin, which are involved in keratinization and formation of barrier function. Further lipid-containing lamellar granules or Odland bodies are present in the SG. Via exocytosis, these granules release their content (ceramides, cholesterol, free fatty acids, cholesterol esters and hydrolytic enzymes) into the intercellular space between the SG and SC. These compounds form the lipid envelope and the extracellular matrix of the SC (Monteiro-Riviere 2010).

The **SS** consists of several layers of irregular polyhedral-shaped cells connected via TJs to one another and via desmosomes to the adjacent cell layers. Small lamellar granules appear in the uppermost layers. Morphologically characteristic features of the SS are the numerous tonofilaments which connect the desmosomes with the cytoskeleton (Monteiro-Riviere 2010).

The **SB** is a single cell layer of columnar or cuboidal cells connected to one another and to the overlying SS via desmosomes. The nucleus of each cell is large, ovoid and occupies most of the cell. The keratinocytes in the SB act either as stem cells that divide and proliferate to continuously replenish the epidermis as the SC cells are shed from the surface or as structure cells which are anchored to the basement membrane via hemidesmosomes.

The **basement membrane** is the boundary between epidermis and dermis. It is undulated and irregular which results in finger-like projections into the dermis (papillae). The number and extent of papillae decreases with age. With constituents like type IV collagen, laminin and fibronectin, the membrane gives mechanical stability to the skin, acts as a selective barrier and influences cell behavior and wound healing (Monteiro-Riviere 2010; Walters & Roberts 2002).

Beneath the basement membrane lies the **dermis**, a network of dense irregular connective tissue. It is composed of collagen and elastic fibers embedded in an amorphous gel of tangled glycosaminoglycans. This structure allows tension in many directions and provides support for nerves, vascular systems and appendages. The cell types of the dermis are the fibroblasts – which produce the connective tissue – as well as mast cells and macrophages. Due to its structure, the dermis is tough and elastic, and is responsible for nutrient support to the skin and for the detection of pressure and temperature via specific sensory receptors (Monteiro-Riviere 2010; Walters & Roberts 2002)

The **hypodermis** or subcutis is loose connective tissue which anchors the dermis to the underlying muscle or bone, but allows free movement over these structures. It carries the vascular and nervous

systems and, depending on the species and location, adipose tissue (e.g. abdominal region in humans). The latter serves as a cushion or fat pad. Taken together the hypodermis acts as a heat insulator, shock absorber and energy storage region (Monteiro-Riviere 2010).

Derived from the skin structure outlined above, a substance present on the skin surface must overcome the SC, the viable epidermis and parts of the dermis to reach the vascular system – to be absorbed. For the main barrier, the SC, three **absorption pathways** have been hypothesized: transcellular, intercellular and transappendageal. All three pathways are restricted to passive diffusion, since no active transport systems are present. Mathematical principles of passive diffusion with special focus on skin permeation are outlined in chapter 1.4.2. Besides diffusion, the second factor determining the partition into SC and deeper skin layers is the solubility of the penetrant in the system. The transcellular route involves repeated partitioning of molecules between lipophilic and hydrophilic compartments including the mainly impermeable keratin bundles in the corneocytes. This theoretical process could not be proven experimentally (Roberts & Cross 2002). Experimental arguments against diffusion of water through corneocytes were obtained by Potts and Francoeur. Therefore, it was argued that the transcellular pathway is unlikely for polar organic molecules in general, when not even water utilizes this pathway (Potts & Francoeur 1991; Pugh 2001). The existence of an intercellular pathway was shown by investigating the histological localization of applied substances within the bilayers and the effect of delipidation as outlined by Roberts and Cross. This route is widely accepted to be the dominant pathway during steady-state permeation of compounds (Roberts & Cross 2002). Hints of lipid and polar pathways ('aqueous pores') through the intercellular lipids were derived from experiments with penetration-enhancing solvents, which changed diffusivity and partitioning of polar, non-polar and intermediate model compounds differently (Blank & Mcauliffe 1985; Southwell & Barry 1983). However, no physical evidence supports the existence of such pores, wherefore it is controversially discussed in the scientific community (Mitragotri et al. 2011; Potts & Guy 1992). Evidence for the transappendageal route including reservoir functions comes from histological studies based on stain localization within the appendages as summarized by Roberts and Cross (Roberts & Cross 2002). Although appendages account for only 0.1 – 1 % of the total human skin surface, their ability to act as shunts for fast absorption probably allow them to dominate the transport through skin until the lag time for intra- or transcellular transport is reached (Scheuplein 1972). For example, remarkable absorption via hair follicles in vivo was observed for caffeine (Otberg et al. 2007). Overcoming the SC subjects compounds to two polar barriers: the viable epidermis and the dermis. These tissues provide less resistance than the SC, but may hinder further permeation of highly lipophilic compounds. The role of tight junctions (TJs) for these barriers is still unclear (Kirschner & Brandner 2012). The density and pattern of TJ proteins in the tissue depends on the epidermal layer. The SG comprises all types of TJ proteins including transmembrane proteins like several claudins (Cldns), occludin and JAM-A (junctional adhesion molecule) as well as scaffold proteins like ZO-1 (tight junction protein 1) and MUPP-1 (multiple PDZ containing protein). The typical TJ structures, the 'kissing points', were observable. Several tight junction proteins were also found in deeper cell layers of the epidermis (Cldn-1, Cldn-4, Cldn-7, JAM-A, MUPP-1) or in the SC (Cldn-1, Occludin) (Brandner 2010; Kirschner & Brandner 2012). TJs are known to provide a paracellular barrier for solutes in

simple epithelia composed of one single cell layer (e.g. in the intestine), whereby the composition and number of TJs determines the restriction (Amasheh et al. 2011). However, the role of TJs in barrier formation in stratified epithelia like the epidermis of the skin is ambiguous. Clear hints for a paracellular inside-out barrier function of TJs in the epidermis were detected by Furuse and co-workers: the distribution of a tracer (primary amine-reactive biotinylation reagent (BR), 557 Da) applied subcutaneously in mice was stopped by TJ structures in the SG (Furuse et al. 2002). Similar findings were made for ex vivo human skin preparations using the same reagent BR or lanthanum nitrate (Hashimot 1971; Kirschner 2010). A similar role of TJs as an outside-in barrier is conceivable, but the interrelation between SC and TJs complicates the evaluation of test results. For example, the removal of the SC by tape-stripping induced the upregulation of TJ proteins in former studies, wherefore the observed barrier function may be absent in non-stripped skin samples and classified as a secondary effect (Kirschner et al. 2011). Furthermore, disturbance of TJ-dependent ion gradients may influence the production and processing of the lipids and proteins for the extracellular space of the SC and therefore disturb the barrier function of the SC (Brandner 2010). Howsoever, the barrier function of the viable epidermis could lead to reservoir formation in the SC (Roberts et al. 2005; Vickers 1972). A reservoir or accumulation of compounds in the SC was firstly shown for topically applied corticosteroids. The vasoconstrictive effect of the compounds – which was gone after removal of the application film from the surface – could be reactivated by occlusion of the same application site. Furthermore, the effect was absent, if the application site was tape-stripped (Vickers 1963). Generally, reservoir formation could result in an inducible release as described above, a prolonged absorption process or a reduced penetration into the SC of freshly-applied molecules of the same compound due to an decreased concentration gradient (Roberts et al. 2005). Finally, active transports into and out of the keratinocytes and metabolic transformation in the viable epidermis or dermis are processes that determine additionally the systemic availability of penetrants (Dancik et al. 2010). The effect of xenobiotic biotransformation on dermal absorption is outlined in chapter 1.4.3.2.

1.3 Skin equivalents

For in vitro experiments – to determine dermal absorption characteristics or toxicity of chemicals – freshly prepared human skin is nearest to the human in vivo situation. But access to human material is limited and storage in the freezer may influence its properties. Furthermore, high variability is possible due to donor or preparation techniques. These factors led to increased efforts to develop high reproducible and cost effective skin equivalents. Many cell-based systems with similar morphology as human skin were developed in the past. Reconstructed human skin possess a fully-stratified, multi-layered and highly differentiated epidermal tissue, and in the case of full-thickness constructs, also a dermis consisting of fibroblast-populated layers. Differentiation of epidermal keratinocytes into distinct layers is promoted by incubation at the liquid-air-interphase. However, other dermal cell types like Langerhans cells or melanocytes as well as skin appendages are absent and neither protective sebum nor sweat is produced from these constructs (Schaefer-Korting & Schreiber 2008). Some epidermis constructs are already accepted for toxicity testing: for example EpiDerm™ from MatTek, Ashland, MA, USA, EpiSkin™ from L'Oreal, Paris, France and SkinEthic™ from SkinEthic laboratories, Nice, France. These constructs are proposed by OECD Guidelines 431 and 439 as well as by European Regulations

761/2009 and 440/2008 for in vitro testing of skin irritation and corrosion (OECD 2010a; OECD 2010b; The Commission of the European Communities 2008). Therewith, these constructs are part of the testing and evaluation strategy outlined in OECD Guideline 404 (OECD 2002). OECD Guidance document 28 for the conduct of skin absorption studies allows the use of reconstructed human skin, if its application leads to absorption results similar to results obtained with excised human skin (OECD 2004a). In a former validation study, reconstructed human epidermis (EpiDerm™, EpiSkin™, and SkinEthic™) showed obviously higher permeability in comparison to ex vivo human skin, but ranking absorption of substances reflected the results with human skin. Furthermore, the results obtained with skin constructs were less variable than results with excised human skin (Schaefer-Korting et al. 2008a). Remarkably higher absorption compared to human skin were also observed for the skin constructs Phenion®FT from Henkel, Düsseldorf, Germany and Graftskin™ LSE™ from Organogenesis, Canton, MA, US (Ackermann et al. 2010; Schmook et al. 2001). In the current work the barrier function of a further human skin construct was tested: StrataTest® from Stratatech, Madison, WI, USA. Reported results of the transepidermal electrical resistance (TEER) – a marker for skin barrier function – were promising: StrataTest® showed only slightly reduced barrier functionality compared to intact human skin, but significantly higher barrier function compared to impaired (tape stripped) human skin (Rasmussen et al. 2010b). The hope for a more effective barrier is based on the different cellular source used for StrataTest® in comparison to other human skin constructs. Despite the human-derived primary epidermal keratinocytes from neonatal/adult foreskin or abdominal skin, so-called NIKS® cells are used to engineer the epidermis of the StrataTest®. NIKS® are spontaneously immortalized cells from a senescing cell culture of BC-1_Ep cells, which are derived from human neonatal foreskin keratinocyte progenitor cells (Allen-Hoffmann et al. 2000; Rasmussen et al. 2010b; Schaefer-Korting & Schreiber 2008). As with other constructs, primary human fibroblasts embedded in a type I collagen matrix are used to build the dermis (Rasmussen et al. 2010b). A histological section as well as a picture of StrataTest® constructs are shown in Figure 3 a and b, respectively.

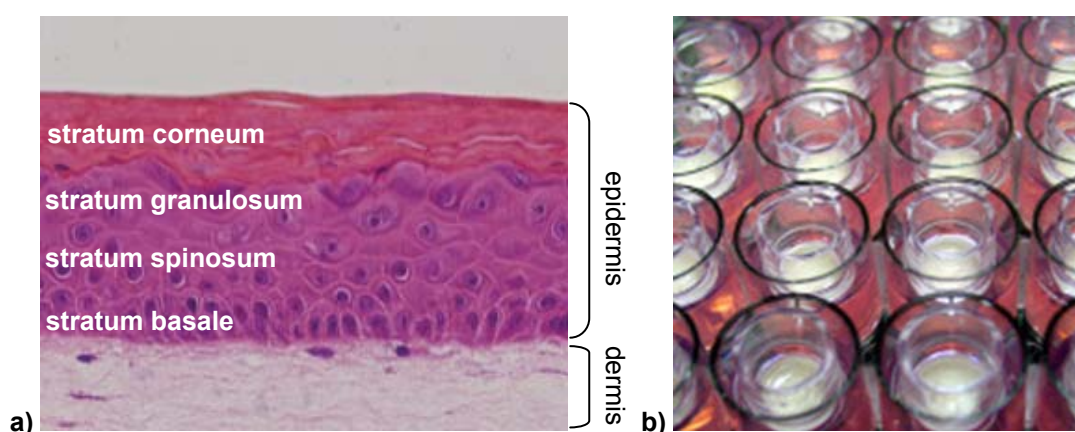


Figure 3: StrataTest® – reconstructed human skin, a) histological section after H&E staining, b) constructs in inserts for shipment. Pictures are copied with permission from the supplier (Rasmussen et al. 2010c).

Advantageously, different sizes of this skin tissue are commercially available, for example preparations with a diameter of 23 mm for diffusion cell experiments and even larger tissues – so-

called StrataGraft[®] – for clinical applications. Successful phase I/II clinical trials with StrataGraft[®] showed the ability to optimize the wound bed and prevent infection until permanent closure. No adverse events were reported (Schurr et al. 2009). Preliminary results from a further clinical trial showed complete wound closure for seven out of seven patients with severe burns (Stratatech Corporation 2012). Due to this promising union and co-operation of damaged in vivo and reconstructed tissue, the question of preserved metabolic activity arose. An activity of xenobiotic-metabolizing enzymes similar to human skin would make the reconstructed tissue a valuable tool for in vitro testings – especially for testings where biotransformation may play a role (e.g. sensitization, genotoxicity testing), since metabolic modulation of chemicals – which affect its local and systemic behavior – would be covered. The profile of xenobiotic-metabolizing enzyme activities in the reconstructed epidermis EpiDerm[™] and in the reconstructed full-thickness skin Phenion[®]FT and EpiDermFT[™] was investigated in line with keratinocytes and ex vivo human skin in a project funded by the German Ministry of Education and Research (BMBF). The authors reported close profiles for the full-thickness skin constructs (Phenion[®]FT and EpiDermFT[™]) and human skin (Henkler et al. 2012). A closer look on the enzyme activities obtained by Henkler et al. is given in chapter 5.2.2, p. 115 and discussed alongside with the activities in the reconstructed human skin StrataTest[®] – investigated in the current work.

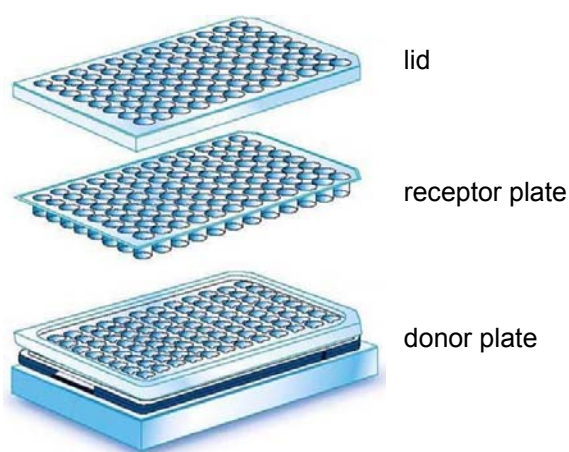


Figure 4: Scheme of skin-PAMPA sandwich printed with permission from the supplier. Each bottom of the receptor plate is an artificial membrane containing SC-specific compounds (Sinkó et al. 2011)

Alternatively to cell-based skin equivalents, abiotic skin membranes are on the market to estimate dermal permeability: e.g. Strat-M from Merck Millipore, Billerica, MA, USA, and skin-PAMPA (parallel artificial membrane permeability assay) from Pion, Billerica, MA, USA. Strat-M consists of multiple layers of polyethersulfone and the membrane of skin-PAMPA contains representative compounds of the intercellular space of the SC (free fatty acids, cholesterol and synthetic ceramides, so-called certramides) (Merck 2006a; Sinko et al. 2012). The latter system is an advancement of former PAMPA models simulating dermal permeation (Ottaviani et al. 2006). It is also closely related to membranes simulating passive membrane diffusion over the gastrointestinal and blood brain barrier (Avdeef et al. 2007; Kansy et al. 1998; Tsinman et al. 2011). Recently, absorption results with the latest skin-

PAMPA were shown to correlate with results obtained with human skin in vitro (Sinko et al. 2012). To check the suitability of this system for screening approaches, performance standards suggested by the manufacturer as well as other reference compounds were applied for the current thesis. Detailed assay description is outlined in chapter 3.5.4. The membranes are provided by Pion as inlets of 96-well plates (see Figure 4).

1.4 Prediction of dermal absorption

1.4.1 Experimental models

Several methods exist to determine dermal absorption of pharmaceuticals, cosmetics, pesticide or industrial chemicals in men. However, not all methods are accepted by the particular regulatory agency as outlined in the following.

Firstly, the most relevant results can be obtained with human volunteer studies. Such studies are suitable for pharmaceuticals and are the basis for precise dosing regimen for clinical routine. However, testing of other chemical classes like pesticides is not feasible due to ethical reasons. The principle of the test method is to apply a ready to use formulation (e.g. patch, gel) and measure concentrations in blood, urine and/or feces at regular time intervals and/or in SC samples obtained from the skin surface via tape stripping. The total absorbed dose can be determined as well as kinetics like absorption and elimination of the compound (European Centre for Ecotoxicology and Toxicology of Chemicals 1993).

In addition to the measurement of dermal uptake via blood, urine and feces (and optional via exhaled air if degradation to CO₂ is expected), mass balance including content in the application site could be determined when conducting animal in vivo studies, e.g. rat or pig studies (OECD 2004c). Therefore, radiolabeled compounds are applied. Advantageously, mammalian studies provide physiologically and metabolically intact systems, but generally overestimate the human in vivo situation. The extent of overestimation depends on the test substance and the species used. Bartek et al. suggest the following order of dermal uptake based on six compounds with logP_{ow} ranging from -0.66 to 5.03 and MW ranging from 163.2 to 361.4 g/mol: rabbits > rats > pigs > humans (Bartek et al. 1972). However, in vivo animal studies are no longer accepted for cosmetic products, and from 2013 on, are also banned for ingredients and all kinds of toxicity testing, regardless of the availability of alternative methods (The Council of the European Communities 1976). In contrast, the Environmental Protection Agency (EPA) of the US requests in vivo studies with rats for pesticides and does not accept in vitro application as a stand-alone method (United states Environmental Protection agency (EPA) 1996).

In Europe, experiments with human skin ex vivo are generally accepted for the assessment of dermal absorption (EFSA Panel on Plant Protection Products and their Residues (PPR) 2012). In such experiments excised skin is mounted on a diffusion chamber, test substance is applied topically and the penetrated and absorbed amount is measured in the skin sample and the underlying receptor fluid. With samples from the receptor fluid taken at distinct time points, kinetic characteristics can be determined (for basic theory see chapter 1.4.2 and for general performance see chapter 3.5.3). However, limited access to human skin preparations implies the necessity of alternatives.

For example, animal skin preparations could be used for in vitro experiments (OECD 2004b). Their use was assessed to be similar (pig) to human skin or over-predictive (rat) (Barbero & Frasch 2009; van Ravenzwaay & Leibold 2004). Over-prediction fulfills the worst case principle in risk assessments, if the systemic dose is calculated from dermal exposure (e.g. exposure scenario of pesticide field application for workers and bystanders). The same is true for the general over estimation of the in vivo situation with in vitro experiments (van Ravenzwaay & Leibold 2004). A triple pack of human in vitro, rat in vitro and rat in vivo data is proposed to provide a more reliable estimation of the human in vivo situation than one of the named experiments alone (van Ravenzwaay & Leibold 2004):

$$\text{Equation 1: } \%h_{\text{vivo}} = \%r_{\text{vivo}} * \frac{\%h_{\text{vitro}}}{\%r_{\text{vitro}}}$$

Parameter $\%h_{\text{vivo}}$ is the estimated percent absorbed for the human in vivo situation, $\%r_{\text{vivo}}$ the determined percent absorbed with rat in vivo experiments and $\%h_{\text{vitro}}$ and $\%r_{\text{vitro}}$ the determined percent absorbed with in vitro experiments using human and rat skin, respectively. The two latter parameters could be replaced by the absorption rate (AR) or the permeability coefficient (Kp) derived with human or rat skin. Furthermore, the use of reconstructed human skin is proposed as an alternative to excised human skin. According to OECD Guidance document no. 28 their use would be acceptable if data from reference chemicals are consistent with those published in the literature for excised human skin (OECD 2004a). As described in section 1.3 similar results were not achieved with any of the human skin constructs tested up to date, but a ranking of compounds parallel to human skin results (Schaefer-Korting et al. 2008a). Despite such restrictions, the broadly defined OECD Guideline and other protocols in the literature, provide only rough frameworks for the performance of in vitro absorption experiments. The resulting various experimental conditions are assumed to be the main reasons for the high variability reported in the literature. This and other critical aspects of the method are outlined in the following chapter (1.4.2).

1.4.2 Quantification of dermal absorption using principles of passive diffusion

Permeation through skin is basically a passive diffusion process over a membrane, since SC is considered to be the main barrier and devoid of active transporters (Blank 1953; Dancik et al. 2010). Therefore, the mathematical description of this mechanism could be derived from Fick's first law. This law states that flux J of a compound – the rate of mass transfer ($\Delta m/\Delta t$) per unit area (A) – at a given time and position is proportional to the concentration difference (Δc) over a distance (Δx) (the concentration gradient ($\Delta c/\Delta x$)) (Kielhorn et al. 2006):

$$\text{Equation 2: } J = \frac{\Delta m}{A * \Delta t} = -D * \frac{\Delta c}{\Delta x}$$

D is the diffusion coefficient or diffusivity in dimension of length²*time, which depends on velocity of diffusing particles. The negative sign indicates a net flux in direction of decreasing thermodynamic activity or – as here simplified – to decreasing concentration. Adapting Equation 2 for steady state flux

(J_{ss}) over a membrane with thickness h and the concentrations c_1 and c_2 at the outermost ($x = 0$) and innermost layers ($x = h$), respectively, leads to

$$\text{Equation 3: } J_{ss} = D * \frac{(c_2 - c_1)}{h}$$

This equation could be used adequately for the membrane 'skin', if it is assumed to consist of homogenous, stable layers. J_{ss} is then equivalent to the absorption rate (AR). In general, the thickness of the stratum corneum (SC) is used for h , since this layer controls mainly the dermal absorption. The real length of the pathway through the SC depends on the substance and their preference to take the inter- or the intracellular route. The generally preferred intercellular way via SC lipids around the corneocytes is obviously longer than the direct route through the cells. Under sink conditions c_2 is (nearly) zero and c_1 is in local equilibrium with the vehicle:

$$\text{Equation 4: } c_1 = K_{mv} * c_v$$

$K_{m/v}$ is the partition coefficient between SC and vehicle and c_v is the vehicle concentration. Combining Equation 3 and Equation 4 leads to

$$\text{Equation 5: } J_{ss} = \frac{D * K_{m/v}}{h} * c_v$$

The permeability coefficient Kp – which characterizes the substance specific membrane permeability – is defined as follows:

$$\text{Equation 6: } Kp = \frac{D * K_{m/v}}{h}$$

Equation 6 was the origin of the first in silico prediction models for dermal absorption as described in chapter 1.4.4. Combining Equation 5 and Equation 6 provides Equation 7 which is a first-order rate process per definition (Kielhorn et al. 2006; Riviere 2011b):

$$\text{Equation 7: } J_{ss} = Kp * c_v$$

J_{ss} and Kp can be derived from in vitro experiments when measuring time-dependently the absorbed amount in the receptor medium. Ideally infinite dose absorption experiments under sink conditions are performed. Infinite dosing (typically $100 \mu\text{L}/\text{cm}^2$ or more) maintains an almost constant concentration in the vehicle. Sink conditions – which are provided by sufficient solubility in and fast removing of penetrant from the receptor fluid – ensure an concentration in the receptor which is close to zero (OECD 2004a). For calculations, the cumulated amount of penetrant per area is plotted against time (black curve in Figure 5). The slope in the linear/steady state range is J_{ss} as described in Equation 2. Using J_{ss} , applied concentration c_v and Equation 7, Kp can be calculated. The intercept of this elongated line with the x-axis represents the lag time. Under finite dose conditions, the concentration in the vehicle is depleted over time which leads to a sigmoidal-shaped absorption curve (grey curve in

Figure 5). For such experiments the maximum flux (J_{\max}), the steepest slope of the absorption curve, is determined, since this is close to J_{ss} . For absorption studies, J_{\max} is equivalent to the maximal absorption rate (maxAR). Finite dose experiments are necessary for determining the percent absorbable dose and simulating in use conditions – often requested from regulatory agencies like ECHA (European Chemicals Agency) (The Commission of the European Communities 2008).

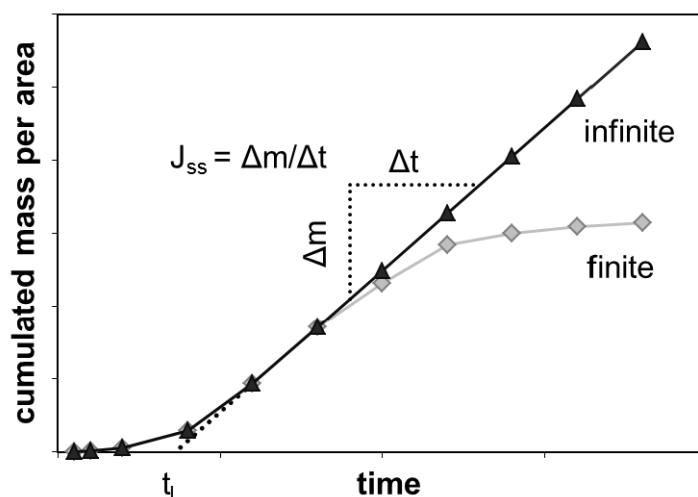


Figure 5: Cumulative absorption of a compound through the skin as a function of time under infinite (black triangles) and finite (grey squares) dose conditions. The slope of the linear portion of the curve represents the flux at steady state (J_{ss}) and the intercept of the extrapolated line with the x-axis provides the lag time (t_{lag}).

1.4.3 Critical aspects of in vitro experiments

1.4.3.1 Experimental influences

The extent to which a substance can penetrate the skin depends mainly on its physicochemical properties. A big size represented by molecular volume (MV) or MW and a low or extreme high lipophilicity quantified by $\log P_{ow}$ hinders dermal absorption (Riviere 2011a). Additionally, caustic effects, binding or other interactions with the skin, volatility and finally dose and volume in the experiment affect the absorption rate and absorbable dose. But beside the substance itself, many other aspects influence the study outcome. This chapter summarizes the knowledge concerning potentially influential parameters with a special focus on experimental parameters (EFSA Panel on Plant Protection Products and their Residues (PPR) 2012; European Centre for Ecotoxicology and Toxicology of Chemicals 1993; Kielhorn et al. 2006; Roberts & Cross 2002; Schaefer & Redelmeier 1996c). Experimental influences restrict the comparison of different studies and laboratories and make general conclusions and development of in silico models based on joint data difficult. Therefore, trend and extent should be considered for appropriate assessments. The susceptibility of the system emphasizes the importance of a widely standardized and accepted protocol – which is the intend of many guidance documents (EFSA Panel on Plant Protection Products and their Residues (PPR) 2012; European Centre for Ecotoxicology and Toxicology of Chemicals 1993; European Centre of the Validation of Alternative Methods ECVAM 2010; OECD 2004a; OECD 2004b). Further investigations –

including mechanistic interpretations – concerning influential parameters, would help to define standardized protocols and therefore increase the robustness and decrease the variance of the method.

The skin tissue has a high influence on the extent of dermal absorption. Since it is a natural material with inherent variability, wide variations are tolerated. In vitro a coefficient of variation (CV) about 43 % was observed for single donors (Southwell et al. 1984). Interindividual variance was observed to be 6 to 110 % (CV) or 2- to 8-fold (Lee et al. 2001; Schaefer & Redelmeier 1996c; Southwell et al. 1984; van de Sandt et al. 2004). To account for the donor effect, the Panel on Plant Protection Products and their Residues (PPR) of the European Food Safety Authority (EFSA) as well as the Scientific Committee on Consumer Safety of the European Commission demand for one experiment, skin preparations from at least two different donors (EFSA Panel on Plant Protection Products and their Residues (PPR) 2012; Scientific Committee on Consumer Safety (SCCS) 2010). A main aspect affecting intraindividual variation is the localization in the body. It was shown in vivo, that forearm, palm and ball of the foot provide larger barrier functions than axilla (3- to 7-fold) and scrotum (11- to 42-fold). The effect was assigned to SC thickness, hair-follicle density and skin flexibility (Maibach et al. 1971). Pathological variations like wounds, psoriasis or atopic eczema decrease the barrier function (Wiechers 1989). Furthermore, observed interindividual variability between human volunteers was not clearly attributable to sex or race (Black, Asian, Caucasian and Hispanics) (Leopold & Maibach 1996; Lotte et al. 1993; Rougier et al. 1988a). Age-related changes in percutaneous absorption were observed in human volunteers (young: 18 – 40 and old: > 65 years), whereby the absorption decreased with increasing age (Christophers & Kligman 1965; Roskos et al. 1989). In contrast, increased absorption of fluorescein with advancing age of the donor (young: 20 – 30 and old 70 – 80 years) was observed in vitro. However, the absorption of water was not affected. Christophers and Kligman explained the conflicting results in their in vitro and in vivo experiments with the minor barrier function of 'old' skin present in vivo and in vitro – which is linked to reduction of sebum production and increased dryness of SC – and the decreased transportation capacities to the systemic circulation due to decreased blood flow and atrophy of capillaries only present in vivo (Christophers & Kligman 1965). Furthermore, individual life-style may affect percutaneous absorption. The effect of stress on the skin is probably mediated by glucocorticoid release and results in limitation of healing processes, predisposition to bacterial infections by immunosuppression and reduction of quantity and quality of collagen by affecting the collagen production and degradation (Kahan et al. 2009). An enhancing effect of ethanol consumption observed in rats, could not be detected in human volunteers (Brand et al. 2004; Jacobi et al. 2005). Influential effects are also known for climatic or experimental conditions. Rising temperature is considered to increase absorption by increasing blood flow, higher fluidity of the intercellular lipids in the SC and enhanced diffusion activities of molecules. Occlusion acts primary by increasing the hydration of the SC – which is under normal relative humidities between 15 and 20 %. Extensive hydration of the skin swells the corneocytes – since the water is preferentially bound to intracellular keratin –, alters the motility of the attached lipids and disrupts the lamellar structures. Mainly decreased barrier functions were observed in vitro (Hotchkiss et al. 1992; Kielhorn et al. 2006; Potts & Francoeur 1990; Roberts & Walker 1993; Vecchia & Bunge 2002; Warner et al.

2003). It is also discussed that the receptor fluid used for in vitro investigations may change the hydration state of the SC or disrupts the barrier function otherwise. However, higher absorption rates were also correlated with increasing solubility in the receptor fluid (Challapalli & Stinchcomb 2002; Safferling 2008). Additionally, repeated dosing may affect the absorption profile. Such scenarios are closer to occupational, therapeutic or cosmetic exposure scenarios than single applications. Increasing, decreasing and no effects were observed in vivo as summarized by Kielhorn and Melching-Kollmuss, whereby disruptive effects or reservoir formation explain both directions (Kielhorn & Melching-Kollmuss 2008). Since OECD Guideline 428 recommends a maximum experimental time of 24 h, only few in vitro data exist concerning repeated dosing scenarios; but these data suggest, that skin could be used up to 96 h without deterioration of the barrier function and that repeated dosing – if at all – slightly increase the dermal absorption (Blank & Scheuplein 1967; Peck et al. 1993; Toner et al. 2009). However, other authors observed signs of skin deterioration at earlier time points (Buist et al. 2005). To complete these observations and to assess the general applicability of a repeated dosing scenario in vitro, effect of time, mechanical and chemical pretreatment – including pretreatment with test compound – were systematically investigated in the current work.

Previous studies with human and pig skin showed, that permeability properties of SC were preserved after excision and freezing and that several freeze-thaw cycles did not affect their barrier function (Harrison et al. 1984; Moody et al. 2009; Safferling 2008). Nevertheless, in vitro experiments are considered to generally overestimate the in vivo situation. For instance, an average overestimation of 14-fold was observed for 25 pesticides when comparing rat in vivo and rat in vitro results (van Ravenzwaay & Leibold 2004). Henning et al. observed that different preparation types (isolated SC, heat separated epidermis, dermatomed skin (DMS) and full-thickness skin (FTS)), which were generally in use for in vitro experiments, led to variant results (Henning et al. 2008). Lower absorptions through FTS compared to DMS were reported. The dermis is hypothesized to provide in vitro an artificial aqueous barrier which is not present in vivo, since vascular systems are present to uptake the substance after passing the epidermis (Diez-Sales et al. 1993; Henning et al. 2008; van de Sandt et al. 2004). In contrast, Vallet et al did not observe different absorption characteristics for two pesticides (demeton-S-methyl and diisopropylfluorophosphate) when using DMS or FTS (Vallet et al. 2007). Therefore, the effect of the dermis was systematically investigated in the current work by comparing dermal absorption of seven compounds through DMS and FTS. The skin preparations were derived from the same human donor to avoid donor-dependent variations.

A general strategy to avoid donor-specific variability is the use of reconstructed human skin. However, up to now none of the tested constructs (EpiDerm™, EpiSkin™ and SkinEthic™) fulfill the OECD requirement and provide absorption data for reference compounds which are consistent with those for excised human skin (OECD 2004a; Schaefer-Korting et al. 2008a). Therefore, barrier properties of a further commercially available human skin construct StrataTest® (details in section 1.3), was investigated in this work.

The effects outlined above for human skin are generally transferable to mammalian skin. However, some effects are discussed controversially in the literature: e.g. Bronaugh et al. observed different

permeabilities for male and female rats as well as for back and abdominal rat skin and in contrast, Gotter reported equal results for rat skin preparations from different sites and genders (Bronaugh et al. 1983; Gotter 2007). Comparison of human skin to pig skin revealed similar morphology and absorption characteristics (Barbero & Frasch 2009). Skin from rat and other rodents is considered to generally overestimate the human situation. Higher absorptions with rat skin compared to human skin were observed in vitro as well as in vivo. Differences may be related to morphology of SC and epidermis as well as density of skin appendages and depend on the physicochemical properties of the substance as well (Bartek et al. 1972; Scott et al. 1986; van Ravenzwaay & Leibold 2004). However, under identical experimental conditions, hairless rat skin showed similar permeability to human breast and thigh skin and Wistar rat and nude mouse skin similar permeability to human cheek, neck and inguinal skin for salicylic acid (Harada et al. 1993). To sum up, the entire information of the skin preparation – e.g. species, localization and preparation – must be considered, not only single aspects.

Beside penetrant and skin sample, a further main influential factor is the vehicle in which the substance is applied – also called donor, mixture or formulation. Two main effects should be considered: the effect on the barrier function of the skin and the effect on the behavior of the substance. Effects on the barrier include delipidation, disorganization of the lipid order, increasing fluidity, forming of water pools, hydration and caustic effects that lead to degradation of desmosomes and disruption of keratin bundles. Various enhancers designed for optimized uptake of pharmaceuticals acting via these mechanisms (Barry 1993; Menon et al. 1998; Roberts & Cross 2002). A direct effect on the substance may affect its permeation characteristics by changing its activity, diffusivity and solubility in the vehicle or by changing its ionization state and therefore its hydrophilicity. Several publications compare absorption from different vehicles. An increasing absorption was generally related to low solubility or high saturation of the compound in the vehicle (Baynes et al. 2002; Bronaugh & Franz 1986; Dugard & Scott 1986; Riviere 2011c; Safferling 2008). A further aspect discussed in the literature is the use of static and flow-through systems. Several working groups observed similar results with both systems (Bronaugh & Stewart 1985; Hughes et al. 1993). However, Shah et al. reported remarkable differences between the two designs (Shah et al. 1988). The current work compared the two approaches as well, using two test compounds under equivalent experimental conditions. The last aspect which could lead to differing results in different laboratories is the calculation (e.g. K_p derived from linear range or maximum slope) and interpretation (e.g. content in SC defined as absorbed or not absorbed) of the data (EFSA Panel on Plant Protection Products and their Residues (PPR) 2012; European Chemicals Agency (ECHA) 2008; Scientific Committee on Consumer Products (SCCP) 2006).

1.4.3.2 Xenobiotic biotransformation in skin

Beside the physical barrier formed mainly by the SC, the skin provides physiological defense mechanisms like xenobiotic-metabolizing enzyme activities (Wilkinson & Williams 2008). Therefore, additionally to the influential factors discussed above, dermal biotransformation may affect the fate of compounds in the skin as well. Functionalization or conjugations can change the physicochemical properties of the penetrant, which may result in accelerated or attenuated permeation. Furthermore,

metabolites – built in the viable epidermis – could diffuse with their concentration gradient bidirectional – which means into deeper tissue layers or in the direction of the skin surface. Additionally, breakdown of the parent molecule changes its concentration gradient and therefore its diffusion pressure. Overall, localization and extent of biotransformation determine the effect on absorption. Furthermore, first-pass effects in the skin determine local and systemic exposure to xenobiotics, which determines the presence and extent of therapeutic, adverse or toxic effects. This property of the skin is under investigation for prodrug strategies (Fang & Leu 2006). Since several enzyme activities were preserved to a certain extent after excision and freezing, the effect on dermal absorption is not limited to in vivo experiments. However, activity of enzymes, e.g. NAT 1 and several CYP-isoforms, was observed to decrease ex vivo – even when stored frozen (Henkler et al. 2012; Kao et al. 1985). Ester cleavage during passage through freshly-excised human skin was shown for the glucocorticoid prednicarbate and ester derivatives of the herbicide fluoxypyr (Gysler et al. 1999; Hewitt et al. 2000). In case of the drug prednicarbate, the content of parent drug and metabolites determines the deliberate anti-inflammatory and adverse atrophogenic – skin-thinning – effects and therefore the benefit/risk-ratio of the drug (Gysler et al. 1999). In case of the pesticide, only the polar metabolite fluoxypyr (free acid) was systemically available, whereby the highly lipophilic esters mainly remain in the SC. Therefore, formation rate and toxicity of the free acid need to be taken into account for suitable risk assessment (Hewitt et al. 2000). The overall esterase activity in human skin – determined with turn-over of substrate fluorescein diacetate in S9 fraction – was $\sim 0.2 - 0.5 \text{ nmol}/(\text{min} \cdot \text{mg})$ (Bätz et al. 2012). For the recent work, the impact of dermal biotransformation on absorption of pesticide MCPA-EHE (2-methyl-4-chlorophenoxyacetyl 2-ethylhexylester) was investigated. Therefore, washing fluid, skin and receptor fluid from dermal absorption studies were analyzed for the parent and degradation products and parallel absorption studies were conducted with the hydrolysis product MCPA (2-methyl-4-chlorophenoxyacetic acid). Additionally, general and specific esterase activity was measured in S9 fraction from cryoconserved human skin samples with substrates fluorescein diacetate and MCPA-EHE.

Besides esterases like carboxylesterases, lipidases and amidases, other xenobiotic-metabolizing enzymes are involved in dermal biotransformation. Broad overviews of enzymatic profiles (transcript, protein and activity) in human and animal skin are given from several authors (Henkler et al. 2012; Hotchkiss 1998; Jaekch et al. 2012; Oesch et al. 2007; United States Environmental Protection Agency (US-EPA) 2011; Wilkinson & Williams 2008). A short summary is given below.

In general the basal activities of xenobiotic-metabolizing enzymes are low considering the surface area of the skin and the activities in the liver. Hotchkiss summarizes expression levels of phase I enzymes to be 0.1 – 28 % and phase II enzymes to be 0.6 – 50 % of the hepatic level (Hotchkiss 1998). The enzymes are mainly localized in keratinocytes of the viable epidermis or sebaceous glands and to a lesser extent in fibroblasts of the dermis (Oesch et al. 2007). Transcripts of several cytochrome P450 isoenzymes (CYPs) were detected in human skin (e.g. CYP 1A1, 1B1, 2E1, 3A4) (Henkler et al. 2012). Generally, low basal activities were measured using microsomes of human skin and enzyme-specific substrates (substrates are given in brackets): e.g. CYP 2E1 (1.8 nmol(p-

nitrophenol)/(min*mg) and 2.8 nmol(chlorzoxazone)/(min*mg)) and CYP 3A (2.4 nmol(midazolam)/(min*mg) and 3.3 nmol(erythromycin)/(min*mg)) (Baron et al. 2001; Rolsted et al. 2008). The activity of CYP 1A was reported to be below the limit of detection (LOD, ~0.0001 nmol (methoxyresorufin/ethoxyresorufin)/(min*mg)) and the limit of quantification (LOQ, 0.002 nmol (ethoxyresorufin)/(min*mg)) when using whole tissue microsomes; however, clearly detectable activities were measured with microsomes derived from isolated primary keratinocytes (0.01 nmol (ethoxyresorufin)/(min*mg)) (Baron et al. 2001; Goetz et al. 2012a; Henkler et al. 2012). Many CYPs were shown to be inducible, leading generally to higher activities. For example, Ledirac et al. reported a 15-fold increase of CYP1A (ethoxyresorufin) activity in the keratinocyte cell line HaCaT after treatment with 3-methylcholanthrene (Ledirac et al. 1997). Several isoforms of aldehyde dehydrogenase (ALDH 1A1, 2) were expressed in the human skin and a general activity of 6.2 nmol(propionaldehyde)/(min*mg) was measured in the cytosol (Henkler et al. 2012). Transcripts of alcohol dehydrogenase isoforms (ADH 1A, 1B, 1C) were detected only in the dermis of human skin, associated with an overall activity of 9.1 nmol (ethanol)/(min*mg) measured in the cytosol (Henkler et al. 2012). Also transcripts of flavin-dependent monooxygenases (FMO 1, 3) were detected in human skin. The reported overall activity of both isoforms in microsomes of human skin was 4.0 nmol (benzylamine)/(min*mg) (Henkler et al. 2012). Additionally, activities of cyclooxygenase (COX) 2 (24 pg(prostaglandin E2)/(min*mg), UDP-glucuronosyltransferase (UGT) 1 (0.1 nmol(4-methylumbelliferone)/(min*mg)) and N-acetyltransferase (NAT) 1 (1.8 nmol(para-aminobenzoic acid)/(min*mg)) were detected in microsomes of human skin samples. However, human skin is devoid of NAT 2 and UGT 2 transcripts (Goetz et al. 2012a; Henkler et al. 2012). General activities of NAD(P)H quinone reductase, glutathione transferases (GSTs) with major representative GST π and isoforms of sulfotransferases (SULT 1A, 2B) were summarized by Wilkinson and Williams for human skin. Additionally, methyl transfer and glycine conjugations were observed (Wilkinson & Williams 2008).

1.4.3.3 Integrity tests

A final critical aspect of in vitro experiments for dermal absorption is the use and suitability of various integrity tests. Performance of an integrity test should ensure an exclusive use of skin samples with intact barrier function and thereby avoid unsuitable over-prediction due to damaged preparations. In addition to a visual examination of the skin, OECD Guidance document 28 proposes different methodologies to assess the barrier function of the skin: Measuring the transepidermal electrical resistance to an alternating current or impedance (TEER), the transepidermal water loss (TEWL) or the absorption characteristics of a reference material like tritium-labeled water (transepidermal water flux, TWF) in advance or at the end of an experiment or adding an internal standard (ISTD), e.g. ^3H -labeled sucrose with high specific activity, to the test preparation and measuring its absorption characteristics concurrently (OECD 2004a; OECD 2004b). Widely used tests in many laboratories are TWF and to a lesser extent TEWL and TEER (Diembeck et al. 1999; Meidan & Roper 2008). But despite intensive investigations, there is still much research and discussion about experimental performances, limit values and fields of application (Brain et al. 1995; Chilcott et al. 2002; Meidan & Roper 2008; Netzlaff et al. 2006). For example, TWF is a widely used and established marker for skin barrier function with a large historical dataset (Bronaugh et al. 1986; Meidan & Roper 2008). However,

the application of an infinite dose of water and therefore hydration for several hours, followed by the necessary removal and wash could cause physical deterioration of the skin and higher permeability afterwards (Brain et al. 1995). In contrast, a measurement at the end of the experiment could lead to rejection of previously intact skin samples. Similar effects due to similar treatment of the skin (application of several milliliters of physiological saline followed by removal and wash) are conceivable for TEER – which was also shown to be a barrier indicator in general (Davies et al. 2004; Fasano et al. 2002). Also TEWL is widely used as a marker for skin barrier function *in vitro* and *in vivo*. This measurement of evaporating water from skin samples avoids physical stress to the skin (Levin & Maibach 2005). However, like TEER and TWF, it provides only a snapshot before or after an experiment – an experiment during which the skin properties could change. For instance, changes of stratum corneum structure and hydration level by vehicle compounds and deterioration with time have been reported (Buist et al. 2005; Shah et al. 2008). Only the application of ISTD provides information of the barrier function over the entire experimental period. However, the presence of an additional compound in the donor may influence the absorption characteristic of the test substance. Changes in solubility or saturation levels of the test substance, and effects on the barrier could be reasons for this influence (Barry 1987; Dugard & Scott 1986). Due to this influence, the inertness of an ISTD must be demonstrated. ³H-sucrose and phenol red have been used as ISTD in the past, but systematic validation and provision of a sufficient database is still missing (Balaguer et al. 2006; Pendlington et al. 1997; Walters et al. 1997). Using absorption characteristics of methylene blue (BLUE) as an integrity parameter is also promising due to the compound's properties: methylene blue is a cationic dye with a minor ability to penetrate and permeate the skin, but binds inside cells on DNA and accumulates in mitochondria (Gabrielli et al. 2004; Johnson et al. 1996). Thus, dermal penetration and absorption could be assessed either by optical examination of a potential blue staining of the skin or by highly sensitive photometrical measurement of methylene blue in the receptor fluid. In the current work five different skin integrity tests (TEER, TWF, TEWL, ISTD and BLUE) were evaluated for their ability to differentiate damaged and undamaged skin samples as well as explain minor differences in barrier function. To verify the ISTD approach, co-analytics and co-absorption of ISTD and test substance were investigated.

1.4.4 In silico prediction models

Besides the explained experimental determination (chapter 1.4.1), several *in silico* models were developed to predict dermal absorption of chemicals (Mitragotri et al. 2011). Although many models are limited to small applicability domains or were insufficiently validated, they may be useful for risk assessment. This is especially true, if appropriate data were missing (e.g. for chemicals under the European REACH (Registration, Evaluation, Authorisation and Restriction of Chemicals) legislation) or if the availability of the test compound is limited (e.g. in early developmental stages of pesticides). Therefore, valid screening tools would reduce the number of experiments as well as time and costs (European Centre for Ecotoxicology and Toxicology of Chemicals 1993; The European Parliament and the Council of the European Union 2006).

The basic assumption that similar chemical structures lead to similar reactivity and biological effects is used to relate experimental absorption results in the form of K_p with physicochemical properties of the penetrant. The obtained relationships can be used to predict the behavior of untested compounds. Structurally or chemically derived as well as theoretically and experimentally derived properties can be used as model descriptors. Some authors define their model by the kind of descriptors used or the endpoint as QSPeR or LSER. QSPeR models (quantitative structure-permeation relationships) are specialized forms of QSAR models (quantitative structure-activity relationships) which use structurally derived properties to predict dermal absorption; LSER models (linear solvation energy relationships) include chemically derived free energy based properties (Cramer et al. 1993; Xia & Riviere 2011). Many other names, e.g. LFER (linear free energy relationships), TLSER (theoretical LSER), QSAR or TQSAR (theoretical QSAR) are used as well. Since the nomenclature is not consistently used in the scientific community, the more general phrase of 'in silico prediction model' is used in the following. Detailed overviews and evaluations of various models are given in the literature and summarized shortly in the following (Fitzpatrick et al. 2004; Geinoz et al. 2004; Mitragotri et al. 2011; Moss et al. 2002).

Many models presented in the literature used the Flynn database (Flynn 1990). This dataset summarizes in vitro absorption results of 94 compounds from 15 different literature sources from 11 different research groups. The listed K_p values were obtained from infinite dose experiments with aqueous donor and receptor solutions and human skin preparations. The other experimental parameters like occlusion conditions or temperature were diverse. One of the first models based on this dataset was developed by Potts and Guy in 1992 (Potts & Guy 1992). They deduced from former investigations, relationships between K_{mv} (membrane/water partition coefficient) and P_{ow} and between D_m (permeant diffusivity within the membrane) and MW:

$$\text{Equation 8: } K_{mv} = P_{ow}^f$$

$$\text{Equation 9: } D_m = D_0 * e^{-\beta * MW}$$

The exponent f accounts for the difference between the partitioning domains octanol and SC lipids, D_0 is the diffusivity of a hypothetical molecule with zero molecular weight and the constant β relate MW exponentially to D_m . Insertion of Equation 8 and Equation 9 in the definition of K_p derived from Fick's first law (Equation 6) provides:

$$\text{Equation 10: } Kp = P_{ow}^f * \frac{D_0}{h} * e^{-\beta * MW}$$

Rearrangement and logarithmic transformation led to the following linear relationship:

$$\text{Equation 11: } \log Kp = \log \frac{D_0}{h} + f * \log P_{ow} - \beta * e^{MW}$$

Using $\log P_{ow}$, MW and $\log Kp$ from the Flynn database, linear regression analysis revealed results for constants $\log D_0/h$, f and β as shown in the following model equation (R^2 0.67) (Potts & Guy 1992):

$$\text{Equation 12: } \log Kp[cm/s] = -6.3 + 0.71 * \log P_{ow} - 0.0061 * MW$$

By explaining 67 % of the variance this model confirmed the theoretical relationship between molecular size and lipophilicity of the penetrant and its dermal absorption (Potts & Guy 1992). Similar to this approach MW and $\log P_{ow}$ were inserted in several *in silico* prediction models including so-called two-pathway models. The latter models account separately for a lipid (lipids of the SC) and aqueous (protein fraction of the SC, epidermis and dermis) barrier (McKone & Howd 1992; Vecchia & Bunge 2002; Wilschut et al. 1995). One and two-pathway models were compared by Wilschut and co-workers (Wilschut et al. 1995). Peck et al. as well as Kushner et al. built their models on the porous pathway theory and therefore on parameters like membrane porosity, tortuosity and thickness (Kushner, IV et al. 2007; Peck et al. 1994). Other researchers expanded the idea of existing linear or exponential relationships between Kp and the variables P_{ow} and MW to other physicochemical properties: For example, Abraham and co-workers introduced five free energy-based properties for the prediction of dermal absorption: $\Sigma\alpha_2^H$, $\Sigma\beta_2^H$, Rf_2 , π_2^H and V_x , where $\Sigma\alpha_2^H$ and $\Sigma\beta_2^H$ are the overall hydrogen bond acidity and basicity, Rf_2 the solute excess molar refractivity, π_2^H the solute dipolarity/polarizability and V_x the McGowan characteristic volume (Abraham et al. 1999). Originally, such parameters were used to correlate solute-solvent interactions (Cramer et al. 1993). By describing transport processes through the skin with these parameters, the relationship describes the different interacting properties of the solute with the skin and the vehicle (Abraham et al. 1999). Based on Kp values of 119 compounds extracted from the Flynn database and various publications, Abraham et al. obtained the following model equation with R^2 0.83 (Abraham & Martins 2004):

Equation 13:

$$\log Kp[cm/s] = -5.426 - 0.473 * \Sigma\alpha_2^H - 3.000 * \Sigma\beta_2^H - 0.473 * \pi_2^H - 0.106 * Rf_2 + 2.296 * V_x$$

Similar to the Potts and Guy model, the term covers size and lipophilicity of the penetrants, but additionally hydrogen bonding capacities. That the latter is a good descriptor for dermal absorption was also observed by other research groups (Ghafourian & Fooladi 2001; Lien & Gao 1995; Pugh 2001). However, many other descriptors are discussed in the literature, e.g. melting point or number of rotatable bonds (Barratt 1995; Dearden et al. 2000; Moody & MacPherson 2003). Also under discussion is the experimental variance in the databases. Several publications addressed this issue by adjusting the absorption results in the form of Kp values to a unique temperature and/or to the amount of neutral compound considering pH and pKa (acid dissociation constant) (Abraham & Martins 2004; Vecchia & Bunge 2002).

The disadvantage of all the models mentioned above were their restriction to aqueous vehicles. A first attempt to insert a vehicle effect was introduced by Hostynek and Magee by using an indicator variable in a linear model (1 for acetone, 2 for ethanol) (Hostynek & Magee 1997). A different attempt was used by Frasch et al. who related the prediction to the solubility in the vehicle (Frasch et al. 2010). Riviere and co-workers applied a more general mixture factor (MF) which was added as an independent model variable (Riviere & Brooks 2005): Their MF was a physicochemical parameter

(refractive index, polarizability or $\log(1/\text{Henry's law constant})$) which was calculated as the sum of the weight percentage of each of the bulk components in the mixtures for this particular parameter. Based on a homogeneous experimental dataset of 16 penetrants in 24 different mixtures containing water, ethanol, propylene glycol, methyl nicotinate and/or sodium lauryl sulfate resulting in 344 combinations, the multiple linear regression on the five Abraham descriptors $\Sigma\alpha_2^H$, $\Sigma\beta_2^H$, Rf_2 , π_2^H and V_x and the refractive index as MF led to the following regression equation (R^2 0.80) (Riviere & Brooks 2005):

$$\text{Equation 14: } \log Kp[cm/s] = 10.751 - 0.525 * \sum \alpha_2^H + 0.329 * \sum \beta_2^H + 0.407 * \pi_2^H \\ - 0.411 * Rf_2 - 1.385 * V_x - 9.242 * MF$$

In the present work this approach was stressed by using a complex 'real world' dataset from BASF SE which consists of in vitro experiments for mainly agrochemicals. The penetrants were applied in typical formulations and dilutions with up to 20 ingredients from a total palette of about 240 ingredients under various experimental conditions. The development and modifications of the current approach were described in detail and the suitability of the final models for future tasks was assessed. During the model development, several decisions, considerations and calculations were made to address the five principles of reliable prediction models postulated by the OECD (OECD 2007): '1. A defined endpoint, 2. an unambiguous algorithm, 3. a defined domain of applicability, 4. appropriate measures of goodness-of-fit, robustness and predictivity and 5. a mechanistic interpretation, if possible.'

2 Objectives

The current work is part of a research project at BASF SE with the aim to identify, better understand and evaluate the impact of influential parameters on dermal absorption in vitro and to improve the routine application. A further aim is the development of screening tests comprising in silico and alternative in vitro approaches. Specific objectives for the current work were derived in the introduction (chapter 1) and summarized in the eight following bullet points. The tasks address influences on dermal absorption in vitro, dermal biotransformation in vitro including its impact on dermal absorption and in silico modeling of dermal absorption:

1. Assessment of the suitability of five skin integrity tests for dermal absorption experiments in vitro and verification of the internal standard (ISTD) approach
2. Comparison of absorption results obtained with the flow-through and the static system
3. Evaluation of the repeated dosing regimen in vitro and systematic investigation of the effect of time, substance as well as physical and chemical stress
4. Comparison of absorption characteristics through DMS (dermatomed skin) and FTS (full-thickness skin) derived from the same human donors
5. Examination and evaluation of alternatives to human skin for the determination of dermal absorption (rat skin, human skin construct (StrataTest®) and abiotic skin surrogate (skin-PAMPA))
6. Measurement of the metabolic transformation of the model substrate MCPA-EHE during absorption experiments
7. Determination of xenobiotic-metabolizing enzyme activities in the human skin construct StrataTest®
8. Development of an in silico model based on BASF SE data that considers mixture effects

3 Materials and methods

3.1 Chemicals, reagents and devices

Central chemicals, reagents and devices used for investigations are listed in this section including their producer or supplier. Some further laboratory chemicals as common solvents were purchased from typical suppliers in appropriate quality and purity. Solutions and buffers were prepared in de-ionized water – produced with Synergy[®] Water Purification Systems – unless stated otherwise.

Chemicals and reagents

acetyl coenzyme A sodium salt	Sigma-Aldrich, St. Louis, MO, USA
adenosine monophosphate disodium salt (5'-AMP)	Sigma-Aldrich, St. Louis, MO, USA
agarose (BioChemika, high melting)	Sigma-Aldrich, St. Louis, MO, USA
benzylamine hydrochloride (BA)	Sigma-Aldrich, St. Louis, MO, USA
benzylxyresorufin (BROD)	Sigma-Aldrich, St. Louis, MO, USA
benzylamine n-oxide hydrogen maleate (BA-nOx)	Sigma-Aldrich, St. Louis, MO, USA
bovine serum albumin (BSA)	Roche, Basel, Switzerland
Bradford reagent	Sigma-Aldrich, St. Louis, MO, USA
Brij [®] 58 (Polyoxyethylene (20) cetyl ether)	Sigma-Aldrich, St. Louis, MO, USA
dimethyl sulfoxide (DMSO)	Sigma-Aldrich, St. Louis, MO, USA
dithiothreitol (DTT)	Sigma-Aldrich, St. Louis, MO, USA
ethylenediaminetetraacetic acid disodium salt (EDTA-Na ₂)	Sigma-Aldrich, St. Louis, MO, USA
ethanol	Sigma-Aldrich, St. Louis, MO, USA
ethoxyresorufin (EROD)	Sigma-Aldrich, St. Louis, MO, USA
fluorescein	Sigma-Aldrich, St. Louis, MO, USA
fluorescein diacetate	Sigma-Aldrich, St. Louis, MO, USA
formic acid	Merck, Darmstadt, Germany
glucose-6-phosphate (monosodium salt)	Sigma-Aldrich, St. Louis, MO, USA
glucose-6-phosphat-dehydrogenase Type XV (Bakers Yeast)	Sigma-Aldrich, St. Louis, MO, USA
glutathione (reduced)	Merck, Darmstadt, Germany
glycerol (86-88%)	Sigma-Aldrich, St. Louis, MO, USA
glycine	Sigma-Aldrich, St. Louis, MO, USA
hydration buffer (P/N 120662)	Pion, Billerica, MA, USA
4-hydroxybiphenyl (HOBI)	Sigma-Aldrich, St. Louis, MO, USA
LSC-cocktail Hionic Fluor [™]	PerkinElmer, Boston, MA, USA
magnesium chloride (MgCl ₂ *6H ₂ O)	Sigma-Aldrich, St. Louis, MO, USA

maintenance medium (StrataTest [®] -medium)	Stratatech, Madison, WI, USA
methylene blue	Sigma-Aldrich, St. Louis, MO, USA
4-methylpyrazole hydrochloride	Sigma-Aldrich, St. Louis, MO, USA
4-methylumbelliferone (MUF)	Sigma-Aldrich, St. Louis, MO, USA
4-methylumbelliferon- β -D-glucuronide	Sigma-Aldrich, St. Louis, MO, USA
nicotinamide adenine dinucleotide – oxidized (NAD ⁺)	Sigma-Aldrich, St. Louis, MO, USA
nicotinamide adenine dinucleotide – reduced (NADH)	Sigma-Aldrich, St. Louis, MO, USA
NADPH (tetrasodium salt, CalBiochem [®])	Merck, Darmstadt, Germany
para-aminobenzoic acid (PABA)	Sigma-Aldrich, St. Louis, MO, USA
pentoxeresorufin (PROD)	Sigma-Aldrich, St. Louis, MO, USA
physiological saline (0.9 %)	B. Braun, Melsungen, Germany
potassium dihydrogen phosphate (KH ₂ PO ₄)	Sigma-Aldrich, St. Louis, MO, USA
prisma HT buffer concentrate (P/N 110238)	Pion, Billerica, MA, USA
propionaldehyde (97 %)	Sigma-Aldrich, St. Louis, MO, USA
pyrophosphate tetrasodium salt	Sigma-Aldrich, St. Louis, MO, USA
resorufin sodium salt	Sigma-Aldrich, St. Louis, MO, USA
saccharose	Sigma-Aldrich, St. Louis, MO, USA
semicarbazide hydrochloride	Sigma-Aldrich, St. Louis, MO, USA
Soluene 350 [®]	PerkinElmer, Boston, MA, USA
Texapon [®] N70	Cognis, Düsseldorf, Germany
trichloroacetic acid (TCA)	Sigma-Aldrich, St. Louis, MO, USA
Trizma [®] base (Tris)	Sigma-Aldrich, St. Louis, MO, USA
uridine 5'-diphospho- α -D-glucuronic acid (UDP-GA)	Sigma-Aldrich, St. Louis, MO, USA

Technical devices

analytical balances

AT 400, AE 240, XP 504, AT 200

Mettler-Toledo, USA

cell warmer

PermGear, USA

centrifuges

Centrifuge 5424

Eppendorf, Germany

Multifuge 3 S-R

Haereus, Germany

L8-M ultracentrifuge

Beckman instruments, USA

clean bench Variolab Mobilien W90

Waldner, USA

cotton swaps	Pezl, Germany
Crystal Clear Tape 600	Scotch, France
dermatome GA 643 and blades GB 228	Aesculap, Germany
diffusion cells	
flow-through (Ø 12 mm)	PermGear, USA
static (1 cm ²)	BASF, Germany
filter Spartan 13/0.45 RC and 13/02 RC	Whatman, UK
Fixomull [®]	BSN medical, Germany
forceps, scissors, scalpels including blades Germany	Aesculap, Tuttlingen,
fraction collector Liquid Handler 222 XL	Abimed, Germany
GC-MS (gas chromatography with mass spectrometry)	
HP-6890	Agilent, USA
MSD 5975B	Agilent, USA
GC-MS column	
HP- 5MS 5 % phenylmethylsiloxane, 30 m, 0.25 mm, 0.25 µm	Agilent, USA
high sensitivity UV plate (P/N 110286)	Pion, USA
HPLC (high-performance liquid chromatography) columns	
Gemini C18, 3 µ, 50*2 mm	Phenomenex, Germany
Hypersil CN, 5 µ, 250 x 4 mm	Fisher Scientific, USA
Luna C18, 5 µ 250*3 mm	Phenomenex, Germany
Nucleosil 120-5, 5 µ, 250 x 4 mm	Macherey-Nagel, Germany
Synergi Hydro-RP, 4 µ, 250 x 3 mm	Phenomenex, Germany
Synergi Hydro RP 4 µ, 250 mm x 3 mm	Phenomenex, Germany
HPLC-UV/FLD (HPLC with ultraviolet and fluorescence detector)	
pump 1312A (binary) (Agilent 1100 Series)	Agilent, USA
UV: DAD G1315A (Agilent 1100 Series)	Agilent, USA
FLD: FP-1520	Jasco, USA
HPLC-UV/RAD I (HPLC with UV radio detector)	
pump 1312A (binary) (Agilent 1100 Series)	Agilent, USA
UV: VWD G1314A (Agilent 1100 Series)	Agilent, USA
RAD: radioflow detector Berthold LB 509 with solid scintillator cell YG150	Berthold, Germany

HPLC-UV/RAD II

pump: PU-1580	Jasco, USA
UV: UV 2075 Plus	Jasco, USA
RAD: HPLC radioactivity monitor LB 507 A with solid scintillator cell YG150	Berthold, Germany
homogenizers	
Potter S	B. Braun, Germany
ultrasonic probe Labsonic 2000	B. Braun, Germany
incubator Haereus 6000	Haereus, Germany
LCR bridge LCR 400	Thurbly Thandar Instruments, UK
liquid scintillation counter (LSC)	
TriCab 2800TR	PerkinElmer, USA
Wallac 1409	PerkinElmer (Wallac), USA
magnetic stirrers	
IKA-Combimag RET	IKA, Germany
Variomag compact stirrers and Telemoduls 20C/40C	Thermo Fisher Scientific, USA
measuring gauge (external) IP 67	Kroeplin, Germany
multichannel peristaltic pump MC 360	IDEX Health & Science, Germany
Parafilm 'M' [®]	Pechiney Plastic Packaging, USA
pH-Meter 766 Calimatic	Knick, Germany
pipettes and tips	Eppendorf, Germany; Gilson; USA
(fluorescence) photometer Infinite200 [®]	Tecan, Switzerland
punch (Ø 22 mm)	Hoffman Group, Germany
rack for diffusion cells	BASF SE, Germany
reaction vessels	Eppendorf and Sarstedt, Germany
receptor reservoir with automated replenishment	BASF SE, Germany
evaporator Rotavapor R-125 including heating bath	Büchi, Switzerland
shakers	
shaker KS 501 digital	IKA, Germany
shaker Unimax 1010	Heidolph Instruments, Germany
vortexer Labdancer	VWR International, USA
steam sterilizer Laboklav	Steriltechnik, Germany
Styrodur [®]	BASF, Germany

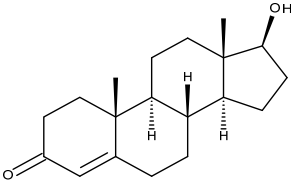
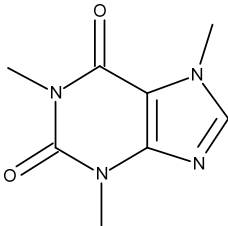
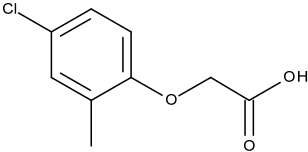
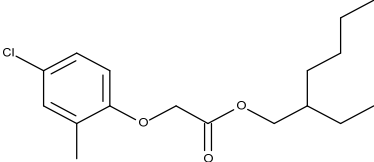
Synergy [®] Water Purification Systems	Millipore, USA
syringe pump	B. Braun, Germany
syringes and canulas	B. Braun, Germany
thermomixer comfort	Eppendorf, Germany
three-port valve	Sarstedt, Germany
tubes	
'Heidelberger Verlängerungen'	B. Braun, Germany
Tygon (Ø 0.38 mm)	IDEX Health & Science, Germany
ultrasonic baths	
Bandelin Sonorex	Bandelin, Germany
Elmsonic S30H, Transsonic T460 and T780/H	Elma, Germany
vacuum concentrator SpeedVac [®]	Thermo Scientific, USA
vacuum pump Laboport [®]	KNF Neuberger, USA
VapoMeter	Delfin Technologies Ltd, Finland
water thermostats	
GFL 1083 including shaker	GFL, Germany
Haake B3 and C1 including pump	Thermo Haake, Germany
Julabo SW 1	Julabo, Germany
well plates (clear and black)	VWR, Germany
Software	
ADME Boxes version 4.95	Advanced Chemistry Development, Canada
Chromeleon 6.8- chromatography data system (HPLC)	Dionex Corporation, USA
ChemOffice 6.0.1 (including ChemDraw)	CambridgeSoft, USA
ChemStation (GC-MS)	Agilent, USA
WinSpectral 2.00.02 (LSC)	Wallac, PerkinElmer, USA
Quantasart 2.03	PerkinElmer, USA
Magellan [™] - Data Analysis Software (photometer)	Tecan, Switzerland
Molinspiration Property Calculator http://molinspiration.com/cgi-bin/properties	Molinspiration Cheminformatics, Slovak Republic
Office 2003 / 2010	Microsoft, USA
PAMPA Explorer Command Software	Pion, USA

PhysProp Database Demo (Syrres), http://www.syrres.com/esc/physdemo.htm	SRC, USA
REIHE13.XCP (Fraction collector)	Abimed, Germany
SAS 9.2 TS Level 2M3	SAS Institute, USA
SigmaPlot 11.0	Systat Software, USA

3.2 Test substances

Testosterone, caffeine, 2-methyl-4-chlorophenoxyacetic acid (MCPA) and 2-methyl-4-chlorophenoxyacetyl 2-ethylhexylester (MCPA-EHE) were used as test substances for dermal absorption experiments. MCPA-EHE was also used as model substrate for biotransformation in human skin systems. Chemical formulas and structures as well as some physicochemical properties of the test substances are listed in Table 1.

Table 1: Chemical structures and physicochemical properties of test substances ($\log P_{ow}$, MW and S_R – the solubility in the respective receptor fluid). If no literature value was available, solubility was determined as described in section 3.5.1.

test substance	chemical structure	$\log P_{ow}$	MW [g/mol]	S_R [g/L]
testosterone		3.32 ¹	288.4	0.49 ± 0.01 (32°C, 5% BSA in tap water)
caffeine		-0.07 ²	194.2	20 (20°C, water) ²
MCPA 2-methyl-4-chlorophenoxyacetic acid		-0.71 (pH 7) ³ 2.75 (pH 1) ³	200.6	293.9 (25°C, water pH7) ³
MCPA-EHE 2-methyl-4-chlorophenoxyacetyl 2-ethylhexylester		6.8 ³ 5.4 ⁴	312.8	0.40 ± 0.13 (32°C, water)

¹ (Yalkowsky et al. 1983)

² (Merck 2006a)

³ (British Crop Protection Council 2011)

⁴ (United States Environmental Protection Agency (US-EPA) 2004)

Testosterone and caffeine were used as model substrates due to their status as performance standards in OECD Guideline 428 (OECD 2004b). This status is based on a broad knowledge about their dermal absorption characteristics from extensive research over the last decades (Bronaugh et al. 1986; Heylings et al. 2001; OECD 2004b; Schaefer-Korting et al. 2008a; Scheuplein et al. 1969; Siddiqui et al. 1989; van de Sandt et al. 2004). The androgen testosterone was used representatively for dermal uptake of lipophilic substances and the xanthine alkaloid and psychostimulant caffeine representatively for more hydrophilic compounds. ^{14}C -labeled standards with specific activities of 9.6 MBq/mg (caffeine) and 7.3 MBq/mg (testosterone) were purchased from PerkinElmer and the unlabeled standards from Sigma-Aldrich.

MCPA and MCPA-EHE were used as model pesticides for dermal absorption and biotransformation studies. On the one hand due to their (metabolic) relationship to each other and on the other hand due to their well-investigated kinetic behavior in plants and animals (van Ravenzwaay et al. 2004). Furthermore, MCPA-EHE – an extremely lipophilic compound ($\log P_{ow}$ of 5.4 – 6.8) – and MCPA – a hydrophilic compound ($\log P_{ow}$ -0.71, pH 7) – supplement the physicochemical spectrum of test compounds for dermal absorption experiments (Table 1). MCPA is a selective, systemic herbicide which inhibits growth of annual and perennial broad-leaved (dicotyledonous) weeds. Structure analogy to auxins – phytohormones – produce uncoordinated growth which led to depletion of nutrients and finally to plant death (British Crop Protection Council 2011). Four active ingredients derived from MCPA are registered for commercial products in the US: MCPA, MCPA sodium salt, MCPA dimethylamine salt (MCPA DMA), and MCPA-EHE (United States Environmental Protection Agency (US-EPA) 2004). In Germany MCPA, MCPA DMA and MCPA sodium salt are registered (Bundesamt für Verbraucherschutz und Lebensmittelsicherheit (BVL) 2012a). In natural waters and soil/water mixtures as well as in plants and animals MCPA-EHE hydrolyses rapidly to MCPA. Main metabolite of MCPA in plants and animals is its oxidation product 2-hydroxymethyl-chlorophenoxyacetic acid (HMCPA) (British Crop Protection Council 2011; van Ravenzwaay et al. 2004). Radiolabeled standards with specific activities of 3.3 MBq/mg for MCPA-EHE and 9.4 MBq/mg for MCPA were received from the Radio Isotope Laboratory of BASF SE. Unlabeled standards as well as formulation ingredients (see 3.5.1) were provided from AH Marks & Co, Wyke, Bradford, UK.

Performance standards for the skin-PAMPA-assay – **atenolol, chlorpromazine, niflumic acid, piroxicam, progesterone, verapamil and warfarin** – were provided by Pion.

3.3 Excised skin samples and skin equivalents

Dermatomed (DMS) and full-thickness (FTS) female **human skin samples** obtained from abdominal surgeries were purchased from Biopredic, France. The thickness was between 340 and 580 μm for DMS and between 825 and 1320 μm for FTS.

Rat skin was excised from the back of eight week old female Crl:WI (Han) rats (Charles River, Germany) after anesthesia with isoflurane and exsanguination. DMS (in the literature also called 'split-thickness skin') with a thickness from 270 to 500 μm was generated with a dermatome after hair trimming. Rat and human skin punches of 20 mm diameter were stored at -20°C for a maximum

period of one year. Before mounting on diffusion cells, skin samples were rehydrated for 10 min in physiological saline.

The reconstructed human skin **StrataTest**[®] was purchased from Stratatech. After arrival the constructs were transferred in 6-well plates with maintenance medium and incubated at 37°C, 5 % CO₂ and 95 % humidity overnight. For absorption studies the tissue samples were mounted on Franz-type diffusion cells. For experiments with testosterone and caffeine the skin constructs were transferred with and without the underlying membrane to compare its effect on absorption results. For studies with MCPA, tissue samples were either stored for 4 d at 8°C and 1 d under culture conditions or for 6 d under culture conditions, before removing from the underlying membrane and mounting on diffusion cells. On average, the tissue was 110 µm and the membrane 180 µm thick. For biotransformation studies, samples were removed from the membrane and homogenized as outlined in chapter 3.6.1.

The artificial stratum corneum surrogate **skin-PAMPA** was provided in 96-well plates by Pion. The samples were stored at 8°C until use (maximum 4 weeks).

3.4 Histological sections

For morphological investigations of different skin models, histological slices were prepared and stained with hematoxylin and eosin (H & E) as follows: Human and rat skin preparations were sliced in smaller pieces, transferred to histological cassettes and fixed with 4 % neutral buffered formalin. StrataTest[®] samples were embedded in high melting agarose before slicing and fixation. An established 19 h standard-protocol with a Tissue-Tek[®] VIP from Miles Scientific was used to embed the samples in paraffin. Therein ascending ethanol series (70 to 100 %) were used to dehydrate the tissue, xylene for replacing ethanol and fluid paraffin to replace xylene as well as to fix the samples for sectioning. From the hardened paraffin block slices of 2.5 µm thickness were prepared with a microtome, straighten on a microscope slide in warm water (40°C) and dried overnight at 50°C. The sections were stained with H & E following an established standard protocol after Lillie and Mayer with an automated tissue stainer (TST 44, Medite Medizintechnik) (Lillie 2012). Therefore, the histological sections were de-waxed with xylene and rehydrated with descending ethanol series (100 to 70 %) and water. Then immersion in hematoxylin solution, acidic ethanol solution (70 % ethanol, 1 % HCl (32 %)) and eosin solution (5 g/L in water) followed including washing steps in between. For hematoxylin solution 10 g hematoxylin were solved in 700 mL water and mixed with 100 g aluminium ammonium sulfate solved in 700 mL water. To this mixture 1 g sodium iodide, 40 mL ice-cold acetic acid and 600 mL glycerin were added. For preservation issues every slide was dehydrated again with alcohol and xylene and then sealed with a cover glass. After this procedure acidic structures like DNA in the nucleus were stained with hematoxylin and obtained a blue-violet color; basic structures like proteins in the cytoplasm or keratin were stained with eosin and obtained a red-pink color (Schrödel 2012). Paraffin embedding and staining with H&E was carried out by the Laboratory for Pathology of BASF SE.

3.5 Dermal absorption experiments in vitro

3.5.1 Solubility tests

Regarding OECD requirements, the solubility of penetrants in the receptor fluid must ensure solvation of at least 10 times the absorbed dose. If water – the receptor fluid of first choice – does not fulfill the requirement, addition of 5 % BSA or ethanol (up to 50 %) was considered. If no literature values were available (here: testosterone, MCPA-EHE), the solubility was determined with the flask method (OECD 1995): In a stepwise procedure, increasing volumes of solvent were added to 0.1 g test substance until complete solvation. Five times that soluble amount was mixed with solvent and shaken for 24 – 48 h at 32°C. Samples with MCPA-EHE were diluted 1/10, v/v, in ACN (acetonitrile), centrifuged at 4500 rpm for 10 min and the supernatants were measured by GC-MS (gas chromatography with mass spectrometry) and quantified via external calibration (method details see Table 2). Samples with testosterone were filtrated (0.2 µm), measured with HPLC-UV (high-performance liquid chromatography with ultraviolet detector) and quantified via external calibration (method details see Table 3). Each of three independent samples was measured in three chromatographic runs.

Table 2: GC-MS conditions for solubility measurement of MCPA-EHE. LOD: limit of detection; LOQ: limit of quantification.

capillary column	HP- 5MS 5 % phenylmethylsiloxane (30 m x 0.25 mm x 0.25 µm)
oven program	180°C, with 10°C/min to 210°C, 4 min at 210°C, with 10°C/min to 250°C, 2 min at 250°C
carrier	helium
flow [mL/min]/Split	1.1 / 20:1
injector temperature [°C]	250
transfer line temperature [°C]	280
solvent Delay [min]	2.00
MS quad temperature [°C]	150
MS source temperature [°C]	230
EM offset	0
SIM parameters	
resolution	low
plot 1 Ion	200
0 – 13 min	mass: 200.0, dwell: 100 mass: 312.2, dwell: 100
LOD [mg/L]	0.04
LOQ [mg/L]	0.12

3.5.2 Test substance preparation and control analyses

For absorption experiments with diffusion cells, the supplied ^{14}C -labeled stock solution of test substance was diluted in solvent and measured with the LSC (liquid scintillation counter) to determine the current specific radioactivity. The radiochemical purity was verified with HPLC-RAD (HPLC with radio detector). Respective solvents and HPLC conditions are listed in Table 3. Based on the results radiolabeled and non-radiolabeled test substance were mixed to achieve the intended specific activity and concentration. The following application solutions were prepared:

- 4 mg/mL ^{14}C -testosterone in ethanol/water (1/1, v/v), 1 MBq/mL:

Appropriate amounts of stock solution ^{14}C -testosterone in toluene and testosterone in ethanol (4 mg/mL) were evaporated to dryness under nitrogen and re-solved in ethanol/water (1/1, v/v).

- 4 mg/mL ^{14}C -caffeine in ethanol/water (1/1, v/v), 1 MBq/mL:

Appropriate amounts of stock solution ^{14}C -caffeine in ethanol and caffeine in ethanol (4 mg/mL) were evaporated to dryness under nitrogen and re-solved in ethanol/water (1/1, v/v).

- 9 mg/mL ^{14}C -MCPA as a DMA(dimethylamine)-salt-formulation in tap water, 3.7 MBq/mL:

13.5 g of DMA (60 %) were added slowly to 38.7 g MCPA under stirring. When all MCPA was dissolved, 125 mg EDTA and 5 mg of silicone antifoam emulsion were added. The pH was adjusted to 8.5 ± 1.0 with DMA (60 %) and the solution was made up to volume (50 mL) at 20°C . This concentrate was diluted 1/83 with tap water. The pH was adjusted to 8 ± 0.8 with HCl or NaOH. Appropriate amount of stock solution ^{14}C -MCPA in toluene was evaporated to dryness under nitrogen and re-solved with the prepared 1/83 dilution. To investigate repeated dosing regimen, a corresponding cold formulation (only unlabeled MCPA) and a blank formulation (without MCPA, DMA neutralized with HCl) were prepared.

- 16 mg/mL ^{14}C -MCPA-EHE as emulsion in water, 3.7 MBq/mL:

Appropriate amount of stock solution ^{14}C -MCPA-EHE in ACN was evaporated to dryness under nitrogen and re-solved in neat MCPA-EHE and water.

The obtained mixtures were treated with ultrasonic and stirred continuously until use. Homogeneity, stability, specific radioactivity and concentration of test substance were analyzed via LSC and HPLC-UV/RAD. HPLC-UV/RAD conditions are shown in Table 3.

For skin PAMPA, the concentrations of DMSO stock solutions were chosen accordingly to the water solubility and the UV activity of the test substances. Under assay conditions, the UV-signal of the samples should be in the linear detection range of the photometer. This was the case for 20 mM stock solutions of caffeine, testosterone and MCPA. No appropriate concentration of MCPA-EHE was feasible, due to too low water solubility and UV activity. 20 mM stock solutions of performance standards atenolol, chlorpromazine, niflumic acid, piroxicam, verapamil and warfarin and 30 mM stock solution of progesterone were used as suggested by the supplier Pion.

Table 3: HPLC-UV/RAD conditions for three test substances. A solid scintillator cell was used; eluent A was 5 ‰ formic acid in water, eluent B 5 ‰ formic acid in ACN and used complementary to eluent A; injection volume was 10 µL for all methods. LOD and LOQ were determined as described in chapter 3.8. LOD (0.75 kBq/mL) and LOQ (2.50 kBq/mL) for RAD detection were estimated with model compound ¹⁴C-MCPA-EHE.

	testosterone	caffeine	MCPA / MCPA-EHE
dilutions in	ACN	water	ACN
column	Luna C18, 5 µ, 250 x 3 mm	Synergi hydro RP, 4 µ, 250 x 3 mm	Gemini C18 3 µ, 50 x 2 mm
eluent/ gradient	40% A	85 % A	0 min: 5 % A 0 – 5 min: from 5 % to 95 % A 5 – 7.0 min: 95 % A, 7.0 – 7.1 min: from 5 % to 95 % A 7.1 – 12 min 5 %A
run time [min]	10	9	12
retention time (UV) [min]	5.1	6.8	MCPA: 5.9 MCPA-EHE: 7.9
flow [mL/min]	0.6	0.7	0.4
UV [nm]	245	273	228
RAD [nuclide]	¹⁴ C	¹⁴ C	¹⁴ C
LOD (UV) [mg/L]	0.001	0.001	0.004 / 2.0
LOQ (UV) [mg/L]	0.005	0.002	0.012 / 4.1

3.5.3 Diffusion cell experiments

3.5.3.1 Standard experiment (static)

Performance of dermal absorption experiments followed the OECD-Guideline 428 and the corresponding technical Guidance document 28 (OECD 2004a; OECD 2004b). Five skin samples per run were mounted on Franz-type diffusion cells with surface area of 1 cm² and a receptor volume of 4 mL (Figure 6 a). The water jacket around the receptor chamber was maintained at a temperature of 32°C with a water thermostat pump. A finite dose was applied on top of the skin under occlusive (Parafilm 'M'[®]) or semi-occlusive (Fixomull[®]) conditions. After the exposure time the substance was washed off with cotton swaps and washing fluid (0.7 % aqueous Texapon[®] N70 solution or ethanol/water, 1/1, v/v). During the entire experimental period of 24 h, samples were taken out of the stirred (450 rpm) receptor fluid at 8 – 12 time points and replaced with fresh receptor fluid by a fraction collector and a multi-channel peristaltic pump. At the end of the run each diffusion cell was dismantled and all parts were processed for balancing. Furthermore, tape strips were used to remove the upper stratum corneum from the skin samples. Each tape was pressed for 5 s on the SC of a skin preparation which was placed evenly, without wrinkles, on a Styrodur[®] block. Due to complete disruption of the tissue during stripping, this procedure was waived for StrataTest[®]. The tapes with stratum corneum and the remaining skin were digested separately with Soluene 350[®]; cotton swaps

as well as the class devices were extracted with ethanol or water – depending on the solubility of the test substance. All samples were diluted with LSC-cocktail and measured by LSC. Specific experimental conditions for ^{14}C -labeled caffeine, testosterone, MCPA, MCPA-EHE are listed in Table 4. The applied formulations were prepared as described in section 3.5.1. Individual experimental conditions on single cell level are listed in the annex (Table 45).

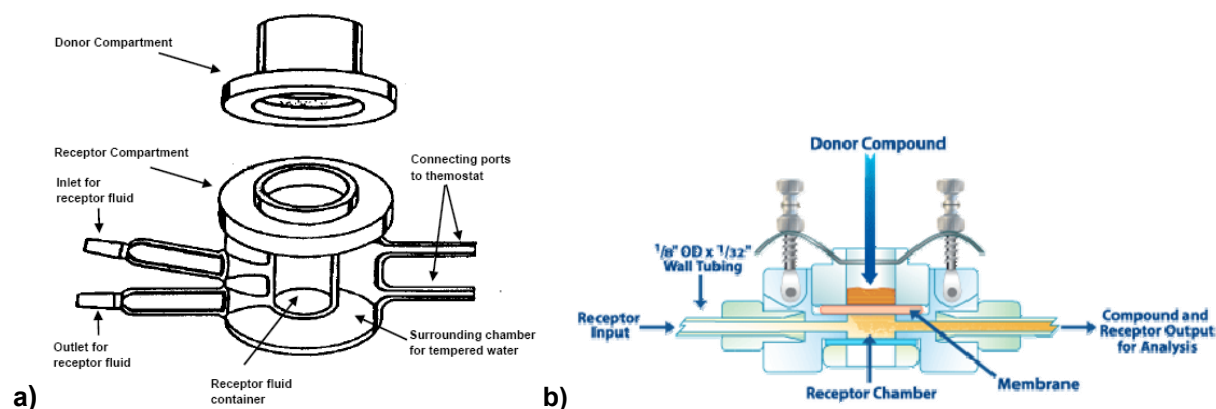


Figure 6: Diffusion cells for a) static and b) flow-through experiments (flow-through cell printed with permission from supplier PermGear (PermGear 2005)).

Table 4: General experimental conditions for the ^{14}C -labeled test substances testosterone, caffeine, MCPA and MCPA-EHE; conc: applied concentration; SRA: specific radioactivity; ARD: applied radioactive dose, vol: applied volume, time: exposure period until first washing / total experimental period; wash: washing fluid; Tex: 0.7 % aqueous Texapon[®] N70 solution, E/W: ethanol/water (1/1, v/v); (T)W: (filtrated tap) water; occ: occlusive; semi: semi-occlusive; extraction: solvent for extractions; tapes: number of tape strips.

test substance	conc [mg/mL]	SRA [MBq/mL]	Dose [$\mu\text{g}/\text{cm}^2$]	ARD [MBq/ cm^2]	vol [$\mu\text{L}/\text{cm}^2$]	time [h]	wash	receptor	covering	extraction	tapes
testosterone	4	1	100	0.025	25	24/24	E/W	5% BSA in TW	occ	ethanol	2
caffeine	4	1	100	0.025	25	24/24	E/W	TW	occ	water	2
MCPA	9	3.7	90	0.037	10	6/24	Tex	W	semi	ethanol	6
MCPA-EHE	16	3.7	160	0.037	10	6/24	Tex	W	semi	ethanol	6

3.5.3.2 Standard experiment (flow-through)

Flow-through experiments were carried out analogously to experiments under static conditions. The applied formulation, receptor fluid, exposure and experimental period, skin preparation, washing procedure and occlusion conditions were equal to static experiments; different were the diffusion cells (surface area: 1.1 cm^2 , receptor volume: $\sim 0.6 \text{ mL}$) (see Figure 6 b), the continuous receptor flow of 2.4 mL/h provided by a syringe pump and the use of a cell warmer. Experiments with ^{14}C -MCPA and

³H-testosterone were carried out under static as well as flow-through conditions to assess the impact of the experimental design.

3.5.3.3 Repeated dosing experiment

Dermal absorption experiments in vitro with repeated dosing regimen were conducted as static experiments following the general procedure outlined in chapter 3.5.3.1 and the following variations: Rat skin preparations – mounted on diffusion cells with physiological saline as receptor fluid – were treated with 10 µL so-called ‘cold’ MCPA formulation (DMA-formulation with unlabeled MCPA, 9 mg/mL) and washed thoroughly after 6 h on three following days. On the fourth day 10 µL ¹⁴C-MCPA formulation (0.037 MBq/mL, 9 mg/mL) were applied and the experiment was finished as a standard experiment (chapter 3.5.3.1). The receptor fluid was stirred over the entire experimental period (96 h) and exchanged every day. On day four it was replaced with water. For evaluation of time-, washing-, test substance- and formulation-specific effects several controls were added. Beside pretreatment with cold formulation, pretreatments with water or blank formulation (DMA-formulation without MCPA) were tested. And beside three washing steps during pretreatment, one or no washing procedure was conducted. Furthermore, untreated controls were added. One untreated control represented the standard experiment with an experimental period of 24 h and the second covers the effect of prolonged experimental time (72 + 24 h). The detailed regimen is listed in Table 5. Additionally, ³H-testosterone was present in the radiolabeled formulation as an internal standard.

3.5.3.4 Skin integrity testing

To ensure an exclusive use of undamaged skin for absorption studies and to compare the suitability of different skin integrity parameters, several skin integrity tests were evaluated in the current work. For comparison, at least two of the five following integrity tests were applied in one experiment to skin samples mounted on diffusion cells: TEER, TWF and TEWL in advance, ISTD concurrently and BLUE at the end of the run. In the case of pretreatment of the skin samples (compare the previous chapter 3.5.3.3), TEER was measured before and TEWL after the pretreatment. In addition visual abnormalities before or at the end of an experiment were recorded. Results outside the classical limit values for TEER, TWF and TEWL led to an exchange of these skin samples in advance of a routine experiment. For investigations concerning the suitability of different skin integrity tests and for experiments with repeated dosing regimen all skin samples were used independently of test results.

TEER: To measure the transepidermal electrical resistance to an alternating current (impedance), the receptor and donor compartment of the diffusion cell were filled with physiological saline (0.9 % aqueous NaCl solution). Electrodes were immersed in each compartment and the impedance was measured via a LCR bridge at a frequency of 1 kHz. The standard limit value was 1 kOhm.

TWF: To determine the absorption characteristics of water, the receptor compartment was filled with physiological saline. Purchased tritium-labeled water (PerkinElmer, (2056 MBq/mg)) was diluted with unlabeled water to 0.123 MBq/mL and applied as an infinite dose (300 µL/cm²) to the skin surface. At distinct time points (0.5, 1, 2, 3, 4 and 5 h) samples were taken out of the receptor fluid using a syringe.

Table 5: Repeated dosing regimen. 10 µL were applied for pretreatments with water, blank or cold formulation and 10 µL for the final absorption experiments with ¹⁴C-MCPA; washing procedure (wash) was conducted after exposure period of 6 h with 0.7 % aqueous Texapon® N70 solution.

experiment / pretreatment	none (standard, 24 h)	none, (72 + 24 h)	3x water, 0x wash	3x water, 1x wash	3x water, 3x wash	3x blank, 0x wash	3x blank, 3x wash	3x cold, 1x wash	3x cold, 3x wash
treatment day 1	---	mounting	mounting, water	mounting, water	mounting, water, wash	mounting, blank formulation	mounting, blank formulation, wash	mounting, cold formulation	mounting, cold formulation, wash
treatment day 2	---	---	water	water	water, wash	blank formulation	blank formulation, wash	cold formulation	cold formulation, wash
treatment day 3	---	---	water	water, wash	water, wash	blank formulation	blank formulation, wash	cold formulation, wash	cold formulation, wash
treatment day 4	mounting, ¹⁴ C-MCPA, wash	¹⁴ C-MCPA, wash	¹⁴ C-MCPA, wash	¹⁴ C-MCPA, wash	¹⁴ C-MCPA, wash	¹⁴ C-MCPA, wash	¹⁴ C-MCPA, wash	¹⁴ C-MCPA, wash	¹⁴ C-MCPA, wash
treatment day 5	end of run	end of run	end of run	end of run	end of run	end of run	end of run	end of run	end of run
non-radiolabeled dose [µg/cm²]	---	---	---	---	---	---	---	3 x 90	3 x 90
radiolabeled dose [µg/cm²]	90	90	90	90	90	90	90	90	90
total experimental period [h]	24	96	96	96	96	96	96	96	96

After the last sampling the skin was thoroughly washed with distilled water and cotton swaps. Kinetic samples were diluted with LSC-Cocktail, measured with the LSC and used to calculate K_p as described in section 3.5.3.5. A generally accepted limit value of $2.5 \cdot 10^{-3}$ cm/h was applied (Bronaugh et al. 1986). To remove the radioactivity from the system the receptor fluid was exchanged several times and the remaining radioactivity was measured every hour. Once a sample has an activity less than 50 dpm (0.8 Bq), the test substance was applied.

TEWL: The transepidermal water loss was measured after 1 – 3 hours of equilibration and drying of the skin sample. With the VapoMeter, the TEWL was determined under closed chamber conditions (Imhof et al. 2009). To this end the donor compartment of the diffusion cell was covered precisely with the VapoMeter. A standard threshold of 10 g/(m²·h) was used considering own historical data and observations from Schaefer and Redelmeier (Schaefer & Redelmeier 1996b).

ISTD: A tritium labeled internal standard was applied to the skin with the test substance formulation. Used ISTDs including physicochemical properties are listed in Table 6. The concentration was determined by the specific radioactivity which was chosen to be equal to the ¹⁴C-activity of the test substance. ³H-activity in all samples was measured along with the ¹⁴C-activity by LSC. Absorption characteristics (AD and maxKp) were determined as described in section 3.5.3.5.

Table 6: Used ³H-labeled internal standards (ISTD) for dermal absorption experiments with ¹⁴C-labeled test compounds. Given are specific radioactivities of supplied standard solution (SAR) including supplier as well as physicochemical properties (logP_{ow}, MW and S_w, water solubility). Furthermore it is indicated in which experiments the ISTDs were used (details in annex, Table 45).

³ H-ISTD	SAR [MBq/mg]	supplier	logP _{ow}	MW [g/mol]	S _w [g/L]	used with ¹⁴ C-compound
testosterone	21 845	PerkinElmer	3.32 ¹	288,4	0,02 (25°C) ¹	caffeine, MCPA, MCPA-EHE
caffeine	11 432	PerkinElmer	-0.07 ²	194,2	20 (20°C) ²	testosterone
mannitol	2 503	American Radiolabeled Chemicals	-3,1 ³	182,17	182.2 (20°C) ⁴	caffeine, testosterone

¹ (Yalkowsky et al. 1983)

² (Merck 2006a)

³ (Leo et al. 1971)

⁴ (Sigma-Aldrich 2007)

BLUE: 250 µL of a 0.025 % aqueous methylene blue solution was applied topically to the skin for 0.5 h. The skin was thoroughly washed with 0.7 % aqueous Texapon® N70 solution and the dye concentration in the receptor fluid was measured with a photometer at 661 nm. The absorbed amount of BLUE was determined by external calibration. Any staining of the skin sample was reported.

To evaluate the different skin integrity tests, two procedures were used in general. Firstly, valid and invalid excised and reconstructed human skin samples were differentiated according to standard

thresholds for TEWL, TWF and TEER (10 g/(m²*h), 2.5*10⁻³ cm/h and 1 kOhm, respectively) and one modified value for each test (13 g/(m²*h), 4.5*10⁻³ cm/h and 2 kOhm, respectively). Then the minimum, maximum and mean absorption results for each test substance (maxKp and AD) were calculated separately for the defined valid and invalid groups. Additionally, single diffusion cell results for the defined valid and invalid skin samples were plotted. Secondly, all experiments with the same test substance (¹⁴C-testosterone, ¹⁴C-caffeine, ¹⁴C-MCPA or ¹⁴C-MCPA-EHE) and the same barrier systems (human, rat or StrataTest[®]) were grouped together. Experiments with at least 10 single data points were used to run linear regression analysis for the integrity test results versus absorption results (AD or maxKp). Slopes and coefficients of determination (R²) were reported. Minimum, maximum and mean values were calculated for each integrity test, but only R² from correlations with the correct algebraic sign were used.

To verify the ISTD approach, co-analytics and co-absorption of ISTD and test compound were investigated. Co-analytics of ³H- and ¹⁴C-analytics were investigated by measuring ¹⁴C-testosterone standards by LSC in the presence and absence of ³H-testosterone and vice versa. High and low levels of matrix isotope were used (on average 12667 and 242 Bq/g for ³H and 1288 and 587 Bq/g for ¹⁴C). Linear regressions were calculated to evaluate potential influences. Absorption characteristics of test substances in presence and absence of an internal standard were checked for three compounds under equal experimental conditions: ¹⁴C-MCPA and ¹⁴C-caffeine in presence and absence of ³H-testosterone; ¹⁴C-testosterone in presence and absence of ³H-caffeine.

3.5.3.5 Data analyses

Mass balance

A single experiment (one diffusion cell) with a total recovery (mass balance) of 100 ± 10 % of ¹⁴C-activity was assessed to be valid for mean calculations. As a first step to determine the mass balance (R_{%total}), the totally applied radioactive dose (R_{appl}) was calculated using the specific radioactivity (SRA_{appl,total}) and absolute weight (W_{appl}) of the applied formulation:

$$\text{Equation 15: } R_{appl} [Bq] = SRA_{appl,total} [Bq / g] * W_{appl} [g]$$

The measured activity (R_{aliqu,i}) in an aliquot with distinct weight (W_{aliqu,i}) of a single sample i was used to calculate the concentration of radioactivity (R_{conc,i}) in that sample i:

$$\text{Equation 16: } R_{conc,i} [Bq / g] = R_{aliqu,i} [Bq] / W_{aliqu,i} [g]$$

The total radioactivity in sample i (R_{total,i}) was determined from the total weight of this sample i (W_{total,i}):

$$\text{Equation 17: } R_{total,i} [Bq] = R_{conc,i} [Bq / g] * W_{total,i} [g]$$

The recovery of the applied radioactivity in sample i (R_{%i}) was calculated as follows:

$$\text{Equation 18: } R_{\%,i} [\%] = R_{total,i} [Bq] / R_{appl} [Bq] * 100$$

The total recovery R_{%total} was the sum of all samples i of the same diffusion cell:

$$\text{Equation 19: } R_{\%,total} = \sum R_{\%,i}$$

Regarded as 'not absorbed' were samples of skin wash, tape stripping and donor compartment extracts. Tape strips were considered as not absorbed for the current work, since they account for the in vivo existing process of desquamation. Regarded as 'absorbed' or named as 'content in the receptor' was the sum of kinetic samples, receptor fluid, extracts of receptor compartment and, if present, the content in the membrane from StrataTest® constructs. Defined as 'potentially absorbable dose' (AD) was the sum of these samples plus the recovery in the skin extract ('content in the skin') – which is the whole skin preparation without the stripped off SC.

To determine the concentration of total test substance – or better concentration equivalents (eq) – in a sample *i* ($C_{subst,i}$) the specific radioactivity of test substance in the applied formulation ($SRA_{subst,appl}$) was used. $C_{subst,appl}$ was the concentration of test substance in the formulation:

$$\text{Equation 20: } SRA_{subst,appl} [Bq / mg] = SRA_{appl,total} [Bq / g] / C_{subst,appl} [mg / g]$$

$$\text{Equation 21: } C_{subst,i} [\mu g_{eq} / g] = R_{conc,i} [Bq / g] / SRA_{subst,appl} [Bq / mg] * 1000$$

The absolute amount of test substance in sample *i* ($D_{subst,i}$) was calculated as follows:

$$\text{Equation 22: } D_{subst,i} [\mu g] = C_{subst,i} [\mu g / g] * W_{absol,i} [g]$$

Kinetics

Calculation of absorption kinetics is based on absorption-time-profiles (theoretical background for infinite and finite dose regimen is outlined in section 1.4.2). Under finite dose regimen – which was used for the ¹⁴C-labeled test substance and ³H-labeled ISTD – the cumulated absorbed dose at time point *t* ($D_{cum}(t)$) is the sum of the compound in the receptor compartment at this time point plus the compound removed with former samples. Under static conditions Equation 23 consists of four terms:

- cumulated absorbed dose at time point *t*-1 ($D_{cum}(t-1)$)
- difference of absolute amount in receptor fluid in diffusion cell at time point *t* ($D_{absol,rec,t}$) and time point *t*-1 ($D_{absol,rec,t-1}$)
- amount in sampled receptor aliquot of time point *t*-1 ($D_{aliqu,rec,t-1}$)
- amount in tube rinse at time point *t*-1 ($D_{rinse,t-1}$)

Terms two and three were calculated with Equation 22. The total weight of 4 mL receptor fluid in the diffusion cell was defined independently from the density of the receptor fluid as 4 g. For term four the total weight of pooled rinsing samples (W_{rinse}) was divided by the number of time points ($\psi_{time\ points}$) and multiplied with the concentration of the receptor sample at time point *t*-2 ($C_{subst,rec,t-2}$) (Equation 24). $C_{subst,rec,t-2}$ represents the concentration in the tube at sampling time point *t*-1.

Equation 23:

$$D_{cum}(t)[\mu g] = D_{cum}(t-1)[\mu g] + (D_{absol,rec,t}[\mu g] - D_{absol,rec,t-1}[\mu g]) + D_{rec,aliqu,t-1}[\mu g] + D_{rinse,t-1}[\mu g]$$

Equation 24: $D_{rinse,t-1}[\mu g] = C_{subst,rec,t-2}[\mu g / g] * W_{rinse}[g] / \psi_{timepoints}$

The cumulated absorbed dose per skin area (A, here 1 cm²), was plotted against the time. The steepest slope – J_{max} or here maxAR – divided by the applied concentration provides the maximum permeability coefficient maxKp:

Equation 25: $\max Kp[cm / h] = \max AR[\mu g / (cm^2 * h)] / C_{subst,appl}[\mu g / cm^3]$

The intercept of the elongated steepest slope line with the x-axis represents the lag time [h]. The kinetics for the infinite dose regimen – which was used for integrity test TWF – is calculated slightly different: Samples were taken directly at the outlet of the diffusion cell, so that term four of Equation 23 is redundant. Furthermore the slope in the linear range represents AR and provides Kp after division with the concentration. For flow-through experiments (finite dose) kinetic values were determined similar, but the cumulated absorbed dose was calculated by adding the samples of distinct periods and for determination of maxAR the cumulated absorbed dose was plotted against the mean time of the sampling period.

3.5.4 Skin-PAMPA

The skin-PAMPA assay was conducted in accordance with the instructions from the supplier Pion and is briefly outlined in the following. Prisma HT and hydration buffer were delivered ready to use by Pion.

The prepared stock solution of test substance in DMSO and DMSO as the solvent control were diluted 1/20 with prisma HT buffer (2.5 % prisma HT buffer concentrate in water, adjusted with NaOH or HCl to pH 6.5 and 7.4). Both buffers (pH 6.5 and 7.4) were applied by default for all tested compounds (performance standards and model substrates). MCPA stock solution was additionally diluted with prisma HT buffer at pH 4.5. 200 µL of each test substance solution were transferred in sextuplicate in the donor plate of the skin-PAMPA sandwich. 200 µL receptor fluid (prisma HT buffer pH 7.4) were filled in the coated receptor plate, which was previously hydrated (overnight) in hydration buffer. Then the sandwich was built with donor and receptor plate. After incubation for 5 h, the plates were separated and donor and receptor phase were transferred into high sensitivity UV plates. UV-scans from 230 to 500 nm with 4 nm steps were run for each sample with a photometer. Prisma HT buffer at applied pH values was measured analogously as blank and each substance solution in buffer as a reference. For analyses with PAMPA Explorer software it was recommended to have corresponding samples (blank, reference, donor, receptor) for each substance/buffer combination at the same well position of the 96-well plates. With the software, the absorption maximum was identified, solvent effects subtracted and remaining test substance in donor and absorbed amount in the receptor fluid was determined in relation to the reference ('single point calibration'). Based on the surface area (0.3 cm²) and the receptor volume (0.2 mL), the software calculated the effective Kp [*10⁻⁵cm/h] and the membrane retention [%] (Pion 2012; Sinko et al. 2012). If no substance was detected in the receptor fluid, Kp was set to 0.036*10⁻⁵cm/h.

3.6 Metabolic activity of skin models

3.6.1 Subcellular fractions

S9 fraction was prepared from human skin, StrataTest[®] constructs and rat liver; cytosol and microsomes from StrataTest[®] and rat liver. Human skin was derived from two different female donors with age of 33 and 68 years and cryoconserved until use. Rat liver was excised from male Crl:WI (Han) rats (Charles River, Germany) with about 440 g body weight, which were previously treated with Aroclor 1254 (ChemService, West Chester, PA, USA, 500 mg/kg body weight i.p., 5 days), anesthetized with isoflurane and sacrificed. Aroclor 1254 is an industrially produced mix of PCBs (polychlorinated biphenyls), which contains 54 % chlorine by mass. It was applied to induce xenobiotic-metabolizing enzymes in the liver (U.S.Department of Health and Human Services.Public Health Service Agency for Toxic Substances and Disease Registry).

The subcellular fractions were prepared at $\leq 4^{\circ}\text{C}$ to guarantee optimal enzyme activities. Used buffers are listed in Table 7. Liver or skin samples were minced, mixed with an appropriate volume of respective homogenization buffer and homogenized with a potter. Volumes of buffer were estimated to obtain a protein concentration higher than 1 mg/mL. For rat liver three times, for human skin two times and for StrataTest[®] half the tissue weight were appropriate. After treatment with ultrasonic probe, cell debris was pelleted at 9000 g for 15 min. The supernatant – the S9 fraction – was used for biotransformation studies or to prepare microsomes and cytosol. For the latter it was ultra-centrifuged at 100 000 g for 1 h. The supernatant – the cytosol – was transferred in new vials. The pellet was re-suspended in washing buffer and ultra-centrifuged again at 100 000 g for 1 h. The supernatant was discarded and the pellet re-suspended in resuspension buffer. To obtain protein concentrations higher than 1 mg/mL, 1 mL buffer per g original weight of rat liver tissue and 0.2 mL per g StrataTest[®] tissue were appropriate. The obtained preparations (S9 fraction, cytosol and microsomes) were stored at -80°C until use (maximum one year).

Table 7: Buffers for the preparation of subcellular fractions

homogenization buffer (for skin models)	50 mM Tris
	1 mM DTT
	pH 7.5 (HCl)
homogenization buffer (for rat liver)	250 mM saccharose
	1 mM EDTA-Na ₂
washing buffer	150 mM KCl
resuspension buffer	0.308 g/mL glutathione (reduced)
	0.732 g/mL EDTA-Na ₂
	0.816 g/mL MgCl ₂ *6H ₂ O
	13.6 g/mL KH ₂ PO ₄
	200 mL/mL glycerol (20 % in water)
	pH 7.5 (NaOH)

Protein concentrations of the subcellular preparations were determined with the Bradford assay according to the manufacturer's protocol: 5 μ L neat sample as well as dilutions in respective matrix (1/2, 1/5, 1/10, v/v) were transferred in 96-well plates in triplicates and mixed with 250 μ L Bradford reagent. After incubation for 10 min under shaking and exclusion of light, the samples were measured at 595 nm photometrically. Additionally, blanks and standard solutions of 10 – 2000 μ g/mL BSA (bovine serum albumin) were processed analogously for external calibration. Dilutions within the linear range of the calibration curve were used to calculate the protein concentration. Based on the obtained results, the samples were normalized to 1 mg protein/mL and verified by a second Bradford assay. Heat-deactivated samples (HDC) were prepared as controls for unspecific protein binding by heating and shaking (99°C, 450 rpm) for 10 min.

3.6.2 Biotransformation of MCPA-EHE in human skin

3.6.2.1 Chemical stability

To determine the chemical stability of MCPA-EHE in water, a stock solution of 14 C-MCPA-EHE in ACN was diluted in water and analyzed for its concentration and possible degradation products with HPLC-UV/RAD after distinct time points over a period of 96 h (conditions see 3.5.1). Over the entire period the mix was stirred. Before injection in the HPLC, the mix was diluted with ACN at a ratio 1:1 (v/v). Considering the LOD of 0.75 kBq/mL for HPLC-RAD detection, a concentration of 41.7 kBq/mL (0.013 mg/mL) was chosen to allow the detection of potential degradation products with amounts ≥ 2 %. The content of ACN was therefore 0.3 %. The recovery of the substrate was calculated in two ways: firstly, based on RAD detection and relating peak areas at later time points to peak areas at time point zero and secondly, based on UV detection and relating concentrations – determined via external calibration – at later time points to the concentration at time point zero. To evaluate a possible loss through evaporation, 14 C-MCPA-EHE solution in ACN (36 kBq/mL, 0.011 mg/mL) was evaporated to dryness under nitrogen and resolved in ACN afterwards. The resistance against evaporation was determined by comparing the radiochromatograms from samples before and after evaporation.

3.6.2.2 In vitro biotransformation in human skin S9 fraction

General esterase activity in S9 fraction derived from cryoconserved human skin (obtained from two different donors) was examined with model substrate fluorescein diacetate as described in chapter 3.6.3. Furthermore, abiotic and biotic breakdown of model substrate 14 C-MCPA-EHE was investigated in human skin S9 fraction. For actual substrate incubations (AI) normalized S9 fraction (1 mg/mL) was mixed with phosphate buffer, 14 C-MCPA-EHE standard in water, NADPH mix and glutathione solution and incubated for 30 min at 37°C and 450 rpm in a thermomixer. Reaction vessels were wrapped with Parafilm 'M'[®] to avoid evaporation. To stop the reaction 1 volume of acetone was added. To distinguish between abiotic and biotic breakdown and detect unspecific protein binding, several controls were processed in a similar manner: heat-deactivated control (HDC), immediately stopped control (t_0) and buffer control without S9 fraction (BC). Individual incubation mixes and composition of reagents are shown in detail in Table 8 a and b. After stopping, the samples were centrifuged at 4600 rpm for 10 min. 14 C-MCPA-EHE and degradation products in the supernatant were determined with HPLC-UV/RAD (using method for MCPA described in section 3.5.2). Standards of

MCPA-EHE, ^{14}C -MCPA-EHE, MCPA, ^{14}C -MCPA and HMCPA were measured along with the samples. The radioactive concentration in the incubation solution was nominal 12.5 kBq/mL (^{14}C -MCPA-EHE) and the total MCPA-EHE concentration 0.065 mg/mL. Considering the dilution with acetone and the LOD of 0.75 kBq/mL for HPLC-RAD measurements of ^{14}C -activity, products with amounts $\geq 6\%$ were detectable. Recovery of radioactivity was calculated in relation to BC. Rat liver S9 fraction was incubated in parallel as a positive control for general assay functionality and substrate testosterone was added as a positive control for CYP-dependent biotransformation (0.2 mM in incubation solution).

Table 8: Metabolic breakdown of ^{14}C -MCPA-EHE in S9 fraction. a) Reagents and b) S9 fraction incubations including processing. AI: actual substrate incubation, HDC: heat-deactivated control, t_0 : immediately stopped substrate incubation, BC: buffer control.

a)

NADPH mix	131 mg/mL glucose-6-phosphate
	33.3 mg/mL NADPH
	142.9 $\mu\text{L}/\text{mL}$ MgCl_2 (1 M in water)
	200 $\mu\text{L}/\text{mL}$ glucose-6-phosphate-dehydrogenase (0.7 U/ μL)
phosphate buffer	500 mL KH_2PO_4 (0.1 M in water)
	pH 7.4 (K_2HPO_4 , 0.1 M)

b)

	AI	HDC	t_0	BC
phosphate buffer, pH 7.4 [μL]	167.5	167.5	167.5	237.5
^{14}C-MCPA-EHE in water (1 Mq/mL, 5.2 mg/mL) [μL]	6.25	6.25	6.25	6.25
40 mM glutathione in phosphate buffer pH 7.4 [μL]	6.25	6.25	6.25	6.25
S9 fraction [μL]	62.5	-	62.5	-
heat-deactivated S9 fraction [μL]	-	62.5	-	-
NADPH mix [μL]	7.5	7.5	7.5	-
acetone (stops reaction) [μL]	250	250	250	250
incubation time [h]	0.5	0.5	-	-

3.6.2.3 In vitro biotransformation in human skin during absorption experiments

To determine if and where MCPA-EHE hydrolysis occurs during permeation through skin, DMS and FTS from the same human donor (female, 68 years) were incubated with ^{14}C -MCPA-EHE under standard experimental conditions (static) as outlined in chapter 3.5.3.1, but with the following variations: a higher radioactive concentration (8.2 MBq/g) was applied, washing was performed with water and the skin samples were homogenized with a potter in homogenization buffer (composition see Table 7). Additionally, kinetic sampling and tape stripping were waived. All samples were measured with the LSC for mass balance. Then samples were grouped to four representative sections of dermal uptake in vitro: application solution, washing fluid, skin and receptor. To gain four HPLC compatible solutions for each skin preparation, the samples were processed as follows:

- The application solution was diluted in ACN at the ratio 1:10.

- The washing fluids after 6 and 24 h including cotton swaps and pipette tips were combined directly and extracted together with about 120 mL ethanol. This extract plus the ethanol rinsing of the diffusion cell donor compartment and the covering were merged and concentrated by evaporation. The cotton swaps and pipette tips were extracted a second time with ethanol, two times with ethyl acetate and two times with dichloromethane (120 mL each time). These extracts were successively added to the former and evaporated to dryness. Acidic water (~pH 1.5, 60 mL) was added to the cotton swaps and pipette tips; the obtained mixture was shaken overnight, treated with ultrasonic several times and extracted two times each with ethyl acetate and dichloromethane (about 60 mL). The extracts were pooled, the pH of the aqueous phase adjusted to ~pH 7 and evaporated to about 1 mL. The pH was checked regularly – and if necessary adjusted – during concentrating. The concentrate was added to the former dried residual and evaporated to dryness. The radioactive residue was re-solved in about 10 mL ACN.

- The aqueous skin homogenates were extracted three times each with ethyl acetate and dichloromethane (~15 mL). The organic phases were collected and evaporated successively. The aqueous homogenate was acidified to ~pH 1.5 with HCl and extracted with ethyl acetate and dichloromethane. The extracts were pooled, the pH adjusted to ~pH 7 and evaporated to ~1 mL. The pH was checked regularly – and if necessary adjusted – during the concentration process. The concentrate was added to the former extracts and evaporated to dryness. The radioactive residue was re-solved in about 0.25 mL ACN.

- The ethanol rinsing of the receptor compartment was evaporated to ~1 mL and added to the receptor fluid sample. This mixture was evaporated to dryness and re-solved in about 0.5 mL ACN.

In general, solvent amounts smaller than 10 mL were dried with a vacuum concentrator and larger amounts with a rotary evaporator. The temperature was kept lower than 38°C for all experimental steps. Acidification of aqueous samples facilitated organic extraction of MCPA, since it was present in its uncharged form. MCPA-EHE was extracted under neutral conditions in advance. To avoid an acidic hydrolysis of the ester after pooling neutral and acidic extracts together, the pH was adjusted constantly to about 7. The final four samples were clarified – if necessary – by centrifugation or filtration and separated via HPLC (conditions see Table 9). Samples were detected with UV/RAD, but due to low sensitivity, the eluent was collected after passing the detectors in one minute fractions, diluted with LSC-cocktail and measured by LSC. Out of the resulting values, the radiochromatograms were reconstructed. LOD and LOQ of LSC measurement were determined with the solvent ACN as described in section 3.8 as 0.6 and 0.9 Bq, respectively, for each one-minute fraction of 0.8 ml. The coefficient of variation, CV, defined as the ratio of the standard deviation (SD) to the mean, was 0.3. Considering specific activity and molecular weight of the parent ^{14}C -MCPA-EHE and the injection volume of 25 μl , 0.03 and 0.04 μM ^{14}C -labeled compound could be detected and quantified in the solutions, respectively. Total recoveries in extracts were calculated in relation to the samples before extraction.

Table 9: HPLC-UV/RAD conditions for analysis of ¹⁴C-MCPA-EHE and degradation products; a solid scintillator cell was used.

column	Synergi Hydro RP 4 μ, 250 mm x 3 mm
eluent	A: 5 ‰ formic acid in water, B: 5 ‰ formic acid in ACN
gradient	0 min: 5 % A 0 – 20 min: from 5 % A to 95 % A 20 – 38 min: 5 % A 38 – 40.1 min: from 5 % A to 95 % A 40.1 – 45 min: 95 % A
flow [mL/min]	0.8
Injection volume [μL]	25
retention time (UV) [min]	HMCPA: 12.7 MCPA: 15.5 MCPA-EHE: 24.4
UV [nm]	280
RAD [nuclide]	¹⁴ C

3.6.3 Xenobiotic-metabolizing enzyme activities in skin construct StrataTest[®]

Different enzyme activities were determined in subcellular fractions of three different batches of the StrataTest[®] skin construct along with subcellular fractions of rat liver from one donor as the positive control. 1 mg/mL normalized samples were applied in duplicates or triplicates. As an exception rat liver S9 with 0.1 mg/mL was used for esterase activity assays.

In general, the turn-over of an enzyme-specific model substrate was determined. Specific substrates for the investigated enzymes are listed in Table 10. Formation of product or respective co-enzyme per volume (Δconc) was measured and transformed into absolute amount with volume (V) and dilution factor (F) and related to assay time (t) and protein content (p) as follows:

$$\text{Equation 26: } \text{activity}[\text{nmol}/(\text{min} \cdot \text{mg})] = \frac{\Delta\text{conc}[\frac{\text{nmol}}{\text{mL}}] * F * V[\text{mL}]}{t[\text{min}] * p[\text{mg}]}$$

The results were stated in nmol/(min*mg). As an exception, UGT 2 activity was given in Δ fluorescence units/(mg*min), since a standard for the glucuronidated product was not available. General assay performances were based on literature (shown in Table 10) and conducted as described recently in Jaeckh et al. and Henkler et al, but are briefly described in the following (Henkler et al. 2012; Jaeckh et al. 2011). LOD and LOQ of the single assays were determined as described in chapter 3.8 and are given alongside the results in chapter 3.6.3.

Table 10: Overview of performed enzyme activity assays. Shown are subcellular fractions (S9: S9 fraction, C: cytosol and M: microsomes) and model substrates used for the assay as well as basic literature about assay performance and substrate specificity. With exception of fluorescein diacetate, which is sensitive to a broad range of hydrolyzing enzymes, the other listed substrates were specific for the named isoforms.

enzyme	subcellular fraction	substrate	Literature
N-acetyltransferase 1 (NAT 1)	S9	para-aminobenzoic acid (PABA)	(Kawakubo et al. 1988; Minchin et al. 1992; Ohsako & Deguchi 1990)
esterase (e. g. lipase, acylase)	S9	fluorescein diacetate	(Guilbault & Kramer 1964; Karmazsin et al. 1979)
alcohol dehydrogenase (ADH)	C	ethanol	(Blair & Vallee 1966; Kawashima et al. 2011; Li 1977)
aldehyde dehydrogenase (AIDH)	C	propionaldehyde	(Jones & Lubet 1992; Lindahl & Evces 1984a; Lindahl & Evces 1984b)
flavin-dependent monooxygenase 1/3 (FMO 1/3)	M	benzylamine (BA)	(Kawaji et al. 1993; Yeung & Rettie 2006)
cytochrome P450 isoenzymes (EROD/PROD/BROD)¹	M	ethoxy-/ pentoxy-/ benzyloxyresorufin (ER/PR/BR)	(Burke et al. 1985; Burke et al. 1994; Jaeckh et al. 2011)
UDP-glucuronosyl-transferase 1	M	4-methylumbelliferone (MUF)	(Lilienblum et al. 1982; Wishart 1978)
UDP-glucuronosyl-transferase 2	M	4-hydroxybiphenyl (HOBI)	(Bock et al. 1979)

¹ EROD: CYP isoform with ethoxyresorufin-O-deethylase activity inducible with 3-methylcholanthrene, mainly CYP 1A, PROD: CYP isoform with pentoxyresorufin-O-deethylase activity inducible with phenobarbital, mainly CYP 2B, BROD: CYP isoform with benzyloxyresorufin-O-debenzylase activity inducible with 3-methylcholanthrene and phenobarbital, mainly CYP 1A/2B/3A

NAT 1 activity was determined with specific model substrate para-aminobenzoic acid (PABA) and calculated by formation of acetylated PABA (acPABA). 25 µL of S9 fraction were incubated with 10 µL PABA (12.5 mM in DMSO), 185 µL TrisHCl buffer (50mM, pH 7.5), 25 µL acetyl-CoA (4 mg/mL in TrisHCl buffer), 2.5 µL DTT (100 mM in TrisHCl buffer) and 2.5 µL EDTA (100 mM in TrisHCl buffer) for 30 min at 37°C and 450 rpm in a thermomixer. The reaction was stopped with one volume (250 µL) of perchloric acid on ice. Heat-deactivated (HDC) and buffer (BC) control were prepared analogously with heat-deactivated S9 fraction and buffer instead of S9 fraction. The supernatant – after centrifugation for 5 min at 10 000 g – was measured with HPLC-UV (conditions see Table 11). The concentration of generated product was determined via external calibration with acPABA standards from 1 to 100 µM in the corresponding matrix. Due to instability of the enzyme, its activity was measured directly after preparation of S9 fraction (Henkler et al. 2012).

Table 11: HPLC-UV and HPLC-UV/FLD conditions for acPABA and BA-nOx, respectively. The methods belong to the enzyme activity assays for NAT 1 and FMO 1/3, respectively. LOD and LOQ were determined as described in chapter 3.8. Injection volume was 10 μ L.

	acPABA	BA-nOx
column	Nucleosil 120-5, 5 μ , 250 x 4 mm	Hypersil CN, 5 μ , 250 x 4 mm
eluent / isocratic	80 % water with 5 ‰ formic acid 20 % ACN with 5 ‰ formic acid	ACN/methanol/ KH_2PO_4 buffer (0.01 M, pH 7) 4/1/2.7 (v/v/v)
flow [mL/min]	1	1.5
run time [min]	8	15
retention time (UV) [min]	5.3	3.3
UV [nm]	263	200
FLD λ_{ex} [nm]	-	305
λ_{em} [nm]	-	375
LOD [μM]	0.013	0.0013
LOQ [μM]	0.043	0.0004

Esterase activity was determined with the model substrate fluorescein diacetate and calculated via formation of fluorescein. The used substrate is sensitive to various hydrolyzing enzymes, such as lipase, acylase and chymotrypsin (Guilbault & Kramer 1964). 30 μ L of S9 fraction were incubated with 170 μ L of fluorescein diacetate (0.06 mM in TrisHCl buffer, 100 mM, pH 8) in a black 96-well plate. The fluorescence of the product fluorescein was measured over 15 min in 1 min steps with excitation wavelength λ_{ex} 490 nm and emission wavelength λ_{em} 514 nm at 37°C with a photometer. In parallel, HDC and BC as well as fluorescein standards of 25 to 3000 nM were measured for external calibration. The linear time period for each sample was chosen to calculate formation rate of fluorescein.

ADH activity was determined with model substrate ethanol and calculated by formation of co-enzyme NADH. Further oxidation and NADH formation by AIDH activity was prevented by depletion of product acetaldehyde with semicarbazide. 25 μ L of cytosol were incubated with 25 μ L ethanol (100 mM in pyrophosphate buffer II), 175 μ L pyrophosphate buffer I and 25 μ L NAD^+ (28 mM in pyrophosphate buffer I) in a 96-well plate (for buffer composition see Table 12). Absorption of co-enzyme NADH was measured for 10 min in 1 min steps at wavelength 340 nm and 37°C with a photometer. Production of NADH was calculated in the linear time period for each sample with an external calibration from 5 to 500 μ M. In addition to HDC and BC, a matrix control with buffer instead of substrate (MC) was prepared in parallel and subtracted as background from the active incubation.

AIDH activity was determined with model substrate propionaldehyde and calculated by formation of co-enzyme NADH. Enzymatic reduction to propanol and consumption of NADH was prevented by adding ADH-inhibitor 4-methylpyrrazole. 25 μ L cytosol were incubated with 150 μ L pyrophosphate buffer III (see Table 12), 25 μ L propionaldehyde (50mM in pyrophosphate buffer III), 25 μ L 4-methylpyrrazole and 25 μ L NAD^+ (10 mM in pyrophosphate buffer III) in a 96-well plate. Absorption of

NADH was measured for 20 min in 1 min steps at wavelength 340 nm and at 37°C with a photometer. Production of NADH was calculated in the linear time period for each sample with an external calibration from 5 to 500 µM. In addition to HDC and BC, MC was prepared in parallel and subtracted from the active incubation.

Table 12: Buffers for ADH and AIDH activity assays

pyrophosphate buffer I	66.6 mM pyrophosphate
	11.25 mM glycine
	100 mM semicarbazide
	15 mM glutathione
	pH 9 (NaOH)
pyrophosphate buffer II	66.6 mM pyrophosphate
	pH 9 (NaOH)
pyrophosphate buffer III	88.9 mM pyrophosphate
	pH 8.8 (NaOH)

FMO 1/3 activity was determined with specific model substrate benzydamine (BA) and calculated by formation of benzydamine-n-oxide (BA-nOx). 10 µL microsomal fraction were incubated with 33 µL TrisHCl buffer (100 mM, pH 8.5), 5 µL BA (100 mM in water), 1 µL EDTA (100mM in water), 1 µL DTT (100 mM in water) and 50 µL NADPH (20 mM in TrisHCl buffer) for 30 min at 37°C and 450 rpm in a thermomixer. The reaction was stopped with one volume (100 µL) of acetone on ice. HDC and BC controls were prepared in parallel. The supernatant – after centrifugation for 5 min at 10 000 g – was measured with HPLC-UV/FLD (HPLC with UV and fluorescence detector) (conditions see Table 11) and the concentration was determined via external calibration with BA-nOx standards from 0.1 to 25 µM in the corresponding matrix. HDC was subtracted as background from the active incubation.

Activity of **CYP 450 isoforms** with ethoxyresorufin-O-deethylase (EROD) activity inducible via 3-methylcholanthrene (mainly CYP 1A) was determined with specific model substrate ethoxyresorufin (ER), activity of CYP 450 isoforms with pentoxyresorufin-O-deethylase (PROD) activity inducible via phenobarbital (mainly CYP 2B) with pentoxyresorufin (PR) and CYP 450 isoforms with benzyloxyresorufin-O-debenzylase (BROD) activity inducible via 3-methylcholanthrene and phenobarbital with benzyloxyresorufin (BR). The activities were determined by measuring formation of resorufin. 10 µL microsomal fraction were incubated with 74.5 µL TrisHCl buffer (100 mM, pH 7.5), 5 µL MgCl₂ (200 mM in TrisHCl buffer), 1 µL 5'-AMP (200 mM in TrisHCl buffer), 1 µL glucose-6-phosphate (500 mM in TrisHCl buffer), 1.5 µL glucose-6-phosphate-dehydrogenase (0.7 U/µL in water), 1 µL dicoumarol (1 mM in TrisHCl buffer) and 1 µL substrate (0.2 mM EROD, 1 mM PROD or 0.5 mM BROD in DMSO) in a black 96-well plate. Fluorescence of the product was measured for 60 min in 5 min steps with λ_{ex} 550 nm, λ_{em} 585 nm at 37°C with a photometer. BC and resorufin standards from 1 to 1500 nM for external calibration were processed in parallel. The linear time period of each sample was chosen to calculate the resorufin production.

UGT 1 and 2 activities were determined with specific model substrates 4-methylumbelliferone (MUF) and 4-hydroxybiphenyl (HOBI), respectively, and determined by formation of respective glucuronides. 25 μ L microsomal solution were incubated with 125 μ L TrisHCl buffer (100 mM, pH 7), 25 μ L $MgCl_2$ (50 mM in TrisHCl buffer), 25 μ L Brij[®] 58 (0.5 % in water) and 25 μ L substrate (5 mM MUF or HOBI in DMSO) for 3 min at 37°C and 450 rpm in a thermomixer. Then 25 μ L UDP glucuronic acid (30 mM in DMSO) were added. For sample t_0 , the reaction was stopped immediately by adding one volume perchloric acid (0.5 M in water) and for sample t_{10} the mix was incubated for 10 min before adding the perchloric acid. The stopped mixture was centrifuged at 4600 rpm for 5 min. To remove remaining substrate 450 μ L of the supernatant were mixed with 1.2 mL chloroform, vortexed thoroughly and centrifuged at 400 rpm for 10 min. Three 100 μ L aliquots of the aqueous supernatant were transferred to a black 96-well plate and mixed with 100 μ L glycine-NaOH solution (1.6 M, pH 10.3) for 4 min. Fluorescence of MUF-glucuronide (λ_{ex} 315 nm, λ_{em} 365 nm) and HOBI-glucuronide (λ_{ex} 278 nm, λ_{em} 327 nm) was measured with a photometer. BC and MUF-glucuronide standards from 0.005 to 50 μ M for external calibration were processed adequately. MUF-glucuronide production was the difference of product in t_{10} and t_0 . Due to the lack of standards for HOBI-glucuronide, the increase in fluorescence units between t_0 and t_{10} was used as an alternative for concentrations to calculate the enzyme activity.

3.7 In silico models for dermal absorption

3.7.1 Data mining and calculation of mixture factors

A BASF SE dataset of routine dermal absorption experiments in vitro was used as the basis for in silico-model development. The database comprises 89 chemicals tested in 569 individual experiments in more than 150 different formulations containing up to 20 ingredients from a palette of more than 240 ingredients. Examples of these ingredients were water, organic solvents, surfactants and thickeners. The active compounds (mainly pesticides and cosmetic ingredients) and their chemical formula, CAS number (if available), given substance number as well as selected physicochemical properties are listed in the annex (Table 47). Molecular weight ranges from 70 (tetrahydrofuran) to 1052 g/mol (fenbutatine oxide) and $\log P_{ow}$ from -2.9 (prohexadione calcium) to 6.2 (Uvinul A Plus). Results, in the form of $\log_{max} K_p$, ranged from -7.48 (very slow) to -1.01 (very fast permeation). Since the Abraham model for dermal absorption was used as the basic model (see section 1.4.4), the five Abraham descriptors were calculated for each compound with ADME Boxes version 4.95: $\Sigma\alpha_2^H$ and $\Sigma\beta_2^H$, the overall hydrogen bond acidity and basicity, Rf_2 the solute excess molar refractivity, π_2^H the solute dipolarity/polarizability and V_x the McGowan characteristic volume (Abraham & Martins 2004). The required SMILES codes (simplified molecular-input line-entry system) were generated with ChemDraw. Compounds no. 5, 19, 34, 41, 53 and 65 were excluded from the dataset due to missing chemical descriptor values. The structures of compounds no. 53 and 65 were not known in detail and the others belong to chemical classes (inorganic, polymers) which could not be processed by the software due to their lack of carbon atoms or extensive or indeterminate size. For the remaining dermal absorption experiments, individual experimental condition and composition of applied formulation (mixture) were extracted from the reports. Skin preparations from human, rat, pig and rabbit as well as different commercial epidermis and skin constructs (StrataTest[®], EpiDerm[™] and EpiSkin[™]) were used for the studies. Due to a small number of experiments with pig, rabbit and reconstructed skin and to form a

more homogeneous dataset, these experiments were excluded from the set. To further simplify the dataset, different kinds of receptor fluids were combined to form seven representative groups: 'water' (de-ionized water, distilled water, tap water, physiological saline, PBS (phosphate buffered saline)), 'water+B' (water and BSA (bovine serum albumin), culture medium and BSA), 'water+x' (water and PEG (polyethylene glycol), Volpo or Igepal, culture medium and PEG), 'PBS, pH4' (PBS at pH4), 'E/W_1' (ethanol/water mixture < 4/6, v/v), 'E/W_2' (ethanol/water mixture > 4/6 ≤ 1/1, v/v) and 'E/W_3' (ethanol/water mixture > 1/1, v/v). Similar to receptor fluid, different exposure and total experimental periods were condensed to form the following periods: < 6 h, 6 – 8 h, 8 – 24 h, 24 h, 25 – 48 h and > 48 h. An exclusive use of experiments within the time frame 6 to 48 h was defined, that is, experiments of duration less than 6 h and greater than 48 h were eliminated from the dataset.

Beside chemical descriptors which describe the penetrant ($\Sigma\alpha_2^H$, $\Sigma\beta_2^H$, π_2^H , Rf_2 and V_x), so-called mixture factors (MFs) which represent the entire formulation of the penetrant, were used as independent variables for the model. Each MF was a combined value for a descriptor X (e.g. $\log P_{ow}$) calculated from the individual values X_i for the single ingredients (i). Each ingredient was weighted by its contribution or weight fraction to the mixture (w_i):

$$\text{Equation 27: } MF_X = \sum_{i=1}^{i=j} w_i * X_i$$

To identify the factors which reflect best the effect of the mixture, 87 different MFs, which cover molecular size, solvatochromatic and lipophilicity properties of the ingredients, were analyzed. The values for each formulation ingredient were generated by the softwares ADME Boxes version 4.95 and Molinspiration Property Calculator. Literature values were extracted from the PhysProp Database Demo (Syrres) or material safety data sheets. Table 13 gives an overview of the descriptors generated with the named software packages. The generated values as well as their logarithm and reciprocal values were used for analysis. Literature values and calculated values for $\log P_{ow}$ and logarithm of water solubility were compared to evaluate the general suitability of the used software programs. For development of the model, only calculated values were used, since these were derived uniformly and hence independent of experimental variations.

Table 13: Software packages and derived chemical descriptors. MW: molecular weight, S_w : water solubility, $\log P_{ow}$: logarithm of the octanol/water partition coefficient, pKa: acid dissociation constant, HBAcc: number of hydrogen bond acceptors, HBDOn: number of hydrogen bond donors, TPSA: topological polar surface area, RotB: number of rotatable bonds.

Software	PhysChem
PhysProp Database Demo (Syrres), literature values	MW, melting point, boiling point, $\log P_{ow}$, S_w , pKa, vapor pressure, Henry's law constant, Atmospheric OH Rate Constant
Molinspiration Property Calculator	$\log P_{ow}$, TPSA, number of atoms, MW, HBAcc, HBDOn, Lipinski number, number of Lipinski violations, RotB, molecular volume
ADME Boxes version 4.95	$\Sigma\alpha_2^H$, $\Sigma\beta_2^H$, π_2^H , Rf_2 , V_x , MW, S_w (at 5 different pH values), $\log P_{ow}$ (two different algorithms), $\log D$ ($\log P_{ow}$ at 5 different pH values), HBAcc, HBDOn, TPSA, RotB, pKa

No descriptor values could be derived for polymeric and inorganic mixture ingredients. Others could not be processed due to missing knowledge of the structure (propriety of the supplier, reaction product or natural product). However, some of these ingredients could be processed by using sparse information combined with simplifications and assumptions. As an example, natural rapeseed oil contains on average 63 % oleic acid, 20 % linoleic acid 9 % α -linolenic acid and traces of other fatty acids (Belitz et al. 2008). Two triglycerides containing oleic acid and one triglyceride containing two linoleic acid and one α -linolenic acid were used as representative molecules for rapeseed oil. As a second example, for different SolvessoTM types the content of C8 – C14 aromatic hydrocarbons was estimated based on distillation ranges and boiling points. For instance, SolvessoTM 150 has a distillation range of 182 – 207°C; for calculations 1,3,5-mesitylene (C9), indene (C10), naphthalene (C10) and 1-methylnaphthalene (C11) with boiling points of 165, 182, 218 and 242 °C, respectively, were used as representatives. In general, it was decided to use only experiments with mixture factors derived from more than 90 % of the composition. That is, if more than 10 % of a formulation were undefined, it was eliminated from the dataset. Considering all decisions, the final dataset consisted of 56 chemical compounds with 342 data points. Results in the form of logmaxKp and experimental conditions for the remaining experiments are listed in the annex (Table 48).

3.7.2 Abraham-based models containing mixture factor(s)

For the first analysis the dataset was split randomly into a training set (2/3) and a validation set (1/3 of the total dataset): random numbers were assigned to each data point and every third point was assigned to the validation set. Therefore, information of one penetrant could be in the training set as well as in the validation set. In a second approach, the set was split up by penetrant: the 56 penetrants were sorted by the penetrant-specific Rf_2 and $\Sigma\alpha_2^H$ values and then every third penetrant was assigned to the validation set. Figure 7 shows the distribution of chemicals in this penetrant-dependent training and validation set according to their Rf_2 , $\Sigma\alpha_2^H$ and $\Sigma\beta_2^H$ values and confirms coverage of similar descriptive clouds.

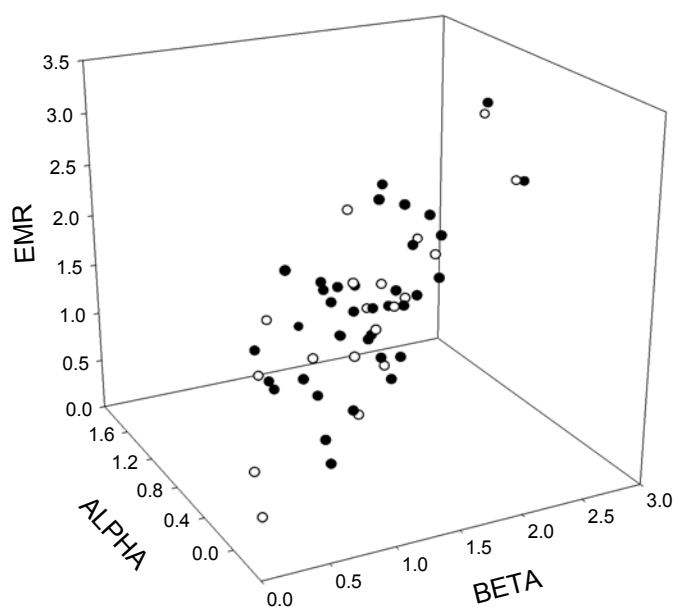


Figure 7: Distribution of chemicals in the penetrant-dependent training set (black circles) and validation set (open circles) based on Rf_2 , $\Sigma\alpha_2^H$ and $\Sigma\beta_2^H$ values.

Since it is broadly accepted by the scientific community, Abraham's prediction model was selected as the basic model for analysis (outlined in section 1.4.4) (Abraham & Martins 2004). Due to mainly finite dose experiments in the dataset, logmaxKp was used as the endpoint instead of logKp. To incorporate mixture effects, a MF was added to the basic equation as previously reported by Riviere and Brooks (Riviere & Brooks 2005). This led to the following model algorithm:

$$\text{Equation 28: } \log \max Kp = c + a * \sum \alpha_2^H + b * \sum \beta_2^H + p * \pi_2^H + e * Rf_2 + v * V_x + m * MF$$

Parameters a, b, p, e, v and m are regression coefficients for corresponding variables and c is the intercept. In a second approach a class variable was added to the model, which represents the species (Spl):

Equation 29:

$$\log \max Kp = c + a * \sum \alpha_2^H + b * \sum \beta_2^H + p * \pi_2^H + e * Rf_2 + v * V_x + m * MF + s * Spl$$

This binary class or indicator variable Spl (species indicator) represents either the species rat (2) or human (1). In the same way a receptor indicator (RI) was incorporated:

Equation 30:

$$\log \max Kp = c + a * \sum \alpha_2^H + b * \sum \beta_2^H + p * \pi_2^H + e * Rf_2 + v * V_x + m * MF + s * Spl + w * RI$$

This binary class variable represents either ethanol/water mixtures (1) or other water-based receptor fluids (2). In addition to this approach, principle component (PC) factors 1 and 2 for variables $\Sigma\alpha_2^H$, $\Sigma\beta_2^H$, π_2^H , Rf_2 and V_x were determined utilizing SAS 9.2 ('Proc Factor') and used as model descriptors as follows:

$$\text{Equation 31: } \log \max Kp = c + s * PC1 + t * PC2 + m * MF$$

Parameter s and t are regression coefficients coupling the PC factors to the endpoint logmaxKp. PC factors are linear combinations of underlying variables which combine and condense the information of these variables. They are determined with the aim to be independent from each other to ensure robust estimates. This was to evaluate, if two PC factors can replace five Abraham descriptors without losing information and predictive power.

The SAS procedure 'Proc Reg' was used to run multiple linear regression analysis based on Equation 28 to Equation 31. The training set was used as the underlying dataset. The procedure generated values for the regression coefficients including their standard error and statistics (p-value), as well as the coefficient of determination (R^2), adjusted R^2 and F-values for the model. In order to identify the most descriptive MF, each of the 87 MFs was used as the additional factor in the models. The most descriptive MF was identified by the highest resulting R^2 value. In a second approach, not all Abraham variables were forced into the model. Utilizing the features '/selection=stepwise' and '/selection=maxR' in the SAS procedure 'Proc Reg', the most descriptive variables for the endpoint logmaxKp, from the total set of 87 MFs, five Abraham descriptors and two class variables (Spl, RI) were identified. Using

'stepwise', only descriptors with a significant influence on the model were added, whereby 'maxR' searched for the combination with the highest R^2 for a given number of variables. The resulting combinations were reported by their R^2 values.

The correlation of the model descriptors were calculated with the SAS procedure 'Proc Corr'. Results were given as Pearson's correlation coefficients (r) including the statistical significance of the correlation. Correlations with r values under 0.7 were considered to be appropriate for reliable models; robust estimates are ensured. Additionally, only significant descriptors ($p < 0.05$, 'Proc Reg') remained in the model.

With the Williams plot, response outliers were identified along with data points with high leverage, as described by Gramatica et al. (Gramatica 2007): The standardized/studentized residuals and the leverage in the form of the hat value were generated with the SAS procedure 'Proc Reg' and plotted against one another. An example of the Williams plot is given in Figure 8. Data points with standardized residuals larger than three times the standard deviation (SD) belong to wrongly predicted values and required special attention when interpreting the model. Data points with hat values higher than the critical hat value h^* belonged to highly influential, or highly leveraged, data points and were excluded from the model. The hat value indicates the standardized distance of each data point to the centroid of the training set. The critical hat value h^* was calculated utilizing the number of observations (n) and the number of variables (p) (OECD 2007):

$$\text{Equation 32: } h^* = 3 * (p + 1) / n$$

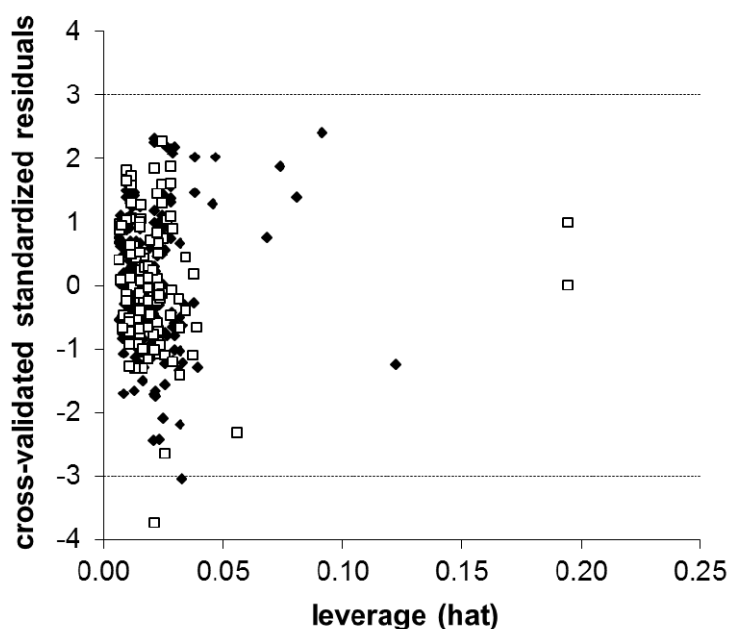


Figure 8: Williams plot for a dataset of 342 data points (human and rat skin experiments). Underlying model variables are $\Sigma\alpha_2^H$, $\Sigma\beta_2^H$, π_2^H , Rf_2 , V_x , Spl and the mixture factor $molinspHBAcc$. The training set (227 points) is shown as black diamonds and the validation set (115 points) as open squares. The horizontal lines depict the limits of three SDs and the vertical line is the critical hat value h^* .

Including all the steps mentioned above, the remaining data and variable set belonged to significant models. For such models R^2 as well as adjusted R^2 – which considers the number of variables and data points – were utilized to determine goodness of fit with SAS 9.2 ('Proc Reg'). Internal and external validation steps followed. Internal predictivity and model robustness were determined via cross-validation using two procedures recommended by the OECD (OECD 2007): leave-one-out (LOO) and leave-many-out (LMO). Both were calculated with the 'Prog Reg' procedure as part of validation loops which exclude either stepwise single data points or randomly selected data groups: With procedure LOO each data point was removed, one-at-a-time and predicted with the model derived from the remaining dataset. Focusing on the training set with n_{tr} data points, n_{tr} reduced models with $n_{tr}-1$ data points were calculated. Q^2LOO , a measure for robustness, was calculated as the sum of the squared differences between the observed and the estimated response, which is equivalent to a coefficient of determination between the two values:

$$\text{Equation 33: } Q^2LOO = 1 - \frac{PRESS}{SS_{tot}} = 1 - \frac{\sum_{i=1}^{n_{tr}} (y_i - \hat{y}_i)^2}{\sum_{i=1}^{n_{tr}} (y_i - \bar{y}_{tr})^2}$$

PRESS is the predictive residual sum of squares and defined as the sum of squared differences between the observed response for the i -th object (y_i) of the training set and the response of the i -th object estimated by using a model obtained without using the i -th object, but the rest of the training set (\hat{y}_i). SS_{tot} is the total sum of squares and defined as the sum of squared differences between the observed response for the i -th object (y_i) and the average response value of the training set (\bar{y}). Similar to the procedure LOO, procedure LMO deleted one part of the entire training set (here randomly selected 25 %) which was then predicted by the model derived from the remaining dataset (here 75 %). This was repeated numerous times and the mean predicted value for each data point ($\hat{y}_{mean,i}$) was used to calculate the $Q^225\%$:

$$\text{Equation 34: } Q^225\% = 1 - \frac{PRESS}{SS_{tot}} = 1 - \frac{\sum_{i=1}^{n_{tr}} (y_i - \hat{y}_{mean,i})^2}{\sum_{i=1}^{n_{tr}} (y_i - \bar{y}_{tr})^2}$$

The predictive power of the model was determined by external cross validation. That is, the model derived from the training set was used to predict the validation or external dataset – which was not used for model derivation. The external explained variance (Q^2Ext) was calculated as follows:

$$\text{Equation 35: } Q^2Ext = 1 - \frac{\sum_{i=1}^{n_{ext}} (y_i - \hat{y}_i)^2}{\sum_{i=1}^{n_{ext}} (y_i - \bar{y}_{tr})^2}$$

where the numerator is the sum of squared differences between the observed response for the *i*-th object (y_i) of the validation set and the response of this *i*-th object estimated by using a model obtained with the training set (\hat{y}_i); the denominator is the sum of squared differences between the observed response for the *i*-th object of the validation set (y_i) and the average response value of the training set (\bar{y}_i) (OECD 2007).

3.7.3 Substance-based models containing mixture factor(s)

In addition to the Abraham-based approach, substance-based models were developed. Using these models the results of one substance were condensed in a class variable SUBST and combined linearly with the MF:

$$\text{Equation 36: } \log \max Kp = c + SUBST + m * MF(+s * Spl)$$

The MF explains the mixture effect on the response using knowledge from all included experiments, from all substances. The class variable Spl was added to the model equation, if the entire dataset with human and rat skin experiments was used. A substance was included in the analysis, if it was tested in at least five different mixtures. One third of these experiments were then assigned randomly to the validation set and two thirds to the training set. Based on the training set, the model analysis was performed with procedure 'Proc Glim' of SAS 9.2. Using this procedure, estimators for the class mean – in this case for each substance – and regression coefficients for the continuously influential variables like MF could be determined simultaneously. Used and compared regarding their ability to explain dermal absorption results, were the same MFs as formerly identified for the Abraham-based approach (molinspTPSA, molinspLogHBAcc, AdmeLogHBDOn, AdmeP_{ow} and Adme1/RotB; for method see the previous chapter 3.7.2 and results chapter 4.4.1). The predictive power was determined with the validation set in the form of Q²Ext as described in the previous chapter 3.7.2, Equation 35. A summary of the SAS 9.2 procedures used to develop the substance-based as well as the Abraham-based models is listed in Table 14.

Table 14: Overview of SAS 9.2 procedures used for analysis

SAS procedure	analysis
Prog Reg	(multiple) linear regression
/ stb	standardized coefficients
/ selection=maxr	parameter selection based on maximum R ²
/ selection=stepwise	parameter selection based on stepwise selection
Proc Glim	linear regression with class variables
Proc Corr	generates correlation matrix
Proc Standard	standardizes input parameters
Proc Factor	generates principle component factors

3.7.4 Interpretation and application

To assess the impact of each descriptor on the model, the standardized regression coefficients were calculated with SAS 9.2 ('Proc Reg' combined with feature '/stb' or 'Proc Standard' before 'Proc Reg' or 'Proc Gln'). These coefficients were independent of the unit of their corresponding descriptors and therefore directly comparable to each other.

To define the applicability domain (ApD) of the final models, minimum and maximum values of the descriptors in the remaining dataset, excluded data points (eliminated during the developmental process), and wrongly predicted data points with standardized residuals larger than three SD were extracted and discussed.

For the prediction of data points (training and validation set), SAS 9.2 procedures 'Proc Reg' or 'Proc Gln' were used. Distinct values, including the upper and lower bounds of a 95 % confidence interval were generated. Calculated hat values for Abraham-based models ('Proc Reg') smaller than the model specific h^* confirms the affiliation of the predicted data point to the defined ApD.

Besides the prediction of distinct values, the models were checked for their ability to assign correct classes of permeability to substance/mixture combinations. Therefore, each predicted and observed $\log_{\max}K_p$ value was assigned to its Marzulli class. Criteria are given in Table 15 (Marzulli & Brown 1969). The number of data points with matching classes for predicted and observed values were counted as well as the number of incorrectly predicted data points.

Table 15: Definition of Marzulli classes based on $\log K_p$ values; K_p values were given in cm/h (Marzulli & Brown 1969).

	logKp
very slow	< -5.22
slow	-5.22 – -4.22
moderate	-4.22 – -3.22
fast	-3.22 – -2.22
very fast	> -2.22

3.8 Statistics

If not stated otherwise results are shown in the form of mean and SD. For statistical comparison of two groups ($n \geq 3$) student's t-test (unpaired, two-sided) was performed with Microsoft Office Excel 2003 or SAS 9.2. Significance (*) was set at $p < 0.05$ and high significance (**) at $p < 0.01$.

Limit of detection (LOD) and limit of quantification (LOQ) were determined in two ways: Firstly, LOD and LOQ of chromatographic methods were calculated based on the signal to noise ratio (S/N) (Equation 37 to Equation 39) (Europäische Arzneibuchkommission 2008). This ratio was determined with a small, but good detectable standard (C_{Kalib}) in the linear range where H is the substance peak height and h the height of background noise before and after the peak:

$$\text{Equation 37} \quad S / N = H / h$$

$$\text{Equation 38} \quad LOD[mg / L] = 3 * C_{Kalib}[mg / L] / (S / N)$$

$$\text{Equation 39} \quad LOQ[mg / L] = 10 * C_{Kalib}[mg / L] / (S / N)$$

Secondly, LOD and LOQ of HPLC-UV methods with background peaks in the blank, as well as limits of photometric and fluorometric methods were calculated based on mean and SD derived from repeated blank measurements ($Mean_{blank}$, SD_{blank}) (Rücker et al. 2008):

$$\text{Equation 40} \quad LOD[mg / L] = Mean_{blank} + 3 * SD_{blank}$$

$$\text{Equation 41} \quad LOQ[mg / L] = 2 * LOD[mg / L]$$

Further processing steps like extraction, dilution and relation to protein content or time were considered. The resulting LOD and LOQ were then used as limits for the entire assay (e.g. enzyme activity assay). The first method was used for chromatographic determination of testosterone, caffeine, MCPA, MCPA-EHE (GC-MS), acPABA and BA-nOx as well as for the entire NAT-1-activity assay. Limit values for radio-detection (HPLC-RAD) were estimated with a ^{14}C -MCPA-EHE standard. The second method was used for esterase, AIDH, CYP 450, UGT 1 and 2 and FMO activity assays. Instead of using BC as the blank, HDC was used for the ADH activity assay and water for MCPA-EHE examinations with HPLC-UV. ACN was used as the blank to determine limit values for LSC measurements.

4 Results

4.1 Histological sections of skin models

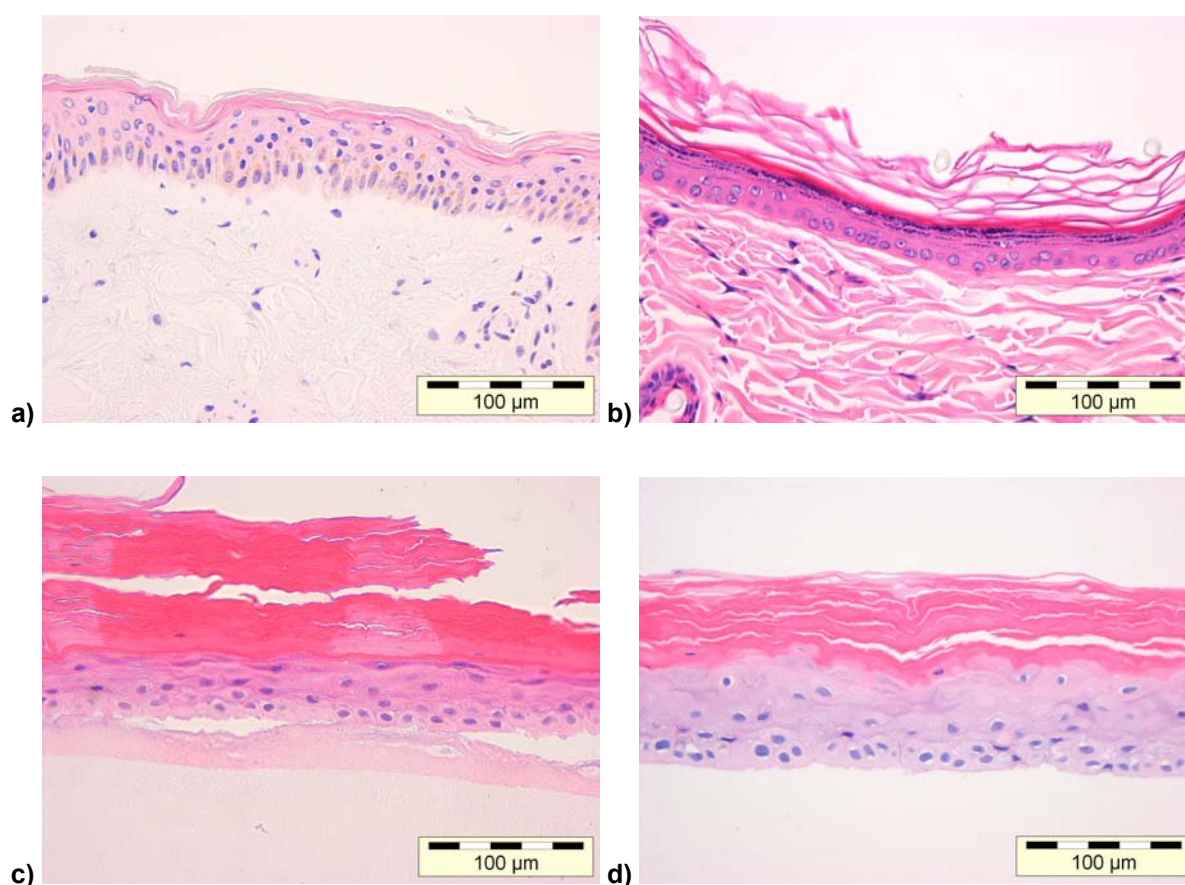


Figure 9: Histological sections stained with hematoxylin and eosin, magnified 20 times: a) human skin (abdomen), b) rat skin (dorsum), c) StrataTest[®] sliced as delivered and d) StrataTest[®] after removing the underlying membrane.

For morphological comparison of the skin models used for dermal absorption experiments, histological sections were prepared and stained with hematoxylin and eosin (see Figure 9). The human abdominal skin section showed – with exception of stratum lucidum that is generally absent in abdominal skin – all distinct epidermal layers described in section 1.1: stratum corneum (SC), stratum granulosum (SG), stratum spinosum (SS) and stratum basale (SB). Connected to the epidermis was a prominent dermis consisting of connective tissue and scattered fibroblasts (Figure 9 a). The reconstructed human skin StrataTest[®] (Figure 9 c – d) consisted of the same typical layers, but the basal cells were more cuboidal and irregularly arranged in comparison to the well-organized columnar cells of the human ex vivo sections. Furthermore, the SC in StrataTest[®] tissue was obviously thicker than that in human skin and only a thin dermis with few fibroblasts was present (Figure 9 c). The dermis was tightly connected to the underlying membrane, but the connection to the epidermis was loosened frequently by preparing the slices as shown in Figure 9 c. By removing the underlying membrane, the layers of the dermis were completely removed as well as the basement membrane (Figure 9 d). The epidermis of rat dorsal skin was thinner than that of human abdominal skin. It consisted of one to two layers of nucleated cells (Figure 9 b). The stratum basale was prominent as well as the stratum corneum, but

only single spinous and granula cells were present. The dermis consisted of single fibroblasts and connective tissue.

A further potential alternative to human skin, skin-PAMPA, was assessed for its barrier function in the current work. However, no histological investigation was feasible, since it is a synthetic membrane consisting of typical compounds of the extracellular space of the SC.

4.2 Aspects of dermal absorption experiments in vitro

The impact of different skin models (including different preparation types and skin equivalents), diffusion cell type, dosing regimen and skin integrity testing for dermal absorption in vitro was investigated in the current work. The annex contains detailed lists with experimental conditions (Table 45), properties of used skin models including integrity test results (Table 44) and absorption characteristics for single diffusion cells (Table 46).

4.2.1 Skin integrity testing

4.2.1.1 Binary classification with standard tests

The suitability of various skin integrity tests was investigated for the current thesis. The purpose of such a test is to ensure the exclusive use of undamaged skin samples for dermal absorption experiments. To evaluate a potential binary classification, the absorption results of four ¹⁴C-labeled penetrants (caffeine, testosterone, MCPA and MCPA-EHE) were assigned to valid and invalid (excised and reconstructed human) skin samples by limit values of standard integrity tests. Table 16 a – c show the mean, minimum and maximum values for the absorption results separated by valid and invalid skin samples according to limit values of TEWL, TEER or TWF.

Table 16: Range of absorption (minimum – maximum) for valid and invalid (excised and reconstructed human) skin samples differentiated by a) TEWL b) TEER c) TWF at two defined limit values each – the stricter limits are given on the left side. Mean values are shown in brackets. AD is given in percent dose and maxKp in $\cdot 10^{-5}$ cm/h; n is the number of skin samples used for calculations. The applied doses of ¹⁴C-labeled test substances testosterone, caffeine, MCPA and MCPA-EHE were 100, 100, 90 and 160 μ g/cm², respectively.

a) TEWL

limit value		10 g/(m ² *h)		13 g/(m ² *h)	
classification		valid	invalid	valid	invalid
testosterone	n	24	11	26	9
	maxKp	12 – 138 (55)	20 – 805 (290)	12 – 169 (58)	123 – 805 (334)
	AD	6 – 44 (22)	27 – 76 (56)	6 – 44 (23)	47 – 76 (61)
caffeine	n	19	11	20	10
	maxKp	25 – 143 (64)	54 – 1647 (909)	25 – 143 (63)	607 – 1647 (995)
	AD	12 – 68 (32)	54 – 98 (84)	12 – 68 (33)	73 – 98 (86)
MCPA	n	9	11	17	3
	maxKp	4 – 18 (11)	15 – 1004 (447)	4 – 1004 (192)	441 – 715 (579)
	AD	9 – 21 (14)	28 – 96 (84)	9 – 94 (45)	95 – 96 (95)
MCPA-EHE	n	3	7	7	3
	maxKp	0.6 – 1.4 (0.9)	0.4 – 2.0 (0.9)	0.4 – 2.0 (0.8)	0.9 – 1.0 (1.0)
	AD	5.2 – 9.7 (6.7)	1.0 – 8.9 (4.4)	1.0 – 9.7 (5.2)	2.6 – 8.7 (4.9)

b) TEER

	limit value classification	2 kOhm		1 kOhm	
		valid	invalid	valid	invalid
testosterone	n	22	8	30	0
	maxKp	12 – 283 (78)	48 – 805 (296)	12 – 805 (136)	-
	AD	6 – 64 (27)	18 – 76 (48)	6 – 76 (33)	-
caffeine	n	20	10	30	0
	maxKp	25 – 994 (110)	54 – 1647 (901)	25 – 1647 (374)	-
	AD	12 – 97 (35)	54 – 98 (82)	12 – 98 (79)	-
MCPA	n	13	7	18	2
	maxKp	4 – 365 (96)	18 – 1004 (537)	4 – 585 (183)	715 – 1004 (860)
	AD	9 – 86 (36)	13 – 96 (83)	9 – 96 (48)	94 – 96 (95)
MCPA-EHE	n	9	1	10	0
	maxKp	0.4 – 2.0 (0.9)	0.4	0.4 – 2.0 (0.9)	-
	AD	1.0 – 9.7 (4.7)	8.9	1.0 – 9.7 (5.1)	-

c) TWF

	limit value classification	2.5*10 ⁻³ cm/h		4.5*10 ⁻³ cm/h	
		valid	invalid	valid	invalid
testosterone	n	8	2	9	1
	maxKp	12 – 37 (26)	20 – 33 (27)	12 – 37 (27)	20
	AD	11 – 24 (17)	11 – 44 (27)	11 – 24 (16)	44
caffeine	n	8	2	8	2
	maxKp	30 – 143 (68)	77 – 130 (103)	30 – 143 (68)	77 – 130 (103)
	AD	30 – 68 (46)	51 – 53 (52)	30 – 68 (46)	51 – 53 (52)
MCPA	n	4	6	8	2
	maxKp	4 – 11 (6)	8 – 18 (14)	4 – 18 (10)	14 – 15 (14)
	AD	9 – 15 (12)	12 – 28 (17)	9 – 28 (15)	15 – 17 (16)
MCPA-EHE	n	3	7	8	2
	maxKp	0.7 – 1.4 (1.0)	0.4 – 2.0 (0.8)	0.4 – 2.0 (0.9)	0.4 – 0.9 (0.7)
	AD	2.6 – 9.7 (5.8)	1.0 – 8.9 (4.8)	1.0 – 9.7 (4.8)	3.3 – 8.9 (6.1)

TEWL as differentiation tool (limit 10 g/(m²*h)) led to obviously higher mean absorption values for test compounds ¹⁴C-caffeine, ¹⁴C-testosterone and ¹⁴C-MCPA when considering invalid skin samples in comparison to valid samples (Table 16 a). However, an obvious overlapping of results was observed. That is, when high maximum values for valid and low minimum values for invalid skin samples were present. This effect on single skin sample level was visualized for maxKp and TEWL-classification in Figure 10. Changing the TEWL limit from 10 to 13 g/(m²*h) did not change the distribution significantly for ¹⁴C-caffeine and ¹⁴C-testosterone. For ¹⁴C-MCPA the valid results increased clearly when applying the higher limit value (see Table 16 a). The defined valid and invalid skin samples for the slow permeating test compound ¹⁴C-MCPA-EHE did not correspond to the potentially absorbable dose (AD) or the Kp values. For both skin classes similar results were obtained. This was also the case for TEWL, TEER and TWF – irrespective of the applied threshold (Table 16 a – c). Considering the other three test compounds, the two different limit values for TEER (1 and 2 kOhm) led to different distributions

(Table 16 b). Only 2 of 90 skin samples were classified as invalid applying 1 kOhm as the limit, but 26 when applying 2 kOhm. Analog to TEWL, differentiation with TEER (limit: 2 kOhm) and TWF resulted in obvious higher absorption means for invalid skin samples than for valid skin samples as well as in significant overlapping of results. Mean, minimum and maximum values did not differ significantly for the two different limit values of TWF (2.5 and $4.5 \cdot 10^{-3}$ cm/h) (Table 16 c).

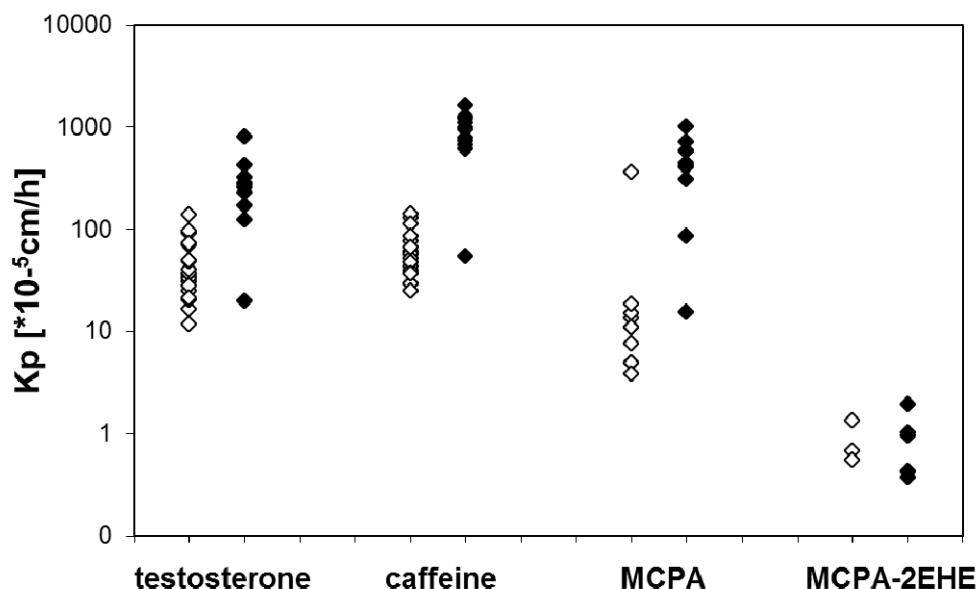


Figure 10: Absorption results for excised and reconstructed human skin in the form of maxKp values of four ^{14}C -labeled test compounds. Values are sorted by integrity class due to TEWL measurements (cut-off-value: $10 \text{ g}/(\text{m}^2 \cdot \text{h})$). Results of valid skin samples are shown in open diamonds, invalid skin samples in filled diamonds.

4.2.1.2 Correlation of integrity test and absorption results

A potential correlation between integrity test results and differences in skin barrier function (in the form of AD and maxKp of various test compounds) was investigated by running linear regression analyses. Only values obtained under equal ('homogeneous') experimental conditions were grouped together (≥ 10 data points). For example, linear regression analyses for TEER were conducted separately for the four penetrants (^{14}C -caffeine, ^{14}C -testosterone, ^{14}C -MCPA and ^{14}C -MCPA-EHE) and the three skin models (human, rat and StrataTest[®]). Table 17 shows mean, minimum and maximum values of slope and R^2 from different experiments. The obtained correlations varied over a wide range for all five methods. The largest R^2 in average (0.579) and maximum (0.986) was achieved with the ISTD. Partly high correlations were observed for TEWL (max R^2 0.895). For TEWL, TEER, TWF and BLUE positive and negative correlations were obtained. This means that at least one homogenous experiment revealed the opposite correlation to the results as expected. Only positive correlations were obtained for ISTD. The largest homogeneous dataset (^{14}C -MCPA-DMA formulation, rat skin, water as receptor, semi-occluded, $n = 45$) – which covers a wide range of absorption (6.4 to 99 %) and permeation rates (Marzulli-Class: slow to very fast) – was highly correlated with the ISTD results (R^2 of 0.859 and 0.911) (Marzulli & Brown 1969). The plots for AD and maxKp are shown in Figure 11 a and b. The broad range was achieved by various pretreatments – conducted to evaluate the effect of repeated dosing regimen (performance see section 3.5.3.3).

Table 17: Correlations between absorption results AD and maxKp and different integrity tests. Correlations were calculated for each homogeneous experiment with at least 10 data points separately for the four test substances (TS) (¹⁴C-caffeine, ¹⁴C-testosterone, ¹⁴C-MCPA and ¹⁴C-MCPA-EHE) and the three skin models (human, rat and StrataTest®). Shown are the mean, maximum (max) and minimum (min) slopes and coefficients of determination (R²) for all experiments (n). Mean values for R² were calculated from experiments with correct positive or correct negative correlations only. Regarding the principle of the tests the slope is expected to be positive for ISTD, TWF, TEWL and BLUE and negative for TEER.

		TEER		TWF		TEWL		³ H-ISTD		maxKp		BLUE	
		Slope	R ²	Slope	R ²	Slope	R ²	Slope	R ²	Slope	R ²	Slope	R ²
AD	N	10	7	4	3	14	14	10	10			4	1
	Mean	-0.06	0.196	4.57	0.257	0.24	0.348	0.75	0.556			-0.63	0.434
	Min	-0.41	0.001	-9.95	0.064	-0.18	0.006	0.31	0.142			-1.9	0.434
	Max	0.07	0.658	19.56	0.628	1.04	0.690	1.15	0.882			0.17	0.434
maxKp	N	10	9	4	2	14	13			10	10	4	3
	Mean	-0.14	0.188	0.451	0.259	0.18	0.281			1.54	0.579	-0.173	0.243
	Min	-0.91	0.003	-10.75	0.212	-0.002	0.006			0.19	0.139	-1.73	0.153
	Max	0.004	0.691	15.76	0.307	1.32	0.895			11.78	0.986	144.34	0.391

Untreated skin samples or samples pretreated with water, but without washing steps in between, resulted in the lowest values which were highlighted in Figure 11 in black and grey. Since these samples represent valid skin samples for the defined experimental conditions, maxKp value of $\sim 40 \cdot 10^{-5} \text{ cm/h}$ and AD of $\sim 35\%$ for ISTD (^3H -testosterone) were indicated as potential thresholds for validity. Using the same skin samples, correlations of AD and maxKp to TEWL (R^2 of 0.53 and 0.45) or TEER (R^2 of 0.41 and 0.48) were lower in comparison to correlations obtained for the ISTD.

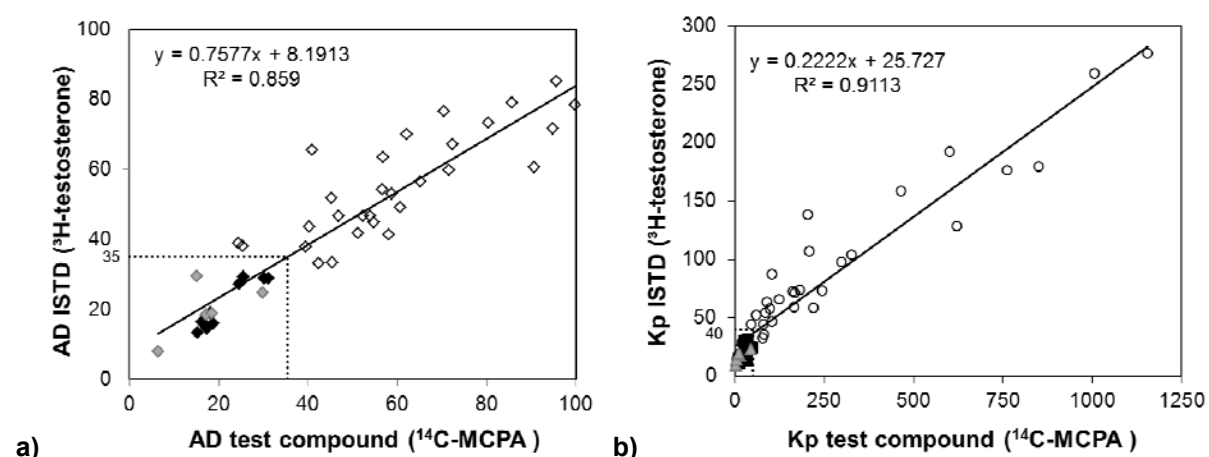


Figure 11: Correlation of a) potentially absorbable dose (AD) and b) maxKp of test compound ^{14}C -MCPA ($90 \mu\text{g}/\text{cm}^2$) and internal standard ^3H -testosterone ($0.0017 \mu\text{g}/\text{cm}^2$) from a shared MCPA-DMA formulation through rat skin. AD is plotted in percent dose and maxKp in $\cdot 10^{-5} \text{ cm/h}$. The large absorption range was achieved by chemical and mechanical pretreatment of the skin samples as outlined in chapter 3.5.3.3 'Repeated dosing experiment'. Filled symbols represent undamaged skin preparations with no pretreatment (black) or with water pretreatment without mechanical washing (grey). Open circles represent all other pretreatments. Linear regression equation including coefficient of determination are shown in the graphics. The dotted lines indicate proposed threshold values for validity: a) AD 35%; b) maxKp $40 \cdot 10^{-5} \text{ cm/h}$.

4.2.1.3 Verification of the internal standard approach

To evaluate **co-analytics** of ^3H - and ^{14}C -activity by LSC under the given technical set up, the measured Bq values of ^{14}C -testosterone standards in presence of ^3H -testosterone at two dose levels were compared with ^{14}C -testosterone standards without ^3H in the matrix (Figure 12 a). The R^2 was 0.9991 and the slope 1.0077. No influential effects were apparent. For the opposite case R^2 was 0.9998 and the slope 1.0008 (see Figure 12 b). In general, the presence of ^{14}C increased slightly the variability of ^3H measurements in the low Bq range. A tendency to higher values was observed in the range $< 25 \text{ Bq}$.

To assess the **co-permeation** of test compound and an internal standard, Table 18 lists absorption characteristics for three ^{14}C -labeled test substances in absence and presence of a ^3H -labeled ISTD. All other experimental conditions were identical: ^{14}C -caffeine was applied to human skin preparations ($0.025 \text{ MBq}/\text{cm}^2$, $100 \mu\text{g}/\text{cm}^2$, $4.0 \text{ mg}/\text{mL}$ in ethanol/water mixture 1/1, v/v) with or without ^3H -testosterone ($0.025 \text{ MBq}/\text{cm}^2$, $0.0013 \mu\text{g}/\text{cm}^2$, $0.00005 \text{ mg}/\text{mL}$); ^{14}C -testosterone was applied to human skin preparations ($0.025 \text{ MBq}/\text{cm}^2$, $100 \mu\text{g}/\text{cm}^2$, $4 \text{ mg}/\text{mL}$ in ethanol/water mixture 1/1, v/v) with or without ^3H -caffeine ($0.025 \text{ MBq}/\text{cm}^2$, $2.5 \mu\text{g}/\text{cm}^2$, $0.1 \text{ mg}/\text{mL}$) and ^{14}C -MCPA was applied to rat skin preparations ($0.037 \text{ MBq}/\text{cm}^2$, $90 \mu\text{g}/\text{cm}^2$, $9 \text{ mg}/\text{mL}$ as MCPA-DMA formulation) with or without ^3H -

testosterone (0.037 MBq/cm^2 , $0.0017 \text{ }\mu\text{g/cm}^2$, 0.00017 mg/mL). With the exception of a significantly different lag time for ^{14}C -testosterone with and without ^3H -caffeine (2.4 ± 0.4 and 4.4 ± 1.5 h, respectively), all endpoints of dermal absorption were similar for the two different experimental conditions. The fastest permeation and highest absorption values were obtained with ^{14}C -testosterone followed by ^{14}C -caffeine and ^{14}C -MCPA.

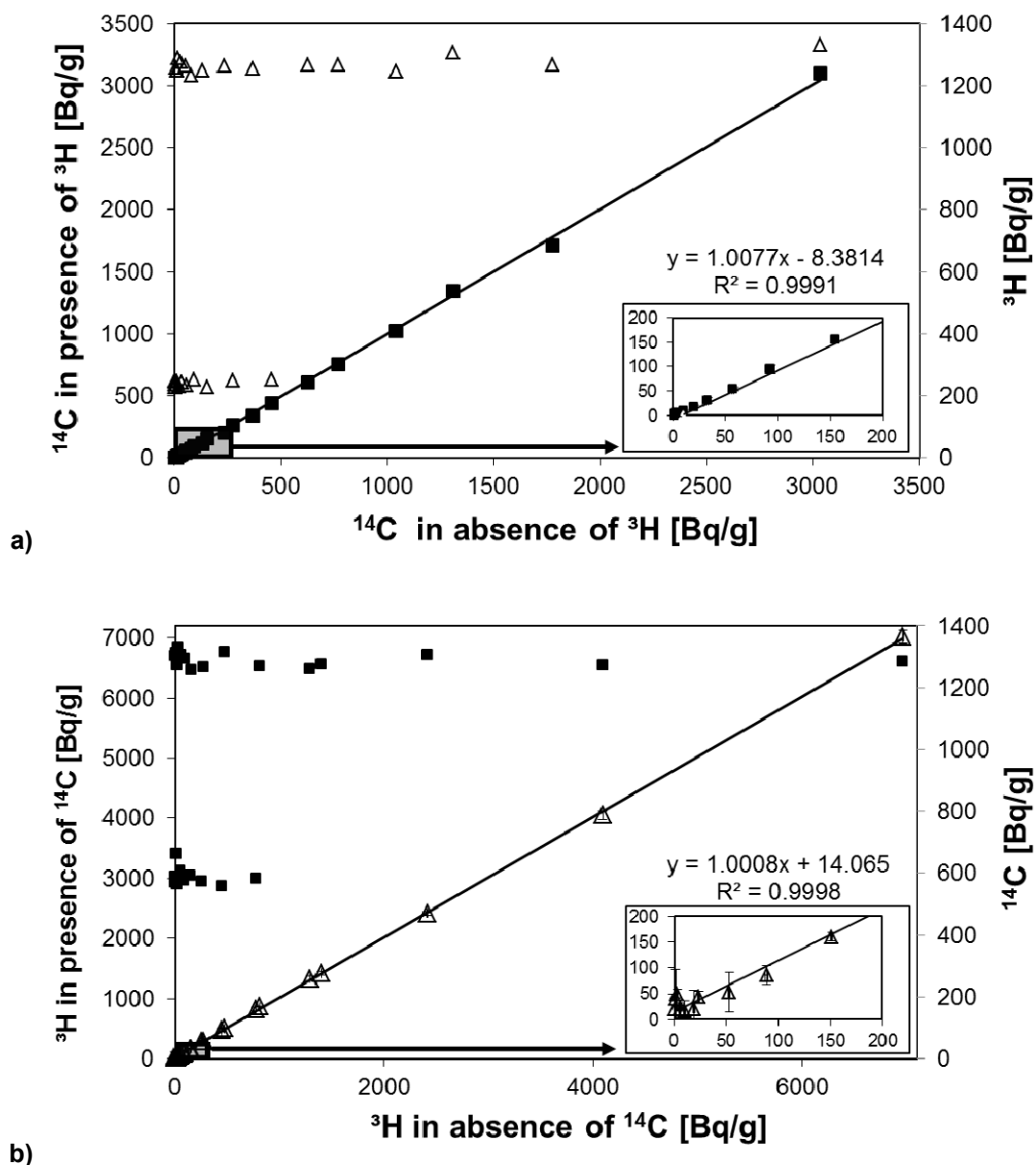


Figure 12: Correlation of a) ^{14}C -testosterone activity in absence and presence of ^3H -testosterone and b) of ^3H -testosterone in absence and presence of ^{14}C -testosterone. Activities were determined by LSC measurements. ^{14}C -activities are shown in filled squares, ^3H -activities in open triangles. Insertions show magnified low activity range (< 200 Bq/g). Correlation equations including coefficients of determination were shown in the graphs.

Table 18: Absorption results of 3 different test compounds in absence (-) and presence of a tritium labeled internal standard (³H-ISTD). Shown are percent dose in skin tissue and receptor fluid, maxKp and lag time. Statistics: students t-test; ** highly, *significant difference to correlated experiment. Experiments with caffeine and testosterone were conducted with human skin preparations from the same donors and MCPA absorption was determined with rat skin.

¹⁴ C- test substance (dose)	³ H-ISTD (dose)	skin [%]	receptor [%]	maxKp [[*] 10 ⁻⁵ cm/h]	lag time [h]
caffeine (100 µg/cm ²)	-	0.5 ± 0.2	19.6 ± 6.0	62.5 ± 13.8	3.0 ± 1.1
	testosterone (0.0013 µg/cm ²)	0.6 ± 0.3	16.5 ± 3.7	40.9 ± 16.6	4.0 ± 0.9
testosterone (100 µg/cm ²)	-	1.7 ± 1.3	24.5 ± 10.6	69.3 ± 25.1	4.4 ± 1.5*
	caffeine (2.5 µg/cm ²)	0.4 ± 0.2	17.3 ± 14.8	61.8 ± 47.0	2.4 ± 0.4*
MCPA (90 µg/cm ²)	-	2.5 ± 2.4	9.2 ± 3.6	15.6 ± 14.6	1.1 ± 0.9
	testosterone (0.0017 µg/cm ²)	4.3 ± 0.9	12.6 ± 1.2	21.4 ± 10.4	0.7 ± 0.4

4.2.2 Flow-through versus static experiments

Experiments with ¹⁴C-MCPA as test substance (9 mg/mL in a MCPA-DMA formulation) including ³H-testosterone as internal standard (0.00017 mg/mL) were conducted under flow-through and static conditions. The following experimental conditions were the same for both approaches: dermatomed rat skin, water as receptor fluid, 0.7 % aqueous Texapon[®] N70 solution as washing fluid, semi-occlusive conditions, 6 h exposure and 24 h total experimental period. Different to static conditions were the continuous receptor flow of 2.4 mL/h under flow-through conditions as well as the surface area and receptor volume of the diffusion cells (1 cm² and 4 mL for static, 1.2 cm² and ~0.6 mL for flow-through).

Table 19: Dermal absorption of ¹⁴C-MCPA (90 µg/cm²) and internal standard ³H-testosterone (0.0017 µg/cm²) from a shared MCPA-DMA formulation through rat skin under static and flow-through conditions; shown are recovered doses in skin tissue and receptor fluid, maxKp and lag time; n, number of replicates. Statistics: students t-test; ** highly, *significant difference of absorption characteristics between static and flow-through experiments.

test substance (dose)	diffusion cell	n	skin [%]	receptor [%]	maxKp [10 ⁻⁵ cm/h]	lag time [h]
¹⁴C-MCPA (90 µg/cm ²)	static	3	4.3 ± 0.9	12.6 ± 1.2	21.4 ± 10.4	0.7 ± 0.4
	flow-through	4	4.5 ± 1.7	11.7 ± 1.4	22.8 ± 18.4	0.6 ± 0.2
³H-testosterone (0.0017 µg/cm ²)	static	3	2.9 ± 0.9	12.7 ± 2.1	13.4 ± 2.8**	0.6 ± 0.1
	flow-through	4	3.7 ± 1.6	15.2 ± 1.8	22.2 ± 2.7**	0.7 ± 0.2

Similar absorption results were obtained for ¹⁴C-MCPA when using the two different experimental designs (Table 19). For ³H-testosterone content in the skin, content in the receptor fluid, AD and lag time were similar, but maxKp was highly significantly faster under flow-through conditions than under

static conditions. However, the values were in the same order of magnitude (22.2 ± 2.7 and $13.4 \pm 2.8 \cdot 10^{-5}$ cm/h, respectively).

4.2.3 Repeated dosing regimen with rat skin

The effect of repeated application of test substance on dermal absorption was evaluated for MCPA. The regimen is summarized in the headline of Table 20 and in more detail in Table 5, p. 37. For experiment '3x cold, 3x wash' ^{14}C -MCPA in the form of a DMA-formulation (9 mg/mL) was applied to skin samples which were pretreated in advance three times with cold formulation (DMA-formulation with unlabeled MCPA, 9 mg/mL) and washed after 6 h on three consecutive days (total experimental period: 96 h). This treatment resulted in fast absorption of the radiolabeled test compound on day 4 (lag time 0.1 ± 0.1 h, maxKp $549 \pm 453 \cdot 10^{-5}$ cm/h) with AD of 75 ± 24 % (see Table 20 a).

Table 20: Dermal absorption of a) ^{14}C -MCPA and b) ^3H -testosterone (ISTD) through rat skin from a shared MCPA-DMA formulation after repeated dosing. For each experiment, skin samples from at least two different female animals from the same strain (CrI:WI (Han) were used. Application volume of $10 \mu\text{L}/\text{cm}^2$ led to doses of $90 \mu\text{g}/\text{cm}^2$ (^{14}C -MCPA) and $0.0017 \mu\text{g}/\text{cm}^2$ (^3H -testosterone); applied radioactive doses were $0.037 \text{ MBq}/\text{cm}^2$ for both compounds. For the repeated dosing scenario skin was pretreated three times on three consecutive days with cold formulation (DMA-formulation with unlabeled MCPA) including washing steps after 6 h with 0.7 % aqueous Texapon[®] N70 solution and cotton swaps ('3x cold, 3x wash'). Several controls were conducted to evaluate the impact of pretreatment, washing procedure and time: experiments with standard (24 h) experimental period without pretreatment ('standard, 24 h'), experiments without pretreatment, but inclusion of skin samples in diffusion cells for three days ('72 + 24 h'), experiments with pretreatment with water or blank formulation (DMA-formulation without MCPA) and experiments in which the number of washing procedures were reduced; the experiment title depicts the number of treatments and washing steps. Detailed regimen is given in Table 5, p. 37. Shown are total experimental period and number of valid replicates (n), AD, maxKp and lag time. Statistics: students t-test, ** highly, * significant difference to untreated control (no pretreatment, standard, 24 h), ** highly, + significant difference to equal pretreatment solution, but without washing steps. No statistically significant differences were observed between skin samples with equal pretreatment solution, but with one instead of three washing steps.

a) ^{14}C -MCPA:

experiment / pretreatment	period [h]	n	AD [%]	maxKp [$\cdot 10^{-5}$ cm/h]	lag time [h]
none (standard, 24 h)	24	12	14 ± 3^1	19 ± 14^1	0.8 ± 0.6^1
none (72 + 24 h)	96	5	$25 \pm 6^{**}$	26 ± 14	0.7 ± 0.3
3x water, 0x wash	96	5	17 ± 8	16 ± 17	$-0.5 \pm 0.8^{**}$
3x water, 1x wash	96	4	$58 \pm 19^{**+}$	$293 \pm 374^{**}$	$0.1 \pm 0.1^*$
3x water, 3x wash	96	4	$56 \pm 14^{**+}$	$173 \pm 112^{**+}$	$0.1 \pm 0.1^*$
3x blank, 0x wash	96	5	$36 \pm 11^{**}$	$51 \pm 31^*$	$-0.7 \pm 1.3^{**}$
3x blank, 3x wash	96	5	$75 \pm 25^{**+}$	$294 \pm 229^{**+}$	$0.1 \pm 0.1^{**+}$
3x cold, 1x wash	96	5	$70 \pm 15^{**}$	$358 \pm 364^{**}$	$0.1 \pm 0.1^*$
3x cold, 3x wash	96	4	$75 \pm 24^{**}$	$549 \pm 453^{**}$	$0.1 \pm 0.1^*$

¹combined values of three individual experiments (experiment 1: n = 3, AD = 17 ± 2 , maxKp = $21 \pm 10 \cdot 10^{-5}$ cm/h, lag time = 0.7 ± 0.4 h; experiment 2: n = 4, AD = 16 ± 3 , maxKp = $23 \pm 18 \cdot 10^{-5}$ cm/h, lag time = 0.6 ± 0.2 h; experiment 3: n = 5, AD = 12 ± 2 , maxKp = $16 \pm 15 \cdot 10^{-5}$ cm/h, lag time = 1.1 ± 0.9 h)

b) ³H-Testosterone:

experiment / pretreatment	period [h]	n	AD [%]	maxKp [$\cdot 10^{-5}$ cm/h]	lag time [h]
none (standard, 24 h)	24	7	17 ± 3 ¹	18 ± 5 ¹	0.7 ± 0.2 ¹
none (72 + 24 h)	96	5	23 ± 7*	22 ± 6	0.6 ± 0.0
3x water, 0x wash	96	5	20 ± 8	17 ± 5**	0.6 ± 0.1
3x water, 1x wash	96	4	52 ± 18***	88 ± 62***	0.2 ± 0.1***
3x water, 3x wash	96	4	50 ± 12***	67 ± 28***	0.3 ± 0.1***
3x blank, 0x wash	96	5	40 ± 5**	38 ± 11**	0.4 ± 0.2**
3x blank, 3x wash	96	5	66 ± 15***	107 ± 67**	0.1 ± 0.1***
3x cold, 1x wash	96	5	67 ± 15**	117 ± 81**	0.2 ± 0.1**
3x cold, 3x wash	96	4	62 ± 16**	142 ± 93**	0.2 ± 0.1**

¹combined values of two individual experiments (experiment 1: n = 3, AD = 15 ± 3 %, maxKp = 13 ± 3 $\cdot 10^{-5}$ cm/h, lag time = 0.6 ± 0.0 h; experiment 2: n = 4, AD = 19 ± 3 %, maxKp = 22 ± 3 $\cdot 10^{-5}$ cm/h, lag time = 0.7 ± 0.2 h)

Several variations of the experiment were performed in parallel to evaluate the effect of pretreatment, washing procedure and time (see Table 20 a). All other experimental conditions like receptor fluid (water) stayed the same. Considering time the untreated control '72 + 24 h' (three days untreated in Franz cell followed by application of test substance on the fourth day) revealed slightly higher absorption results than the untreated control under standard conditions ('standard, 24 h'): AD was significantly higher (25 ± 6 compared to 14 ± 3 %). In comparison to these two experiments, pretreatment with water without washing procedures over three days led to results in the same range ('3x water, 0x wash'): AD was 17 ± 8 %. Inclusion of washing steps after water pretreatment increases significantly the absorption of ¹⁴C-MCPA. However, no difference was observed between three washing procedures after every water treatment ('3x water, 3x wash') or one washing procedure after the last water application ('3x water, 1x wash'); AD was 56 ± 14 and 58 ± 19 % of the dose, respectively. Similarly, skin samples washed only once after three pretreatments with cold formulation ('3x cold, 1x wash') led to similar results as skin samples washed each time after three treatments with cold formulation (AD 70 ± 15 and 75 ± 24 %, respectively). Comparing the groups with the same number of washing steps, pretreatment with cold formulation led to obviously higher absorption of ¹⁴C-MCPA than water treatment. Skin samples treated three times with blank formulation (corresponding DMA-formulation without MCPA) including three washing steps in between ('3x blank, 3x wash') led to the same absorption results as the parallel treatment with cold formulation (AD 75 ± 25 and 75 ± 24 %, respectively). Waiving washing after three applications of blank formulation led to significantly lower absorption results for ¹⁴C-MCPA (AD 36 ± 11 %). However, in comparison to water treatment without washing, the results were higher. The ISTD ³H-testosterone was applied along with the test compound ¹⁴C-MCPA in the DMA-formulation (0.00017 mg/mL). The effects of the several treatments on the absorption results of ³H-testosterone parallel the results obtained for ¹⁴C-MCPA (see Table 20 b). Congruent were the increased absorption in comparison to the standard experiment over 24 h after pretreatment with water ('3x water, 1x wash' and '3x water and 3x wash'), cold ('3x cold, 1x' wash and '3x cold, 3x wash') or blank DMA-formulation ('3x blank, 3x wash') if accompanied by washing

procedures, the lower effect observed for blank formulation if the washing procedure was waived ('3x blank, 0x wash'), the total absence of effect when applying water and waiving the washing procedure ('3x water, 0x wash') and the absence of any effect for elongation of the experimental period without additional treatments ('72 + 24 h').

4.2.4 Preparation types of human skin ex vivo

The impact of skin preparation type on absorption results was investigated by using DMS (dermatomed skin) and FTS (full-thickness skin) samples from the same human donors. The thickness was about 450 and 1000 μm , respectively. ^{14}C -MCPA-EHE was applied as emulsion in water (16 mg/mL) and ^{14}C -MCPA as DMA-formulation (9 mg/mL) semi-occlusively. Water was used as receptor fluid. ^3H -testosterone was applied as ISTD alongside with each of these two compounds in lower concentration of 0.00017 mg/mL. No general differences were observed for both applications of ^3H -testosterone, wherefore the average absorption results are reported in Table 21. The same applies to ^3H -mannitol which was applied as ISTD (0.0004 mg/mL) alongside with ^{14}C -caffeine (4 mg/mL) or ^{14}C -testosterone (4 mg/mL) in ethanol/water-mixture 1/1, v/v, occlusively. Tap water was used as receptor fluid for the experiments with ^{14}C -caffeine and 5 % BSA in tap water for the experiments with ^{14}C -testosterone.

Table 21: Dermal absorption results with human DMS and FTS. The same donors were used for the different preparation types (prep), but only valid experiments were compared, why the number of individual experiments can differ (n). The other experimental conditions were identical. The vehicle (EW, ethanol/water mixture (1/1, v/v), W, water, DMA, aqueous dimethylamine-formulation) and the applied dose are given in the table. Shown are results of different test substances: percent dose in the skin and the receptor fluid, AD, maxKp and lag time. Statistics: student's t-test, ** highly, * significant difference between the two preparation types.

test substance (vehicle, dose)	prep	n	skin [%]	receptor [%]	AD [%]	maxKp [10^{-5}cm/h]	lag time [h]
^{14}C -MCPA-EHE (W, 160 $\mu\text{g}/\text{cm}^2$)	DMS	5	1.7 \pm 1.5	1.8 \pm 1.2	3.5 \pm 1.9	0.9 \pm 0.7	12.7 \pm 0.9
	FTS	4	3.6 \pm 2.3	4.1 \pm 2.5	7.6 \pm 2.9	0.8 \pm 0.3	10.6 \pm 2.1
^{14}C - testosterone (EW, 100 $\mu\text{g}/\text{cm}^2$)	DMS	4	0.5 \pm 0.2**	11.6 \pm 1.1	12.1 \pm 1.2*	35.1 \pm 2.0**	2.3 \pm 0.6**
	FTS	5	6.3 \pm 2.5**	13.4 \pm 3.9	19.7 \pm 5.4*	20.9 \pm 7.3**	5.9 \pm 0.5**
^3H -testosterone (DMA or W, 0.0017 $\mu\text{g}/\text{cm}^2$)	DMS	10	3.2 \pm 1.2**	18.9 \pm 6.9**	22.1 \pm 7.1	16.4 \pm 8.3**	1.4 \pm 0.7**
	FTS	8	17.4 \pm 9.5**	8.2 \pm 2.1**	25.6 \pm 9.2	3.0 \pm 1.2**	7.6 \pm 4.1**
^{14}C -MCPA (DMA, 90 $\mu\text{g}/\text{cm}^2$)	DMS	5	1.8 \pm 1.2*	9.9 \pm 3.2	11.7 \pm 2.3*	10.7 \pm 6.3	5.6 \pm 1.5
	FTS	4	5.8 \pm 3.4*	10.9 \pm 2.9	16.7 \pm 2.8*	9.3 \pm 3.8	7.6 \pm 2.0
^{14}C -caffeine (EW, 100 $\mu\text{g}/\text{cm}^2$)	DMS	5	4.0 \pm 3.6	43.0 \pm 14.5	47.0 \pm 14.0	90.1 \pm 36.8	4.9 \pm 2.1
	FTS	5	17.1 \pm 17.3	30.2 \pm 16.0	47.3 \pm 11.7	59.3 \pm 40.4	8.4 \pm 5.2
^3H -mannitol (EW, 0.01 $\mu\text{g}/\text{cm}^2$)	DMS	9	4.7 \pm 4.1	8.7 \pm 6.7	13.3 \pm 5.3	19.0 \pm 16.5	4.3 \pm 2.4*
	FTS	10	13.3 \pm 13.2	9.0 \pm 7.2	22.3 \pm 12.8	15.5 \pm 15.9	7.4 \pm 3.3*

Generally, the obtained results were slightly or significantly different for both scenarios, but in the same order of magnitude (see Table 21). The percentage amount of the radioactivity remaining in the

skin was higher if FTS was used. Significant differences were observed for ^{14}C -MCPA (DMS: 1.8 ± 1.2 , FTS: 5.8 ± 3.4 %), ^{14}C -testosterone (DMS: 0.5 ± 0.2 , FTS: 6.3 ± 2.5 %) and ^3H -testosterone (DMS: 3.2 ± 1.2 , FTS: 17.4 ± 9.5 %). The percentage amount of the radioactivity recovered in the receptor fluid was independent of skin preparation type for test substances ^3H -mannitol, ^{14}C -testosterone and ^{14}C -MCPA; lower values in the receptor fluid were obtained when FTS was used instead of DMS for ^{14}C -caffeine (FTS: 30.2 ± 16.0 , DMS: 43.0 ± 14.5 %) and ^3H -testosterone (FTS: 8.2 ± 2.1 , DMS: 18.9 ± 6.9 %, statistically significant) and higher values for ^{14}C -MCPA-EHE (FTS: 4.1 ± 2.5 , DMS: 1.8 ± 1.2 %). In sum, AD was higher with FTS for all compounds (statistically significant for ^{14}C -testosterone and ^{14}C -MCPA) except ^{14}C -caffeine; ^{14}C -caffeine led to close AD values with FTS and DMS (47.3 ± 11.7 and 47.0 ± 14.0 %, respectively). The lag time was generally longer when using FTS. Significant differences were observed for ^{14}C -testosterone (FTS: 5.9 ± 0.5 , DMS: 2.3 ± 0.6 h), ^3H -testosterone (FTS: 7.6 ± 4.1 , DMS: 1.4 ± 0.7 h) and ^3H -mannitol (FTS: 7.4 ± 3.3 , DMS: 4.3 ± 2.4 h). Only ^{14}C -MCPA-EHE revealed a slightly, but not significantly, shorter lag time when using FTS (10.6 ± 2.1 h) in comparison to DMS (12.7 ± 0.9 h). The maxKp values were lower when using FTS with all test compounds. Significantly slower absorption was observed for ^{14}C -testosterone (FTS: 20.9 ± 7.3 , DMS: $35.1 \pm 2.0 \cdot 10^{-5}$ cm/h) and ^3H -testosterone (FTS: 3.0 ± 1.2 , DMS: $16.4 \pm 8.3 \cdot 10^{-5}$ cm/h). In contrast, the average Kp values for ^3H -water – originated from integrity test TWF – were similar for FTS ($248 \pm 156 \cdot 10^{-5}$ cm/h) and DMS ($302 \pm 188 \cdot 10^{-5}$ cm/h).

4.2.5 Skin equivalents

4.2.5.1 StrataTest[®]

Using the reconstructed human skin StrataTest[®] as barrier system for dermal absorption experiments in vitro, led to generally high and fast absorption of ^{14}C -caffeine (4 mg/mL in ethanol/water mixture 1/1, v/v), ^{14}C -testosterone (4 mg/mL in ethanol/water mixture 1/1, v/v) and ^{14}C -MCPA (9 mg/mL in MCPA-DMA-formulation including ISTD ^3H -testosterone, 0.00017 mg/mL) (see Table 22). The comparison to human skin is given in chapter 4.2.6.

Different storage conditions after delivery of constructs did not influence the results for test compound ^{14}C -MCPA (see Table 22): For example, AD obtained with StrataTest[®] stored for 6 d under culture conditions was 90 ± 6 % and 94 ± 3 % with constructs stored 4 d at 8°C and 1 d under culture conditions. For the ISTD ^3H -testosterone storage under culture conditions decreased significantly AD (72 ± 5 %) in comparison to storage at 4°C (85 ± 4 %). Presence of the underlying membrane led to similar AD (here including content in membrane) for ^{14}C -caffeine and ^{14}C -testosterone, but slightly lowers maxKp values in comparison to skin constructs without this membrane. Highly significantly lower maxKp values were obtained for ^{14}C -caffeine ($746 \pm 131 \cdot 10^{-5}$ cm/h in comparison to $1242 \pm 247 \cdot 10^{-5}$ cm/h). In general, a substantial amount of test compound was bound to the membrane (25 ± 2 and 14 ± 9 % of dose for ^{14}C -caffeine and ^{14}C -testosterone, respectively).

Table 22: Dermal absorption results with reconstructed human skin StrataTest®. Four different substances were tested under two different test conditions each. ¹⁴C-caffeine and ¹⁴C-testosterone were tested with and without the underlying membrane of the skin construct. ¹⁴C-MCPA and the ISTD ³H-testosterone were tested after storage at 8°C for 4 d and 1 d under culture conditions or under culture conditions for 6 d, but generally without the membrane. All other experimental conditions were identical. The vehicle (EW, ethanol/water mixture (1/1, v/v), DMA, aqueous dimethylamine-formulation) and the applied dose are given in the table. Shown are AD (defined as sum of recovered dose in skin, receptor fluid and – for experiments with membrane – in membrane), maxKp and lag time. Statistics: student's t-test, ** highly, * significant difference between the two experimental conditions.

test substance (vehicle, dose)	conditions	n	membrane [%]	AD (incl. membrane) [%]	maxKp [10 ⁻⁵ cm/h]	lag time [h]
¹⁴C-caffeine (EW, 100 µg/cm ²)	- membrane	5	-	96 ± 1**	1242 ± 247**	0.2 ± 0.04
	+ membrane	5	25 ± 2	101 ± 1**	746 ± 131**	0.3 ± 0.1
¹⁴C-testosterone (EW, 100 µg/cm ²)	- membrane	3	-	60 ± 9	290 ± 155	0.5 ± 0.2*
	+ membrane	5	14 ± 9	65 ± 22	242 ± 46	0.8 ± 0.1*
¹⁴C-MCPA (DMA, 90 µg/cm ²)	4 d 8°C + 1 d culture	5	-	94 ± 3	547 ± 123	0.2 ± 0.2
	6 d culture	5	-	90 ± 6	433 ± 342	0.3 ± 0.2
³H-testosterone (DMA, .0017 µg/cm ²)	4 d 8°C + 1 d culture	5	-	85 ± 4**	408 ± 152	0.04 ± 0.08
	6 d culture	5	-	72 ± 5**	309 ± 156	0.03 ± 0.07

4.2.5.2 Skin-PAMPA

To evaluate skin-PAMPA, permeation characteristics of performance standards were investigated. Donor solutions of 1 mM (atenolol, chlorpromazine, niflumic acid, piroxicam, verapamil and warfarin) and 1.5 mM (progesterone) were prepared in prisma HT buffer at two different pH levels (6.5 and 7.4) and applied to skin-PAMPA membranes for 5 h. Resulting Kp values and percent dose in the membrane are listed in Table 23 a. Similar Kp values at pH 6.5 and 7.4 were observed for performance standards progesterone (3650 ± 994 and 3123 ± 746 *10⁻⁵cm/h), and atenolol (183 ± 12 and 124 ± 25*10⁻⁵cm/h). Higher absorption at pH 6.5 in comparison to pH 7.4 was observed for warfarin (352 ± 71 and 103 ± 14*10⁻⁵cm/h) and piroxicam (983 ± 49 and 207 ± 25*10⁻⁵cm/h). Lower absorption at pH 6.5 in comparison to pH 7.4 was obtained with chlorpromazine (781 ± 62 and 3316 ± 251*10⁻⁵cm/h) and verapamil (94 ± 19 and 1138 ± 184*10⁻⁵cm/h). The fastest absorptions were observed for verapamil and chlorpromazine at pH 7.4 and for progesterone at pH 6.4 and 7.4. The slowest absorption was observed for atenolol.

Model compounds caffeine, testosterone and MCPA were applied in concentrations of 1 mM in prisma HT buffer at two pH levels (pH 6.5 and 7.4) for 5 h. MCPA was additionally applied in prisma HT buffer at pH 4.5. Different pH values were chosen to examine the effect of ionization on the diffusion over the skin-PAMPA barrier. The results are listed in Table 23 b. The fastest absorption was observed for testosterone with similar results for the two different pH values (pH 6.5: 2358 ± 292, pH 7.4: 2528 ± 226*10⁻⁵cm/h). Also close results for both pH values were obtained for caffeine (pH 6.5: 206 ± 17, pH 7.5: 241 ± 38*10⁻⁵cm/h). For MCPA a tendency to higher absorption with lower pH was observed. The fastest absorption was obtained with pH 4.5 (307 ± 43*10⁻⁵cm/h) followed by pH 6.5 (89 ± 27*10⁻⁵cm/h)

and pH 7.4 ($67 \pm 42 \cdot 10^{-5} \text{cm/h}$). The comparison of the absorption results to human skin results is given in chapter 4.2.6.

Table 23: Permeation results of a) performance standards and b) model compounds through skin-PAMPA. Given are concentration of compounds in donor (prisma HT buffer), pH of donor, absorption maximum (λ) and results in the form of Kp and membrane retention in percentage of the applied dose. Statistics: student's t-test, ** highly, * significant difference between pH 6.5 and pH 7.4; ** highly, + significant difference between pH 4.5 and pH 6.5 or pH 7.5.

a) performance standards

compound (concentration in mM, mg/mL)	pH	λ [nm]	membrane [%]	Kp [* 10^{-5} cm/h]
progesterone (1.5, 0.47)	6.5	249	57 \pm 4	3650 \pm 994
	7.4	249	55 \pm 2	3123 \pm 746
warfarin (1, 0.31)	6.5	308	2 \pm 1	352 \pm 71
	7.4	308	1 \pm 1	103 \pm 14
niflumic acid (1, 0.28)	6.5	287	4 \pm 6	551 \pm 118
	7.4	287	2 \pm 2	172 \pm 26
atenolol (1, 0.27)	6.5	270	0 \pm 0	183 \pm 12
	7.4	270	2 \pm 1	124 \pm 24
verapamil (1, 0.49)	6.5	278	7 \pm 0	95 \pm 17
	7.4	278	19 \pm 1	1138 \pm 184
piroxicam (1, 0.33)	6.5	354	3 \pm 3	983 \pm 49
	7.4	354	3 \pm 2	207 \pm 25
chlorpromazine (1, 0.32)	6.5	254	24 \pm 2	781 \pm 62
	7.4	254	44 \pm 2	3316 \pm 251

b) model compounds

compound (concentration in mM, mg/mL)	pH	λ [nm]	membrane [%]	Kp [* 10^{-5} cm/h]
testosterone (1, 0.29)	6.5	249	0.0 \pm 0.0	2358 \pm 292
	7.4	249	0.0 \pm 0.0	2528 \pm 226
caffeine (1, 0.20)	6.5	273	0.5 \pm 0.6	206 \pm 17
	7.4	273	0.3 \pm 0.5	241 \pm 38
MCPA (1, 0.20)	4.5	282	1.5 \pm 0.8	307 \pm 43
	6.5	282	0.2 \pm 0.4	89 \pm 27 ⁺⁺
	7.4	282	0.8 \pm 1.6	67 \pm 42 ⁺⁺

4.2.6 Cross-comparison of various skin models

Absorption characteristics of ^{14}C -labeled caffeine, testosterone and MCPA through different skin models are shown in Figure 13 a – c. For direct comparison, diffusion cell (static) experiments with human skin, rat skin and StrataTest[®] were conducted under the same experimental conditions (e.g. identical application solution, receptor fluid and occlusion conditions): For ^{14}C -caffeine a solution in ethanol/water-mixture 1/1, v/v, (100 $\mu\text{g}/\text{cm}^2$, 4mg/mL) was applied occlusively using tap water as

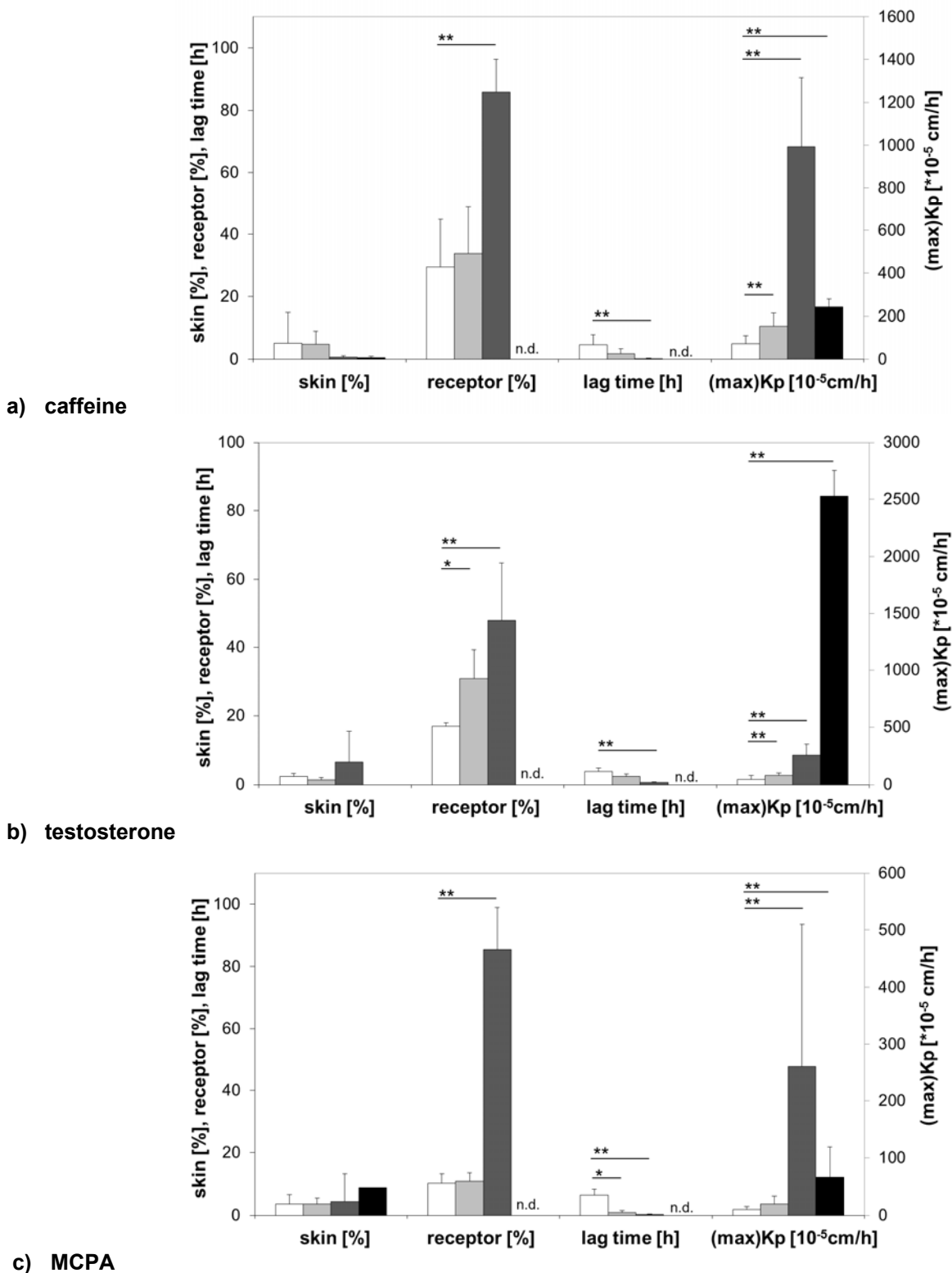


Figure 13: Comparison of a) caffeine, b) testosterone and c) MCPA absorption through different barrier systems: human skin (white), rat skin (light grey), StrataTest® (dark grey) and skin-PAMPA (black); with exception of skin-PAMPA, identical diffusion cell (static) experiments were conducted (details given in the text); experiments with skin-PAMPA were conducted as similar as possible to the other experiments; membrane retention from skin-PAMPA is shown as skin content and Kp values in direct comparison to maxKp values; content in receptor fluid and lag time was not determinable with skin-PAMPA (n.d.); percentage of the recovered dose in skin and receptor [%] as well as lag time [h] refer to the left y-axis, maxKp [10^{-5} cm/h] refer to the right y-axis; Statistics: students t-test, ** highly, * significant difference to human skin.

receptor fluid; for ^{14}C -testosterone a solution in ethanol/water-mixture 1/1, v/v, (100 $\mu\text{g}/\text{cm}^2$, 4mg/mL) was applied occlusively using 5 % BSA in tap water as receptor fluid and for ^{14}C -MCPA a DMA-formulation was applied (90 $\mu\text{g}/\text{cm}^2$, 9 mg/mL) semi-occlusively using water as receptor fluid. Mean values for human skin experiments (FTS and DMS), mean values for StrataTest[®] approaches and results for untreated rat skin with total experimental period of 24 h were used for the comparisons. Experiments with skin-PAMPA were conducted as similar as possible to the above listed conditions, but remarkably different: Unlabeled compounds were diluted in prisma HT buffer at pH 7.4; MCPA together with DMA, but without other formulation ingredients. The receptor fluid was prisma HT buffer pH 7.4 and the system was occluded during the experimental period of 5 h – which was shorter than in diffusion cell experiments (24 h). A further difference was the infinite dose regimen for skin-PAMPA and the finite regimen for diffusion cell experiments. Therefore Kp values were compared with maxKp values. The membrane retention obtained for skin-PAMPA was compared with the skin content from the other models. No receptor content due to infinite dose conditions and no lag time due to missing kinetic samples could be determined with skin-PAMPA.

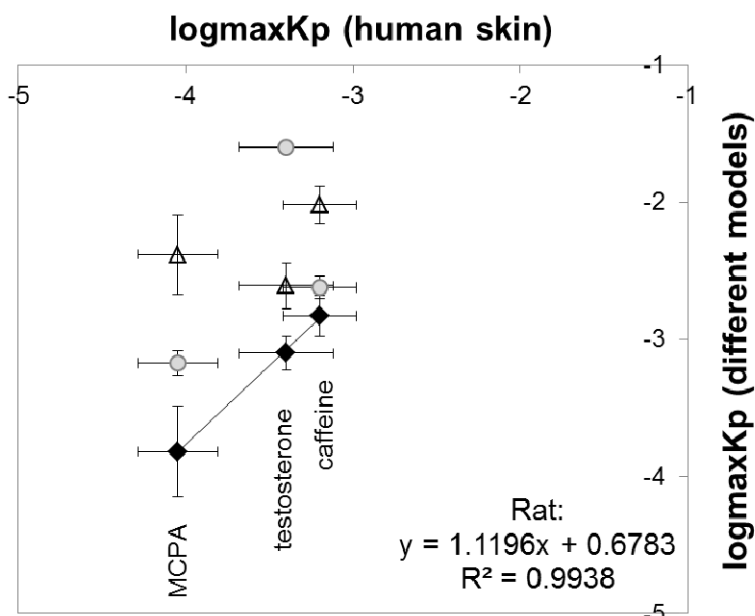


Figure 14: LogmaxKp values for MCPA, testosterone and caffeine generated with human skin preparations plotted against logmaxKp values generated with other skin models. Against rat skin: black diamonds, against StrataTest[®]: open triangles, against skin-PAMPA: grey circles. Resulting linear regression between human and rat skin preparations is shown in the graph including equation and coefficient of determination.

Test substance absorption through rat skin preparations was slightly faster and higher than through human skin preparations. Significantly different were maxKp values for ^{14}C -caffeine (rat: 154 ± 62 , human: $71 \pm 39 \cdot 10^{-5} \text{cm/h}$), the recovered dose in receptor fluid (rat: 30 ± 8 , human: $17 \pm 10 \%$) and maxKp values for ^{14}C -testosterone (rat: 82 ± 21 , human: $47 \pm 33 \cdot 10^{-5} \text{cm/h}$), and the lag time for ^{14}C -MCPA (rat: 0.8 ± 0.6 , human: $6.5 \pm 2.0 \text{h}$). StrataTest[®] as well as skin-PAMPA led to significantly higher and faster absorption than human skin in general (see Figure 13 a – c). The use of StrataTest[®] resulted in 5 – 49 times higher maxKp and 3 – 4 times higher AD values compared to human skin; the use of skin-PAMPA resulted in 3 – 53 times higher Kp values.

An obvious linear relationship between results generated with different skin models was apparent for logmaxKp from human and rat skin experiments, but for no other combination (see Figure 14).

4.3 Metabolic activity of skin models

4.3.1 Biotransformation of MCPA-EHE in human skin

4.3.1.1 Chemical stability

Chemical stability of ^{14}C -MCPA-EHE in water (41.7 kBq/mL, 13 mg/L, 0.3 % ACN, acetonitrile) at pH 4 – 5 was investigated up to 96 h. The test substance preparation was stirred over the entire period and diluted with ACN (1/1, v/v) for HPLC-UV/RAD measurements. The recoveries in percentages of the initial concentration after distinct time points up to 96 h were 98 ± 4 and 97 ± 7 % for RAD and UV detection, respectively. Under these abiotic conditions neither time dependent decrease of ^{14}C -MCPA-EHE nor ^{14}C -MCPA formation was detectable (see Table 24). In an additional test ^{14}C -MCPA-EHE solution in ACN (36 kBq, 11 mg/L) was evaporated to dryness under nitrogen and resolved in ACN. The recovery based on radiodetection was 103 ± 0.7 %.

Table 24: Stability analysis of ^{14}C -MCPA-EHE emulsion in water containing 0.3 % ACN. Shown are chromatographic (HPLC-UV/RAD) results at distinct time points after preparation; the test substance preparation was stirred over the entire period and diluted with ACN for measurements; concentrations of MCPA-EHE were determined via external calibration with cold standards; the recovery was calculated in relation to the initial concentration at time point 0 h (recovery UV). The recovery based on radiodetection (recovery RAD) was calculated in relation to the peak area of time point 0 h. No other peaks were detected at any time point.

time point [h]	MCPA-EHE conc. [mg/L]	recovery UV [%]	recovery RAD [%]
0	13.2		
1.5	12.4	94.0	98.7
2.5	13.0	98.5	102.1
3	14.0	106.6	102.0
5	13.8	105.0	97.3
7	11.6	88.4	101.0
24	11.8	90.0	91.8
96	13.0	99.2	95.2

4.3.1.2 In vitro biotransformation in human skin S9 fraction

Chemical stability and biotic breakdown of ^{14}C -MCPA-EHE were determined in S9 fraction derived from cryoconserved human skin obtained from two different donors. Model substrate fluorescein diacetate was applied as a positive control for hydrolysis and used to determine the overall esterase activity. Testosterone was used as model substrate for CYP-dependent activity. Rat liver S9 fraction was incubated in parallel to human skin S9 fraction for general assay functionality.

Esterase activity measured via the model substrate fluorescein diacetate (0.051 mM) in S9 fraction of human skin and rat liver resulted in a turn-over of 0.7 ± 0.6 and 5.4 ± 0.4 nmol/(min*mg protein), respectively. The LOQ of the method was 0.02 nmol/(min*mg protein). In the actual substrate

incubation (AI) of human skin S9 fraction, 59 % of the applied substrate ^{14}C -MCPA-EHE was recovered unchanged and 9 % as the hydrolysis product ^{14}C -MCPA – when relating the peak areas from HPLC-RAD measurement to the buffer control (BC). In the heat-deactivated control (HDC) and the immediately-stopped substrate incubation (t_0) the recovery of ^{14}C -MCPA-EHE was 55 % and 92 %, respectively. No degradation products were detectable in these two controls (see Figure 15 a). The recovery of the parallelly applied model substrate testosterone related to BC was on average 92 % and no metabolites were detectable. Incubating rat liver S9 fraction (AI) with testosterone resulted in several metabolites and a 21 % turn-over of testosterone. No turn-over was observed in the corresponding controls (HDC and t_0) (data not shown). Incubation of rat liver S9 with substrate ^{14}C -MCPA-EHE resulted in a total metabolic turn-over after 30 min (AI). 96 % of the radioactivity was recovered as ^{14}C -MCPA and 3 % as ^{14}C -HMCPA when relating the amounts to BC. In the control t_0 19 % of the substrate was hydrolyzed to ^{14}C -MCPA and 77 % recovered as the parent molecule. In the heat-deactivated control (HDC) 32 % were recovered in the form of the parent ^{14}C -MCPA-EHE, whereas no degradation products were detected (see Figure 15 b).

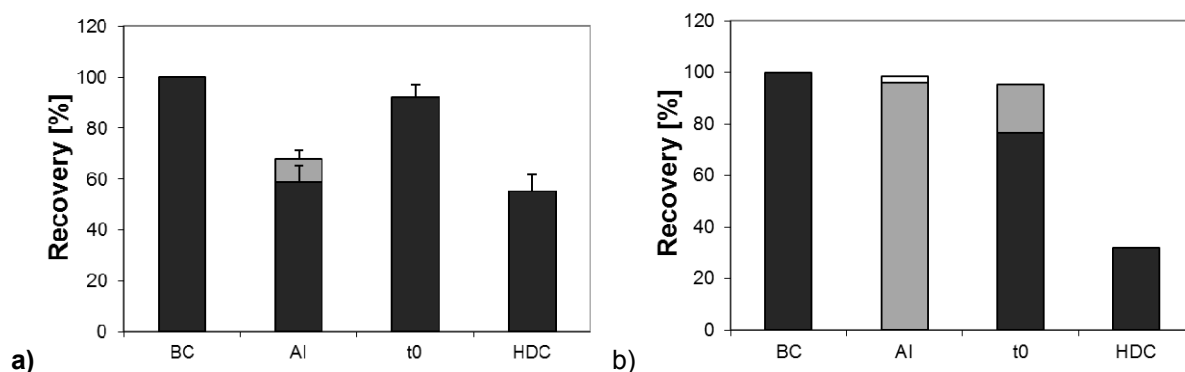


Figure 15: Biotransformation of ^{14}C -MCPA-EHE in S9 fraction of a) human skin (two different donors) and b) rat liver (positive control). AI: actual substrate incubation, t_0 : immediately-stopped substrate incubation, HDC: heat-deactivated control, BC: buffer control. Shown are recoveries of radioactivity in the form of ^{14}C -MCPA-EHE (black), ^{14}C -MCPA (grey) and ^{14}C -HMCPA (white) in relation to the parent molecule ^{14}C -MCPA-EHE in buffer control (BC) determined via HPLC-RAD.

4.3.1.3 In vitro biotransformation in human skin during absorption experiments

To determine if and where biotransformation occur during a standard absorption experiment in diffusion cells (static), ^{14}C -MCPA-EHE was used as model substrate and applied in an aqueous emulsion (8.2 MBq/g, 160 $\mu\text{g}/\text{cm}^2$, 16 mg/mL) on DMS and FTS from the same human donor. Water was used as the receptor fluid (solubility 0.4 ± 0.13 g/L). Furthermore, water was used as matrix for skin homogenization at the end of the run. The mass balance of the absorption experiments was 100 ± 2 %. The various samples of one experiment were extracted with several solvents (ethanol, ethyl acetate and dichloromethane), concentrated and combined to four samples: application solution, washing fluid, skin and receptor fluid. These samples were separated via HPLC in one-minute fractions and measured with LSC. The measured radioactivities were used to calculate the recoveries of the four samples after these steps. Results are given in Table 25. Recoveries for the application and

receptor fluid were > 90 %, for the washing fluid 76 ± 15 % in average and 8 or 37 % for the skin homogenates.

Table 25: Recovery of radioactivity after extraction. The recovery was calculated by relating the radioactivity collected after extraction steps and HPLC separation to the activity in the samples before these steps.

	DMS	FTS	mean \pm SD
application solution	99	97	98 ± 1
washing fluid	87	66	76 ± 15
skin	8	37	23 ± 21
receptor fluid	91	101	96 ± 7

Using the LSC-measured one-minute fractions, radiochromatograms were reconstructed. Figure 16 shows an overlay of the chromatograms for washing fluid, skin and receptor fluid using DMS. Resulting peak areas are reported in Table 26. With exception of the skin homogenate derived from experiments with DMS, ^{14}C -MCPA-EHE was detected in all compartments of both skin preparations. The corresponding acid ^{14}C -MCPA was not detected in the original application solution, but with 0.14 and 0.04 μM – or 1.7 and 0.5 % – in the washing fluids when using DMS or FTS, respectively. Furthermore it was present in the skin homogenate originated from DMS and in both receptor fluids.

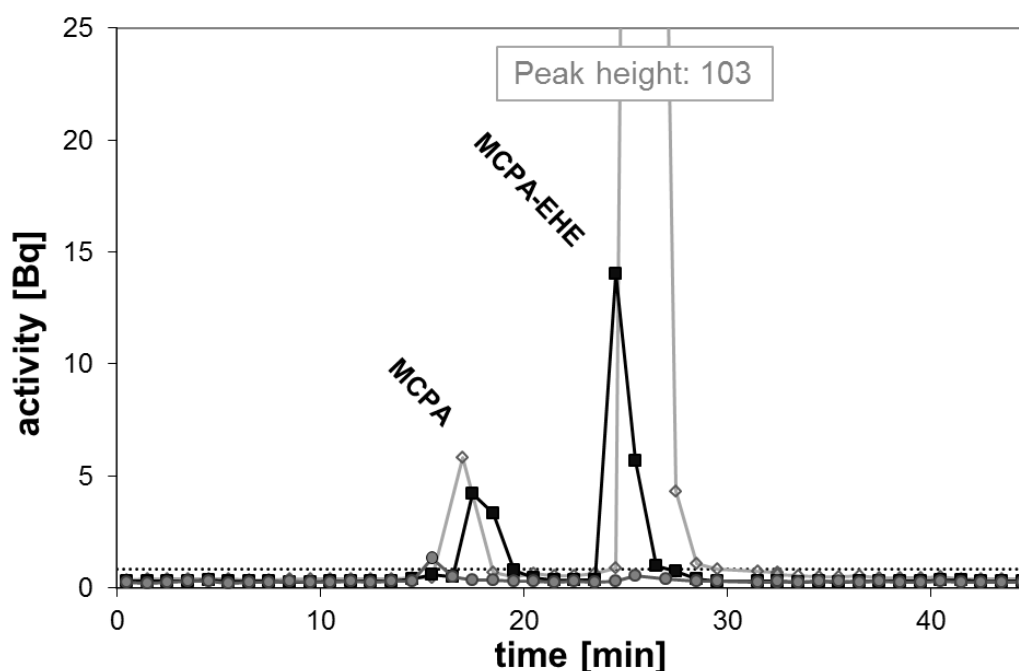


Figure 16: Reconstructed radiochromatograms of washing fluid (open diamonds, light grey), skin (filled circles, dark grey) and receptor fluid (filled squares, black) from dermal absorption experiment with ^{14}C -MCPA-EHE and DMS from a human donor. Samples were separated via HPLC; and collected one-minute fractions were measured via LSC. Retention time of MCPA was about 17.5 min and of MCPA-EHE about 25.5 min. The dotted line represents LOQ (0.9 Bq) for one single LSC sample of one minute and 0.8 mL; LOQ was determined with collected fractions from blank (ACN).

Table 26: Presence of ^{14}C -MCPA-EHE and ^{14}C -MCPA in different compartments after dermal absorption experiments with DMS and FTS from one human donor. Absolut peak areas in Bq – derived from radiochromatograms reconstructed with HPLC-separated one-minute fractions measured via LSC – were transformed with the specific activity and the molecular weight of the parent ^{14}C -MCPA-EHE and the injection volume of 25 μl into concentrations [μM]. LOD and LOQ were 0.03 and 0.04 μM .

	MCPA [μM]		MCPA-EHE [μM]	
	DMS	FTS	DMS	FTS
application solution	-	-	6.82	8.27
washing fluid	0.14	0.04	8.19	6.15
skin	0.07	-	-	0.41
receptor	0.37	0.43	0.96	0.14

4.3.2 Xenobiotic-metabolizing enzyme activities in skin construct StrataTest[®]

Table 27: Xenobiotic-metabolizing enzyme activities in StrataTest[®] skin constructs. Beneath activities in subcellular fractions (S9: S9 fraction, C: cytosol, M: microsomes) of StrataTest[®] and the positive control (rat liver), the table shows LOD, LOQ as well as the basis for their calculation: BC: buffer control, HDC: heat-deactivated control. N: number of charges, n: number of replicates.

enzyme	subcellular fraction	basis for LOD/LOQ	enzyme activity [nmol/(min*mg)]				N	n
			LOD	LOQ	rat liver	Strata Test [®]		
NAT 1	S9	BC	0.009	0.03	3.3 \pm 0.1	7.2 \pm 1.6	3	3/4
esterase	S9	BC	0.01	0.02	5.4 \pm 0.4	3.6 \pm 0.1	3	3
ADH ¹	C	HDC rat HDC strata	R: 9 S: 36	R: 19 S: 71	> LOD, < LOQ	< LOD	3	3
AIDH	C	BC	1.3	2.5	20.6 \pm 2.3	3.1 \pm 0.8	2	3
FMO 1/3	M	BC	0.1	0.3	6.8 \pm 0.3	0.5 \pm 0.1	3	2
EROD ²	M	BC	0.001	0.002	0.977 \pm 0.006	< LOD	3	3
PROD ³	M	BC	0.004	0.007	0.100 \pm 0.002	< LOD	3	3
BROD ⁴	M	BC	0.001	0.002	0.428 \pm 0.011	< LOD	3	3
UGT 1	M	BC	0.5	0.9	51.0 \pm 0.004	< LOD	3	2
UGT 2 ⁵	M	BC	1457	2914	95577	< LOD	3	2

¹ LOD and LOQ for ADH were calculated based on HDC (heat-deactivated control), so that each species has its own limit values; S: StrataTest[®], R: rat liver

² CYP isoform with ethoxyresorufin-O-deethylase activity inducible with 3-methylcholanthrene, mainly CYP 1A

³ CYP isoform with pentoxyresorufin-O-depentyase activity inducible with phenobarbital, mainly CYP 2B

⁴ CYP isoform with benzyloxyresorufin-O-debenzylase activity inducible with 3-methylcholanthrene and phenobarbital, mainly CYP 1A/2B/3A

⁵ UGT 2-activity is given in Δ fluorescence units/(min*mg protein)

To characterize the metabolic activity of the human skin construct StrataTest[®], 10 xenobiotic-metabolizing enzyme activities were determined via individual model substrate turn-over in respective subcellular fractions (see Table 27). High enzyme activities of 7.2 \pm 1.6 and 3.6 \pm 0.1 nmol/(min*mg protein) were measured for NAT 1 and esterase in S9 fraction, respectively. Used model substrates

were PABA and fluorescein diacetate, respectively. Slightly over quantification limits were activities for AIDH and FMO 1/3 (3.1 ± 0.8 and 0.5 ± 0.1 nmol/(min*mg protein), respectively), whereby propionaldehyde and BA were used as model substrates and cytosol and microsomes as subcellular fraction, respectively. ADH activity measured with ethanol as substrate in cytosol was below LOD of 36 nmol/(min*mg protein). EROD, PROD and BROD activities were not detectable in microsomes (LOD 0.001, 0.004, 0.001 nmol/(min*mg protein), respectively). MUF-specific UGT 1 activity was below LOD (0.5 nmol/(min*mg protein)) as well as the HOBI-specific UGT 2 activity (LOD 1457 Δ fluorescence units/(min*mg protein) – both measured in microsomes. LOD and LOQ of the assays as well as activities in the positive control (rat liver) are given in Table 27. ADH activity was detectable in the positive control, but not quantifiable (LOD 9, LOQ 19 nmol/(min*mg protein)). Since a clear linear turn-over was observed, it was assessed as a positive response.

4.4 In silico models for dermal absorption

In silico prediction models for dermal absorption were developed on the basis of routine in vitro experiments conducted at and for BASF SE. Active compounds, including their chemical formula, CAS number and calculated Abraham-descriptors are listed in Table 47 (annex). Experimental conditions like species and receptor fluid, results in the form of logmaxKp and calculated mixture factors (MF) of single experiments are given in Table 48 (annex). Out of 87 MFs used for calculations, values for molinspTPSA, molinspLogHBAcc, AdmeLogHBDon, AdmeP_{ow} and Adme1/RotB are given as examples (the prefix indicates the software used for the calculation of the value: 'Adme', ADME Boxes version 4.95 and 'molinsp', Molinspiration Property Calculator, respectively). To evaluate the relation between calculated and experimental data, linear regression analyses were run for two examples: logP_{ow} and logS_w (the logarithm of water solubility). The obtained R² values were 0.75 and 0.76, respectively (Figure 17 a and b).

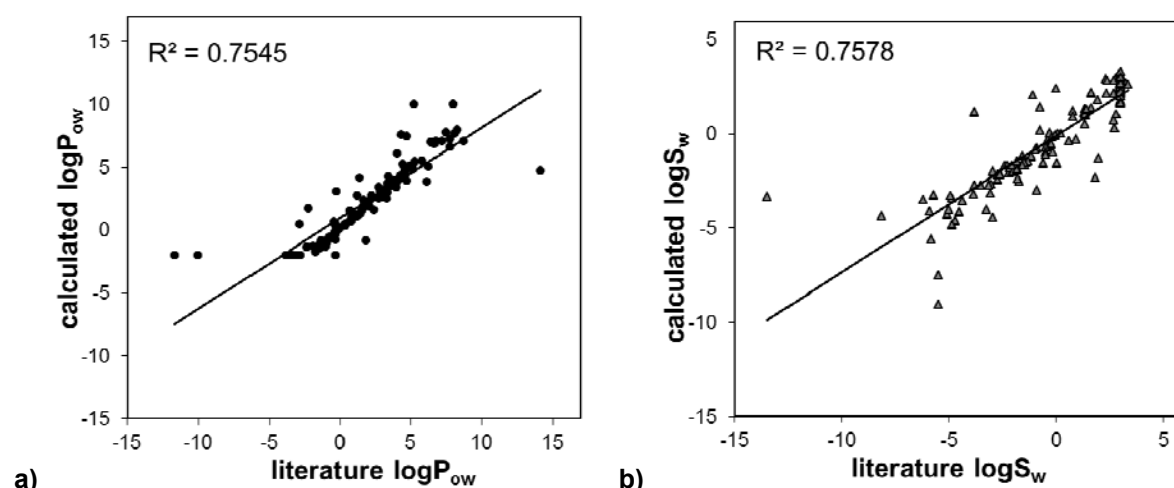


Figure 17: Correlation of software predicted and literature (experimental) values for 125 randomly selected chemical compounds of the dataset: a) logP_{ow} calculated with Molinspiration Property Calculator and literature values generated by PhysProp Database Demo (Syrres), b) logarithm of water solubility (logS_w) calculated with ABLab feature of software ADME Boxes 4.95 and literature values generated by PhysProp Database Demo (Syrres).

The original dermal absorption database containing results for 89 compounds in 569 individual experiments was heterogeneous considering experimental conditions and data processing. To generate a more homogeneous set with an adequate number of data points, only experiments corresponding to the following study design were used for calculations: Experiments with human or rat skin preparations in the time frame of 6 to 48 h with mixture factors derived from more than 90 % of the composition and reasonable data processing. Response logmaxKp was used as the endpoint. Due to these selections, the dataset was reduced to 342 data points for 56 compounds (see Table 48 in annex).

4.4.1 Abraham-based models containing mixture factor(s)

For the first analysis, the dataset was split up randomly into a training (2/3) and a validation (1/3) set. Using the training set, multiple linear regression analyses were performed on the basis of Equation 28, p. 53, comprising the five Abraham descriptors plus one of the 87 MFs. A hit list (decreasing R²) of MFs was generated (Table 28). Addition of a MF for TPSA (topological polar surface area) or HBAcc (number of H-bond acceptors) led to the highest values for rat, human or rat plus human datasets. Since MF molinspLogHBAcc (logarithmic transformed HBAcc calculated with the Molinspiration Property Calculator software) led to high values with all three datasets, it was chosen for the next steps.

Table 28: Hit list of MFs sorted by decreasing R². Basic Abraham model ($\Sigma\alpha_2^H$, $\Sigma\beta_2^H$, π_2^H , Rf_2 and V_x) and one of the 87 mixture factors were used to run regressions for endpoint logmaxKp based on training set alone (Equation 28, p. 53). The four highest R²s and associated MFs for human, rat and human plus rat datasets are given. Abbreviations for the MFs contain the name of the software and the derived property.

Human		Rat		Human & Rat	
R ²	MF	R ²	MF	R ²	MF
0.402	Adme1/TPSA	0.382	molinspTPSA	0.326	molinspLogHBAcc
0.398	molinsp1/TPSA	0.361	AdmeTPSA	0.318	AdmeLogHBAcc
0.389	molinspLogHBAcc	0.335	AdmeLogHBAcc	0.312	Adme1/TPSA
0.367	AdmeLogHBAcc	0.335	molinspLogHBAcc	0.308	molinsp1/TPSA

To build significant and reliable models, a correlation matrix based on all 342 data points was calculated for the Abraham descriptors molinspLogHBAcc and molinspTPSA (Table 29). Abraham descriptors $\Sigma\beta_2^H$, π_2^H , Rf_2 and V_x were significantly correlated to each other with Pearson's correlation coefficients between 0.478 and 0.831. Correlations between $\Sigma\alpha_2^H$ and the other descriptors were low with r values from 0.017 to 0.222. MF molinspLogHBAcc and molinspTPSA were poorly correlated to the Abraham descriptors (0.046 – 0.141, 0.056 – 0.274, respectively), but significantly to each other (0.619). Combined use of two variables with high correlation to each other may lead to unstable models. Therefore, only descriptors with r values smaller than 0.7 and p-values smaller than 0.05 were accepted for the model. Furthermore, data points which lied outside the domain and had high leverage on the model were identified with the Williams plot ($\hat{h} > h^*$) and excluded from the calculations. The number of eliminated data points and the final significant model descriptors are given in Table 30 as

well as the results of internal (Q²LOO, Q²25%) and external validation (Q²Ext). The most frequently eliminated data points are given in Table 42 and addressed in the discussion (chapter 5.3.4). The first fully-validated models (no. 2, 4, 6 in Table 30) with datasets human, rat or human and rat, respectively, contain $\Sigma\alpha_2^H$ and Rf_2 as significant descriptors and show adjusted R² values from 0.33 to 0.45 if using molinspLogHBacc as MF. Corresponding models without MF revealed values from 0.21 to 0.26.

Table 29: Correlation matrix for Abraham descriptors and two mixture factors (molinspLogHBacc and molinspTPSA). Shown are Pearson's correlation coefficients (r); ** indicates highly significant values (p < 0.01).

	$\Sigma\alpha_2^H$	$\Sigma\beta_2^H$	π_2^H	Rf_2	V_x	molinspLogHBacc	molinspTPSA
$\Sigma\alpha_2^H$	1						
$\Sigma\beta_2^H$	0.222	1					
π_2^H	0.212	0.730**	1				
Rf_2	0.041	0.658**	0.831**	1			
V_x	0.017	0.485**	0.478**	0.600**	1		
molinspLogHBacc	0.046	0.141	0.135	0.137	0.113	1	
molinspTPSA	0.170	0.189	0.274	0.165	0.056	0.619**	1

Plotting the observed values against predicted values with model no. 6 separately for each species, revealed an imbalance of prediction (Figure 18 a). Ratio of over-predicted and under-predicted experiments was 1.9 for human and 0.4 for rat. A binary class variable (Spl) which accounted for human (1) and rat (2) was included in the dataset and used as an independent variable. Models no. 7 and 8 originated from Equation 29, p 53 which contains this variable. These models had higher values for R², adjusted R², Q²LOO, Q²25% and Q²Ext than their analogous models no. 5 and 6 without Spl (see Table 30; e.g. R² 0.22 (model 5) vs. 0.28 (model 7) and 0.37 (model 6) vs. 0.41 (model 8)). Ratios for over- and under-predicted experiments with model no. 8 were 1.2 and 0.9 for human and rat, respectively (Figure 18 b).

Plotting the observed values against predicted values with model no. 8 separately for the seven defined receptor groups ('water', 'water+B', 'water+x', 'PBS, pH4', 'E/W_1', 'E/W_2' and 'E/W_3') revealed no obvious bias for distinct groups (Figure 19). Combined examination of all ethanol/water mixtures led to a ratio of over- and under-predicted experiments of 0.9 and combination of all other water-based receptor fluids to a ratio of 1.8. Insertion of the binary class variable RI (1 for ethanol/water mixtures and 2 for other water-based receptor fluids, Equation 30, p. 53), changed only slightly the regression equation. However, neither the number of over- and under-predictions nor the following ratios were changed. Furthermore, the additional variable RI was not significant in the model (p 0.162) and therefore excluded during further validation steps.

Table 30: Validated (significant) Abraham-based models. Q²LOO: internally cross-validated explained variance obtained with LOO procedure, Q²25%: internally cross-validated explained variance obtained with LMO (25%) procedure, Q²Ext: externally explained variance, h: human, r: rat, rdm: randomly, Acc: molinspLogHBacc, TPSA: molinspTPSA, AP_{ow}: Adme1/P_{ow}, Don: molinsp1/HBDon, Don: AdmeLogHBDon, PC1: principle component factor 1. Highlighted is the model with the highest validation scores (no. 20).

model no.	species	data splitting	n training set (n full set)	model descriptors	eliminated data points	R ²	adjusted R ²	Q ² LOO	Q ² 25%	Q ² Ext	standard error	F-value
1	h	rdm	133 (200)	$\Sigma\alpha_2^H$ Rf ₂	11	0.27	0.26	0.22	0.22	0.21	1.06	24
2	h	rdm	133 (200)	$\Sigma\alpha_2^H$ Rf ₂ Acc	11	0.46	0.45	0.41	0.42	0.38	0.91	37
3	r	rdm	86 (129)	$\Sigma\alpha_2^H$ Rf ₂	2	0.23	0.21	0.17	0.16	-0.26	0.93	12
4	r	rdm	86 (129)	$\Sigma\alpha_2^H$ Rf ₂ Acc	2	0.35	0.33	0.28	0.27	0.03	0.86	15
5	h + r	rdm	221 (332)	$\Sigma\alpha_2^H$ Rf ₂	10	0.22	0.22	0.20	0.20	0.05	1.05	31
6	h + r	rdm	221 (332)	$\Sigma\alpha_2^H$ Rf ₂ Acc	10	0.37	0.36	0.34	0.34	0.26	0.94	43
7	h + r	rdm	223 (334)	$\Sigma\alpha_2^H$ Rf ₂ Spl	7	0.28	0.27	0.25	0.25	0.14	1.01	28
8	h + r	rdm	223 (334)	$\Sigma\alpha_2^H$ Rf ₂ Spl Acc	7	0.41	0.40	0.38	0.38	0.32	0.91	38
9	h + r	rdm	225 (337)	PC1 Spl	5	0.17	0.17	0.15	0.15	0.13	1.08	23
10	h + r	rdm	225 (337)	PC1 Spl Acc	5	0.33	0.32	0.30	0.30	0.27	0.97	36
11	h	AE	126 (187)	Rf ₂	14	0.17	0.16	0.17	0.14	0.19	0.92	25
12	h	AE	126 (187)	Rf ₂ Acc	14	0.36	0.35	0.34	0.33	0.34	0.81	35
13	h + r	AE	221 (330)	Rf ₂ Spl	12	0.21	0.21	0.19	0.19	0.16	1.06	27
14	h + r	AE	221 (330)	Rf ₂ Spl Acc	12	0.37	0.36	0.34	0.34	0.33	0.80	40
15	h + r	AE	220 (341)	Rf ₂ Spl	1	0.16	0.16	0.14	0.14	0.13	0.91	21
16	h + r	AE	220 (341)	Rf ₂ Spl Acc AP _{ow}	1	0.36	0.35	0.33	0.33	0.41	0.80	30
17	h + r	AE	218 (339)	Rf ₂ Spl	3	0.16	0.15	0.14	0.14	0.13	0.91	21
18	h + r	AE	218 (339)	Rf ₂ Spl Acc Don	3	0.37	0.36	0.34	0.34	0.41	0.80	31
19	h + r	AE	213 (328)	Rf ₂ Spl	13	0.18	0.17	0.15	0.15	0.35	0.27	23
20	h + r	AE	213 (328)	Rf₂ Spl TPSA	13	0.38	0.37	0.35	0.35	0.41	0.78	42
21	h + r	AE	218 (332)	Rf ₂ Spl	10	0.18	0.17	0.16	0.16	0.11	0.89	23
22	h + r	AE	218 (332)	Rf ₂ Spl TPSA Don	10	0.39	0.38	0.36	0.36	0.30	0.78	33

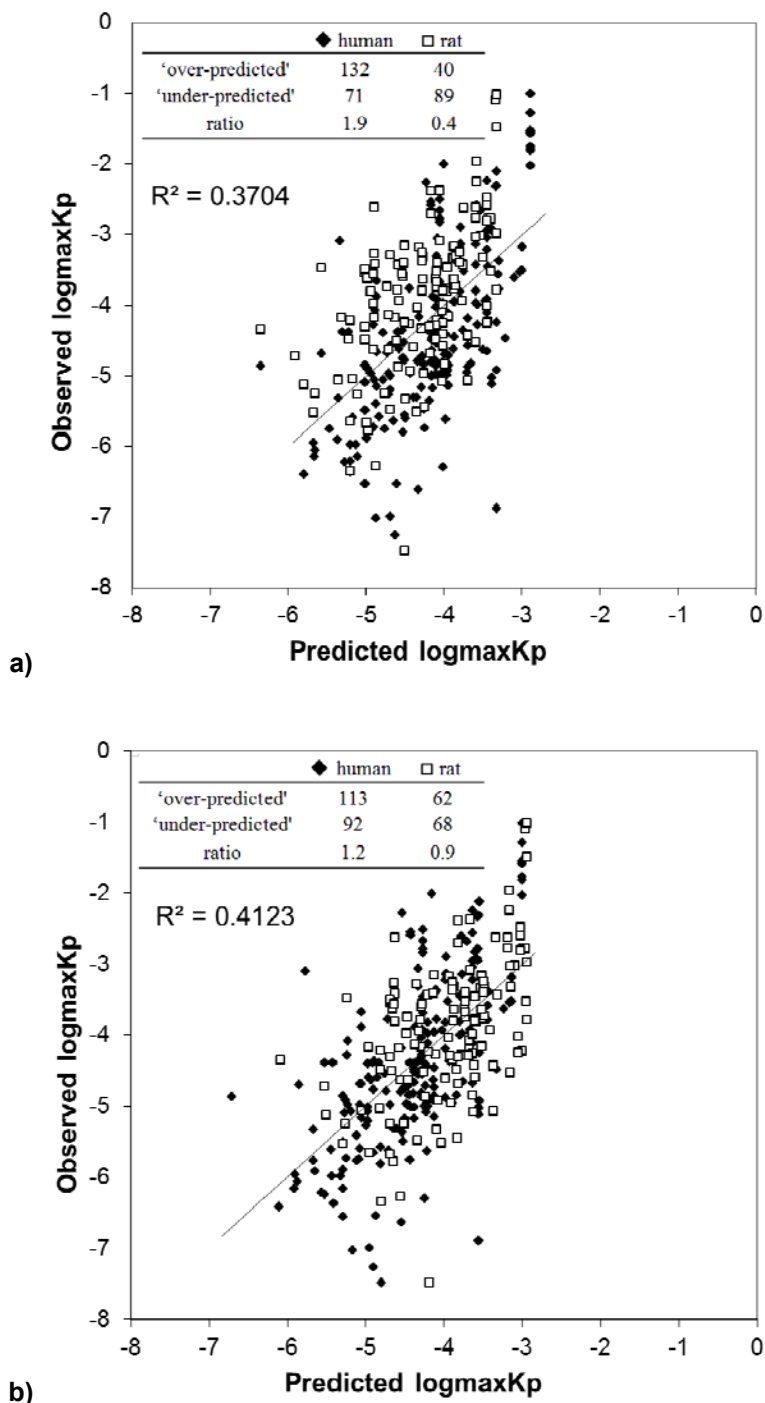


Figure 18: Predicted and observed logmaxKp values a) without (model no. 6) and b) with variable Spl, the species indicator (model no. 8). The other descriptors were the same for both approaches: $\Sigma\alpha_2^H$, overall hydrogen bond acidity, Rf_2 , solute excess molar refractivity – both calculated with software ADME Boxes 4.95 – and molinspLogHBAcc, number of hydrogen bond acceptors calculated with software Molinspiration Property Calculator. Model equations are for a) $\log\max Kp [cm/h] = -2.5 - 1.2 \cdot \Sigma\alpha_2^H - 0.7 \cdot Rf_2 - 3.5 \cdot \text{molinspLogHBAcc}$ and for b) $\log\max Kp [cm/h] = -3.4 - 1.2 \cdot \Sigma\alpha_2^H - 0.7 \cdot Rf_2 - 3.3 \cdot \text{molinspLogHBAcc} + 0.6 \cdot \text{Spl}$. Correlations are based on the training set. Data points were plotted separately for the different species: human: filled diamonds, rat: open squares. The inserted tables show numbers and ratios of under- and over-predicted data points for both species.

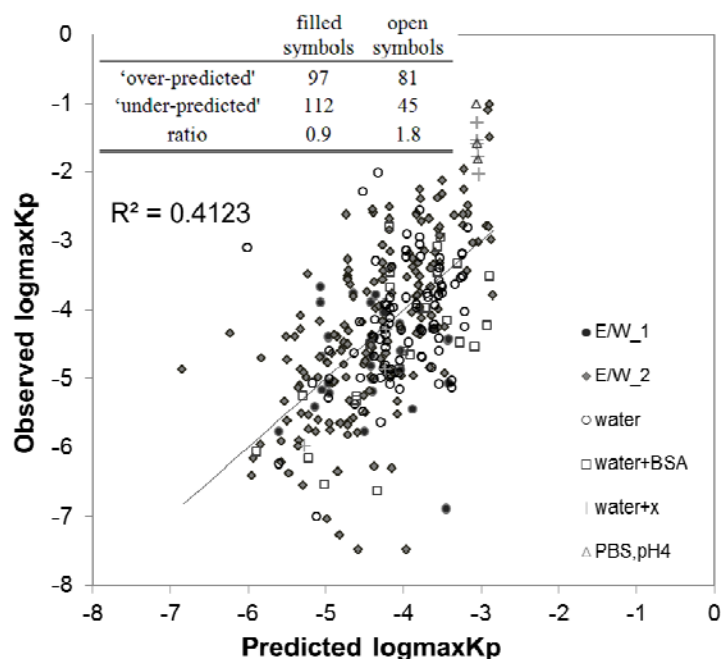


Figure 19: Predicted and observed logmaxKp values (model no. 8). The model descriptors were $\Sigma\alpha_2^H$, overall hydrogen bond acidity, Rf_2 , solute excess molar refractivity – both calculated with software ADME Boxes 4.95 – and molinspLogHBacc, number of hydrogen bond acceptors calculated with software Molinspiration Property Calculator and Spl, species indicator. The model equation is $\log\max Kp [cm/h] = -3.4 - 1.2 \cdot \Sigma\alpha_2^H - 0.7 \cdot Rf_2 - 3.3 \cdot \text{molinspLogHBacc} + 0.6 \cdot \text{Spl}$ and the correlation is based on the training set. Data points were plotted separately for the different receptor fluids as assigned in the graph. Filled symbols belong to ethanol/water mixtures and open symbols to other water-based receptor fluids. Inserted tables show numbers and ratios of over- and under-predicted data points for both receptor groups.

In models no. 1 to 8, Abraham descriptors $\Sigma\beta_2^H$, π_2^H and V_x were excluded due to high correlation to Rf_2 (see Table 29) and missing significance to the model. This exclusion of information was compared to the condensation of information by using principle components (PC) as model descriptors. PC factors 1 and 2 were calculated for the five Abraham descriptors. Factor 1 with eigenvalue 2.7 had a high association to $\Sigma\beta_2^H$, π_2^H , Rf_2 and V_x and factor 2 with eigenvalue 0.4 a main association to $\Sigma\alpha_2^H$ (Table 31). Using these factors as independent variables for linear prediction models (models no. 9 and 10 based on Equation 31, p. 53) resulted in lower values for R^2 , adjusted R^2 , $Q^2\text{LOO}$, $Q^2\text{25\%}$ and $Q^2\text{Ext}$ than models containing the significant original Abraham descriptors $\Sigma\alpha_2^H$ and Rf_2 (models no. 7 and 8) (see Table 30, e.g. R^2 0.17 (model 9) vs. 0.28 (model 7) and 0.33 (model 10) vs. 0.41 (model 8)). Factor 2 was excluded due to missing significance to the model.

Table 31: Factor pattern of principle component factor 1 and 2 based on Abraham descriptors.

	factor 1	factor 2
$\Sigma\alpha_2^H$	0.19867	0.44495
$\Sigma\beta_2^H$	0.81023	0.19276
π_2^H	0.90079	0.15104
Rf_2	0.89137	-0.18801
V_x	0.62652	-0.34004

Since the 342 data points belong to 56 substances, randomly splitting into training and validation sets may result in presence of one substance in both sets. Therefore the next optimization step was a substance-based splitting: after sorting by substance-specific values (Rf_2 and $\Sigma\alpha_2^H$), each third compound was assigned to the validation set (19 compounds). The other compounds were assigned to the training set (37 compounds). Except for this different training set, the regression analysis for model no. 14 was run on the same basis as model no. 8: human and rat dataset, Abraham descriptors, Spl and molinspLogHBAcc as MF. The derived model (no. 14 in Table 30) obtained a lower adjusted R^2 (0.36) than model no. 8 (0.40), but a slightly higher Q^2_{Ext} (0.33 in comparison to 0.32). Furthermore, descriptor $\Sigma\alpha_2^H$ was excluded due to missing significance to the model. A similar model was obtained by using the human dataset alone. This model (no. 12) with R^2 0.36 revealed as significant descriptors Rf_2 and molinspLogHBAcc (Table 30). Using only rat data resulted in exclusion of all five Abraham descriptors. The final significant model contains only MF molinspLogHBAcc and possesses a minor fit (R^2 0.14).

The basic model above was defined by adding each possible MF individually to the Abraham descriptors and reducing the approach afterwards to only significant variables. To see which significant variables were chosen by direct selection of model parameters from the total set of MFs, Abraham descriptors and indicator variables, two different commands were added to the regression calculation in SAS 9.2: 'stepwise' and 'maxR'. The results of the first seven steps for both versions using the substance-specific training set with rat and human data are given in Table 34. Step 1 and 2 were the same for both procedures and revealed Rf_2 and molinspLogHBAcc as the best 2-variables model. 'Stepwise' select Spl as the third variable and then other MFs. 'MaxR' excluded in the third step molinspLogHBAcc from the set and replace it with molinspTPSA. The best 3-variable model was molinspTPSA, Rf_2 and Spl. The next selected variables were other MFs. The listed descriptors were all significant to the model, but may be correlated to each other. Therefore, the correlation matrices for the models at step seven are shown in Table 32 ('stepwise') and Table 33 ('maxR'). With r values higher than 0.7 significantly correlated were the MFs for the number of H-bond donors calculated with Molinspiration Property Calculator (molinspHBDOn) and the logarithm of it calculated with ADME Boxes (AdmeLogHBDOn) as well as the inverse partition coefficient calculated with ABLab feature of ADME Boxes (Adme1/ P_{ow}) and AdmeLogHBDOn.

Table 32: Correlation matrix for the descriptors selected at step seven using 'stepwise'. Shown are Pearson's correlation coefficients (r), ** indicates highly significant values ($p < 0.01$).

	Rf_2	Spl	molinsp LogHBAcc	Adme 1/ P_{ow}	molinsp HBDOn	AdmeLog HBDOn	Adme 1/RotB
Rf_2	1.00						
Spl	0.07	1.00					
molinspLogHBAcc	0.14	0.03	1.00				
Adme1/ P_{ow}	0.06	0.01	-0.53**	1.00			
molinspHBDOn	0.13	0.02	-0.37	0.89**	1.00		
AdmeLogHBDOn	0.13	0.01	-0.39**	0.92**	0.97**	1.00	
Adme1/RotB	0.05	0.01	0.51**	-0.38**	-0.28**	-0.33**	1.00

Table 33: Correlation matrix for the descriptors selected at step seven using 'maxR'. Shown are Pearson's correlation coefficients (r), ** indicates highly significant values (p < 0.01).

	Rf ₂	Spl	molinsp TPSA	molinsp 1/HBDon	molinsp P _{ow}	Adme 1/RotB
Rf ₂	1.00					
Spl	0.07	1.00				
molinspTPSA	0.17	0.05	1.00			
molinsp1/HBDon	0.03	0.05	0.13	1		
molinspP _{ow}	0.06	0.07	0.40**	-0.11	1.00	
Adme1/RotB	0.05	0.01	0.18**	-0.01	0.04	1.00

Table 34: Results for the linear regression analysis including stepwise selection of the most predictive descriptors. The first seven steps for stepwise and 'maxR' function of SAS 9.2 are shown. Given are R² for the selected set of descriptors, and in the case of stepwise also the partial R² for each descriptor. Abbreviations for the MFs contain the name of the software and the derived property.

step	stepwise			maxR	
	R ²	partial R ²	model descriptors	R ²	model descriptors
1	0.1902	0.1902	molinspLogHBAcc	0.1902	molinspLogHBAcc
2	0.2553	0.1902	molinspLogHBAcc	0.2553	molinspLogHBAcc
		0.0651	Rf ₂		Rf ₂
3	0.3114	0.1902	molinspLogHBAcc	0.2677	molinspTPSA
		0.0651	Rf ₂		Rf ₂
		0.0562	Spl		
4	0.3636	0.1902	molinspLogHBAcc	0.3218	molinspTPSA
		0.0651	Rf ₂		Rf ₂
		0.0562	Spl		Spl
		0.0522	Adme1/P _{ow}		
5	0.4009	0.1902	molinspLogHBAcc	0.3639	molinspTPSA
		0.0651	Rf ₂		Rf ₂
		0.0562	Spl		Spl
		0.0522	Adme1/P _{ow}		molinsp1/HBDon
		0.0373	molinspHBDDon		
6	0.4258	0.1902	molinspLogHBAcc	0.3963	molinspTPSA
		0.0651	Rf ₂		Rf ₂
		0.0562	Spl		Spl
		0.0522	Adme1/P _{ow}		molinsp1/HBDon
		0.0373	molinspHBDDon		molinspP _{ow}
		0.0249	AdmeLogHBDDon		
7	0.4619	0.1902	molinspLogHBAcc	0.4221	molinspTPSA
		0.0651	Rf ₂		Rf ₂
		0.0562	Spl		Spl
		0.0522	Adme1/P _{ow}		molinsp1/HBDon
		0.0373	molinspHBDDon		molinspP _{ow}
		0.0249	AdmeLogHBDDon		Adme1/RotB
		0.0361	Adme1/RotB		

Considering the results of the correlation matrices and the stepwise selection of parameters, integration of a second and third MF into the basic model (no. 14) was tested. Addition of $\text{Adme1/P}_{\text{ow}}$ to Rf_2 , Spl and molinspLogHBAcc (model no. 16 in Table 30) did not increase R^2 (0.36), but revealed an obviously higher $Q^2\text{Ext}$ in comparison to model no. 14 (0.41 and 0.33, respectively). Addition of AdmeLogHBDOn (model no. 18 in Table 30) obtained the same $Q^2\text{Ext}$ as model no. 16 (0.41) and slightly higher R^2 of 0.37. Integration of the MF for the inverse number of rotatable bonds (Adme1/RotB) or MF for the number of H-bond donors (molinspHBDOn) as the second MF led to lower R^2 -values (0.32 and 0.34, respectively). Three MFs (molinspLogHBAcc , AdmeLogHBDOn , $\text{Adme1/P}_{\text{ow}}$) in addition to Rf_2 and Spl required exclusion of many data points due to too high leverage. For the remaining dataset this combination was not significant. Since 'maxR' selection supported replacement of molinspLogHBAcc with molinspTPSA , model no. 20 was validated (Table 30). The resulting significant model (Rf_2 , Spl and molinspTPSA) provided validation parameters (R^2 0.38, adjusted R^2 0.37, $Q^2\text{LOO}$ 0.39, $Q^225\%$ 0.38, $Q^2\text{Ext}$ 0.41) similar to the parameters (R^2 0.37, adjusted R^2 0.36, $Q^2\text{LOO}$ 0.38, $Q^225\%$ 0.38, $Q^2\text{Ext}$ 0.41) obtained with model no. 18 (Rf_2 , Spl , molinspLogHBAcc and AdmeLogHBDOn). The F-value for the former model was 42 and for the latter 31. Addition of $\text{molinspP}_{\text{ow}}$ or Adme1/RotB as second MF in addition to molinspTPSA did not lead to significant models after validation. The presence of molinsp1/HBDOn as a second MF led to a significant model with R^2 of 0.39 and $Q^2\text{Ext}$ of 0.30 (model no. 22 in Table 30). The model using three MFs (molinsp1/HBDOn , $\text{molinspP}_{\text{ow}}$ and molinspTPSA) was not significant after several validation steps.

Figure 20 a and c shows example plots of observed versus predicted $\log\text{maxKp}$ values for model no. 20 and its corresponding model without mixture factor molinspTPSA (model no. 19). Concomitant residual plots against molinspTPSA are given in Figure 20 b and d. A trend to negative residuals with high values for molinspTPSA and positive residuals with low values was obvious for model no. 19 (Figure 20 d). If molinspTPSA was included in the model, no trend was observable (model no. 20, Figure 20 d).

The Abraham-based models with the highest R^2 (0.37 and 0.38) and $Q^2\text{Ext}$ (0.41 and 0.41) were models no. 18 and 20. Original and standardized regression coefficients of both models are shown in Table 35. Negative contributions to the models were observed for Rf_2 , molinspLogHBAcc , AdmeLogHBDOn and molinspTPSA . Spl showed a positive contribution to the model. The highest standardized coefficients provided molinspLogHBAcc for model no. 18 and molinspTPSA for model no. 20. For these two models, the predictability of Marzulli classes was determined: results are given in Table 38 and outlined together with the substance-based models no. 25 and 35 in the following chapter. A reasonable drawing of ApD boundaries is discussed in chapter 5.3.4, p. 129.

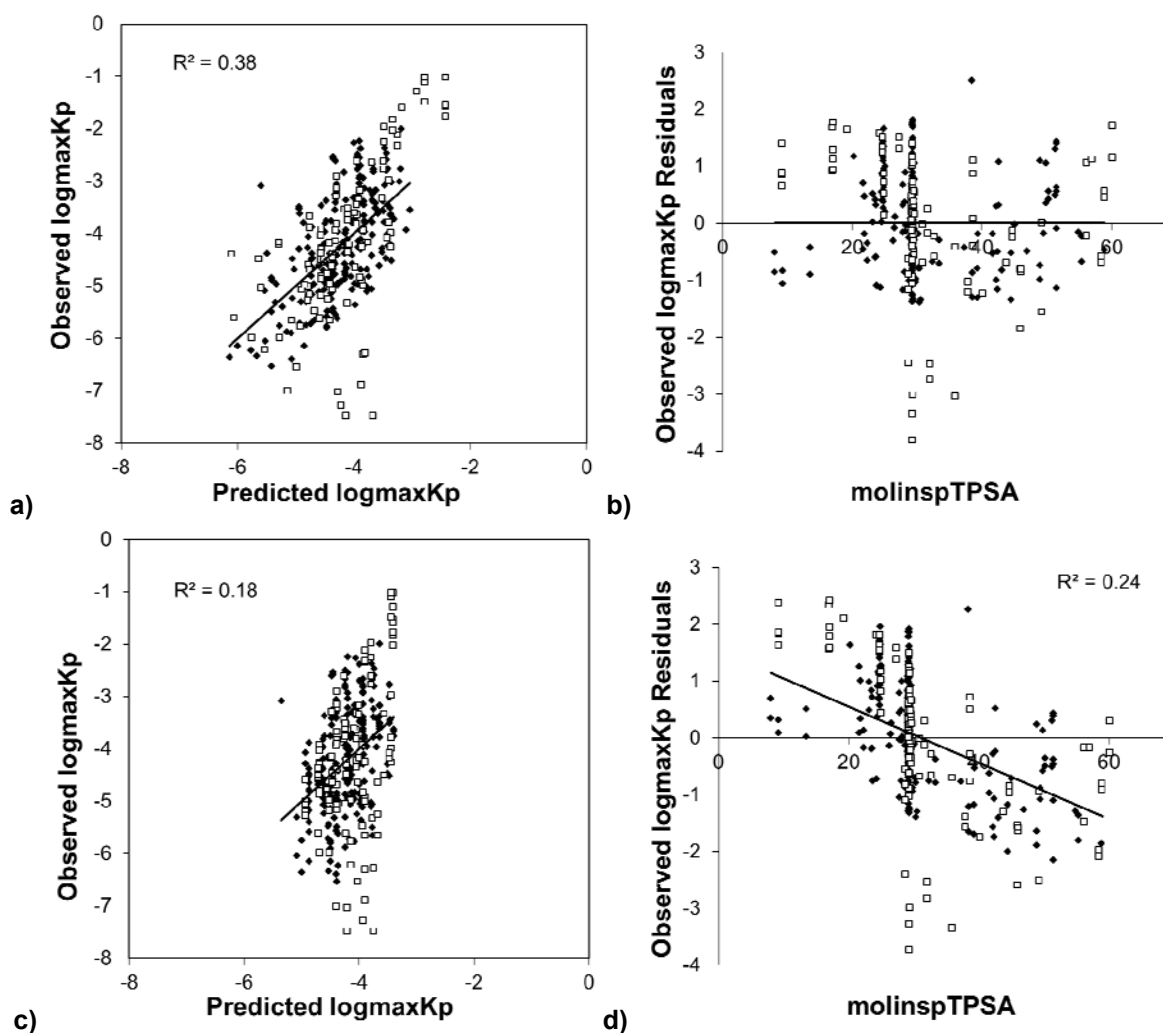


Figure 20: Predicted versus observed logmaxKp values for a) model no. 20 and c) its corresponding model without mixture factor (model no. 19). The model descriptors were Rf_2 , solute excess molar refractivity calculated with software ADME Boxes 4.95, molinspTPSA, topological polar surface area calculated with software Molinspiration Property Calculator and Spl, the species indicator. Model equations are for a) $\log_{\max}Kp [\text{cm/h}] = -2.3 - 0.6 \cdot Rf_2 - 0.1 \cdot \text{molinspTPSA} + 0.5 \cdot \text{Spl}$ and for c) $\log_{\max}Kp [\text{cm/h}] = -3.7 - 0.6 \cdot Rf_2 + 0.5 \cdot \text{Spl}$. The respective residual plots against the mixture factor molinspTPSA are shown in b) for model no. 20 and d) for model no. 19. Data points assigned to the training set are depicted with black diamonds and data points of the validation set with open squares. Existing correlations for the training set are shown in the graphics, including the coefficient of determination.

Table 35: Original and standardized regression coefficients for model descriptors and intercept c of model no. 18 and 20.

	model no. 18		model no. 20	
	original	standardized	original	standardized
intercept c	-3.0	$-4 \cdot 10^{-15}$	-2.3	$-4 \cdot 10^{-15}$
Rf_2	-0.5	-0.3	-0.6	-0.3
Spl	0.5	0.2	0.5	0.2
molinspHBacc	-4.3	-0.6		
AdmeLogHBDon	-2.7	-0.3		
molinspTPSA			-0.1	-0.5

4.4.2 Substance-based models containing mixture factor(s)

In addition to the Abraham-based models derived in the previous chapter, substance-based models were developed. In these models the results of one substance were condensed in a class variable called SUBST, which was combined via linear regression analysis with MFs and Spl (Equation 36, p. 56); Spl was only included if human and rat data were combined. The derived models could predict dermal absorption of a known compound from novel mixtures. For external validation, data points for one substance were divided into training (2/3) and validation sets (1/3). Substances applied in less than five substance-mixture combinations were excluded from the dataset. For the dataset containing only results obtained with human skin, 16 substances (no. 2, 3, 4, 6, 9, 12, 13, 17, 22, 26, 28, 30, 42, 57, 58 and 59), and for the dataset comprising human and rat data, 17 substances (the former plus no. 71) were used in the models. The same MFs as in the previous chapter were tested (molinspTPSA, molinspLogHBAcc, AdmeLogHBDOn, AdmeP_{ow} and Adme1/RotB). Table 36 gives an overview of the resultant significant models.

Table 36: Validated (significant) substance-based models. Q²Ext: external explained variance, h: human, r: rat, rdm: randomly, Acc: molinspLogHBAcc, TPSA: molinspTPSA, AP_{ow}: Adme1/P_{ow}, Don: molinsp1/HBDOn, LogDon: AdmeLogHBDOn, RotB: Adme1/RotB. Highlighted is the model with the highest validation scores (model no. 35).

model no.	species	data splitting	n training set (n full set)	model descriptors	R ²	Q ² Ext
23	h+r	rdm	114 (199)	SUBST Spl	0.49	0.56
24	h+r	rdm	114 (199)	SUBST Spl Acc	0.56	0.68
25	h+r	rdm	114 (199)	SUBST Spl Acc AP _{ow}	0.67	0.69
26	h+r	rdm	114 (199)	SUBST Spl Acc LogDon	0.66	0.65
27	h+r	rdm	114 (199)	SUBST Spl Acc LogDon RotB	0.69	0.50
28	h+r	rdm	114 (199)	SUBST Spl TPSA	0.54	0.60
29	h+r	rdm	114 (199)	SUBST Spl TPSA RotB	0.59	0.37
30	h	rdm	83 (129)	subst	0.59	0.60
31	h	rdm	83 (129)	SUBST Acc	0.65	0.73
32	h	rdm	83 (129)	SUBST TPSA	0.68	0.70
33	h	rdm	83 (129)	SUBST Acc AP _{ow}	0.73	0.69
34	h	rdm	83 (129)	SUBST Acc LogDon	0.73	0.70
35	h	rdm	83 (129)	SUBST Acc AP_{ow} RotB	0.75	0.73
36	h	rdm	83 (129)	SUBST Acc Don RotB	0.75	0.66

The linear model for the human dataset consisting of class variable SUBST only, obtained an R² of 0.59 and Q²Ext of 0.60 (model no. 30 in Table 36). Addition of molinspLogHBAcc or molinspTPSA led to R²-values of 0.65 and 0.68, respectively (models no. 31 and 32). Addition of a second MF to molinspTPSA was not significant. Addition of a second MF to molinspLogHBAcc was significant for Adme1/P_{ow} with R² of 0.73 (model no. 33) and AdmeLogHBDOn with R² of 0.73 (model no. 34). A combination of three MF in addition to the class variable SUBST was significant for molinspLogHBAcc,

Adme1/RotB and AdmeLogHBDon with R^2 of 0.75 (model no. 36) or for molinspLogHBAcc, Adme1/RotB and Adme1/ P_{ow} with R^2 of 0.75 (model no. 35). Corresponding Q^2_{Ext} were 0.66 and 0.73, respectively. Combining datasets for human and rat and adding the variable Spl to the class variable, revealed an R^2 of 0.49 and Q^2_{Ext} of 0.56 (model no. 23). Addition of molinspLogHBAcc or molinspTPSA increased the R^2 to 0.56 or 0.54, respectively (models no. 24 and 28). Combined use of molinspTPSA and a second MF was significant for Adme1/RotB and revealed R^2 of 0.59 and Q^2_{Ext} 0.37 (model no. 29). The combination of molinspLogHBAcc and Adme1/ P_{ow} or molinspLogHBAcc and AdmeLogHBDon are significant models with R^2 0.67 and 0.66, respectively (models no. 25 and 26). Combination of three MFs was only significant for molinspLogHBAcc, AdmeLogHBDon and Adme1/RotB with R^2 of 0.69 and Q^2_{Ext} of 0.50 (model no. 27). For the model with the highest R^2 and Q^2_{Ext} (no. 35) the improvement with and without MFs is visualized in Figure 21. Table 37 shows original and standardized regression coefficients as well as estimators for the class variable SUBST for models no. 25 and 35. Negative contributions were observed for model parameters molinspLogHBAcc, Adme1/ P_{ow} and Adme1/RotB and a positive contribution was observed for Spl.

Table 37: Original and standardized regression coefficients, intercept c and estimators for individual substances of model no. 25 and 35.

	model no. 25		model no. 35	
	original	standardized	original	standardized
<u>regression coefficients</u>				
intercept c	-3.5	-0.4	-0.1	1.3
Spl	0.6	0.2		
molinspLogHBAcc	-5.4	-0.6	-3.1	-0.4
Adme1/ P_{ow}	-0.1	-0.5	-0.1	-0.5
Adme1/RotB			-4.5	-0.5
<u>estimators for</u>				
substance 2	0.3	0.2	-2.5	-2.1
substance 3	-0.4	-0.3	-2.4	-2.1
substance 4	0.5	0.4	-1.7	-1.5
substance 6	0.1	0.1	-1.7	-1.5
substance 9	-0.3	-0.3	-2.5	-2.1
substance 12	-0.3	-0.3	-2.4	-2.1
substance 13	1.4	1.2	-0.6	-0.5
substance 17	1.4	1.2	-0.9	-0.7
substance 22	0.5	0.4	-1.2	-1.0
substance 26	0.7	0.6	-1.0	-0.9
substance 28	0.8	0.6	-1.5	-1.3
substance 30	-0.4	-0.3	-2.2	-1.9
substance 42	0.6	0.5	-2.1	-1.8
substance 57	0.9	0.8	-1.2	-1.0
substance 58	0.7	0.6	-1.5	-1.3
substance 59	2.1	1.8	0.0	0.0
substance 71	0.0	0.0		

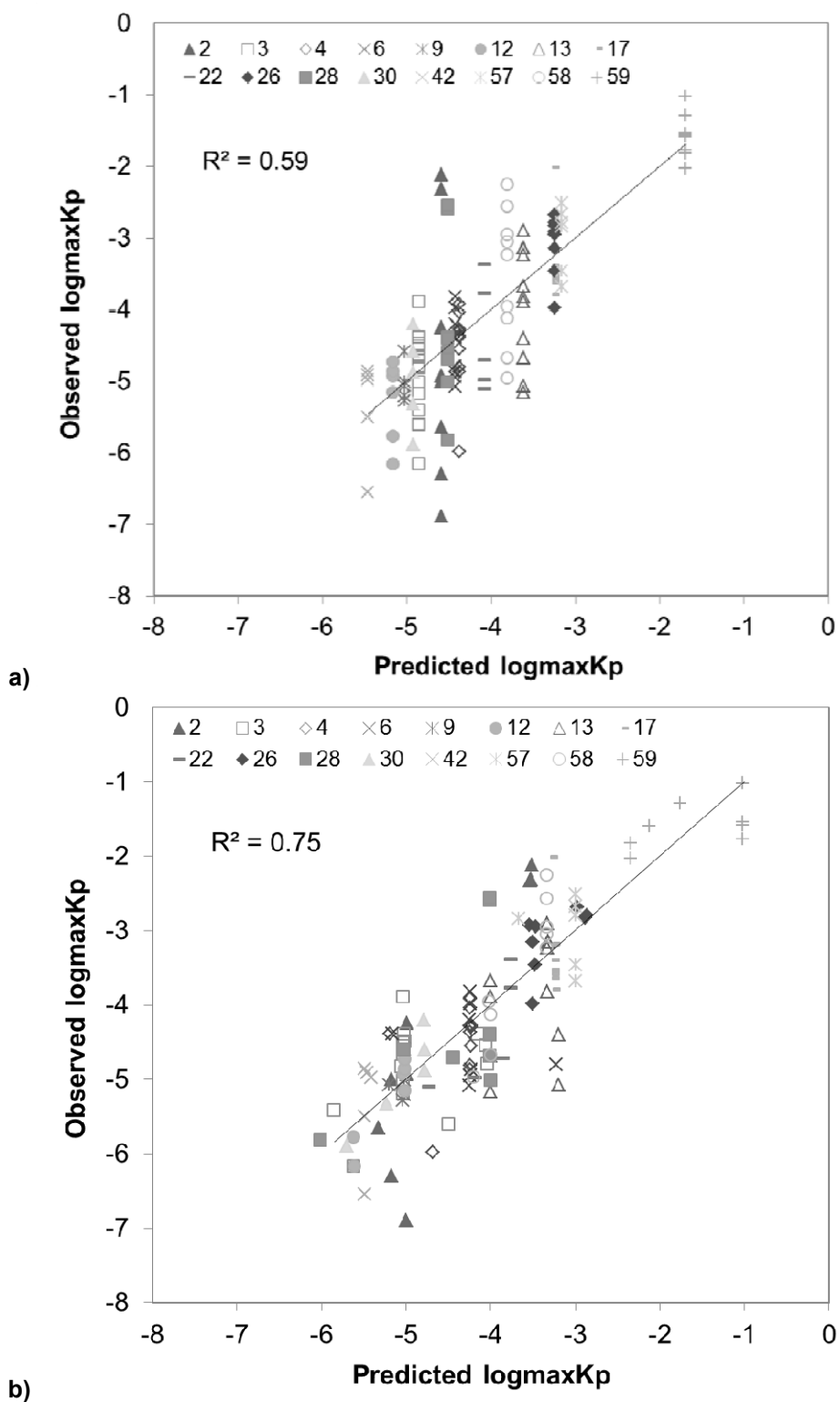


Figure 21: Predicted and observed logmaxKp values a) without (model no. 30) and b) with mixture factors (model no. 35). The correlation is based on the training set. Data points were plotted separately for each substance as assigned in the graph; numbers correspond to numeration in Table 47 (annex).

Besides correlation as a quality criterion for the models, their ability to assign the correct Marzulli class to the substance and corresponding mixture was assessed (Marzulli & Brown 1969). This is visualized as an example for model no. 35 in Figure 22. Horizontal and vertical lines depict the class limits and dark grey fields are areas of correctly predicted Marzulli classes. The percentages of correctly

assigned data points was 47.2, 44.7, 53.3 and 58.9 % for models no. 18, 20, 25 and 35, respectively (see Table 38). 52.8, 55.3, 46.7 and 41.1 % of the data points were wrongly predicted whereas 44.5, 48.9, 45.2 and 40.3 % failed by one class (light grey areas in Figure 22).

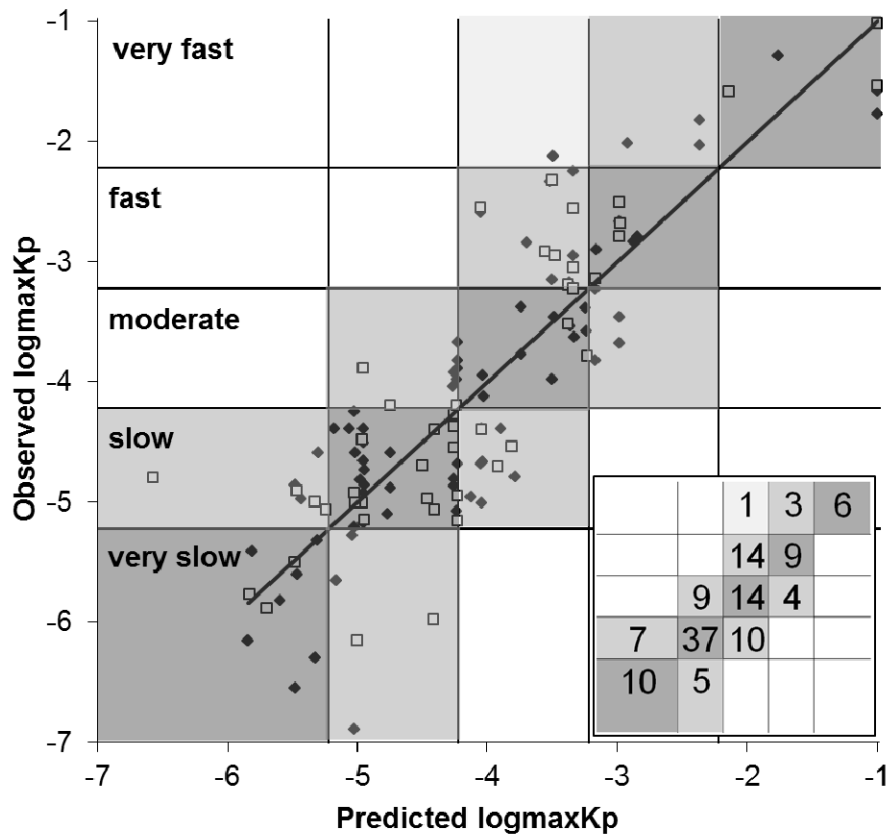


Figure 22: Checkerboard of predicted versus observed logmaxKp values based on Marzulli classes (model no. 35, R^2 0.75). Limits of classes were depicted with horizontal and vertical lines. Colored in dark grey are areas of identical Marzulli classes for observed and predicted values. Lighter grey marks areas with wrongly predicted Marzulli classes. The inserted graphic lists the number of data points in each field. Values derived from the training set are shown as black diamonds and values of the validation set as open squares.

Table 38: Relative number of correctly predicted Marzulli classes as well as number of wrongly predicted data points. Values are given in percentages.

model no.	correctly predicted	wrongly predicted	
		failed by one class	failed by more than one class
18	47.2	44.5	8.3
20	44.7	48.9	6.4
25	53.3	45.2	1.5
35	58.9	40.3	0.8

5 Discussion

5.1 Aspects of dermal absorption experiments *in vitro*

5.1.1 Skin integrity testing

Dermal absorption testing *in vitro* is a regulatory accepted alternative method in the EU. Although OECD Guideline 428 and Guidance document 28 give technical guidance how to conduct valid experiments, many experimental aspects and the overall high variability are still under discussion (OECD 2004a; OECD 2004b). Therefore, main motivation of several research projects – including the current one – is to decrease variability and increase accuracy and robustness of the method. In this context several skin integrity tests were assessed, the influence of selected experimental conditions (skin preparation type, dosing regimen and diffusion cell type) on study outcome was investigated and results of different barrier systems were compared (human skin, rat skin, reconstructed human skin (StrataTest[®]) and abiotic skin surrogate (skin-PAMPA)). To improve the readability of the discussion, the radiolabels of the applied test substances are only indicated if they are important for the context.

A skin integrity test, which is required by OECD Guideline 428, should ensure exclusive use of undamaged skin samples and avoid inadequate over-prediction (OECD 2004b). Suggested tests in OECD Guidance document 28 are TEER (transepidermal electrical resistance), TEWL (transepidermal water loss) or measuring the absorption characteristics of a reference material, e.g. tritium-labeled water (TWF, transepidermal water flux), in advance or at the end of an experiment or measuring in parallel the absorption of an internal standard (ISTD) (OECD 2004a). TEWL, TEER and TWF were intensively investigated and evaluated as skin integrity tests (Bronaugh et al. 1986; Davies et al. 2004; Elkeeb et al. 2010). They are widely used in laboratories to classify skin samples as valid or invalid (Diembeck et al. 1999; Meidan & Roper 2008). Nevertheless there are many discussions about the experimental performances, limit values and fields of application (Chilcott et al. 2002; Meidan & Roper 2008; Netzlaff et al. 2006). Impairment of the skin barrier identified by these methods is expected to allow excessive absorption of the test compound through the impaired skin preparation and therefore yield invalid results. Usually cut-off values are used to distinguish impaired from intact skin preparations with no intermediate stages: a skin preparation is either valid or invalid. Compromising the barrier of a skin preparation is, however, a continuous phenomenon ranging from intact to increasingly more permeable barriers and can occur before the study started, during the test compound application (sometimes even caused by the compound) or after the application (e.g. during washing of the skin). An integrity test that detects the continuum of barrier impairments and therefore provide a complete picture of the barrier integrity would be advantageous. Such a test is expected to correlate with the absorption of the test compound through the very skin preparation. In this respect, the idea to measure a reference compound in a parallel skin sample from the same donor as validity parameter is not sufficient, since it covers only barrier impairments inherent to the donor, but no disruptions caused during the preparation or the experiment.

The suitability of different skin integrity tests for dermal absorption studies was assessed in the current thesis based on their potential to effectively differentiate between intact and damaged skin samples (binary classification) and to correlate continuously with absorption data of test compounds. To

address the binary differentiation of skin samples, the absorption results (AD and maxKp) of four ^{14}C -labeled test compounds (MCPA, MCPA-EHE, testosterone and caffeine) applied to excised or reconstructed human skin were grouped by integrity test classification (valid/invalid) accordingly to the three standard tests TEWL, TEER and TWF. The chosen test compounds represent a wide range of lipophilicity ($\log P_{\text{ow}}$ -0.71 – 6.8) and hence use differently the pathways through the skin (polar- and lipid-intercellular, intracellular and appendageal) (British Crop Protection Council 2011; Merck 2006a; Yalkowsky et al. 1983). Therefore, various changes in the different diffusion pathways were covered by the chosen compounds. Sorting by TEWL or TWF resulted in generally higher mean values for invalid-classified skin samples than for valid-classified skin samples. The valid absorption results for caffeine and testosterone (Table 16 a and c, p. 60) were in good accordance with literature values for these reference substances obtained under similar experimental conditions (identical donor (ethanol/water, 1/1, v/v), dose ($100 \mu\text{g}/\text{cm}^2$), concentration (4 mg/ml), washing fluid (ethanol/water 1/1, v/v), occlusion condition (occlusive) and similar receptor fluid (tap water or 5 % BSA in tap water instead of saline or 5 % BSA in saline): caffeine $30 \pm 14 \%$ (AD) and $56 \pm 36 \cdot 10^{-5} \text{ cm/h}$ (maxKp); testosterone $20 \pm 16 \%$ (AD) and $41 \pm 49 \cdot 10^{-5} \text{ cm/h}$ (maxKp) (van de Sandt et al. 2004). 29 out of 30 reconstructed human skin samples (StrataTest[®]) were identified as invalid by TEWL measurements, which was in accordance to obviously higher absorption values in comparison to human skin. Generally higher absorption through reconstructed human skin in comparison to native human skin was reported previously (Schaefer-Korting et al. 2008a). The outlined observations confirm a meaningful differentiation of skin samples using integrity tests TEWL or TWF. It should be noted, that with the mentioned results for caffeine and testosterone a further requirement of the guideline was fulfilled. This requirement demands application of reference substances like caffeine and testosterone to show general reliability of the test system used in a performing laboratory (OECD 2004b). However, the clear differentiation between absorption characteristics of impaired and intact skin samples was only true when comparing mean values. On single skin sample level, some samples with average permeability were identified as invalid and a few as valid despite of obvious too high maxKp and/or AD. Deterioration of the skin during the experiment just due to time or caused by soap and mechanical treatment during washing procedure could be reasons for the falsely valid classified samples (Buist et al. 2005). Such effects could only be considered and evaluated by concurrent or post-experimental integrity tests. Interestingly the EFSA 'Guidance on Dermal Absorption' recommends to avoid post experimental integrity tests (EFSA Panel on Plant Protection Products and their Residues (PPR) 2012). Prevention of inappropriate skin rejection due to substance related barrier damages could be reasons for this recommendation. However, diminished barrier function of single skin preparations after an experiment could provide valuable information.

Falsely invalid classified samples could be due to too strict limit values. To address this, higher limit values for TEWL and TWF were applied ($13 \text{ g}/(\text{m}^2\cdot\text{h})$ and $4.5 \cdot 10^{-3} \text{ cm/h}$ (the latter proposed by (Meidan & Roper 2008)) in parallel to the standard limits of $10 \text{ g}/(\text{m}^2\cdot\text{h})$ and $2.5 \cdot 10^{-3} \text{ cm/h}$ (the latter suggested by (Bronaugh et al. 1986)). For TEWL it makes no significant difference. With both restrictions the valid mean for caffeine and testosterone was in accordance with reference values from van de Sandt (van de Sandt et al. 2004). But inclusion of several high maxKp values and ADs for MCPA – due to the less strict limit value – led to obviously higher mean values for valid classified skin

samples (192 in comparison to $11 \cdot 10^{-5}$ cm/h and 45 in comparison to 14 %). To avoid inclusion of such apparent over-predictive values for mean calculations, the stricter limit value for TEWL is advisable. Both limit values for TWF led to similar mean values for valid- and invalid-classified skin samples. However, with both limits many skin samples were considered as invalid in contrast to absorption results in reasonable ranges and TEWL classifications. To avoid unnecessary rejection of skin samples by this sensitive method, the higher limit value is recommendable. A bulk of known impaired barrier systems were not identified as invalid with the standard TEER limit of 1 kOhm; but almost all with the stricter limit of 2 kOhm. Furthermore, this stricter limit value provides more reasonable mean values for valid samples: AD of caffeine (35 %) and testosterone (27 %) were close to values obtained from van de Sandt et al. (30 ± 14 % and 20 ± 16 %, respectively) (van de Sandt et al. 2004). Absorption experiments with MCPA-EHE resulted in homogeneous absorption values, which mean that no impaired skin sample was apparent. However some skin samples were identified as invalid using TEWL, TWF and TEER (2 kOhm) (compare Table 16, p. 60). This highlighted again the probability to discard integer skin samples and the usefulness of concurrent or post-experimental integrity tests.

To investigate and assess continuous changes of barrier function, a correlation between integrity test results and test compound absorption is postulated. Rougier et al. observed good correlations between TEWL and absorption of benzoic acid in vivo (Rougier et al. 1988b). However, the comparability of water flow through skin tissue in vivo and in vitro is limited. Levin and Maibach deduced from different studies a general correlation of TEWL and compound absorption in vivo, but discussed a lack of correlation to highly lipophilic test compounds and a lack of correlation in vitro (Levin & Maibach 2005). Previous work from Netzlaff et al. about TEWL application in vitro came to the conclusion that severe damages could be detected, but no small changes (Netzlaff et al. 2006). The same conclusion was drawn for the current work where no, poor or even inverse correlations were observed between TEWL and test compound absorption (Table 17, p. 63, the linear regression analyses were run for experimental datasets ($n \geq 10$) derived under equal conditions: same test compounds and vehicle, same skin type and same receptor fluid). Absence of correlation to test substance absorption, but detection of severe barrier disruption was also true for TEER and TWF. This is in accordance with work from Lawrence who stated a general applicability of TEER and TWF for in vitro testing, but neither correlation between TEER and TWF nor between TEER and absorption results of ^{14}C -mannitol (Lawrence 1997). No correlation between TEWL and TWF and TEWL and ^{35}S -sulfur mustard absorption in vitro was found in work from Chilcott et al (Chilcott et al. 2002).

Taken together all three standard tests are able to sort out a substantial part of impaired skin samples in general. Limit values of $10 \text{ g}/(\text{m}^2 \cdot \text{h})$, $4.5 \cdot 10^{-3} \text{ cm}/\text{h}$ and 2 kOhm for TEWL, TWF and TEER, respectively, seem appropriate to judge between unwanted use of impaired skin and unnecessary rejection of skin samples. However, destruction of barrier function during the experiment could not be evaluated by these tests and – shown by falsely classified skin – only a rough differentiation was possible. Additional application of TEER or TEWL at the end of the run may enhance their utility, since skin samples which were impaired during the run could be identified afterwards. Application of TWF after the run is not feasibility due to remarkable elongation of experimental period and therefore

influence on absorbed and penetrated dose. But, independent of pre- or post-experimental performance, none of the named integrity tests seems universally applicable. Defined 'applicability domains' for each integrity test which limits their use to test compounds in specific physicochemical spaces or to specific experimental conditions (in vitro and/or in vivo, human and/or rat skin ...) would help to choose the most indicative test for the relevant case.

Because of the observations for the standard integrity test (TEER, TWF and TEWL), two other integrity parameters (ISTD, BLUE) were checked for their ability to correlate with absorption results and explain continuous differences of the skin barrier function. Absorption of methylene blue (BLUE) at the end of an experiment clearly identified two extreme outliers, but correlations to test compound absorption were poor and partly inverse. This is understandable since the barrier disruption could have happened during the stressful washing procedure which has no effect on the absorption process before this time point. However, if an enhancement of the penetration and permeation is observed after the washing step ('wash-in' effect), a post-experimental test may help to relate the effect to general barrier disruption or substance-specific behavior. So, a general applicability of BLUE cannot be ruled out and it highlights the benefit of an additional post-experimental test, but lack of remarkable advantages over established tests makes further investigations redundant. The opposite was true for the integrity test ISTD, since the resulting absorption characteristic of a parallelly applied ISTD was positively and highly correlated to test compound results. The correlation (R^2) over a wide absorption range of ^{14}C -labeled MCPA (6 – 100 %) to the ^3H -labeled internal standard testosterone under equal experimental conditions (MCPA-DMA formulation 9 mg/mL, rat skin and receptor fluid water, $n = 45$) was 0.859. The wide range was achieved by pretreatment of skin samples; the data originate from repeated-dose experiments (for regimen see chapter 3.5.3.3, p. 36). Comparison of results for undamaged and intentionally damaged skin samples suggests provisional cut-off values for ISTD ^3H -testosterone of 35 % (AD) and $40 \cdot 10^{-5} \text{cm/h}$ (maxKp) (see Figure 11, p. 64) In contrast to the recommendation of the OECD-Guideline, ^3H -sucrose was not chosen as ISTD for the current investigations for several reasons: Firstly, poor information was found about applicability and the set limit value of 5 % absorption (Walters et al. 1997). Secondly, the highly hydrophilic substance sucrose is not representative for the routinely tested, mainly lipophilic test compounds (pesticides). It is known that contribution of polar- and lipid-intercellular, intracellular and appendageal pathways through skin depend on the physicochemical properties of the test substance (Flynn et al. 1974; Roberts & Cross 2002). Though changes in any of these pathways could have different effects on different penetrants; e.g. disturbance of stratum corneum (SC) by ethanol may increase the solubilizing ability of the aqueous site for lipid like molecules as steroids, but not for very hydrophilic molecules like sucrose (Barry 1993). Therefore, the ISTD should be selected on the basis of the physicochemical properties of the test compound, to indicate representatively the barrier function. This would be in accordance with the above-mentioned 'applicability domain' for integrity tests. In this context ^3H -sucrose could be an ISTD for highly hydrophilic compounds. Another ISTD used in the literature is phenol red, but a 100 times higher concentration of phenol red would be needed to achieve the same analytical sensitivity as the tritium labeled standards used in this work. And the higher the solutes concentration the higher is the risk to influence the test results (Dugard & Scott 1986). In this respect, application of ^3H -water as

ISTD for hydrophilic compounds in aqueous formulations would be an appealing way to assess the barrier function without changing the formulation.

The mentioned risk of influential effects of the ISTD on the test results is addressed in the following: LSC analytics of ^{14}C -testosterone (test compound) in presence and absence of ^3H -testosterone (ISTD) were compared. It could be demonstrated that ^{14}C -analytics using LSC was independent of the presence of ^3H -activity (Figure 12, p. 65). In contrast, ^3H -analytics was slightly influenced by the presence of ^{14}C -labeled compound; the variability of the test results was generally increased and a tendency to higher values was observed in the range < 25 Bq. This effect is probably due to the overlap of electron energy spectra of the two isotopes, whereby the ^{14}C -spectrum (0 to 156 keV) interferes with the complete ^3H -spectrum (0 to 19 keV), but the ^3H spectrum affects only a small part of the ^{14}C -spectrum. However, for the current approach this effect is negligible, since the magnitude of ^3H -ISTD is decisive for skin barrier evaluation, not the exact values. But a change of labeling (^3H -labeling for test compound and ^{14}C -labeling for the internal reference) is based on these results not recommendable. The observed effects on the ^3H analytics were probably the reasons for observed recoveries outside the defined valid range of 90 – 110 %. Therefore, if the ^{14}C -test compound was recovered in the valid range, the total experiment including the ISTD was assessed as valid. Moreover, the independency of dermal absorption of three different ^{14}C -labeled test compounds from the presence of ^3H -ISTD was shown (Table 18, p. 66). Thus means that the alteration of formulation by adding traces of the used ^3H -compounds were marginal and acceptable.

An obstacle for the routine application of the ISTD approach is the need of a broad historical dataset. This dataset should be a matrix of various ISTDs with different physicochemical properties (at least high, medium and low $\log P_{\text{ow}}$ ranges) applied under several experimental conditions. The former to be able to adjust the ISTD to the physicochemical properties of the test compound and address the same pathway through the skin and the latter to have reference values for various scenarios, since different conditions (like donor or receptor fluid) can influence the ISTD results (Kielhorn et al. 2006; Schaefer & Redelmeier 1996a). Based on these data the influential effects could be evaluated and cut-off values could be determined.

Overall, the ISTD is a promising tool considering the observed correlations to test substance absorption and the provided continuous picture of the barrier function over the whole experimental period. It is advantageous over the 'solitary' integrity tests conducted in advance or after an experiment, since outliers or abnormalities observed for the kinetics of the test compound could be interpreted in parallel with the kinetics of the ISTD. For instance, an abrupt increase of absorption of the test compound after the washing procedure could be classified as a wash-in effect due to mechanical disruption of the barrier function if the ISTD shows a parallel effect, or it could be classified as a substance-specific wash-in effect if the absorption of the ISTD was not affected. The latter case – washing increases the test substance absorption – could be relevant for regulatory purposes. Furthermore, systematic errors could be evaluated. For instance, if higher skin temperatures or higher receptor flow rates were logged during an experiment, ISTD results in the reference range would argue against an effect of these variations on the test substance absorption or in other words would argue for a valid experiment. And finally a continuous test avoids any kind of pretreatment and

elongation of the experiment which could alter the skin properties as outlined above (Buist et al. 2005). However, besides all these advantages, a continuous test is unsatisfactory as a stand-alone method, since a preselection of skin samples does not take place. Therefore, impaired skin samples might be used which may lead to an insufficient number of valid skin samples for the entire study. Therefore, we recommend a combined use of the binary standard test TEWL in advance of an experiment – which is able to identify the majority of defect skin samples without pretreatment of the skin samples – and the outlined continuous ISTD approach – to evaluate effects observed during the absorption experiment.

5.1.2 Flow-through versus static experiments

Beside integrity tests, also effects of experimental conditions on dermal absorption results are continuously under discussion (EFSA Panel on Plant Protection Products and their Residues (PPR) 2012; Kielhorn et al. 2006). One example is the application of static and flow-through scenarios. The latter provides more physiological sink conditions than the former by continuous removal of absorbed test substance. An advantage from this is the ensurance of adequate solubility of lipophilic compounds by less organic receptor fluids – and waiving organic solvents avoids (negative) effects on the tissue (Kielhorn et al. 2006). However, the receptor fluid must not be rate-limiting in general, since this could lead to higher absorption under flow-through conditions compared to static conditions (Bronaugh & Stewart 1985; Crutcher & Maibach 1969; Hughes et al. 1993; OECD 2004a). This and variability caused by skin samples were most likely the reason for frequently observed differences between the two systems (Shah et al. 1988). Studies conducted under equal conditions (e.g. same receptor fluid, skin preparation and species), but using static or flow-through systems, led to close results (Bronaugh & Stewart 1985; Clowes et al. 1994). Therefore, it is crucial to use similar experimental conditions and to ensure an adequate solubility of test compound in the receptor fluid when comparing both systems. This was done in the current investigations aiming to establish flow-through systems in our laboratory. Similar absorption results (absorbable dose, K_p , lag time) were obtained for MCPA and testosterone using both systems. An exception was the significantly higher K_p value for ^3H -testosterone under flow-through conditions (22.2 ± 2.7 compared to $13.4 \pm 2.8 \cdot 10^{-5} \text{cm/h}$) (Table 19, p. 66). However, the values are in the same order of magnitude and rather close – if considering the inherent variability of the methodology and the general interindividual variability (EFSA Panel on Plant Protection Products and their Residues (PPR) 2012). This fact and the absence of a systemic tendency – considering both substances – make the flow-through system a suitable alternative to the static system.

5.1.3 Repeated dosing regimen with rat skin

The dosing regimen (single or repeated) may influence the dermal absorption of a penetrant. On the one hand, repeated dosing could enhance the absorption by direct effects on the barrier function and on the other hand decline absorption by saturation of the skin. Knowledge of such effects on human skin in vivo is limited to pharmaceutical products. For example, Bucks et al. reported no changes of absorption and therefore nor reservoir formation or barrier disruption for several steroids after daily application of human volunteer skin (Bucks et al. 1985). In contrast, azone – used as an enhancer for effective drug delivery – increases slightly its own penetration and permeation through human skin in vivo after several treatments. As soon as a steady state of enhancement was reached, azone did not only alter the barrier function, but also formed a reservoir (Wester et al. 1994). Furthermore, salicylic

acid alters its own absorption by repeated application. Barry et al. observed declined absorption after weekly application on rabbit skin in vivo and Roberts and Horlock reported an initially increased absorption followed by declined absorption using in vivo daily-pretreated rat skin for in vitro experiments. These observations were connected to the keratolytic effect of salicylic acid, but the precise cytological changes in the epidermis were not completely understood (Barry et al. 1972; Roberts & Horlock 1978). For pesticides repeated dosing may be relevant for workers in large-scale farms which are in contact with the substance and the entire formulation for several consecutive days. However, there is no consensus if and how repeated dosing effects should be taken into account for pesticide risk assessment (Kielhorn et al. 2006). In addition, no in vitro system is validated and human volunteer studies are not applicable for agrochemicals. Therefore, such questions can be answered by complex in vivo animal studies only. The current investigations should answer if a study design with repeated dosing in vitro is generally possible and if formulation-specific barrier disruption or reservoir formations are detectable. Potential effects, related to experimental time and physical stress caused by washing steps should be evaluated. Following the OECD Guideline 428 dermal absorption experiments are restricted to 24 h to avoid deterioration of the skin preparations (OECD 2004b). However, repeated application of caffeine in vitro up to 72 h revealed only slightly over additive absorption why barrier disruption due to time or washing procedures were assessed to be negligible (Toner et al. 2009). Even longer experimental periods were reported in the literature: Blank et al. used the same skin preparation consecutively for several absorption experiments over days. With each experiment they changed the temperature (declining in a first and increasing in a second experiment), but applied the same substance (n-alcohols). Since the observed exponential increase of K_p with increasing temperature was substance specific (steeper with longer chain length) and apparent in experiments with declining and increasing temperatures, the effect was related to an increase of temperature and activity of molecules and not to the time and possible degradation of the skin barrier function (Blank & Scheuplein 1967). Peck et al. obtained similar results for successive experiments over five days when isolated human epidermis was stabilized by a porous synthetic membrane. Decreasing barrier properties were associated with mechanical stress on the skin samples by rinsing and sampling (Peck et al. 1993). Therefore, in the current repeated dose experiment, dermatomed skin was used which is considered to be more robust against mechanical forces than epidermal membranes and experiments were performed up to 96 h. Additionally, rat skin was used to reduce donor-dependent variability. Furthermore, an internal standard (^3H -testosterone) was added to distinguish between substance-related and more general effects on the barrier.

The single dose experiment with a total experimental period of 24 h (standard) differs significantly from the single dose experiment with an experimental period of 96 h (72 + 24, three days untreated in Franz cell followed by application of test substance on the fourth day) (e.g. AD of MCPA 14 ± 3 in comparison to 25 ± 6.5 %). However, the values are in the same order of magnitude – and rather close considering the overall interexperimental variation. A further control with three water treatments without washing steps in between over 96 h (AD of 17 ± 8 %) was not significantly different to both experiments – no destruction was apparent. These results support the general usability of excised human skin up to 96 h as proposed by Peck et al (Peck et al. 1993). However, any pretreatment – except water without washing steps – increased the absorption results (ADs of 36 – 75 %). The effects

on the ^3H -labeled internal standard testosterone were parallel to the effects on the ^{14}C -labeled MCPA, which speaks for a general enhancing or barrier-disrupting effect. A possible protective reservoir formation could not be detected due to deterioration of the skin. Complete waiving of washing weakened also the effect of pretreatment with blank-formulation (AD of 36 ± 11 in comparison to 75 ± 25 %). Hence, mechanical stress, short-term hydration or surfactant application during washing could be reasons for the barrier impairment. Reliable experiments including pretreatment with cold formulation could not be done without washing steps, since residuals from pretreatment would change the applied concentration and therefore falsify the results. At least one wash must be performed after the last pretreatment. No differences were observed between the effect of such a single wash and three consecutive washes (AD of 70 ± 15 and 75 ± 24 %, respectively). It seems that the time made the skin less resistant to mechanical and chemical stress. It also needs to be considered that in vivo maintenance mechanisms like proliferation, differentiation and desquamation are reduced or absent in skin ex vivo (Hautier et al. 2008; OECD 2004a). Since Buist and co-workers observed only slight effects of washing in vitro after 55 h and Toner et al. after 72 h, the current experiment may have been too long (Buist et al. 2005; Toner et al. 2009). However, less than three pretreatments are questionable to represent repeated dosing regimen.

Irrespective of washing effects, an enhancing effect of blank or cold formulation pretreatment could be detected. The effect was similar and therefore related to formulation ingredients other than MCPA. Beside MCPA the formulation contains DMA, EDTA and silicone antifoam – a polymeric organosilicon. The latter prevents foaming and facilitates an evenly distribution of the formulation on a surface. It is of low chemical reactivity and does not cause toxic effects (Wacker 2009). DMA is a base with caustic effects (Sigma-Aldrich 2006). However, in the application solution it was neutralized to pH 8 with MCPA or HCl (HCl in case of blank formulation) wherefore an effect on the skin is unlikely. EDTA was added to bind free ions like Mg^{2+} and Ca^{2+} and therefore prevents possible precipitation of MCPA salt in the formulation and in aqueous dilutions of it. The chelating agent is irritant to skin and the respiratory system (Merck 2006b). Considering this, an enhancing effect of the formulation may be due to skin irritation and disruption caused by EDTA.

Taken together, the in vitro system seems not to be appropriate to investigate reservoir effects caused by repeated exposure. Furthermore, stability over 96 h is questionable since higher susceptibility to mechanic and chemical stress was observed. However, barrier disruption related to the formulation was observed. Additionally, the experiments point out how an ISTD could help to distinguish between substance-related effects and general barrier degradation – especially if no controls were available. For further improvements of repeated dosing scenarios in vitro, reconstructed skin could be considered. Since they consist of living cells able to proliferate and differentiate, they may be more appropriate for longer cultivation periods than excised human skin. Furthermore, degradation processes are avoided. However, constructs reported in the literature and tested for the current work (discussed in chapter 5.1.5, p. 103) provided generally poor barrier functions and limited stability against mechanical washing procedures (ECVAM (European Centre for the Validation of Alternative Methods) 2010). Therefore, none of the commercially-available skin constructs – tested up-to-date – is appropriate for such an attempt. A further idea is to develop a short time-scale (hours) method for

predicting in-use, long-term (days) scenarios (Pendlington et al. 2004). In silico modeling would be a further option, but the published data on repeated dosing are not sufficient to develop a reliable model.

5.1.4 Preparation types of human skin ex vivo

With absorption experiments using isolated dermis it was shown that beside the epidermis, especially the SC, also the dermis provides a barrier against permeation of xenobiotics (Flynn et al. 1981; Henning et al. 2008). However, the impact of the skin preparation type on dermal absorption results in vitro is controversially discussed. Henning et al. and Wilkinson et al. observed faster permeation (higher flux and shorter lag time) when using DMS compared to FTS (human skin) and Vallet and co-workers observed close absorption characteristic under finite dose conditions with a tendency to lower values using DMS in comparison to FTS (human and pig skin) (Henning et al. 2008; Vallet et al. 2007; Wilkinson et al. 2006). The reported observations were only partly significantly different and vary maximum 2- to 3-fold. Since the authors did not report whether the same donors were used for both preparation types, it cannot be ruled out that observed differences were caused by donor variability. The general variance caused by donor (in vivo) is reported to be about 2- to 4-fold (Schaefer & Redelmeier 1996c). The donor variances observed in the current work were with 1- to 2-fold for AD and 1- to 3-fold for Kp in this range. Diez-Sales et al. compared directly FTS and epidermal membranes from the same donor (hairless rat). They observed a tendency to lower Kp values using FTS. However, the differences were less than 2-fold for five substances and 2- and 4-fold for the two compounds with the largest P_{ow} and MW. They suggest that the dermis is mainly a barrier for lipophilic substances (Diez-Sales et al. 1993). The observed effect seems correlated to preparation, but not exclusively to thickness. Also heating to 60°C during preparation of epidermal membranes should be taken into account, since it may affect the barrier by denaturation processes (Maid-Kohnert 2001). An increase of absorption up to 2-fold for heat-treated FTS compared to native FTS was actually observed by Flynn et al. (Flynn et al. 1981). In the current work, the effect of skin preparation type – especially the presence of a prominent dermis – on dermal absorption in vitro was investigated. Therefore, four ^{14}C -labeled (MCPA-EHE, MCPA, testosterone and caffeine) and three ^3H -labeled (testosterone mannitol and water) test compounds with various physicochemical properties ($\log P_{ow}$ from -3.1 to 6.8, MW from 18 to 312 g/mol) were applied on FTS and DMS, whereby preparations from the same human donors were compared.

The process of dermal absorption in vitro is a series of partition and diffusion processes between and in several layers: Diffusion in the donor, partition between donor solution and SC, diffusion through SC, partition between SC and viable epidermis, diffusion in the epidermis, partition between epidermis and dermis and – depending on preparation – a longer or shorter diffusion part through the dermis and finally the partition from the dermis into the receptor fluid. Each step and therefore the absorption depend on physicochemical properties of the penetrant (e.g. size, lipophilicity) and experimental conditions (e.g. temperature, donor and receptor fluid). When using FTS, the volume increases in which the substance could distribute. On average the volume was roughly doubled using FTS (thickness ~1000 μm) instead of DMS (~400 μm). This explains why generally higher amounts of applied test substance were recovered in the FTS preparations compared to DMS preparations in the current studies. The presence of a dermis affected most and highly significantly skin contents of

testosterone. This could be due to a preferred protein binding of this molecule or accumulation within adipocytes in the lower dermis which may form a skin reservoir as shown previously by Lee et al. (Lee et al. 2002; Römpf 2010). That also MCPA-EHE has a high unspecific-protein binding capacity was observed with S9-fraction incubations (discussed in chapter 5.2, p. 110). Since protein binding is related to lipophilicity, this effect may be important for other lipophilic compounds, too.

Compared to the substance bound to the skin, the content in the receptor fluid was less affected by the preparation type. Similar values were obtained for test compounds mannitol and MCPA, higher values using FTS for MCPA-EHE and lower values using FTS for caffeine. Similar and lower values were observed with testosterone. The differing observations for testosterone may be related to the applied dose which was about 50 000 times lower when using the ^3H -labeled compound instead of the ^{14}C -labeled version. The resulting relative testosterone binding in the skin – higher for the lower concentration – may hinder a further distribution into the receptor fluid. A relation to lipophilicity of penetrant was not apparent in the current results. However, other researchers see in the aqueous dermis mainly a barrier against lipophilic compounds (Reifenrath et al. 1991; Wilkinson et al. 2006). The current sum of substance in receptor and skin rather close for both preparation types matches the theory, that the main barrier of the skin is the SC. Once penetrated into the skin and permeated through the SC, only the preparation determines the partition between the different layers. The observed tendency to higher ADs with FTS fits to the observations from Vallet et al., but explanations are rare (Vallet et al. 2007). An additional follicular pathway could be discussed – which plays an important role for caffeine or steroids like testosterone –, since FTS may contain more hair follicles than DMS (Otberg et al. 2007). Preparing DMS may remove some anchoring and therefore the hair bulb with the hair shaft. At those positions only pores would be left which could be closed during rehydration. Since the number of root sheaths with and without hair shafts was not counted in the current experiments, this hypothesis cannot be confirmed. Furthermore, the presence of adipocytes or fat droplets in the lower dermis could be of relevance. Additional to the change of solubility in the dermis, lipids may leak into the receptor fluid and raise its dissolving power for lipophilic compounds and change the diffusion pressure (Lee et al. 2002).

The rate of permeation was generally slower through FTS than DMS: The lag time was longer and maxKp was smaller and reached later. Significantly slower absorption was obtained for testosterone. This observation is in line with results from Wilkinson et al. who observed smaller absorption rates and longer lag times for caffeine and testosterone and it fits to reports from van de Sandt and co-workers who observed a higher impact of skin preparation type on testosterone than on caffeine (van de Sandt et al. 2004; Wilkinson et al. 2006). Due to the longer pathway it may take longer until a steady state or maximum rate is reached. However, in some cases it might not be reached in the experimental time frame. This was the case for MCPA-EHE which did not reach a plateau for cumulated amount in the receptor fluid in the experimental period of 24 h. And in case of one testosterone experiment a steeper slope in FTS experiments might be concealed due to missing kinetic samples between 10 and 24 h. However, the main reasons for lower maxKp values with FTS are more likely the deceleration of movements due to more protein binding interactions and the finite dose regimen. Since no steady state is reached with finite doses, the calculation of the maxKp is only an approximation of the steady

state K_p which is normally determined under infinite dose conditions. By the time a substance – applied under finite dose regimen to FTS – reaches the receptor fluid and a balanced concentration in the skin sample, the diffusion pressure coming from the skin surface is already lower than it would have been with DMS. This would also explain why Schreiber et al. did not observe an influence of skin preparation on K_p of caffeine and testosterone under infinite dose conditions and why Gotter observed similar K_p values for infinite doses of 1-Naphthol using rat FTS and DMS (Gotter 2007; Schreiber et al. 2005). Similar K_p values obtained for an infinite dose of ^3H -water (integrity test TWF) confirm this theory as well.

Taken together the current data demonstrate that FTS and DMS are both applicable for dermal absorption studies in vitro, leading generally to results in the same order of magnitude – which confirms conclusions from Vallet et al. (Vallet et al. 2007). Small differences are due to a complex conglomerate of skin thickness, lipophilicity and applied concentration of test compound as well as interaction between skin and compound. Although the barrier function of the dermis was confirmed with the current studies and the partitioning between the dermal compartments was affected, it did not change the potentially absorbable dose significantly. Furthermore, a negative effect of dermatomizing could be excluded. In total, using DMS is advantageous, since effects of fatty droplets are excluded, a missing of important kinetic phases avoidable and the resulting $\text{max}K_p$ closer to the steady state K_p . Therefore, DMS was used for all other studies reported in this work. Other preparation types like epidermal membranes or isolated SC were not considered for routine applications. On the one hand to avoid the effect of heat-separation and on the other hand for the practical reason that a tape stripping – which is the only way to take desquamation of a substance into account in in vitro experiments – would not be possible.

5.1.5 Comparison of skin models

The limited availability of human skin samples for research due to the limited number of plastic surgeries, ethical aspects, bureaucracy and high costs, is the reason for an intensive research for alternative systems. In the current work results obtained with human skin were compared with results obtained with rat skin, a human skin construct (StrataTest[®]) and an abiotic skin surrogate (skin-PAMPA). A suitable alternative should provide similar or correlated results to human skin and a better availability. A benefit over human skin would be a higher reproducibility. Observed variability (coefficient of variation, CV) of absorption experiments using human skin samples was on average 41 % for AD and 47 % for K_p which is in accordance to the general high inter- and intraindividual variability observed for this type of experiment (e.g. 43 – 66 % (Southwell et al. 1984)). To evaluate the above mentioned models, histological sections were prepared from the cell-derived systems and absorption experiments were conducted under comparable conditions.

Rat skin is widely used to determine dermal absorption ex vivo. Histological sections of abdominal human and dorsal rat skin showed clearly the well-known morphological differences between the two species and locations used for absorption experiments: the epidermis of rat dorsal skin (22 μm) was thinner than human abdominal skin (57 μm) with values close to literature data (rat, dorsal: ~22 μm and human, abdomen: ~47 μm). The 1 – 2 layers of nucleated cell in the rat skin were less than in the

human skin (4 – 6 layers) (Monteiro-Riviere 2010; Whitton & Everall 1973). Furthermore, SG (stratum granulosum), SS (stratum spinosum) and SB (stratum basale) were differentiable in human skin, but not in rat skin sections (Elwell et al. 1990; Monteiro-Riviere 2010). These differences between human and rat skin morphology were often interpreted to be responsible for the observed different barrier functions against topically present compounds. For instance, a study of 14 pesticides revealed on average a 10.9 ± 8.8 -fold higher absorption rate through rat epidermal membranes in comparison to human epidermal membranes *ex vivo* (van Ravenzwaay & Leibold 2004). However, also smaller interspecies factors and close results were reported in the literature (Monteiro-Riviere et al. 2000; Scott et al. 1986). Even a general interspecies factor for $\log K_p$ of 1.9 was proposed by Vecchia and Bunge (Vecchia & Bunge 2006) and a constant factor of 2 for $\max K_p$ was observed in the current study of MCPA, testosterone and caffeine using dermatomed rat and human skin. The resulting correlation revealed an R^2 value of 0.97. The remarkably different observations reported in the literature and observed here may be due to varying experimental conditions. For instance, in the present study dermatomed skin samples were used – which were prepared equally for the two species. Van Ravenzwaay and Leibold compared human heat-separated epidermis and rat sodium-bromide-separated epidermis. However, the effect of preparation seems of minor importance, since Safferling reported also highly variable interspecies factors from 1 to 10 depending on the test substance and the formulation for equally prepared dermatomed rat and pig skin (Safferling 2008). A vehicle effect on the interspecies variability (human/rat) was also outlined by Davis et al. who argue that the composition of the SC lipids is species-specific and that therefore effects of chemicals and enhancers on the SC lipids and on the absorption through rat skin and human skin are different (Davis et al. 2002). Considering the effects of test compound and vehicle on the interspecies factor, the constant factor 2 obtained in the current work is rather coincidental for the small number of compounds tested and cannot be generalized without expansion of the data set.

Nevertheless, rat skin is a suitable model for dermal absorption studies *in vitro*, since it revealed results in the same order of magnitude as human skin preparations and fulfilled at the same time the regulatory principle of ‘worst case’ for risk assessment of e.g. pesticides. However, for more precise predictions of the human *in vivo* situation a combined approach of human and rat *in vitro* as well as rat *in vivo* experiments is necessary (triple pack approach). For that regulatory accepted approach, a test-substance and donor-specific interspecies factor (rat/human) derived *in vitro* is used to extrapolate from rat *in vivo* data to the human *in vivo* situation (van Ravenzwaay & Leibold 2004). The applicability of rat data for the triple pack approach and the moderate overestimation of the human situation, make rat skin superior to the other investigated skin equivalents StrataTest[®] and skin-PAMPA.

Several structural aspects of skin tissue are connected with its barrier function: a stratified epidermis with tightly connected keratinocytes, a SC with compact keratin bundles in the keratinocytes and a typical composition and arrangement of SC lipids. The histological sections of the StrataTest[®] constructs showed all typical morphological structures of native human skin (see Figure 9, p. 59): a completely stratified epidermis consisting of SC, SG, SS and SB and a dermis. Importantly, the SC was remarkably thick. Furthermore, biochemical processes are involved to build up and maintain the barrier function. Transglutaminase-1 crosslinks proteins of the cornified envelope and filaggrin

interconnects the keratin bundles. Both proteins were detected in the upper epidermis of the StrataTest[®] tissue. Furthermore, E- and P-cadherin were detected throughout the viable epidermis which are parts of desmosomes and therefore responsible for the cell-cell-adhesion and stability (Green & Jones 1996; Monteiro-Riviere 2010; Rasmussen et al. 2010a). Additionally, measuring the TEER, the barrier function of StrataTest[®] appeared similar to human skin (Rasmussen et al. 2010a). TEER results from the current investigations (1.7 ± 0.6 kOhm) were lower, but still in the range of human skin results (4.9 ± 3.3 kOhm) and exceeded the standard threshold for undamaged skin samples (1 kOhm). However, despite all these hints of a suitable barrier function, the permeation of test compounds was generally fast and was completed for caffeine and MCPA (90 – 100 %) already after 4 – 6 h. Furthermore, the lag time was less than one hour in general. Only the absorption of testosterone was slightly retarded by the reconstructed tissue; after 24 h the absorption was ongoing and 20 – 40 % of the dose could be washed off. The fact that TEER results are not necessarily correlated to absorption results of test substances is discussed in chapter 5.1.1, p. 93. The remarkable thick SC in StrataTest[®] conforms to a hyperkeratosis. Hyperkeratosis is often associated with barrier defects, probably as a compensatory response. For instance, skin with epidermolytic hyperkeratosis possesses an abnormal barrier function which is related to a reduction and abnormal organization of extracellular lipid bilayers due to an impaired secretion of lamellar bodies from the SG (Schmuth et al. 2001). A similar impairment in the amount, composition or arrangement of the extracellular lipid matrix in StrataTest[®] would explain the increased permeability for hydrophilic compounds (caffeine and MCPA) in comparison to the lipophilic compound testosterone.

In addition to the thick SC, histological sections of StrataTest[®] revealed more differences to human skin that may explain the limited barrier function of the tissue: The basal cells were cuboidal and irregularly arranged and the nuclei density in the living epidermis was lower in StrataTest[®] compared to human skin. Similar observations were made for the constructs EpiDerm[™], EpiSkin[™] and SkinEthic[™] (Netzaff et al. 2005). These morphological differences are probably due to an imbalance of proliferation and differentiation. Such an imbalance was detected in the named skin constructs by immunostaining of keratin 6A and skin-derived antileukoproteinase – since both compounds are absent in normal skin, but present in hyperproliferative tissue or during wound healing – and by measuring premature expression of transglutaminase and involucrin – two proteins necessary for a fully-functional cornified envelope (Boelsma et al. 2008). The same could be true for StrataTest[®]. A deficit in differentiation and therefore changed structure, composition and biochemical activity of cells would affect the properties of the entire tissue – especially the barrier function. Additionally, differences of lipid profile in the SC may change the properties. An incomplete ceramide profile was reported for EpiDerm[™], EpiSkin[™] and SkinEthic[™], previously (Schaefer-Korting & Schreiber 2008). However, the StrataTest[®] ceramides profile is unknown. Another point worthy to discuss is the dermis which provides a certain barrier, too. This compartment is negligibly small (1 – 2 cell layers) in the StrataTest[®] constructs and even removed by separating the tissue from its supporting synthetic membrane (see Figure 9, p. 59).

These observations explain the generally high and fast permeation through reconstructed human skin tissues – observed for EpiDerm[™], EpiSkin[™] and SkinEthic[™] previously (Schaefer-Korting et al.

2008a) and observed for StrataTest[®] in the present study. Generally higher absorption compared to human skin was also observed for the human skin constructs Phenion[®]FT and Graftskin[™] LSE[™] (Ackermann et al. 2010; Schmook et al. 2001). To our knowledge, at present there is no reconstructed human skin available which fulfill the requirement of the OECD Guidance document 28 concerning absorption results for reference compounds close to human skin results (OECD 2004a). However, Schaefer-Korting et al. observed correlations between Kp values of 4 – 5 compounds tested in epidermis constructs (EpiDerm[™], EpiSkin[™] and SkinEthic[™]) and in native human skin under infinite dose conditions (r 0.707 – 0.932). Therewith, these constructs appear suitable for screening approaches (Schaefer-Korting et al. 2008a). Additionally, SkinEthic[™] and EpiDermFT[™] from MatTek, USA, were able to reflect vehicle effects on dermal absorption through human skin (Schaefer-Korting et al. 2008b). However, the influence of cosmetic vehicles, especially alcohol-containing formulations, on absorption through human skin was not reflected from EpiDerm[™] or EpiSkin[™] (Dreher et al. 2002). For the finite dose experiments in the present study no correlation was apparent between results obtained with StrataTest[®] and human skin. Thus StrataTest[®] appears less suitable to predict dermal absorption than the human skin constructs tested previously (e.g. SkinEthic[™]).

Nevertheless, some practical aspects of using StrataTest[®] for absorption experiments are discussed, since they may be transferable to other skin constructs. Absorption experiments were conducted with and without the underlying membrane. A remarkable binding of test compound to the membrane was observed (caffeine: 25 ± 2 %, testosterone: 14 ± 9 %, Table 22, p. 71). Adding this to AD, the values were close to AD from experiments without the membrane. However, maxKp values tended to be lower, which was significant for caffeine. This was caused by changed diffusivity and partitioning due to considerable interactions with the membrane. The effect is similar to the increased protein-binding in a thicker dermis and the resultant hampered flow (5.1.4, p. 101). Removing the supportive membrane made the handling more difficult and increased the mechanical stress to the tissue caused by taking receptor fluid samples during the study and by washing procedures. Histological sections showed that with removing of the artificial membrane also the dermis and the basement membrane were removed. Absence of the supporting basement membrane explains also the destabilization of the system. The connections between the SB and the basement membrane seem generally loose: Besides the splitting caused by removing the synthetic membrane, these layers were only partly attached in histological sections where the membrane was present. Furthermore, a tape stripping was impossible. The entire tissue was removed with one tape. In total, the hemidesmosomes detected in StrataTest[®] tissue (Rasmussen et al. 2010a) seem not that effective or maybe less in number than in native human skin. Finally, a potential influence of different storage conditions on absorption results was tested. The supplier recommends storage at 2 – 8°C or under culture conditions until use (Stratatech Corporation 2010). A slight tendency to higher absorption with samples stored at 4°C may be due to decreased activities of enzymes responsible for maintaining the barrier function in the colder environment.

Summing up, the minor barrier function of the reconstructed human skin StrataTest[®] caused overestimation of absorption in ranges of 3- to 4-fold (AD) and 5- to 49-fold (maxKp) compared to human skin. This and the absence of correlation to human skin results make the construct suboptimal

for regulatory issues. It is also of limited use for screening approaches and provides no advantages over other commercially available reconstructed skin. However, if someday the biological processes for barrier formation are completely understood, missing tools could be inserted by the manufacturer using transfection techniques – since stable transfections were already achieved in the underlying cell line (NIKS[®]) (Allen-Hoffmann et al. 2000). In general, such an approach would be limited to skin constructs which are derived from immortalized cell lines.

Skin-PAMPA is a membrane consisting of typical compounds of the intercellular space of the SC: synthetic ceramides, free fatty acids and cholesterol. The molecules are presumed to be arranged as in native human SC (Sinko et al. 2012). Since the SC is the main barrier of the skin and the intercellular pathway the preferred route through it, the model is assumed to provide a barrier function close to human skin. Reported Kp values for several compounds reveal a general over-prediction of human in vitro data, but a remarkable correlation to these values (R^2 0.66, $n = 22$) (Sinko et al. 2012). Seven of these compounds were used as performance standards in the current work (see Table 39). These compounds cover moderate to fast absorption through human skin in vitro and a $\log P_{ow}$ range from -0.1 to 5.3 (Lee et al. 2010). The obtained Kp values differed less than 2-fold from the reference values provided by the supplier Pion (see Table 39). The results confirm a small inter- and intralaboratory variability of the system.

Table 39: Absorption results of performance standards using skin-PAMPA. Given are the pH of the donor medium (prisma HT buffer), the reference values obtained by the supplier (Pion)¹ and values determined in the current work.

test substance	pH	Kp [$\cdot 10^{-5}$ cm/h] (Pion) ¹	Kp [$\cdot 10^{-5}$ cm/h] (current work)
progesterone	6.5	3600	3650 ± 994
	7.4	3600	3123 ± 746
warfarin	6.5	497	352 ± 71
niflumic acid	6.5	925	551 ± 118
atenolol	6.5	< 363	183 ± 12
	7.4	< 363	124 ± 24
verapamil	7.4	1433	1138 ± 184
piroxicam	6.5	844	983 ± 49
chlorpromazine	7.4	4133	3316 ± 251

¹(Pion 2012)

With model substrates caffeine, testosterone, MCPA and MCPA-EHE, the system was checked for its applicability as screening tool under in use conditions. Initially, MCPA-EHE could not be tested under screening conditions, since no concentration was achievable in which MCPA-EHE was soluble in prisma HT buffer and detectable in the assay using photometry. This was due to its high $\log P_{ow}$ (5.4 – 6.8), low water solubility (0.4 g/L at 32°C) and low UV activity (British Crop Protection Council 2011; United States Environmental Protection Agency (US-EPA) 2004).

Due to UV activity, the concentrations in the donor fluid were adjusted for the other three compounds and were therefore different to the concentrations in the diffusion cell experiments with human skin. Furthermore, only solutions in aqueous prisma HT buffer could be used instead of MCPA-DMA-

formulation or caffeine and testosterone solutions in ethanol/water mix as applied in the experiments with human skin in vitro. To be close as possible to the diffusion cell experiments, DMA – no interference with the absorption maximum of MCPA – was added to the MCPA solution in Prisma HT buffer. However, the addition of other formulation ingredients (EDTA and silicone antifoam) were not feasible. Furthermore, infinite dose conditions (skin-PAMPA) were compared with finite dose conditions (human skin in vitro). To sum up, the transfer of experimental conditions used in diffusion cell experiments to skin-PAMPA is limited. Using chromatographic methods for detection would widen the possible concentration range, but lower the time and cost-effectivity of the screening approach at the same time.

Comparing skin-PAMPA results (K_p) with prisma HT buffer pH 7.4 with diffusion cell experiments ($\text{max}K_p$) with human skin conducted under neutral pH, revealed over-predictions of 3-, 6- and 53-fold for caffeine, MCPA and testosterone, respectively. Neither a correlation was obtained nor a correct order from the slowest to the fastest active compound (see black triangles in Figure 23, p. 109). This could be due to the different experimental conditions applied (different receptor, different donor ...). To be closer to the skin-PAMPA conditions, in vitro $\text{max}K_p$ values for caffeine and testosterone were replaced with literature K_p values obtained in human skin in vitro experiments with aqueous donor solutions under infinite dose conditions. The literature K_p values were mean K_p values from three references for caffeine ($79 \pm 72 \cdot 10^{-5} \text{cm/h}$) (Bronaugh & Franz 1986; Schaefer-Korting et al. 2006; Southwell et al. 1984) and three references for testosterone ($235 \pm 294 \cdot 10^{-5} \text{cm/h}$) (Bronaugh & Franz 1986; Schaefer-Korting et al. 2006; Scheuplein et al. 1969). Given three compounds – now all applied in aqueous solution and arranged in the correct order – the degree of over-prediction declined (3- to 9-fold) and the correlation to human skin results was enhanced (R^2 0.89, open diamonds in Figure 23, p. 109). This highlights again that close experimental conditions including the donor fluid and dosing regimen are of utmost importance for absorption kinetics. Up to date only aqueous ($\pm 45\%$ PEG 400) solutions were investigated in skin-PAMPA resulting in absorption profiles correlated to human skin in vitro (Sinko et al. 2012). The compatibility of the membrane with other vehicles was not examined. Skin-PAMPA is an abiotic combination of lipophilic constituents of the SC without a cell scaffold. Therewith, application of an organic solvent may extract ingredients or dissolve in the membrane and therewith impair the barrier function. In this respect, the application of caffeine and testosterone in ethanol/water mixture (1/1, v/v) according to the human in vitro experiments was not reasonable without additional stability tests – which were not compatible with the screening claim.

Comparing the K_p values obtained at pH 6.5 and 7.4 revealed no differences for testosterone or caffeine. However, absorption of MCPA increased with decreasing pH; K_p at pH 4.5 ($307 \pm 43 \cdot 10^{-5} \text{cm/h}$) was significantly higher than at pH 6.5 ($89 \pm 27 \cdot 10^{-5} \text{cm/h}$) or 7.4 ($67 \pm 42 \cdot 10^{-5} \text{cm/h}$). These effects are well in accordance with the pK_a values of the compounds. With pK_a values of 16 (testosterone, calculated with ADME Boxes version 4.95) and 10.4 (caffeine, derived from PhysProp Database Demo (Syrres)), testosterone and caffeine are weak acids and at both pH values predominantly present in their non-ionized form. With pK_a of 3.1 MCPA is a strong acid and predominantly ionized at pH 6.5 and 7.4 (Cessna & Grover 1978). At pH 4.5 more molecules are present in their protonated – neutral – form. The ionized molecules are more polar than neutral

molecules, wherefore diffusion over the lipophilic skin-PAMPA membrane is hampered. Therefore, mainly non-ionized molecules cross – which explain the observed increase with higher amounts of neutral molecules. This pH-dependency applies generally for the diffusion over biological membranes (Riviere 2011c; Vecchia & Bunge 2002).

Taken together, skin-PAMPA is an easy, cost-effective and robust screening tool to get rough estimates of dermal absorption from aqueous solutions. However, many practical aspects as UV-activity and water solubility limit its applicability especially for lipophilic compounds – such as many pesticides. Furthermore, no complex (agrochemical) mixtures could be applied under screening conditions, since the stability of the membrane is not ensured and interference of UV-detection is likely. To improve the system, the stability of the membrane against typical pesticide formulations should be determined. Therefore, the membranes could be pretreated with ingredients like surfactants or organic solvents (e.g. Solvesso™) followed by absorption experiments with reference compounds. The necessary adaptation of the detection method (HPLC-UV, LC-MS or LSC) would allow the use of various formulations and broader concentration ranges, but would also increase effort and costs of the screening approach.

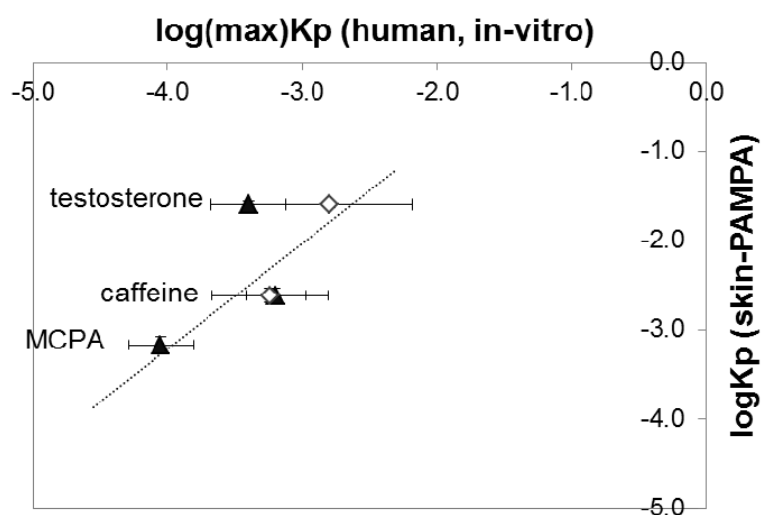


Figure 23: Donor fluid dependency of skin-PAMPA predictions. Given are logKp values obtained with skin-PAMPA against maxKp values obtained with human skin in the current study for MCPA, testosterone and caffeine (black triangles). Since ethanol/water-mixture (1/1, v/v) was used as donor vehicle for testosterone and caffeine in the human skin experiments in contrast to water in the skinPAMPA approach, literature logKp values obtained with aqueous vehicle and human skin were supplemented (open diamonds). Literature Kp values were mean logKp values from three references for testosterone (Bronaugh & Franz 1986; Schaefer-Korting et al. 2006; Scheuplein et al. 1969) and three references for caffeine (Bronaugh & Franz 1986; Schaefer-Korting et al. 2006; Southwell et al. 1984). The dotted line depicts the linear correlation between skin-PAMPA and human skin experiments for aqueous solutions (R^2 0.89).

5.1.6 Relation between AD and maxKp

As an additional aspect of in vitro absorption experiments, the relation between the endpoints AD and maxKp was investigated. A close connection of these two endpoints is expected theoretically for infinite dose experiments, since a high steady state flow leads to a high AD and a low flow to low AD. In the current work, the relation was investigated for finite dose experiments, thus no or only a short

steady state was reached. Data from all absorption experiments conducted in the current work – regardless of the skin types used – are plotted in Figure 24. A general relationship is apparent (polynomial regression analysis, R^2 0.76). However, skin samples providing the fastest maxKp in one experiment did not always led to the highest AD; and the slowest maxKp value did not always originate from the same skin sample as the smallest AD. These slight deviations are due to the finite dose design, where maxKp is an approximation of Kp and therefore only a snapshot of the entire process. In contrast, AD is affected over the entire experimental period. In this context, several aspects have to be discussed. For example, a skin sample which shows a relative high maxKp value in relation to a relative low AD, could have provided a general low barrier function but concomitant to a faster depletion of the substance on the surface. Depletion is depending on solvent evaporation, but also on hydration of SC and therefore from the individual skin sample. Furthermore, wash-in effects may lead to a short-term increase of absorption – resulting in a sharp increase of maxKp, but only a moderate increase of AD – or in a prolonged diffusion phase – resulting in an increase of AD, but a less affected maxKp value. Taken together, also AD and maxKp derived from finite dose dermal absorption experiments tend to be correlated to each other, but deviations on single skin sample level are conceivable.

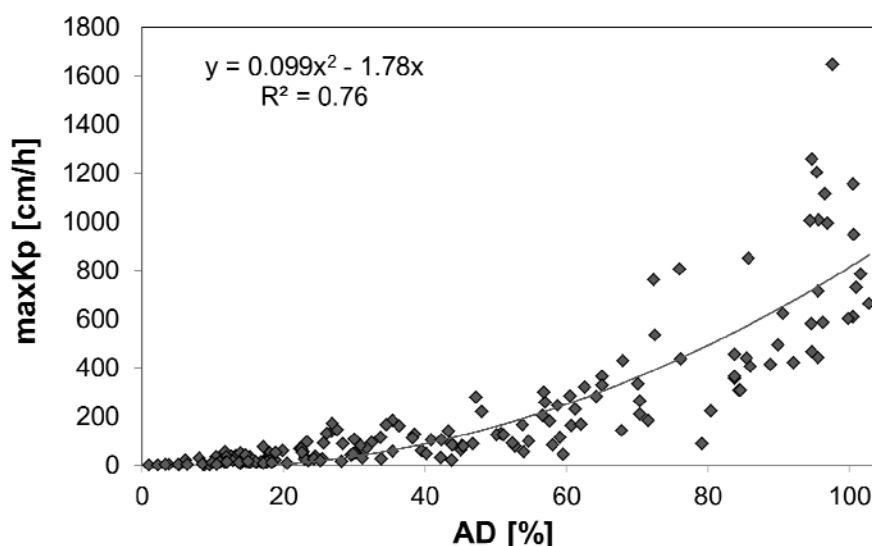


Figure 24: Correlation between potentially absorbable dose (AD) and maximum permeability coefficient (maxKp) on single skin sample level. Human skin, rat skin and reconstructed human skin (StrataTest[®]) are included. A polynomial regression analysis was run; equation and R^2 are given in the graph.

5.2 Metabolic activity of skin models

5.2.1 Biotransformation of MCPA-EHE in human skin

Biotransformation during skin permeation is a crucial point when considering therapeutic action, toxicology or kinetics of a substance. Since the mentioned properties are substance-specific, a transformation to another compound with other physicochemical properties may change the behavior and effects. Several xenobiotic-metabolizing enzymes are present and active in human skin as summarized by Hotchkiss, Oesch or Wilkinson and Williams: isoforms of CYPs, hydrolases, ADHs, AIDHs, FMOs, NATs, SULTs, GSTs, NAD(P)H Quinone reductase, COXs and UGTs (Hotchkiss 1998;

Oesch et al. 2007; Wilkinson & Williams 2008). Extensive 'first pass' biotransformation via various enzymes during *in vitro* skin absorption experiments with freshly prepared mouse and human skin was described for testosterone and benzo[a]pyrene. However, the extent decreased with the use of cryoconserved skin samples (Kao et al. 1985). Ester cleavage during skin passage was shown for the glucocorticoid prednicarbate and the herbicide fluoxypyr in fresh human skin preparations. However, it was not clarified which hydrolase out of the wide range present in the viable epidermis (carboxylesterases, lipidases and proteases) is responsible for these reactions (Gysler et al. 1999; Hewitt et al. 2000; Oesch et al. 2007). Lipase and protease activities were also detected in the intercellular space of the SC. Physiologically the enzymes are thought to be involved in barrier function and desquamation processes (Beisson et al. 2001). Non-specific esterase staining and cleavage of acetylsalicylic acid was distributed over SC and the other epidermal layers. As with other enzymes, a decrease of activity was observed when cryoconserved (-20°C, 1 week) porcine skin samples were used instead of freshly-prepared samples (Lau et al. 2012). Similarly, decreased hydrolyses of ethyl butyrate in cytosolic fraction of pig ear skin was observed when using cryoconserved skin (-20°C, > 6 months) instead of freshly excised pig skin (Abdulmajed et al. 2006).

In the current work, it was investigated, if the cryoconserved human skin samples (-20°C, up to 1 year), which are in use for routine absorption experiments due to limited access to fresh skin, preserve generally xenobiotic-metabolizing enzyme activity. The focus of the investigations was rather qualitative than quantitative and laid on hydrolase activity, since this enzyme group is highly active in human skin (Oesch et al. 2007). MCPA-EHE was chosen as the model substrate, since it is sensitive against hydrolysis. However, also a CYP 450-dependend biotransformation is addressed, since the product of MCPA-EHE hydrolysis, MCPA, is known to be oxidized to HMCPA in plants and animals (British Crop Protection Council 2011; van Ravenzwaay et al. 2004). The biotransformation of MCPA-EHE was investigated during dermal absorption experiments in intact human skin and in human skin S9 fraction. General esterase activity was tested in human skin S9 fraction with the positive control for non-specific hydrolysis: fluorescein diacetate (Guilbault & Kramer 1964). S9 fraction from rat skin was tested in parallel to ensure assay functionality and testosterone was used as a model substrate for CYP-dependent biotransformation (Arlotto et al. 1991).

The protocol from Baetz et al. was used to determine general hydrolase activity with substrate fluorescein diacetate (Baetz et al. 2012). Hydrolase activity of 0.7 ± 0.6 nmol/(min*mg) for S9 fraction derived from cryoconserved (-20°C, up to 1 year) human skin samples in this study is close to results obtained with S9 fraction of freshly-excised human skin ($\sim 0.15 - 1.5$ nmol/(min*mg, mean ~ 0.5 nmol/(min*mg)) (Baetz et al. 2012). In studies from Baetz et al. activity in cryoconserved (2 – 3 months) human skin samples appears lower (~ 0.2 nmol/(min*mg)), however, the range ($\sim 0.06 - 0.6$ nmol/(min*mg)) overlaps with the range for freshly-prepared human skin (Baetz et al. 2012). Thus the observed differences are assignable to enzyme degradation during storage and/or donor variance. Taken together, we could show for the current case (human skin, cryoconserved up to one year) a preserved esterase activity, however – recalling the observations from the literature – this activity is probably lower than that of freshly-prepared human skin.

Next, S9 fraction of human skin was incubated with the ^{14}C -labeled substrate MCPA-EHE at a concentration of about 0.065 mg/mL. After 30 min incubation 59 % MCPA-EHE was recovered and 9 % of the parent was cleaved to MCPA. The low total recovery of 68 % was due to an unspecific protein binding, since the heat-deactivated control (HDC) revealed a low recovery of 55 % as well. The occurring substrate-protein-interaction may explain – beside the extreme high lipophilicity of MCPA-EHE – the very slow permeation through skin samples. Loss of MCPA-EHE via evaporation could be excluded, since the reaction vessels were wrapped with Parafilm 'M'[®] and evaporation to dryness of MCPA-EHE solution in acetonitrile (ACN) and re-solvation in ACN resulted in a recovery of 103 ± 0.7 % (RAD detection). The latter fits to the relatively low vapor pressure (0.000002 hPa) and high boiling point ($> 220^\circ\text{C}$) of MCPA-EHE (BASF SE 2009).

In rat liver S9 fraction, MCPA-EHE was completely cleaved to MCPA, whereby 3 % were oxidized to HMCPA. Therefore, the turn-over in rat liver S9 fraction was 100 % and therewith exceeded the turn-over in human skin S9 fraction. A ~10-fold higher esterase activity in rat liver S9 compared to human skin S9 was also observed with fluorescein diacetate (5.4 ± 0.4 compared to 0.7 ± 0.6 nmol/(min*mg)). A ~100-fold higher hydrolysis rate was reported for several alkyl-paraben-esters (Harville et al. 2007). An abiotic degradation of MCPA-EHE did not occur, since only the parent was recovered in BC (buffer control) and HDC. The further stability test of MCPA-EHE in water with recoveries of 97 ± 7 % and the absence of degradation products like MCPA up to 96 h confirmed these findings. The hydroxylated metabolite HMCPA known from in vivo rat experiments (van Ravenzwaay et al. 2004) was not formed during the incubation with S9 fraction of human skin. The oxidation of the methyl-group would need CYP activity. A general activity of CYP isoforms in skin was previously shown with testosterone which was metabolized to several oxidation and reduction products. For example, the formation of 6- β -hydroxytestosterone was observed, which is dependent on CYP 1A1, 2A2, 2C13 or 3A1/2 activity. However, the turn-over decreased with the use of cryoconserved skin samples (Arlotto et al. 1991; Henkler et al. 2012; Kao et al. 1985; Waxman et al. 1991). Additionally, Baron and co-workers detected EROD and PROD activity in freshly prepared human skin samples, albeit the basal activities were low (0.011 and 0.001 nmol/(min*mg), respectively) and close to the quantification limits of the current work (0.002 and 0.007 nmol/(min*mg), respectively) (Baron et al. 2001). Using cryoconserved human skin samples, EROD, PROD or BROD activities were not quantifiable (Henkler et al. 2012). For liver systems, CYP activity could be preserved up to 5 years by storage at -80°C . However, decreasing activities were reported for storage at higher temperatures (Yamazaki et al. 1997). Therefore, the absence of the oxidation product HMCPA and testosterone metabolites in the current investigations is consequential, when considering general low basal CYP activity in human skin and the decrease in activity with storage time (at -20°C) (Kao et al. 1985; Yamazaki et al. 1997). Taken together, a potential CYP-dependent biotransformation during skin passage is probably not covered when using cryoconserved (-20°C) skin samples. Induction of CYP isoenzymes could be considered for future experiments – which was previously shown to be feasible in human skin and reconstructed human skin (Goetz et al. 2012a; Harris et al. 2002).

In a third step, the actual metabolic transformation of substrate MCPA-EHE during skin passage was investigated using a modified diffusion cell experiment. Modifications include washing with water

instead of soap solution to facilitate extraction and allow HPLC separation, and waiving kinetic samples to avoid losses in tubings and vials. However, the resulting decreased concentration gradient was probably the reason for the similar, but slightly lower absorption results in comparison to the standard experiments. In total four samples representing the four compartments of dermal absorption *in vitro* (application solution, washing fluid, skin and receptor) were prepared, separated via HPLC and collected in one-minute fractions. The fractions were measured via LSC and combined to radiochromatograms. To identify the peaks in the reconstructed radiochromatograms, radiolabeled standards (^{14}C -MCPA-EHE and ^{14}C -MCPA) as well as unlabeled standards (MCPA-EHE, MCPA and HMCPA) were measured in parallel via HPLC-UV/RAD. HMCPA was not detectable in any of the samples. Therefore, no quantifiable CYP-dependent biotransformation occurred during passage – matching results from S9 fraction above. No MCPA was detected in the application solution, confirming the purity of the used standards ^{14}C -MCPA-EHE and MCPA-EHE. In the other compartments, MCPA was present. The deeper the compartment, the more MCPA in relation to MCPA-EHE was detected (e.g. DMS, washing fluid 1/59 and receptor fluid 1/3). Since contamination of the substrate with MCPA and abiotic degradation were excluded, the detected amounts of MCPA were derived from metabolic activities in the skin.

Since metabolites were observed in the washing fluid, degradation started in the SC, or the metabolites built in the viable epidermis re-diffused into the SC. The SC provides lipase and protease activities (Beisson et al. 2001; Egelrud 1992). Considering the structure of MCPA-EHE (see Table 1, p. 29), especially the branched alkyl chain, the molecule is unlikely a substrate of lipases – which hydrolyze substrates like triolein and 4-methylumbelliferyl 7-oleate (Beisson et al. 2001). Proteases like chymotryptic enzymes cleave peptide bonds with low specificity, but mainly at a carboxyl end of aromatic amino acids like tryptophan, tyrosine and phenylalanine (Belitz et al. 2008; Egelrud 1992). A cleavage of MCPA-EHE by these enzymes is likely. Additionally, carboxylesterases are eligible which are located in the viable epidermis and known to cleave alkyl-parabens (Harville et al. 2007). That cleavage could occur in the SC in general weakens the assessment from the EFSA Panel on Plant Protection Products and their Residues (PPR). This panel argued against a great importance of dermal biotransformation on dermal absorption, since metabolically active cells are localized below the main barrier, the SC (EFSA Panel on Plant Protection Products and their Residues (PPR) 2012).

MCPA-EHE was detected in the receptor fluid and in the FTS skin preparation, but not in the DMS preparation. No detectable amounts in the homogenized DMS were probably due to the generally low recovery from this tissue (here 8 %). The apparent binding to proteins – also observed with S9-fraction incubations – and the formation of a gelatinous plaque during extraction may hamper the success of the extraction. Future experiments may be improved by the addition of a proteinase mix – but degradation of MCPA-EHE needs to be excluded beforehand. However, that MCPA-EHE was detectable in the receptor fluid shows an incomplete cleavage. To assess this, a cleavage rate was calculated from S9-fraction incubations which were performed with tissue from the same human donors: From applied 0.07 mg/mL MCPA-EHE, 9 % were recovered as MCPA. Considering protein concentration (1 mg/mL), incubation time (30 min) and molecular weight of MCPA-EHE (312 g/mol), an enzyme activity of 0.67 nmol/(mg*min) was achieved. Therefore, during an absorption study of 6 h

with a skin sample of roughly 200 mg, which contains approximately 4.8 mg S9 protein, maximal 1.2 μmol could be cleaved – which is more than the applied dose of 160 μg = 0.5 μmol . Considering only the 1 – 4 % of compound penetrated into skin (max. 0.02 μmol), the general turn-over capacity is ~60 times higher than the actually observed activity. These results confirm previous findings, that not only the general capacity, but also the access to the enzyme determines its impact (Clark et al. 1993). The extreme lipophilic character of MCPA-EHE ($\log P_{ow}$ 5.4 – 6.8) may impede its diffusion over biological membranes and therefore its presence in viable cells; extreme lipophilic compounds tends to remain in the membrane (British Crop Protection Council 2011; Riviere 2011c; United States Environmental Protection Agency (US-EPA) 2004). Therefore, the incomplete degradation could be due to limited access to carboxylesterases which are located in the cytoplasm of keratinocytes in the viable epidermis (Mccracken et al. 1993). Protease-dependent cleavage in the SC seems of lower impact, since these enzymes are located in the intercellular space and therefore freely accessible; a remarkably higher turn-over would be expected (Egelrud 1992). A more exact localization of the cleavage would be possible with cryosectioning of skin samples and extraction afterwards. Additionally, the responsibility of carboxylesterases in MPCA-EHE cleavage could be tested by specific inhibition experiments using bis-(*p*-nitrophenyl) phosphate as described by Harville and colleagues (Harville et al. 2007).

When reconstructed skin was used as the barrier system, only MCPA was recovered in the receptor fluid (data not shown, but reported in Henkler et al.). This may be due to the observed higher esterase activities in the skin constructs, the higher permeability and therefore a better accessibility of the enzyme, but also due to a less sensitive detection method (GC-MS, LOQ 0.12 mg/L instead of 0.002 mg/L via LSC) (Henkler et al. 2012).

Taken together it was shown, that MCPA-EHE penetrates into and permeates through cryoconserved human skin and thereby undergo biotransformation probably due to carboxylesterase activity preserved in the viable epidermis. It was concluded, that (hydrolase-dependent) biotransformation – and therefore a probable change of physicochemical properties – during absorption experiments in vitro is qualitatively covered when using cryoconserved (20°C, up to one year) human skin. However, it should be noted, that the extent is probably lower than the activity in vivo or in freshly-excised skin and therefore not reflected quantitatively. Furthermore, CYP-dependent biotransformation is lower and maybe absent in cryoconserved human skin, since no CYP related biotransformation could be detected. Decreased activities with storage time were observed previously for several xenobiotic-metabolizing enzymes, e.g. CYP isoforms and NAT 1 (Kao et al. 1985; Land et al. 1989). It could be discussed, if the underestimation of the metabolic activity in vitro leads to an underestimation of dermal absorption in vitro. The argument is, that metabolites are generally more hydrophilic and therefore penetrate into deeper – aqueous – skin layers more easily and distribute in the entire organism more rapidly than the more lipophilic parent compound. However, this is only true, if the transformation takes place in the viable epidermis. If the metabolite is formed in the SC, its higher hydrophilicity compared to the parent compound would impede its penetration into deeper layers of this highly lipophilic tissue and therefore hinder its absorption. Furthermore, a metabolite can generally diffuse into deeper skin layers, but also towards the skin surface – due to the concentration gradient.

Overall, under- and overestimation could result theoretically. Focusing on the current case and considering the faster absorption of MCPA compared to MCPA-EHE through human skin *ex vivo*, extensive hydrolysis of MCPA-EHE in SC or deeper skin layers forming MCPA would probably increase the overall dermal absorption. Therefore, skin models devoid of xenobiotic-metabolizing enzyme activities may underestimate the extent. However, compared to the general overestimation of the *in vivo* situation with *in vitro* absorption experiments (on average factor 14 for the absorbed dose, derived for 14 pesticides in 25 experiments with rats and rat skin) makes the effect of biotransformation negligible for dermal absorption assessment (van Ravenzwaay & Leibold 2004). But beside the influence of absorption, the metabolic transformation may change toxicological or therapeutic aspects. In the present case a high hydrolase activity in the skin may cleave effectively MCPA-EHE and therefore decrease its activity as a skin sensitizer (derived from experiments in guinea pig) (United States Environmental Protection Agency (US-EPA) 2004). Hence, an *in vitro* strategy for skin sensitization should cover the effect of biotransformation in skin.

5.2.2 Xenobiotic-metabolizing enzyme activities in skin construct StrataTest®

Reconstructed human epidermis is already validated for specific toxicological endpoints like skin irritation and corrosion (OECD 2010a; OECD 2010b). Furthermore, reconstructed epidermis and full-thickness skin constructs are taken under consideration for dermal absorption experiments and other endpoints like genotoxicity (Henkler et al. 2012; Schaefer-Korting & Schreiber 2008). Beneficial for the mentioned endpoints would be a morphology, barrier function and metabolic activity close to the human *in vivo* situation. In a former project funded by the German BMBF, the expression, presence and activity of several xenobiotic-metabolizing enzymes were investigated in the following skin systems in comparison to human skin: in a epidermis construct (EpiDerm™), in two full-thickness skin constructs (EpiDerm™FT and Phenion®FT), in a transformed keratinocyte cell line (HaCaT) as well as in primary keratinocytes (for esterase activity measurements only) (Henkler et al. 2012; Jaekch et al. 2010a). In the current work the further construct StrataTest® was metabolically characterized using the same assays as in the mentioned project (Henkler et al. 2012).

Figure 25 shows the enzyme activities in direct comparison to results from Henkler et al. normalized to human skin (Henkler et al. 2012). Although the authors reported the presence of several transcripts of CYP isoform and CYP-dependent metabolites of testosterone in all skin systems (including cryoconserved human skin), no basal EROD, PROD or BROD activity could be detected (Henkler et al. 2012). This apparent contradiction could be explained by low sensitivity of the enzyme activity assays (LOQ 0.002 – 0.005 nmol/(min*mg)) combined with relatively low (CYP1A1) or not detectable (CYP2B6) transcript levels of EROD-/PROD-/BROD-specific CYP isoforms (Henkler et al. 2012). Additionally, the substrate testosterone could have been oxidized by CYP isoforms which were not covered by the enzyme activity assays e.g. CYP2C (Arlotto et al. 1991; Jaekch et al. 2011). Low and undetectable CYP activities were also reported for human skin and EpiDerm™ by Goetz et al. (Goetz et al. 2012a). Basal EROD, PROD, BROD activity below the LOD for the StrataTest® construct line up with findings for EpiDerm™, EpiDerm™FT and Phenion®FT (Henkler et al. 2012). This also holds true for the absence of UGT 2 transcripts and activity in the various constructs (Henkler et al. 2012; Jaekch et al. 2010b). Esterase activity in StrataTest® (3.6 ± 0.1 nmol/(min*mg)) was close to the other skin

constructs ($\sim 0.9 - 5.5$ nmol/(min*mg)) and exceeded the activity in human skin (current data: 0.7 ± 0.6 nmol/(min*mg), Baetz et al: $\sim 0.2 - 0.5$ nmol/(min*mg) (Baetz et al. 2012). The consortium reported NAT 1 activities in the various tested skin systems of $1.8 \pm 0.7 - 16.8 \pm 5.4$ nmol/(min*mg), whereby cryoconserved human skin provided the lowest values (Henkler et al. 2012). NAT 1 activities in StrataTest[®] were found to be in the same order of magnitude (7.2 ± 1.6 nmol/(min*mg)). Using a different substrate (p-toluidine) activity was lower for human skin and EpiDermTM (~ 1.4 and ~ 0.8 nmol/(min*mg), respectively) (Goetz et al. 2012b). mRNA transcripts of ADH isoforms were detected in the dermis, but not in the epidermis. This fits to the ADH activities in reconstructed full-thickness skin (EpiDermTMFT and Phenion[®]FT), and the absence of activity in the epidermal construct EpiDermTM and in keratinocytes (Henkler et al. 2012). In contrast, StrataTest[®] – also a full-thickness skin construct – did not provide detectable activities. Considering the very thin dermis hardly removable from the synthetic membrane (chapter 5.1.5, p. 103) StrataTest[®] is rather an epidermal construct. The negligible amount of fibroblast could also explain the relatively low FMO 1/3 activity, because FMO 3 transcripts were only detected in the dermis (Henkler et al. 2012). Finally, UGT 1 activity was not detectable in StrataTest[®] constructs either, yet UGT 1 transcripts and activity were found in human skin and the three tested constructs EpiDermTM, EpiDermTMFT and Phenion[®]FT – but not in keratinocytes (Henkler et al. 2012).

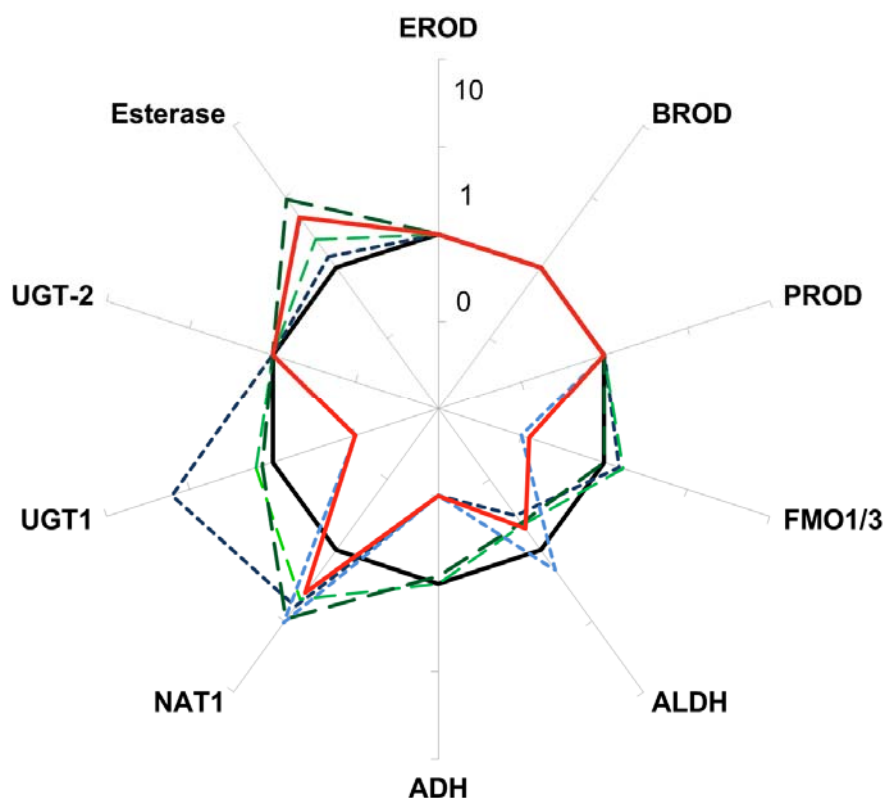


Figure 25: Comparison of xenobiotic-metabolizing enzyme activities in several skin systems in relation to human skin, which were given the value 1 (solid, black): three full-thickness skin constructs StrataTest[®] (solid, red), EpiDermTMFT (dashed, light green) and Phenion[®]FT (dashed, dark green), one epidermis construct, EpiDermTM (dotted, dark blue), and keratinocytes (dotted, light blue). Results for StrataTest[®] and esterase activity in human skin samples were obtained in the current study. The other results were measured by Henkler et al. (Henkler et al. 2012). CYP isoforms with EROD, PROD and BROD activity as well as UGT-2 activity were under the LOD in all tested systems.

To sum this up, the metabolic activity in StrataTest[®] reflected the activity in keratinocytes, but less the activity in other skin constructs and native human skin. Therefore, its use as surrogate for human skin in toxicological investigation would be suboptimal, since it is less representative than the previously investigated full-thickness skin constructs (EpiDermTMFT and Phenion[®]FT) (Henkler et al. 2012). The close results to the keratinocyte cell line are understandable, when recalling StrataTest[®] as a constructed tissue derived from an immortalized cell line (NIKS[®]) (Rasmussen et al. 2010b). Loss of specific function – in this example loss of xenobiotic-metabolizing enzyme activity – is a well-known issue in senescing cell cultures (Allen et al. 2005).

5.3 In silico models for dermal absorption

5.3.1 Abraham-based models containing mixture factor(s)

Besides experimental approaches to predict dermal absorption, in silico prediction tools have gained in importance. The last aim of the current work – the development of a prediction model which considers vehicle effects – is discussed in this section. With such a screening tool, chemicals falling under the REACH regulation could be estimated as a first approach and prioritized for further testing (The European Parliament and the Council of the European Union 2006). Additionally, the simulation of the vehicle effect would facilitate early developmental stages of pharmaceutical, pesticide or cosmetic formulations reducing the need of costly experiments. For regulatory purposes the EFSA Guidance document on dermal absorption of pesticides restricts data transfer to closely related formulations (EFSA Panel on Plant Protection Products and their Residues (PPR) 2012). However, a well-established and validated in silico model providing reliable interpolations may be acceptable for risk assessments (The European Parliament and the Council of the European Union 2006).

As outlined in more detail in chapter 1.4.4, p. 19, most models are restricted to infinite doses of aqueous solutions on human skin and mixture-related effects were only recently addressed (Abraham & Martins 2004; Potts & Guy 1992; Riviere & Brooks 2005). The basic Abraham model for aqueous solutions is widely accepted in the community, since it provides causal connection between physicochemical descriptors like H-bond acidity and dermal permeation (Abraham & Martins 2004). This approach is a single pathway model which represents only the intercellular route. However, such models were assessed to be generally sufficient (Pugh 2001). Riviere and Brooks added to the basic Abraham model a so-called 'mixture factor' (MF). Each MF was a composite value for one descriptor, calculated with the single values for each formulation ingredient and their weight percentage in the mixture. In their first model, they added the refractive index as MF. Based on data from 16 penetrants in 24 different mixtures resulting in 344 combinations they obtained a model describing 80 % of the variability (R^2 : 0.80, Equation 14, p. 22). The underlying database consisted of highly standardized in vitro tests in terms of experimental conditions (dermatomed pig skin, bicarbonate buffer as receptor fluid) and the 24 different mixtures contained maximal five of the following ingredients: water, ethanol, propylene glycol, methyl nicotinate and sodium lauryl sulfate (Riviere & Brooks 2005). For the current work, this approach was stressed with in vitro data from BASF SE derived mainly from regulatory studies for pesticides. This database consists of 89 compounds in more than 150 different formulations containing more than 240 possible ingredients applied on various skin preparations

(human, rat, pig, reconstructed skin, epidermal membranes, dermatomed skin, full-thickness skin ...) in 569 individual experiments conducted at different laboratories. Furthermore, a wide palette of receptor fluids was applied as well as varying occlusion conditions and exposure periods. The transfer was conducted in cooperation with the group of Professor Riviere at the Center for Chemical Toxicology Research and Pharmacokinetics, NC State University, Raleigh, NC, USA. That such inhomogeneous datasets could be used for prediction models of dermal absorption in general was previously shown by different research groups. For instance, Potts and Guy generated a model with R^2 0.67 based on the Flynn database (94 compounds, 15 different literature sources, 11 research groups) comprising various experimental conditions like receptor fluid or temperature (Flynn 1990; Guy & Potts 1992). By including indicator variables and other modifications in their model Samaras et al. obtained a correlation of 0.572 for a combined analysis of widely differing experiments (Samaras et al. 2012). However, the correlations were lower compared to models derived with more homogeneous datasets.

To establish a valid model, the 'OECD principles of (Q)SAR validation' were addressed in the current work. Principle 1 demands 'a defined endpoint' ideally obtained with a single protocol (OECD 2007). To fulfill this point in spite of the inhomogeneous database, only experiments with human or rat skin preparations performed in an experimental period of 6 to 48 h were included in the model development. Additionally, experiments with human and rat skin were considered separately, and species and receptor fluid indicators were used to address specific variables in the prediction model (discussed below). As in all classical dermal absorption prediction models, the logarithmic permeability coefficient ($\log K_p$) was defined as the endpoint. More precisely, the $\log \max K_p$ value was used – derived from the steepest slope of the absorption-time-profile – to include both, infinite as well as finite dose protocols. This value, derived from a pseudo-steady-state, is at least close to the steady state situation represented by $\log K_p$. The same simplification was used previously (Hostynek & Magee 1997). Similar to a homogeneous endpoint, OECD principle 1 also demands a homogeneous derivation of descriptors used in the model (OECD 2007). For instance, experimentally derived $\log P_{ow}$ values could be derived with different protocols. Therefore, only software generated and hence uniformly derived MFs were used in the current approach. Additionally, experimental data do not exist for all relevant compounds. An example comparison of $\log P_{ow}$ (calculated with Molinspiration Property Calculator) and logarithm of water solubility ($\log S_w$, calculated with ABLab feature of ADME Boxes 9.45) to literature (experimental) values – derived from PhysProp Database Demo (Syrres) – revealed a general accord of calculated and measured values with correlations of R^2 0.75 and 0.76, respectively, and therefore confirm the suitability of 'synthetic' values (Figure 17 a and b, p. 79).

OECD principle 2 ('unambiguous algorithm') refers to transparency. A detailed description of the developmental steps and the underlying dataset should be provided with the prediction model (OECD 2007). The final database for the current approach comprised 56 substances tested in 342 individual experiments and is given in Table 48 (annex). Analysis and modifications were described in detail in the method and result sections (3.7, p. 50 and 4.4, p. 79). The basic Abraham model was used as a starting point and extended by one factor, the mixture factor (MF), as described previously (Abraham & Martins 2004; Riviere & Brooks 2005). Multiple linear regression analyses were run with the software SAS 9.2 using this basic equation (Equation 28, p. 53) and refined versions of that. R^2 ,

adjusted R^2 and F-value were obtained, structurally influential compounds were identified with the leverage value (hat) and excluded as outliers and finally insignificant or highly correlated descriptors ($r > 0.7$) were excluded from the model. OECD principle 4 'appropriate measures of goodness-of-fit, robustness and predictivity' was fulfilled by internal (LOO, leave-one-out, and LMO, leave-many-out – her 25 % – procedures) and external validation (prediction of validation set) (OECD 2007). For the first models, the splitting into training and validation set was done randomly.

Riviere et al. tested various MF as the additional factor to the Abraham descriptors. They obtained highest correlations using MF refractive index, polarizability or the logarithm of the inverse Henry's law constant (Riviere & Brooks 2005). However, a clear favorite which explains the mixture effect on dermal absorption with a straight forward mechanistic and hence causal relationship was not identified. Therefore, 87 different MFs were tested in the current approach. In general, the highest correlations for the current dataset were obtained with the factors TPSA (topological polar surface area) – directly or as its inverse value – or logHBAcc (the logarithmic number of hydrogen bond acceptors) calculated with different software tools. The descriptor molinspLogHBAcc was chosen as the starting point for the developmental process. A 'mechanistic interpretation' (OECD principle 5) of the descriptors and their relationship to the endpoint are discussed in chapter 5.3.3, p. 126.

The simplest significant and fully-validated model (no. 6, Table 30, p. 82) used three descriptors, namely $\Sigma\alpha_2^H$, Rf_2 and molinspLogHBAcc. The model was robust with Q^2_{LOO} and $Q^2_{25\%}$ values close to R^2 , but R^2 itself was low (0.37) and Q^2_{Ext} even lower (0.26). The OECD Guidance document states that the goodness depends on the specific model and that the end-user should decide what correlation is suitable for the specific issue (OECD 2007). However, Kubinyi demands a minimum R^2 of about 0.64 when using in vivo data and 0.8 when using in vitro data for an appropriate in silico model (Kubinyi 1993). Therefore, this first attempt was assessed to have a low predictive power. However, comparing this model with the corresponding model without MF, the R^2 was increased about 0.15. This means, that MF was able to explain 15 % of the variance. Over all the models reported in this work, the MF explained between 12 and 21 % of the variance. This is similar to observations from Riviere and Brooks who observed improvements of about 20 % (Riviere & Brooks 2005; Riviere & Brooks 2007). The effect of inserting a MF in the prediction model is visualized in Figure 21, p. 91: Without a MF (Figure 21 a) the predicted logmaxKp values for one substance were identical – independent of the applied formulation and other varying aspects like species or receptor fluid. Therefore, each substance is represented by a 'column' of values whereby the height is related to the deviation observed for one substance. The highest column was obtained for substance no. 2 fenpropimorph. Its structure is given in Figure 26. The observed variance from -6.89 to -1.0, a range of more than 5 orders of magnitude, was partly explained by the MF. This is visualized by redistribution of the column and a closer alignment of predicted values to observed values (Figure 21 b). That is, the observed logmaxKp values still range from -6.89 to -1, but the MF has adjusted the predictions and therefore, repositioned the data points such that they are no longer columnar. The highest logmaxKp values for fenpropimorph (-2.3 to -1.0) were observed for solutions in cyclohexanone. This is plausible, since cyclohexanone is known to enhance dermal uptake, which is probably related to its lipid-

extracting properties. Derivatives of cyclohexanone are under investigation as enhancers for pharmaceutical applications (Monteiro-Riviere et al. 2001; Quan et al. 1991; Roberts et al. 2008).

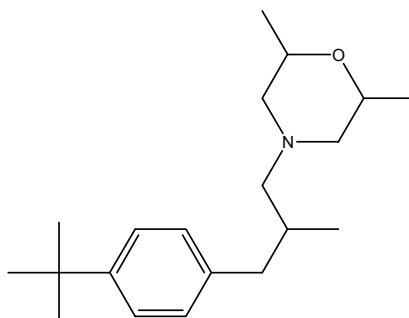


Figure 26: Compound no. 2, fenpropimorph, C₂₀H₃₃NO.

Besides a mixture effect, the huge variation within a substance could be due to other reasons. One possibility is the ionization state of the compound, since ionized molecules cannot permeate the skin (Riviere 2011c). Regarding the example fenpropimorph, the molecules are undissociated at pH 5 – 9, but $\log P_{ow}$ changes with the pH (pH 5: 2.6, pH 7: 4.1, pH 9: 4.4) (Standing Committee on Biocidal Products 2009; United States Environmental Protection Agency (US-EPA) 2006). The decreasing lipophilicity with decreasing pH is due to a protonation of the nitrogen atom. The database reported no details about the pH-values of application solutions, but it is known that generally only neutral formulations were applied to avoid negative effects on the skin samples. Therefore, the pH effect seems of low impact for the current database. However, the ionization state of the molecules under neutral conditions was not considered, since all properties were calculated for the neutral molecules. Therefore, a modification of the model regarding rate of neutral/ionized molecules may improve its predictive power. Such refinements were conducted previously by Vecchia and Bunge (Vecchia & Bunge 2002).

A comparison of other experimental conditions leading to the highest and lowest $\log_{max}Kp$ values for the example fenpropimorph, revealed a complex interaction and no clear rules: highest values were obtained with cyclohexanone vehicle applied on rat or human epidermis and receptor fluid composed of ethanol/water 1/1, v/v, and the lowest values with SolvessoTM- or water-based formulations using dermatomed human skin samples and receptor fluid composed of ethanol/water 2/8, v/v. In between were results with a water-based formulation on human and rat epidermis and receptor ethanol/water 1/1, v/v.

Since the species is a well-known influential factor, the data points derived with human and rat skin samples were depicted separately in the graph of predicted versus observed values (Figure 18, p. 83) (Vecchia & Bunge 2006). This and the calculated residuals revealed a clear bias to over-predict absorption through human skin samples and under-predict absorption through rat skin samples when using model no. 6 (Figure 18 a). However, combination of both seems generally suitable, since linear regression analysis for the human (model no. 2) or rat (model no. 4) dataset alone resulted in tendentially similar model equations:

$$\text{Model 2: } \log \max Kp = -2.6 - 1.0 * \sum \alpha_2^H - 0.8 * Rf_2 - 4.3 * Acc$$

$$\text{Model 4: } \log \max Kp = -2.3 - 1.6 * \sum \alpha_2^H - 0.6 * Rf_2 - 2.6 * Acc$$

Insertion of a binary class variable for the species (Spl) – 1 for human and 2 for rat – revealed the following model equation which was free from bias for the species (compare Figure 18 b) and additionally of higher robustness (Q²LOO 0.38, Q²25% 0.38) and predictive performance (Q²Ext 0.32) than the model without Spl (model no. 6, Table 30, p. 82, Q²LOO 0.34, Q²25% 0.34, Q²Ext 0.26):

$$\text{Model 8: } \log \max Kp = -3.4 - 1.2 * \sum \alpha_2^H - 0.7 * Rf_2 - 3.3 * Acc + 0.6 * Spl$$

However, the model using only the human dataset has with R² 0.46 and Q² 0.38 a remarkably higher predictive power in comparison to the combined approach. A focus on human experiments alone should be considered in the following developmental steps and weighed against the advantageous use of larger, information-rich datasets.

The use of indicator variables representing experimental conditions was firstly introduced by Hostynek and Magee. They used one for occlusion condition and one for vehicle – whereby only two different vehicles (ethanol and acetone) were apparent in their dataset (Hostynek & Magee 1997). To address the well-known influence of dosing vehicle in a manner analogous to the species, model no. 8 was plotted separately (Figure 19, p. 84) for the seven receptor groups defined in section 3.7.1 ('water', 'water+B', 'water+x', 'PBS,pH4', 'E/W_1', 'E/W_2' and 'E/W_3') (Challapalli & Stinchcomb 2002; Safferling 2008). However, no obvious biases were observable. Combining the seven receptor groups into two groups (ethanol/water mixtures and other water-based receptor fluids) and calculating residuals and ratios for over and under-predicted values, tendencies to lower values with ethanol/water mixtures and to higher values with other water-based receptor fluids were observed. However, addition of a binary variable RI, the so-called receptor indicator, with value 1 for the former and 2 for the latter did not change the ratio of over- and under-predicted values. Additionally, the new parameter was not significant. Since the receptor effect was very small and a separate use of the seven receptor groups would be inadequate due to too small groups, the entire set was left in the database and the small effect assessed as acceptable. In general, the influence of the receptor fluid was less obvious than the effect of the species. For future optimization of the model a breakdown into seven values for the RI may increase the fit. However, this approach was waived for the present work, since predefined values and therefore a predefined effect and ranking of the receptor fluid would be necessary with SAS 9.2 procedure 'Proc Reg'. Use of procedure 'Proc Glim' would allow the insertion of class variables which adjust the impact of the different receptor fluids, but this would mean seven additional model parameters and would renounce the internal validation procedures. In general, such indicator variables are conceivable for other experimental parameters that are known to influence absorption, such as occlusion condition (non-, semi- and occlusive) or skin preparation type (epidermis, dermatomed, full-thickness). However, Samaras et al. observed no significant contribution of the two mentioned indicator variables to their prediction model (Samaras et al. 2012). In contrast, Hostynek and Magee applied successfully an occlusion variable (Hostynek & Magee 1997). An indicator variable

for infinite/finite dose experiments was significant in analysis from Samaras and co-workers (Samaras et al. 2012). Application of several indicator variables would help to assess influential factors and determine their usefulness in prediction models. However, over-fitting must be avoided when extending the prediction model. One marker for over-fitting is the standard error. This value should not be smaller than the experimental error of the data (OECD 2007; Wold et al. 1984). This condition is fulfilled for the current model (no. 8, Table 30, p. 82) with a standard error of 0.91 in comparison to the average experimental SD of 0.26.

The use of PC factors was another attempt to enhance the model. The idea was that defining the five Abraham descriptors in fewer PC factors may be superior to models which excluded information by expelling insignificant descriptors. From the resulting PC factors, only the first was significant in the prediction model. This factor was highly associated with $\Sigma\beta_2^H$, π_2^H , Rf_2 and V_x and represented with an eigenvalue of 2.7, roughly half of the total variance of 5. With R^2 0.33 and Q^2Ext 0.27, the 'PC model' (model no. 10) was not superior to the analogue descriptor model using $\Sigma\alpha_2^H$ and Rf_2 (model no. 8, R^2 0.4, Q^2Ext 0.32) (see Table 30).

In classical QSAR approaches each data point represents an individual substance (OECD 2007). In the present model each data point represents a substance-mixture combination applied under individual experimental conditions. Therefore, random splitting into training and validation sets would bias the prediction, if substance-related information is present in both sets. This was the case in the former models (no. 1-10). To build more reliable models, a substance-based splitting was performed. After sorting the substances accordingly to substance-specific value Rf_2 as level one and $\Sigma\alpha_2^H$ as level two, every third compound was assigned to the validation set. A prerequisite for successful predictions is the coverage of the same parameter space by the training and validation sets. That this was the case was illustrated in Figure 7, p. 52). The goodness of fit of the resulting model (no. 14, Table 30) was lower (R^2 0.37) in comparison to the parallel model with the randomly defined training set (no. 8, R^2 0.41). However, the model was reduced to three (Rf_2 , Spl , $molinspLogHBAcc$) instead of four descriptors ($\Sigma\alpha_2^H$, Rf_2 , Spl , $molinspLogHBAcc$) and provided a higher predictive power (Q^2Ext 0.33 compared to 0.27).

In contrast to the observation with the randomly defined training set, this model (no. 14, rat and human data) led to similar validation results as the analogous model containing only human data (no. 12, Table 30). Therefore, both are applicable for predicting the human situation. The predictive power for the rat situation was improved for both training sets when using rat and human data together: For random data splitting, compare model no. 4 (only rat, R^2 0.35, Q^2Ext 0.03) with model no. 8 (human and rat, R^2 0.41, Q^2Ext 0.32) (Table 30). With substance-based splitting, model no. 14 (human and rat, R^2 0.37, Q^2Ext 0.33) was of higher predictive power than the parallel significant model comprising only rat data with R^2 0.13 and only $molinspLogHBAcc$ as a single descriptor. Descriptor Rf_2 was excluded due to a p-value of 0.133. The information provided by the 82 data points of the rat training set seems insufficient to build a good model, but incorporation of human data filled important gaps. The benefit was remarkable. Since the combined approach improves the predictions for rat and does not weaken the predictions for human, it was used for further modifications.

At this point, the descriptor *molinspLogHBAcc* was replaced by the other promising MF identified at the beginning: *molinspTPSA*. The resulting validated model (no. 20, Table 30) provided a similar fit and robustness (R^2 0.38, Q^2_{LOO} 0.35, $Q^2_{25\%}$ 0.35) as the parallel model no 14 with *molinspLogHBAcc* (R^2 0.37, Q^2_{LOO} 0.34, $Q^2_{25\%}$ 0.34), but a remarkably higher predictive power (Q^2_{Ext} 0.41 and 0.33, respectively). However, after all these modifications, the fit and the predictive power were still relatively low. Therefore, an extension of the basic model from Riviere and Brooks containing one MF to two or more MFs was considered (Riviere & Brooks 2005). A combination of the two MF used above (*molinspTPSA* and *molinspLogHBAcc*) was not suitable due to a highly significant correlation to one another (r 0.619) leading to insignificant models. This was also the reason why *molinspLogHBAcc* was eliminated in stepwise analysis using the feature 'maxR' of the software. However, the procedure suggested addition of the descriptors *Adme1/P_{ow}*, *molinspHBDOn*, *AdmeLogHBDOn* and *Adme1/RotB* to *molinspLogHBAcc*, Rf_2 and *Spl*. Considering correlations of the descriptors and p-values derived from regression analysis, only the combinations *molinspLogHBAcc*, Rf_2 , *Spl* and *Adme1/P_{ow}* (model no. 16, Table 30) and *molinspLogHBAcc*, Rf_2 , *Spl* and *AdmeLogHBDOn* (model no. 18) were valid. Goodness of fit and robustness were similar to the parallel model no. 14 (with *molinspLogHBAcc* as the only MF), but the predictive power increased from 0.33 to 0.41. However, in comparison to model no. 20 (*molinspTPSA*, Rf_2 , *Spl*) no improvement was obtained. Using SAS procedure 'maxR', the addition of *molinsp1/HBDOn*, *molinspP_{ow}*, *Adme1/RotB* to *molinspTPSA*, Rf_2 and *Spl* seemed suitable. However, only combination with *molinsp1/HBDOn* led to a valid model (no. 22, Table 30). Although model no. 22 revealed a slightly higher goodness of fit (R^2 0.39 instead of 0.38) and robustness (Q^2_{LOO} 0.36 instead of 0.35) as model 20 (*molinspTPSA*, Rf_2 and *Spl*), the predictive power decreased (Q^2_{Ext} 0.30 in comparison to 0.41). Therefore, no valuable information was added with the second MF in this case. Taken together, the best model was no. 20 with the following regression equation:

$$\text{Model 20: } \log \max Kp = -2.3 - 0.6 * Rf_2 + 0.5 * Spl - 0.1 * molinspTPSA$$

The improvement caused by incorporation of the MF *molinspTPSA* in comparison to the model without any MF is visualized in Figure 20, p. 88. However, with R^2 0.37 the model explains less than half of the variance and was of lower fit than models reported in the literature (R^2 0.83, 0.67, 0.80 (Abraham & Martins 2004; Potts & Guy 1992; Riviere & Brooks 2005), respectively). Only Kirchner et al. reported a correlation in the same dimension (R^2 0.32) using a combined dataset of the Flynn dataset and data from regulatory reports (Kirchner et al. 1997). They improved the predictions by subdividing their set into five groups based on molecular volume. R^2 from 0.55 to 0.86 were reached for subgroups containing 8 to 58 data points. A similar division could be discussed for the current approach. But considering the modifications discussed above for the species, the insertion of indicator variables representing separate groups is more promising than the reduction of the model to less data points. Such an approach would be less restrictive and hence more useful for routine work. Nevertheless, it is questionable, if the required effort to insert all possible variables, will finally lead to a remarkably improved prediction model.

The confidence interval for predicted logmaxKp values using model no. 20 was ± 1.6 log units. The resulting range covers three log units or three orders of magnitude. This was only partly caused by the average SD of the underlying experimental dataset, which was with 0.26 log units on an acceptable level. Nevertheless, it is relatively high in comparison to more standardized in vitro tests. Therefore, the question arises, if a model derived from highly variable data should be used to predict a specific value, or if estimation of classes would be more reasonable. Classification analyses like discriminant analysis are conceivable. But due to the theoretical continuous distribution of logmaxKp, the present study focused on the prediction of the five predefined Marzulli classes (Marzulli & Brown 1969; OECD 2007; Worth & Cronin 2003). Marzulli classes for the rate of dermal permeation, ranging from very slow (< -5.22) to very fast (> -2.22), were assigned to penetrants based on their logmaxKp values (see Table 15, p. 57). Each class comprises one order of magnitude. The ability of models no. 18 and 20 – the two models with the best fit and predictivity from above – to predict the magnitude of dermal absorption was assessed by comparing the Marzulli classes derived from experimental and predicted logmaxKp values. The percentage of data points which were assigned to the correct Marzulli class were 47.2 % (no. 18) and 44.7 % (no. 20). Only one class apart from the correct class were 44.5 and 48.9 %, respectively. Therefore, more than 90 % were predicted with a maximum error of one Marzulli class.

To sum up, the derived modified Abraham model no. 20 with descriptors molinspTPSA, Rf_2 and Spl provided the highest predictive power. However, with R^2 of 0.38 and Q^2Ext of 0.41, the model is of limited use to predict exact logmaxKp values and for regulatory purposes. However, rough estimation of Marzulli class and therefore order of magnitude of dermal uptake is possible, which could save time and costs in the early stages of development. Additionally, further modifications are conceivable which may improve the approach.

5.3.2 Substance-based models containing mixture factor(s)

Due to relatively poor fit and predictive power of the Abraham-based model, a substance-based model was developed which predicted mixture effects. For this the substance-specific descriptors ($\Sigma\alpha_2^H$, $\Sigma\beta_2^H$, π_2^H , Rf_2 and V_x) were replaced by a class variable SUBST. The idea was to use the existing experimental information of a substance instead of predicting it by descriptors. The variation within one substance is due to experimental conditions and therefore describable by linear combinations of class variable SUBST, MF and indicator variables like Spl. Such a model predicts only the mixture and species effect of integrated substances, but not the absorption of unknown substances. At least five data points per substance derived from five different mixtures were defined as basic prerequisites for inclusion in the model. One third was assigned to the validation and two thirds to the training set. When concentrating on human data 16 substances were includable; when combining human and rat data a seventeenth substance could be added. SAS procedure 'Proc Glim' was used to run multiple linear regression analyses while including class variables. However, no stepwise analyses are possible with Glim, therefore, the MFs identified for the Abraham approach were used. Furthermore, no internal validation (LOO and LMO) was possible, thus, only external validation was conducted. Since one substance was always part of the training and validation sets, Q^2Ext was a measure of predictive power as well as a measure for robustness.

The basic models no. 23 (class variable SUBST and Spl; human and rat data) and no. 30 (class variable SUBST; human data) resulted in R^2 0.49 and 0.56 and $Q^2\text{Ext}$ 0.56 and 0.60, respectively (see Table 36, p. 89). Therefore, the substance explained about half of the variance. Addition of one MF explained additionally 5 – 9 % of the variance and using two or three MFs 10 to 20 %. The model comprising human and rat data with the best fit (R^2 0.67) and the highest predictive power ($Q^2\text{Ext}$ 0.69) was model no. 25:

Model 25:

$$\log \max Kp = -3.5 + SUBST - 5.4 * molinspLogHBAcc - 0.1 * Adme1 / P_{ow} + 0.6 * Spl$$

Considering only human data, model no. 35 provided the best fit (R^2 0.75) and the highest predictive power ($Q^2\text{Ext}$ 0.73):

Model 35:

$$\log \max Kp = -1.0 + SUBST - 3.1 * molinspLogHBAcc - 0.1 * Adme1 / P_{ow} - 4.5 * Adme1 / RotB$$

The substance-specific estimators for class variable SUBST are listed in Table 37, p. 90. In contrast to the Abraham-based models discussed in chapter 5.3.1, the inclusion of rat data decreased R^2 and $Q^2\text{Ext}$ and therefore did not provide valuable additional information, but was rather disadvantageous for predicting human data. This is comprehensible, since the species was not considered when calculating the class variable SUBST. It seems that Spl could not compensate for the varying ratios of rat and human experiments underlying each class variable. Considering this problem, makes the usability of other indicator variables accounting for experimental conditions less likely. However, the added MF is almost independent from the class variable, since only few repetitions were present in the dataset. The resultant model no. 35 with R^2 0.75 was better than the Guy and Potts model (R^2 0.67) and close to the original Abraham model (R^2 0.83) (Abraham & Martins 2004; Potts & Guy 1992). Furthermore, the fit was better than requested for reliable prediction models based on in vivo data (R^2 0.64) and close to the requested value for in vitro data (R^2 0.8) (Kubinyi 1993). Additionally, the prediction of Marzulli classes was improved. With model no. 35 59 % were exactly correctly predicted and 40.3 % one class apart from the correct class. Therefore more than 99 % were predicted with a maximum error of 1 Marzulli class. Taken together, this model is a suitable model to predict mixture effects for included substances (mainly pesticides). Therefore, it is a promising tool to evaluate changes in pesticide formulations in the early stages of development. Extension to other substance classes is generally possible by including appropriate experimental data to the training set.

Besides the effect of various mixtures on the absorption of one substance, the model implies a ranking of absorption for different substances from one mixture/formulation. A substance with a high estimator for SUBST would more easily permeate the skin than a substance with a low estimator – if applied in the same formulation. In the current database six formulations were used for different compounds as listed in Table 40. The numerical code used in Table 40 (and in Table 47, annex) shows the test compound number before the underscore and the formulation number after the underscore. For instance, formulation 3_9, 9_1 and 4_4 were the same, but in the respective experiments absorption

of compound 3, 9 or 4 were investigated. Table 40 shows the ranking of the substances experimentally and the ranking based on the estimators of the model (no. 35). For instance, with estimators -2.5 for substance no. 9, -2.43 for substance no. 3, and -1.74 for substance no. 4, the absorption from a joint formulation was ranked as $9 \approx 3 < 4$. The ranking was the same when using model no. 25 (human and rat data). In total, only three of six rankings were correctly predicted. This indicates that the mixture effect is not equal for the different substances as implied by the model. This is reasonable, since the applied formulation may affect the absorption of a substance by direct interaction or indirectly by changing the properties of the skin barrier. If only the skin is affected – possibly by changing lipid fluidity, lipid content or hydration grade – such a ranking would be correct. However, once the substance is directly affected by increased or decreased solubility and therefore changed diffusion behavior, such a ranking may not be correct. These considerations lead over to OECD principle 5, ‘a mechanistic interpretation’, and the reliability of the parameters (see the following chapter).

Table 40: Ranking substance absorption from a joined mixture by experimental data and based on the estimators from model no. 35. Substance and mixture no. are in accordance with the compound no. in Table 47, annex.

mixture no.	ranking substances (experimental)	ranking substances (model)	conformance
3_9 = 9_1 = 4_4	$3 \leq 9 < 4$	$9 \approx 3 < 4$	✓
3_10 = 9_2 = 4_5	$3 < 9 \leq 4$	$9 \approx 3 < 4$	-
28_5 = 4_6	$28 < 4$	$4 < 28$	-
28_6 = 4_7	$28 < 4$	$4 < 28$	-
9_3 = 12_5 = 4_8	$9 \leq 12 < 4$	$9 \approx 12 < 4$	✓
12_6 = 4_9 = 28_7	$12 < 4 < 28$	$12 < 4 < 28$	✓

5.3.3 Mechanistic interpretation of the models

The underlying principle of in silico prediction models is that properties and biological activities are inherent to the structure of a molecule and that similar chemical structures lead to similar reactivity and biological effects. Therefore, developed relationships should provide a mechanistic insight. In the current model, the main parameter explaining the substance-specific variance of absorption was Rf_2 . If the randomly defined training set was used, also $\Sigma\alpha_2^H$ was significant. The MFs most effectively explaining the influence of the mixture on the permeating behavior were molinspTPSA and molinspLogHBAcc. Parameter Spl allowed the combined use of rat and human data in the Abraham-based models.

Several Abraham descriptors were redundant (highly correlated) or insignificant in the current approach. To provide only robust prediction tools, they were excluded from the model equation. In comparable literature models, all five Abraham descriptors were part of the model equation. However, a significance of the single descriptors in the form of p-value was not reported and the remarkable correlation between $\Sigma\alpha_2^H$ and $\Sigma\beta_2^H$ (0.85) stated by Riviere and Brooks would suggest a reduction of the model (Abraham & Martins 2004; Riviere & Brooks 2005).

The relative impact of the individual descriptors could be assessed with the standardized coefficients (Table 35, p. 88 and Table 37, p. 90). Rf_2 has a standardized coefficient of -0.3 for the models no. 18 and 20. This value is smaller than the corresponding values for the MFs (model 18: -0.6 molinspLogHBAcc and 0.3 AdmeLogHBDon, model 20: -0.5 molinspTPSA) and therefore of less impact. Compared to Spl (0.2 in both models) Rf_2 is of higher impact. The same order was achieved when using grade of significance for each model (p-values). On this basis, it could be concluded that dermal absorption was mainly determined by the application solution, followed by the properties of the penetrant and the species of the skin donor. However, with the substance-based approach, the class variable SUBST was the main determinant followed by the MFs and Spl.

Negative coefficients for the substance-specific parameter Rf_2 were also observed from Riviere and Brooks (-0.4) and Abraham and co-workers (-0.1) (Abraham & Martins 2004; Riviere & Brooks 2005). The solvatochromatic parameter Rf_2 , the solute excess molar refractivity – a measure of the speed of light in that medium compared to a vacuum – contains information about molecular volume and polarizability (Todeschini & Consonni 2009). This explains the observed highly significant correlation to V_x and π_2^H (0.60 and 0.83, respectively, see Table 29, p. 81). The Rf_2 value is higher for bigger and more polar molecules. Therefore, a negative contribution to the model is logical, since it is well-known that smaller, nonpolar molecules permeate the skin more easily than bigger and more polar molecules (Grice et al. 2010). This is also the reason, why almost all prediction models published in the literature contain size-parameters (Geinoz et al. 2004).

Regression coefficients for $\Sigma\alpha_2^H$ were generally negative. This is in accordance to former analyses (Abraham & Martins 2004; Riviere & Brooks 2005). Parameter $\Sigma\alpha_2^H$, or the overall hydrogen bond acidity, describes the ability of a compound to donate a proton for a hydrogen bond; high values are related to high polarity and size (Kamlet et al. 1983). Significance of $\Sigma\alpha_2^H$ was also observed in models from El Tayer and co-workers. It was deduced that the highly lipophilic SC, rich in H-bond acceptor groups like phosphate groups or ester linkages, interacts extensively with H-bond donors (El Tayer N. et al. 1991). The higher $\Sigma\alpha_2^H$, the higher is the grade of interaction, the more hindered is the diffusion over the SC and the smaller is the flux or logmaxKp.

Similar straightforward interpretations are difficult for the identified MFs. Also, Samaras et al. who identified the vehicle as a main influential parameter and the gap between melting and boiling point as a good descriptor for the mixture effect, had trouble finding mechanistic explanations (Samaras et al. 2012). However, the need for a factor accounting for vehicle effects was confirmed with this and the current study. The most effective MFs in the current investigation were molinspLogHBAcc and molinspTPSA. Since HBAcc is inserted in its logarithmic form, it is exponentially associated with logmaxKp and therefore linearly with maxKp, but – with a negative sign – generally inversely related. HBAcc is the number of H-bond acceptors in a molecule. So it is the number of electronegative atoms (oxygen, nitrogen) with free electron pairs. Therefore, it is a measure of polarity, probability of interactions with H-bond donors and – since larger molecules could contain more H-bond acceptors – partly a measure of size. In the current work it was not used as a parameter for a single molecule, but as a property for the entire mixture – calculated from the values for the single ingredients and their weight percentages.

As mentioned previously the formulation may affect the penetration and permeation of a substance directly by changing its solubility and diffusional behavior or indirectly by changing properties of the skin like lipid content, fluidity or hydration grade and therefore its barrier function. A mixture with a high value for molinspLogHBAcc contains mainly large polar molecules which highly interact with SC lipids. Such a mixture is less likely to penetrate into the skin and further permeation is severely hampered. This is in accordance to the 'Lipinski rule of 5' which predicts a poor absorption of compounds with more than 10 H-bond acceptors (Lipinski et al. 1997). In contrast, mixtures with low values may easily penetrate into the skin. And once a mixture is present in the skin, it could act as an enhancer. It may increase the solubility of the penetrant in the skin, may disturb the lipid arrangements, or moisturize the SC (Bodde et al. 1989). This theory is in compliance with the negative regression coefficient. Furthermore a mixture with a high MF molinspLogHBAcc could widely interact with itself, and a substance highly soluble and interactive with its donor has a lower diffusion pressure and therefore slower absorption kinetics (Baker 1986). However, if the penetrant is only a minor contributor to the MF (low concentration) the MF does not represent the behavior of the penetrant in the mixture. Therefore, the use of the current MFs may not be sufficient to explain and predict the complex mixture effect. More mechanistic consideration may improve the current approach. For instance, two different factors were conceivable whereby factor one provides information about the mixture as such – this is in general what the current factor does – and factor two relates the substance to the mixture. The latter should take into account the concentration as well as the interaction between mixture and penetrant. One idea is the use of ratios like $\text{HBacc}(\text{mixture}) / \text{HBacc}(\text{penetrant})$.

MF molinspTPSA represents the topological polar surface area and is therefore a measure for polarity and size. This is similar to HBacc which explains the highly significant correlation of these two parameters and suggests a similar mechanistic explanation (see above). Combinations of molinspTPSA with another MF did not improve the prediction. In contrast, besides a slight increase of R^2 , Q^2_{Ext} was even decreased when adding molinsp1/HBDonor. This is an example for an over-fitted model. Some combinations with molinspLogHBacc significantly improved the model; for instance, the combination with AdmeLogHBDon in the Abraham-based approach. This factor is size-dependent and the greater the value, the more H-Bond donors are present in the molecule. The considerations are similar to the ones for H-bond acceptors, but are now representative for other chemical classes. However, the combined use makes sense, since the interactions inside a mixture are highly increased if both numbers – donors and acceptors – are increased. And wide interactions would increase solubility and therefore slow down the permeation. The substance-based models could be improved using a combination of molinspLogHBacc, $\text{Adme1}/P_{\text{ow}}$ and $\text{Adme1}/\text{RotB}$ – all with a negative contribution to \log_{maxKp} . Therefore, the penetration and permeation increased with higher lipophilicity (P_{ow}) and flexibility (RotB) of the mixture. That must be understood in terms of enhancing effects. That lipophilic molecules could permeate through the skin more easily than hydrophilic ones is well-known (Grice et al. 2010). That highly flexible molecules could easier overcome the tight barrier of lipids, keratin and cells is also a logical consideration. A mixture possessing these properties would penetrate easily into the skin and once inside the skin, it would change barrier functions and solubility of the penetrant in the skin and therefore may act as an enhancer.

Finally, the parameter Spl had a high impact on the model. With this factor, the influence of the species could be addressed, namely the generally higher absorption with rat skin compared to human skin. The higher absorption through rat skin is not limited to the current data, but widely reported (Monteiro-Riviere et al. 2000; Scott et al. 1986; van Ravenzwaay & Leibold 2004). The linear addition of Spl implies a constant interspecies factor rat/human. However, this is not true when considering individual data for specific penetrant-mixture combinations. The absence of a fixed factor was discussed before (chapter 5.1.5, p. 103). However, the application of the fixed parameter Spl is suitable for first estimations using *in silico* models.

The three most important factors identified by stepwise regression ($molinspLogHBAcc$, Rf_2 and Spl or $molinspTPSA$, Rf_2 and Spl) were the same as the parameters obtained with a predefined model equation (e.g. Equation 29, p. 53), which was reduced afterwards to the specific parameters. Therefore, backward and forward analyses confirmed each other and identified the importance of the main descriptors.

5.3.4 Applicability domain

In the last section of the discussion OECD principle 3, 'a defined domain of applicability', is addressed. An applicability domain (ApD) identifies the parameter space covered by the prediction model. The model would only be applicable to substances inside the domain. The difficulty is to find the balance between too restrictive limits leading to specialized models and the reliability of the predictions. In general, it is defined by the included data, the training set. Minimum and maximum values of single descriptors were rough estimates to make only interpolations and avoid extrapolations. In the current case, new predictions must not only be inside the structural domain of the penetrant, but also inside the domain of the formulation. Furthermore, response outliers (residuals $> 3 \cdot SD$) should be considered when drawing lines of ApD.

The ApD for the substance-based model no. 35 is not defined by substance properties, but directly by the included 16 substances (no. 2, 3, 4, 6, 9, 12, 13, 17, 22, 26, 28, 30, 42, 57, 58 and 59 or namely, fenpropimorph, pyraclostrobin, epoxiconazole, dimethomorph, boscalid, prochloraz, metazachlor, N-methylpyrrolidone, pyrimidinotriazole, RS-dimethenamid P, metconazole, ametotradin, dimoxystrobin, testosterone, caffeine and tetrahydrofurane; compare Table 47, annex). Furthermore, the predictions are restricted to human skin, since only human data were used for model development. The only response outlier (substance no. 2 in mixture no. 2_4, human skin) was associated with the lowest $\log_{max}Kp$ value (-6.89). This value was lower than the lowest predicted value (-6.57). Therefore, minimum and maximum values of observed (training set) and predicted $\log_{max}Kp$ values were considered, hence predictions inside the range of -6.5 to -1.0 were defined as valid. Values outside this range should be assessed with caution. A mechanistic explanation for the very slow permeation of data point 2_4 is not obvious, since the formulation contains water, organic solvents, an emulsifier and an antifoaming agent, as do many other formulations. Furthermore, the MFs of the data point were clearly inside the data range ($Adme1/P_{ow}$: 23.8, $Adme1/RotB$: 0.0006, $molinspLogHBAcc$: 0.003). Therefore, limits for MFs were defined by minimum and maximum values of the entire training set (Table 41). The final ApD is given in Table 41.

Although the best Abraham-based model (no. 20) is of limited use, a sensible definition of ApD is discussed in the following. A look on the boundaries and outliers may also help to identify weaknesses of the model and to improve the approach. Therefore, all outliers appearing in different stages of model development were reported and assessed. The excluded experiments were listed by their frequency of elimination from models no. 2, 4, 8, 10, 14, 18 and 20. Furthermore, logmaxKp values of the eliminated protocols were predicted with the corresponding models and the ranges of deviation to the observed results (residuals) were calculated (Table 42). Minimum and maximum values of observed logmaxKp as well as minimum and maximum values of model descriptors were extracted from the total dataset and reported in Table 43.

Table 41: Minimum and maximum descriptor values for 83 data points (training set of model no. 35). Given are the limits of MFs AdmeLogHBD_{on}, Adme1/P_{ow} and molinspLogHB_{Acc} which describe the distinct mixtures and the final ApD limits – derivation is described in the text. Matching of both limits is indicated with a hook (✓).

	min	max	ApD
Adme1/P _{ow}	7*10 ⁻⁵	31.2	7*10 ⁻⁵ – 31.2 [✓]
Adme1/RotB	0	0.31	0 – 0.31 [✓]
molinspLogHB _{Acc}	0	0.7	0 – 0.7 [✓]
logmaxKp	-1.02	-6.89	-1.02 – -6.5

Table 42: Excluded data points sorted by frequency of elimination from the Abraham-based models no. 2, 4, 8, 10, 14, 18 and 20. ‘Residual range’ gives the range of deviation of the observed response from the predicted values calculated with the corresponding models; ‘protocol’ gives the compound and mixture number, used species and receptor fluid; Acc: molinspLogHB_{Acc}, TPSA: molinspTPSA.

protocol	frequency	residual range	remarks
28_8_hum_E/W_1	6	0.3 – 1.5	highest Acc: 0.7, highest TPSA: 64
10_1_hum_water	5	-0.04 – -1.9	highest $\Sigma\alpha_2^H$: 1,71
70_1_rat_E/W_2	5	-0.3 – -0.8	highest MW: 1052.7, V _x : 7.15
50_1_hum_water	5	2.2 – 3.5	highest $\Sigma\beta_2^H$: 2.77, π_2^H : 3.6, high MW: 520
70_1_hum_E/W_2	5	0.7 – 0.9	highest MW: 1052.7, highest V _x : 7.15
79_1_hum_E/W_2	4	1.1 – 2.3	high Acc: 0.44, TPSA: 64 π_2^H : 3.2
79_1_rat_E/W_2	4	1.2 – 2.0	high Acc: 0.44, TPSA: 64, π_2^H : 3.2
47_1_hum_water	4	2.2 – 2.9	high $\Sigma\beta_2^H$ 2.68, V _x : 3.3
48_1_hum_water	4	1.8 – 2.5	high $\Sigma\beta_2^H$: 2.75
75_2_hum_water	3	-0.7 – 1.2	high $\Sigma\alpha_2^H$: 0.88
75_1_hum_water	2	-0.9 – -1.5	high $\Sigma\alpha_2^H$: 0.88
16_1_hum_water+B	2	-2.2 – 2.6	high MW: 642
71_3_rat_E/W_2	1	0.8	high TPSA: 62, high Acc: 0.49
49_1_hum_water	1	2.2	highest Rf ₂ : 3.27, high $\Sigma\beta_2^H$: 2.39, π_2^H : 3.51, V _x : 3.68, MW: 531
82_1_hum_E/W_2	1	-0.6	high $\Sigma\alpha_2^H$: 0.81, high TPSA: 58
27_1_hum_water+B	1	-2.3	no TPSA or Acc: 0, smallest $\Sigma\beta_2^H$: 0.17

Focusing on the standardized residuals, only one of the eliminated data points has ever resulted in residuals larger than three SDs (50_1_hum_water, Table 42). This confirms, that an outlier due to too high leverage on a model is not necessarily associated with a weak prediction using the resulting model and therefore not necessarily outside the ApD. Therefore, each outlier was assessed individually for its impact on the ApD, but generally conservative limits were set to increase the reliability of the predictions.

The mentioned data point 50_1_hum_water was the only experiment with substance no. 50 (see the structure in Figure 27). In this experiment, it was applied as a solution in water (0.1 %). Substance no. 50 has the highest $\Sigma\beta_2^H$ (2.77) and the highest π_2^H (3.6) of the current dataset as well as a high MW (520 g/mol) (calculated for the neutral molecule). Substances no. 47, 48 and 49 are closely related to substance no. 50. Similar to the latter, they were only applied once in aqueous solutions (0.1 %). Furthermore, they were also eliminated from several models and possess the next highest $\Sigma\beta_2^H$ values (2.68 – 2.75) with a remarkable distance to the rest (0.17 – 1.90). Therefore, a conservative upper limit for $\Sigma\beta_2^H$ was set to 1.9. The substance with the lowest $\Sigma\beta_2^H$ value (no. 27, 0.17) was an outlier in model 20 and therefore also excluded. The lower limit was set to 0.22 – the value of the next higher, well-predicted compound (no. 59).

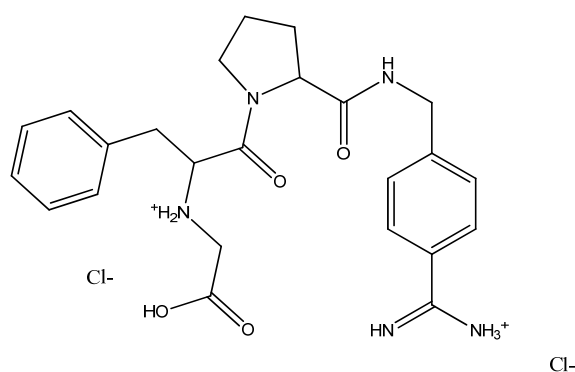


Figure 27: Compound no. 50, IUPAC-name [2-[2-[[4-(azaniumylcarbonimidoyl) phenyl] methylcarbamoyl] pyrrolidin-1-yl]-1-benzyl-2-oxo-ethyl]-(carboxymethyl) ammonium dichloride, $C_{24}H_{31}N_5O_4Cl_2$.

Additionally, substances no. 50 and 49 were, with 525 and 531 g/mol, respectively, two of the six heaviest compounds in the dataset. The heaviest compounds no. 16 (642 g/mol) and 70 (1053 g/mol) were identified as outliers in several models as well. Although compounds 24 (506 g/mol) and 72 (543 g/mol) were constantly well-predicted and included in the set, the upper limit for parameter MW was conservatively defined as 500 g/mol. Therefore, a prediction of compounds with molecular weight greater than 500 g/mol is not reliable with the current linear model. This indicates a very slow or no absorption of such compounds. This fits to the rule, that dermal absorption rapidly declines for molecules over 500 Da or 500 g/mol (Bos & Meinardi 2000). Furthermore it is in accordance with the 'Lipinski rule of 5' – which limit the transition over membranes inter alia to molecules smaller than 500 g/mol. This rule was originally defined for absorption in the gastrointestinal tract, but is transferable to other barrier systems (Lipinski et al. 1997). The two smallest compounds no. 59

(72 g/mol) and 17 (19 g/mol) were well-predicted and always inside the model. Hence, the lower limit was defined as 72 g/mol.

Table 43: Minimum and maximum descriptor values for 342 data points of the human and rat dataset used for models no. 6 – 10 and 13 – 22. Given are the limits for the Abraham descriptors $\Sigma\alpha_2^H$, $\Sigma\beta_2^H$, π_2^H , Rf_2 and V_x which describe the distinct substances, the limits for MFs molinspTPSA, AdmeLogHBDOn and molinspLogHBAcc which describe the distinct mixtures and the final ApD limits – derivations are described in the text. Matching of both limits is indicated with a hook (✓).

	min	max	ApD
$\Sigma\alpha_2^H$	0	1.71	0 – 0.88
$\Sigma\beta_2^H$	0.17	2.77	0.22 – 1.90
π_2^H	0.42	3.63	0.42 – 3.22
Rf_2	0.25	3.27	0.25 – 2.85
V_x	0.62	7.15	0.62 – 3.52
MW	72	1053	72 – 500
logP _{ow}	-2.9	6.8	-2.9 – 6.8 ✓
molinspTPSA	0	64.6	8 – 60
AdmeLogHBDOn	0	0.41	0 – 0.33
molinspLogHBAcc	0	0.70	0 – 0.43
logmaxKp	-1.02	-7.48	-6.14 – -2.43

The parameter V_x is closely related to MW, but does not arrange the compounds in exactly the same order. Since the two largest molecules (no. 49 and 70 with V_x 3.68 and 7.15, respectively) were frequently eliminated and the smallest (no. 59 with V_x 0.62) was inside and well-predicted, the limits were set at V_x 0.62 and 3.53. For the parameter Rf_2 the three substances (no. 49, 50 and 70) with the highest values (3.51, 3.63 and 2.93, respectively) were frequently eliminated. The resulting boundaries based on the rest were set at Rf_2 0.25 and 2.85. The three compounds (no. 10, 50 and 75) with the highest $\Sigma\alpha_2^H$ values (1.71, 1.17 and 0.88, respectively) were eliminated in several models. However, compound no. 75 was not completely excluded, this means that experiments with human skin were eliminated and parallel experiments using the same formulation on rat skin were not excluded. Therefore, the high $\Sigma\alpha_2^H$ was not responsible for exclusion and the valid range was set from 0 to 0.88. However, the discrepancy for compound no. 75 (prohexadione calcium) may indicate a larger species-dependent difference for this substance than standardly covered by the model. This points out again, that the species effect depends on the substance and the formulation and is hardly covered by a fixed factor. Furthermore, compound 75 provides the lowest logP_{ow} (-2.9). Since the effect was not clearly related to the lipophilicity, the boundaries were left at -2.9 and 6.8. However, looking on the distribution of logP_{ow} values in the dataset, revealed a limited coverage of hydrophilic compounds. If there is a significant porous pathway through the skin – which is still controversially discussed – absorption characteristics of hydrophilic compounds may not be covered adequately by the model based on this dataset (Mitragotri et al. 2011). Therefore, predictions of very hydrophilic compounds < -1 should be assessed with caution. For the fifth Abraham descriptor π_2^H , also the compounds (no. 49, 50 and 79) with the highest values were eliminated from several models (π_2^H 3.51, 3.63 and 3.22, respectively).

However, compound 79 was only excluded when applied in formulation 79_1 which possessed very high values for MFs molinspTPSA (64), molinspLogHBAcc (0.44) and AdmeLogHBDOn (0.41). Therefore and since there were no outliers in the lower range, the boundaries for π_2^H were defined as 0.42 and 3.22. Similarly, exclusion of compound 82 applied in formulation 82_1 from one model, was probably due to the combination of high values for $\Sigma\alpha_2^H$ (0.81) and molinspTPSA (58). Also the formulation and not the compound were the reason for excluding data point 28_8_hum_E/W_1 and 71_3_rat_E/W_2 considering the high values for molinspTPSA (64.6 and 62.4, respectively) and molinspLogHBAcc (0.70 and 0.49, respectively). Data point 27_1_hum_water+B was eliminated due to the non-calculable values for molinspTPSA and molinspLogHBAcc which were hence set to zero. The valid range for molinspTPSA was therefore defined from 8 – 60. The valid range for molinspLogHBAcc was set from 0 to 0.43. This is a conservative assessment, since two out of the six data points with the highest molinspLogHBAcc values were excluded despite being constantly well predicted and included in the model (12_1 and 3_9). The data points with the highest values for parameter AdmeLogHBDOn (formulations no. 79_1, 47_1, 48_1, 49_1) were eliminated frequently and the valid range defined by the rest as 0.33 – 0.41.

In addition to the limits set above, each new prediction should be accompanied by calculation of the hat value for this data point. A lower value than the model-specific critical hat value (h^*) confirms the affiliation to the structural domain. However, despite all these considerations, there could be 'empty spaces' inside the ApD. Therefore, prospective extension of the training set would increase the reliability of predictions and may increase the fit. Substance no. 78 applied in various formulations is probably localized in such an empty space: Although the properties were clearly inside the above defined ApD ($\Sigma\alpha_2^H$ 0.76, $\Sigma\beta_2^H$ 0.71, π_2^H 2.16, Rf_2 1.5, V_x 2.15, MW 381, $\log P_{ow}$ 4.56, molinspTPSA 29 – 32, molinspLogHBAcc 0.0001 – 0.11, AdmeLogHBDOn 0.28 – 0.30) and – when using model no. 20 – the hat values (0.005 – 0.009) were clearly lower than h^* (0.034), the predictions were poor and resulted in residuals from -2.8 – -4.3 mainly outside the accepted range of three SDs (response outliers). Furthermore, no crucial difference to the other compounds was apparent based on the structure (Figure 28) or reported experimental conditions. However, the results were in the very slow permeation range (-7.48 – -6.28) which was covered only by 4 of 213 data points of the training set. Based on these observations and the range of observed and predicted values, only predictions inside the range of -6.14 – -2.43 should be assessed as reliable.

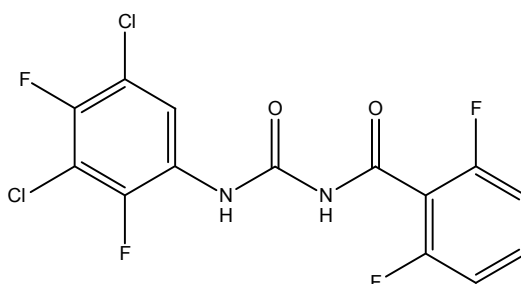


Figure 28: Compound no. 78, teflubenzuron, $C_{14}H_6Cl_2F_4N_2O_2$.

Taken together, substances no. 10, 16, 27, 47 – 50 and 70 were excluded from the dataset and assessed as outliers of the parameter space, whereas substances no. 28, 71, 75, 79 and 82 were excluded only in combination with a specific formulation. However, the excluded formulations contained instead of conspicuous ingredients, only water, organic solvents, antifoaming agents, thickeners or emulsifiers as do many other formulations inside the dataset. A clear pattern did not exist. This is not surprising, considering the number of individual ingredients (> 240). This emphasizes again the difficulty of using 'real world' data instead of highly standardized data as used by Riviere and Brooks (Riviere & Brooks 2005). The final ApD for the Abraham-based models is given in Table 43.

5.3.5 Final remarks

With the current approach, it was shown that a general relationship between physicochemical properties of chemicals and dermal absorption exists and that mainly size and polarity of a compound explain the difference in permeation through skin. A similar impact was shown for the mixture which seems to be mainly dependent on enhancing effects. Furthermore, inclusion of some experimental conditions into the model in the form of indicator variables was generally possible and in case of the species (Spl) shown to enhance the predictions and enables the joint approach for various data sources without reduction of the dataset. Many such modifications are imaginable to transfer the current Abraham-based approach (model no. 20) into a reliable prediction tool – potentially acceptable for risk assessment. But considering the discussion above, it is questionable if the effort is appropriate in relation to the potential improvements in R^2 and Q^2_{Ext} values. Considering the underlying inhomogeneous database and the general high experimental variability a more rough estimation in the form of Marzulli classes seems more suitable. Therefore, it is recommended to use the Abraham-based approach (model no. 20) as a screening tool for estimation of Marzulli classes of dermal absorption e.g. for compounds in early developmental stages or for compounds where data are missing (e.g. chemicals under European REACH legislation) (The European Parliament and the Council of the European Union 2006). However, for substances – for which already dermal absorption data exist – the substance-based approach (model no. 35) provides a respectable tool to extrapolate dermal absorption characteristics to new formulations. This approach may reduce the time and the number of experiments for pesticides in developmental process and – if accepted from the regulatory agency – for risk assessments. By extending the database, the model could be transferred to other chemical classes like pharmaceuticals or cosmetics.

As a final comment, further prediction models could be developed addressing other, more real-life, endpoints of dermal uptake like absorbed dose or specific subgroups like different classes of molecular volume (Kirchner et al. 1997). For the current work $\log_{max}K_p$ was chosen as the endpoint to be comparable to the classical models in the literature, but to develop models for risk assessment, endpoint absorbed dose would be more relevant. Furthermore other statistical analyses could be tested, such as linear partial least square analysis or classifying discriminant analysis (OECD 2007). Finally, more mechanistic models as proposed by the groups of Schaefer, Kasting or Frasch, for instance, could be considered – which may better describe and predict the complex interplay of penetrant, skin and mixture (Dancik et al. 2013; Hansen et al. 2008; Nitsche & Frasch 2011).

6 Conclusion

The following conclusions are the main results extracted out of the discussion above and are related to the numbers of the tasks outlined in chapter 2, p. 23:

1. It was shown, that TEER (transepidermal electrical resistance), TWF (transepidermal water flux), and TEWL (transepidermal water loss) were suitable integrity tests to roughly differentiate between intact and impaired skin samples in advance of an absorption experiment when using limit values 2 kOhm, 10 g/(m²*h) and 4.5*10⁻³ cm/h, respectively. However, only the absorption characteristics of a parallelly applied internal standard (ISTD) were continuously correlated to absorption results of the test compounds and enabled to interpret changes of barrier properties over the entire experimental period and distinguish them from substance-specific effects. The independence of ³H-ISTD and ¹⁴C-test compound analytics as well as the independence of their absorption characteristics was shown. However, an obstacle for the routine application of this methodology is the need of historical datasets for various ISTDs – representative for various physicochemical properties – applied under various experimental conditions.
2. It was confirmed that dermal absorption experiments under analogue flow-through or static study design lead to similar results in general.
3. It was concluded, that a dermal absorption study design in vitro with repeated dosing is not feasible. Additional to the disruptive effects of the MCPA-DMA-formulation on rat skin, a lower resistance against mechanical treatment was observed with proceeding time. The alternative use of living tissue like the human skin construct StrataTest[®] was not applicable due to the thin dermis and the fragility already observed in standard experiments of 24 h.
4. Different preparation types of skin samples derived from the same human donor (DMS, dermatomed skin, and FTS, full-thickness skin) led after finite dosing to absorbed doses in the same order of magnitude. Only the partitioning between the compartments was different – which confirms the SC as the main barrier of the skin. However, since the rate of diffusion was more hampered in FTS and the maxKp derived with DMS closer to the steady state situation, the latter was assessed to be more appropriate for routine experiments.
5. It was observed, that the use of rat skin, StrataTest[®] as well as skin-PAMPA over-predicts absorption through human skin in vitro. Rat skin was assessed to be the most suitable alternative to human skin with results in the same order of magnitude and fulfilling at the same time the regulatory principle of 'worst case' for risk assessment of e.g. pesticides. The reconstructed human skin StrataTest[®] provided neither remarkable advantage in respect of cost- or time-effectiveness, nor in handling. Additionally, no correlation to absorption in human skin was obtained. In contrast, relations between skin-PAMPA and human skin absorption were obtained when focusing on aqueous solutions. However, further test are needed to assess its usability for other vehicles which would be crucial for its application as screening tool during pesticide development.

6. Although there are hints of esterase degradation during storage, a preserved esterase activity was detected in S9 fraction derived from cryoconserved human skin (-20°C, up to 1 year) using model substrates MCPA-EHE and fluorescein diacetate. Furthermore, model substrate MCPA-EHE was partly cleaved to MCPA during skin passage in dermal absorption experiments in vitro. It was concluded, that a change of absorption characteristic due to metabolic hydrolysis and changed physicochemical properties is covered qualitatively when using cryoconserved human skin. However, considering the hints of enzyme degradation during storage, a considerably lower extent is likely.
7. Several xenobiotic-metabolizing enzyme activities were detected in StrataTest[®]. However, the enzyme-activity profile of this reconstructed human skin was closer to the profile of keratinocytes than to profiles of excised human skin, reconstructed epidermis (EpiDerm[™]) or reconstructed full-thickness skin (EpiDerm[™]FT and Phenion[®]FT) reported in the literature. The differences are ascribable to the thin dermis and a probable loss of enzyme activity in senescing cell cultures of the underlying immortalized keratinocyte cell line (NIKS[®]). Therefore, StrataTest[®] was assessed to be a minor alternative to human skin for investigations that require activities of xenobiotic-metabolizing enzymes.
8. In silico prediction models for dermal absorption were developed on an internal database comprising more than 342 experiments for 56 substances in more than 100 formulations. Substance, mixture and species of skin sample were confirmed as main sources for variability. Appropriate descriptors were identified to explain and predict these variances in the model. The model based on Abraham descriptors – whereby only one of the five descriptors was significant (R_{f_2} , solute excess molar refractivity) – in combination with a mixture-related factor (TPSA, topological polar surface area) and a species indicator (Spl) was inadequate to predict distinct values, yet the estimation of Marzulli classes for permeation (order of magnitude) was appropriate and makes the Abraham-based model a suitable screening tool for early stages of development. In contrast, a substance-based model (bundling substance-related information in a class variable) combined with mixture factors (molinspLogHBacc, logarithmic number of hydrogen bond acceptors, $Adme1/P_{ow}$, inverse partition coefficient between octanol and water and $Adme1/RotB$, inverse number of rotatable bonds) predicts effectively absorption of an integrated compound from unknown formulations. Its use as an interpolation tool for regulatory purposes is potentially possible. Many modifications like insertion of further indicator variables, more mechanistic considerations, the use of non-linear or classification models or extension to further substance classes are conceivable to improve the approach.

7 Summary

Dermal absorption – the uptake of compounds via the skin – is a relevant parameter for risk assessment of chemicals, cosmetics and plant protection products. Besides *in vivo* tests, *in vitro* determination is accepted by many regulatory agencies – if experiments are conducted in accordance to OECD Guideline 428 and Guidance document 28. However, the named documents provide a framework whereupon variability regarding performance and results may be observed in different laboratories. A way to minimize variability is to understand the influence of experimental conditions and higher standardization of the system. Regarding the latter, the Guideline requests an integrity test which should ensure the exclusive use of undamaged skin preparations. Proposed tests are TEWL (transepidermal water loss), TEER (transepidermal electrical resistance), application of a reference compound like water (TWF, transepidermal water flux) or the integrated use of an internal standard (ISTD). However, contradictory opinions concerning applicability, experimental performances and limit values have been reported. To evaluate the suitability of different tests and review the present limit values, absorption results of four ¹⁴C-labeled test compounds (MCPA (2-methyl-4-chlorophenoxyacetic acid), MCPA-EHE (MCPA 2-ethylhexylester), testosterone and caffeine) were compared with results of five integrity tests: TEWL, TWF, TEER in advance, ISTD (³H-mannitol, ³H-caffeine, or ³H-testosterone) concurrently and BLUE (transepidermal methylene blue absorption) at the end of the run. The standard methods TEWL, TWF and TEER were assessed to be appropriate tools for rough differentiation between intact and impaired skin samples in advance of experiments, when using limit values 10 g/(m²*h), 4.5*10⁻³ cm/h and 2 kOhm, respectively. However, only the absorption characteristics of a parallelly applied ISTD were highly correlated with absorption results of the ¹⁴C-labeled test compound (e.g. R² 0.86 for maxKp (maximum permeability coefficient) ¹⁴C-MCPA and ³H-testosterone). Further advantages of the ISTD approach are the possibility to rate the barrier function over the entire experimental period and to distinguish substance-specific wash-in effects from barrier-disruption related effects. The independence of ³H-ISTD and ¹⁴C-test compound analytics as well as the independence of their absorption characteristics were shown in the current work. An obstacle for routine application is the need of historical datasets for various ISTDs – representative for various physicochemical properties – applied under various experimental conditions.

Regarding investigation of possible influential experimental parameters, the use of flow-through and static study design was compared. Therefore, ¹⁴C-MCPA and ³H-testosterone were applied on dermatomed rat skin semi-occlusively with water as the receptor fluid. In accordance with the literature, similar absorption results were obtained with the two experimental designs, e.g. maxKp values for ¹⁴C-MCPA of 21.4 ± 10.4*10⁻⁵cm/h under static and 22.8 ± 18.4*10⁻⁵cm/h under flow-through conditions. Repeated application of a formulation containing the pesticide MCPA over three days in advance to the application of the corresponding radio-labeled formulation on rat skin led to a significant increase of the absorption (AD 75 ± 24 %) compared to the standard experiments with a single application of ¹⁴C-MCPA (14 ± 3 %). This effect was only partly due to the formulation, but also due to mechanical and chemical stress during washing procedures between the applications. It was observed that the skin became less resistant to mechanical treatment with increasing time. Therefore, the study design with repeated dosing *in vitro* was assessed as not feasible for routine applications. Furthermore, absorption characteristics of dermatomed (DMS) and full-thickness (FTS) skin samples derived from

the same human donor were compared under identical experimental conditions. Absorption results for four ^{14}C -labeled (MCPA-EHE, MCPA, testosterone and caffeine) and two ^3H -labeled (testosterone and mannitol) penetrants under finite dose conditions were in the same order of magnitude for both preparation types (e.g. ^3H -testosterone, absorbed dose (AD) $22.1 \pm 7.1\%$ for DMS and $25.6 \pm 9.2\%$ for FTS). However, DMS was assessed to be more suitable for routine studies due to Kp values closer to the steady state situation.

Since the availability of human skin is limited, rat skin, StrataTest[®] (a commercially available reconstructed human skin) and skin-PAMPA (an abiotic stratum corneum membrane) were assessed for their suitability to determine dermal absorption. Therefore, experiments were conducted with ^{14}C -labeled and unlabeled model compounds (testosterone, caffeine and MCPA) under similar experimental conditions. In accordance with the literature, rat skin was assessed to be an appropriate alternative to human skin due to absorption results in the same order of magnitude and fulfilling the regulatory principle of 'worst case' for purposes of risk assessment (e.g. for pesticides). Skin-PAMPA was highly over-predictive in comparison to human skin ((max)Kp 3- to 53-fold). If focusing on aqueous solutions skin-PAMPA was less over-predictive ((max)Kp 3- to 8-fold) and the results were correlated to human skin results (R^2 0.89). However, further tests are needed to assess its usability for other vehicles – which would be crucial for its application as screening tool during pesticide development. In contrast, formulations could be applied on the cell-based construct StrataTest[®]. However, the system was highly over-predictive in comparison to human skin (maxKp 5- to 49-fold, AD 3- to 4-fold), not correlated to human in vitro experiments and therefore assessed as inappropriate to determine dermal absorption.

Besides the absorption, also xenobiotic-metabolizing enzyme activities were investigated for StrataTest[®] using subcellular fractions. Remarkable esterase and NAT 1 activities were detected in S9 fraction (3.6 ± 0.1 and 7.2 ± 1.6 nmol/(min*mg), respectively). But lacking UGT 1 and ADH activity and providing low AIDH and FMO 1/3 activities (3.1 ± 0.8 and 0.5 ± 0.1 nmol/(min*mg), respectively) – measured in microsomes or cytosol – StrataTest[®] was closer to a keratinocyte cell line than to the metabolic properties of excised human skin, reconstructed human epidermis (EpiDermTM) or other full-thickness skin constructs (EpiDermTMFT and Phenion[®]FT). Additionally, cryoconserved human skin (-20°C, up to 1 year) was examined for preserved esterase activity. Using S9 fraction and model substrates MCPA-EHE and fluorescein diacetate resulted in activities of 0.67 ± 0.26 nmol/(mg*min) and 0.7 ± 0.6 nmol/(min*mg), respectively. Furthermore, model compound MCPA-EHE was partially cleaved to MCPA during dermal absorption experiments in vitro. It was concluded, that a change of absorption characteristic due to metabolic hydrolysis and changed physicochemical properties is covered qualitatively when using cryoconserved human skin. However, considering the hints of enzyme degradation during storage, a considerably lower extent is likely.

Finally, in silico prediction models for dermal absorption with special focus on mixture-related effects were developed. Data from more than 342 dermal absorption experiments in vitro were used, which comprised 56 test compounds in more than 100 formulations. A model based on one substance-specific Abraham descriptor (Rf_2 , solute excess molar refractivity), a mixture-specific factor (TPSA, topological polar surface area) and a species indicator (Spl) was assessed to be appropriate to

estimate the magnitude of permeation of compound-mixture combinations and therefore to be a suitable screening tool for early stages of development (e.g. for pesticides). More precise predictions were possible with the substance-based approach where substance-related information were bundled in class variables and combined with mixture factors (molinspLogHBAcc, logarithmic number of hydrogen bond acceptors, Adme1/P_{ow}, inverse octanol/water partition coefficient, Adme1/RotB, inverse number of rotatable bonds). This model allows reliable interpolations for included test substances to novel formulations.

Taken together, the current work supplements current knowledge about the in vitro methodology as well as the in silico predictions for dermal absorption. However, further improvements are needed to enhance the reproducibility of the former and allow the routine application of the latter.

8 Zusammenfassung

Die dermale Resorption – die Aufnahme von Stoffen über die Haut – ist ein relevanter Parameter für die Risikobewertung von Chemikalien, Kosmetika und Pflanzenschutzmitteln. Neben in vivo Versuchen werden für die Bewertung Ergebnisse aus in vitro Tests in der EU regulatorisch anerkannt, sofern die Experimente entsprechend der OECD Guideline 428 und dem Guidance document 28 durchgeführt wurden. Allerdings definieren die Dokumente nur ein Grundgerüst der Methode, weshalb die Durchführung und auch die Ergebnisse verschiedener Labore unterschiedlich ausfallen können. Eine Möglichkeit die experimentelle Variabilität zu minimieren, ist den Einfluss variabler Testbedingungen zu verstehen und die Standardisierung des Testsystems voranzutreiben. Ein Validitätskriterium nach OECD Guideline ist z. B. die Durchführung eines Integritätstest, der den exklusiven Einsatz intakter Hautproben gewährleisten soll. Zu den vorgeschlagenen Methoden zählen TEWL (transepidermaler Wasserverlust), TEER (transepidermaler elektrischer Widerstand), die Applikation einer Referenzsubstanz wie z. B. Wasser (TWF, transepidermaler Wasserfluss) oder der Einsatz eines internen Standards (ISTD). Allerdings wird die Anwendung einzelner Methoden kontrovers diskutiert und für andere fehlt ein gemeinsamer Konsens hinsichtlich der Durchführung und der anzuwendenden Grenzwerte. Um die Zweckmäßigkeit der verschiedenen Methoden und die aktuellen Grenzwerte zu beurteilen, wurden in der vorliegenden Arbeit die Ergebnisse von Resorptionsuntersuchungen von vier ¹⁴C-markierten Testsubstanzen (MCPA (2-Methyl-4-chlorphenoxyessigsäure), MCPA-EHE (MCPA-2-ethylhexylester), Testosteron, und Coffein) mit den Ergebnissen von fünf Integritätstests verglichen: TEWL, TWF, TEER, jeweils im Vorfeld, ISTD (³H-Mannitol, ³H-Coffein, oder ³H-Testosteron) zusammen mit der Testsubstanz und BLUE (transepidermale Resorption von Methyleneblau) am Ende des Versuches. Die Standardmethoden TEWL, TWF und TEER erwiesen sich als geeignet zur Vorselektion von intakten Hautproben bei Einhaltung folgender Grenzwerte: 10 g/(m²*h), 4,5*10⁻³ cm/h und 2 kOhm. Indessen war die Korrelation zu den Resorptionsergebnissen der ¹⁴C-markierten Testsubsubstanz gering. Im Gegensatz dazu, bestand eine Korrelation zwischen den Ergebnisse des ISTD und den Ergebnissen der Testsubstanz (z. B. R² 0.86 für maxKp (maximaler Permeabilitätskoeffizient) von ¹⁴C-MCPA und ³H-Testosteron). Weitere Vorteile des Integritätstests ISTD sind die Bewertung der Hautbarriere über die gesamte Expositionszeit hinweg und die Unterscheidung von substanzspezifischen ‚wash-in‘ Effekten von Effekten, die auf eine gestörte Hautbarriere zurückzuführen sind. Weiterhin wurde in der vorliegenden Arbeit gezeigt, dass sich die ¹⁴C-markierte Testsubstanz und der ³H-markierte ISTD nicht gegenseitig hinsichtlich Analytik oder Resorptionsverhalten beeinflussen. Für eine Routineanwendung des Integritätstests ISTD fehlen allerdings noch historischen Daten. Es wird empfohlen, Daten für mehrere ISTDs – repräsentativ für verschiedene physikalisch-chemische Eigenschaften – unter verschiedenen experimentellen Bedingungen als historischen Vergleichsdatensatz zu generieren.

Bezüglich experimenteller Einflussfaktoren auf die dermale Resorption in vitro, wurden in der vorliegenden Arbeit Ergebnisse von statischen und ‚Durchfluss‘-Experimenten verglichen. Dazu wurde ¹⁴C-MCPA und ³H-Testosteron semi-okklusiv auf Rattenhaut appliziert. In Übereinstimmung mit der Literatur wurden für beide Systeme ähnliche Ergebnisse erzielt (z. B. ein maxKp (¹⁴C-MCPA) von 21.4 ± 10.4*10⁻⁵cm/h im statischen und von 22.8 ± 18.4*10⁻⁵cm/h im Durchflusssystem). Wiederholte

Applikation einer MCPA-Formulierung über drei Tage auf Rattenhaut, führte zu einer verstärkten Resorption der anschließend applizierten ^{14}C -MCPA Dosis ($\text{AD } 75 \pm 24 \%$) im Vergleich zur Applikation einer Einzeldosis ^{14}C -MCPA ($14 \pm 3 \%$). Dieser Effekt war auf die Formulierung, aber auch auf den mechanischen und chemischen Stress durch die Waschungen zwischen den Applikationen zurückzuführen. Die Hautproben waren mit voranschreitender Zeit weniger resistent gegenüber solchen Einflüssen. Insgesamt erwies sich dieser *in vitro* Ansatz zur routinemäßigen Untersuchung des Einflusses einer wiederholten Applikation als nicht geeignet. Weiterhin wurde der Einfluss der Hautpräparation auf die Resorption *in vitro* untersucht. Dazu wurde unter identischen experimentellen Bedingungen, dermatomisierte Haut (DMS) und Vollhaut (FTS) vom selben humanen Spender eingesetzt. Vier ^{14}C -markierte (MCPA-EHE, MCPA, Testosteron und Coffein) und zwei ^3H -markierte (Testosteron und Mannitol) Testsubstanzen wurden als finite Dosen appliziert. Die Resorptionsergebnisse lagen für beide Hautpräparationsarten im gleichen Größenbereich (z. B. absorbierte Dosis (AD, ^3H -Testosteron) $22.1 \pm 7.1 \%$ für DMS und $25.6 \pm 9.2 \%$ für FTS). Insgesamt wurden beide Präparationsarten für Routinestudien als geeignet bewertet. Allerdings ist DMS FTS vorzuziehen, da die erzielten maxKp -Werte mit DMS näher am ‚steady state‘ lagen als die maxKp -Werte, die mit FTS generiert wurden.

Da die Verfügbarkeit von Humanhaut für Forschungszwecke begrenzt ist, wurde die Eignung von Rattenhautpräparaten, StrataTest[®] (ein kommerziell erhältliches Humanhautkonstrukt) und skin-PAMPA (eine synthetische Stratum-corneum-Membran) hinsichtlich einer Anwendung zur Bestimmung dermalen Resorption überprüft. Dazu wurden Experimente mit ^{14}C -markierten und nicht markierten Modellschubstanzen (Testosteron, Coffein und MCPA) unter vergleichbaren experimentellen Bedingungen durchgeführt. In Übereinstimmung mit der Literatur, wurde Rattenhaut als geeignete Alternative zur Humanhaut bewertet, da deren Einsatz zu Resorptionen in der gleichen Größenordnung führte und gleichzeitig das regulatorische Prinzip des ‚worst case‘ für Risikobewertungen von z. B. Pflanzenschutzmitteln erfüllte. Skin-PAMPA erwies sich als überprädiktiv ((maxKp) 3- bis 53-fach höher im Vergleich zu den Ergebnissen mit Humanhaut *in vitro*). Wurde der Effekt der Mischung mit berücksichtigt und nur die Daten für wässrige Lösungen miteinander verglichen, so lagen die Resorptionsergebnisse mit skin-PAMPA näher an den Referenzwerten ((maxKp) 3- bis 8-fach höher im Vergleich zu den Ergebnissen mit Humanhaut *in vitro*) und es ergab sich eine Korrelation von $R^2 0.89$. Ob skin-PAMPA auch für andere Vehikel als Wasser geeignet ist – was für die Untersuchung von Pflanzenschutzmittelformulierungen unablässig wäre – muss noch gezeigt werden. Im Gegensatz dazu, können verschiedenste Formulierungen auf StrataTest[®] appliziert werden. Allerdings waren die Resorptionsergebnisse mit diesem Konstrukt im Vergleich zur Humanhaut überprädiktiv (maxKp 5- bis 49-fach, AD 2- bis 4fach), zeigten keine Korrelation zu den Humanhautdaten und wurden deshalb zur Bestimmung dermalen Resorption als nicht geeignet bewertet.

Neben der Barrierefunktion von StrataTest[®] wurden auch Aktivitäten von fremdstoffmetabolisierenden Enzymen charakterisiert. Mit hohen Esterase- und NAT 1- Aktivitäten (3.6 ± 0.1 and 7.2 ± 1.6 nmol/(min*mg)) in S9 Fraktion, geringen AIDH- und FMO 1/3- Aktivitäten (3.1 ± 0.8 and 0.5 ± 0.1 nmol/(min*mg)) und der Abwesenheit von UGT 1- und ADH- Aktivität – gemessen in Zytosolfraction

oder mikrosomaler Fraktion –, entspricht das Profil des Konstrukts mehr dem Profil einer Keratinozyten-Zelllinie als dem exzidiertes Humanhaut oder anderen humanen Epidermis- (EpiDerm™) oder Vollhautkonstrukten (EpiDerm™FT and Phenion®FT) aus der Literatur. Weiterhin wurde die Esteraseaktivität in gefrorenen Humanhautproben untersucht. Bei Einsatz von S9 Fraktion und Modellsubstrat MCPA-EHE und Fluoresceindiacetat wurden Aktivitäten von 0.67 ± 0.26 nmol/(mg*min) und 0.7 ± 0.6 nmol/(min*mg) gemessen. Eine partielle Spaltung von MCPA-EHE zu MCPA wurde auch während dermalen Resorptionsexperimente in vitro beobachtet. Berücksichtigt man die Hinweise auf Abbau des Enzyms während der Lagerung, kann man schließen, dass teilweise – aber nicht quantitativ – hydrolaseabhängige Veränderungen der physikalisch-chemischen Eigenschaften und damit mögliche Änderungen der Resorptionscharakteristika bei Verwendung solcher Hautstücke in dermalen Resorptionsstudien in vitro mit erfasst werden.

Schließlich wurde ein in silico Modell für dermale Resorption unter spezieller Berücksichtigung von Mischungseffekten entwickelt. Dazu wurden Daten von mehr als 342 in vitro Experimenten mit 56 Substanzen in mehr als 100 Formulierungen verwendet. Ein Modell basierend auf einem substanzspezifischen Abraham Deskriptor (Rf_2 , ‚solute excess molar refractivity‘), einem Mischungsspezifischen Faktor (TPSA, ‚topological polar surface area‘) und einem Speziesindikator (Spl) erwies sich als geeignet, die Größenordnung der Resorption einer Substanz-Mischungs-Kombination vorherzusagen. Damit stellt dieses Modell ein geeignetes Werkzeug für die frühen Entwicklungsphasen von z. B. Pflanzenschutzmitteln dar. Präzisere Vorhersagen waren mit dem substanzbasierten Modell möglich. In diesem Modell wurden substanzbezogene Informationen in Klassenvariablen gebündelt und mit Mischungsfaktoren (molinspLogHBacc, Logarithmus der Anzahl an Wasserstoffbrückenbindungsakzeptoren, $Adme1/P_{ow}$, inverser Verteilungskoeffizient Oktanol/Wasser, $Adme1/RotB$, inverse Anzahl an rotierbaren Bindungen) kombiniert. Dieses Modell erlaubt die Interpolation zu neuen Formulierungen für integrierte Substanzen.

Insgesamt ergänzt die vorliegende Arbeit aktuelle Kenntnisse hinsichtlich Einflussparameter der in vitro Methode zur Bestimmung der Hautpermeabilität und der Eignung verschiedener Hautintegritätstests aber auch die Forschung zur Entwicklung von validen in silico Prädiktionsmodellen. Allerdings sind weitere Untersuchungen zu empfehlen, um die Reproduzierbarkeit der Methode weiter zu erhöhen und die Routineapplikation der Prädiktionsmodelle zu ermöglichen.

9 References

- Abdulmajed, K., McGuigan, C. & Heard, C. (2006) Topical delivery of retinyl ascorbate co-drug - 5. In vitro degradation studies. *Skin Pharmacology and Physiology*, 19, 248-258.
- Abraham, M.H., Chadha, H.S., Martins, F., Mitchell, R.C., Bradbury, M.W. & Gratton, J.A. (1999) Hydrogen bonding - Part 46: A review of the correlation and prediction of transport properties by an LFER method: physicochemical properties, brain penetration and skin permeability. *Pesticide Science*, 55, 78-88.
- Abraham, M.H. & Martins, F. (2004) Human skin permeation and partition: General linear free-energy relationship analyses. *Journal of Pharmaceutical Sciences*, 93, 1508-1523.
- Ackermann, K., Borgia, S.L., Korting, H.C., Mewes, K.R. & Schaefer-Korting, M. (2010) The Phenion (R) Full-Thickness Skin Model for Percutaneous Absorption Testing. *Skin Pharmacology and Physiology*, 23, 105-112.
- Allen, D.D., Caviedes, R., Cardenas, A.M., Shimahara, T., Segura-Aguilar, J. & Caviedes, P.A. (2005) Cell lines as in vitro models for drug screening and toxicity studies. *Drug Development and Industrial Pharmacy*, 31, 757-768.
- Allen-Hoffmann, B.L., Schlosser, S.J., Ivarie, C.A.R., Sattler, C.A., Meisner, L.F. & O'Connor, S.L. (2000) Normal growth and differentiation in a spontaneously immortalized near-diploid human keratinocyte cell line, NIKS. *Journal of Investigative Dermatology*, 114, 444-455.
- Amasheh, S., Fromm, M. & Guenzel, D. (2011) Claudins of intestine and nephron - a correlation of molecular tight junction structure and barrier function. *Acta Physiologica*, 201, 133-140.
- Arlotto, M.P., Trant, J.M. & Estabrook, R.W. (1991) Measurement of Steroid Hydroxylation Reactions by High-Performance Liquid-Chromatography As Indicator of P450 Identity and Function. *Methods in Enzymology*, 206, 454-462.
- Avdeef, A., Bendels, S., Di, L., Faller, B., Kansy, M., Sugano, K. & Yamauchi, Y. (2007) PAMPA - Critical factors for better predictions of absorption. *Journal of Pharmaceutical Sciences*, 96, 2893-2909.
- Baetz, F.M., Klipper, W., Korting, H.C., Henkler, F., Landsiedel, R., Luch, A., von Fritschen, U., Weindl & Schaefer-Korting. (2012) Esterase activity in excised and reconstructed human skin - Biotransformation of prednicarbate and the model dye fluorescein diacetate. *Eur J Pharm Biopharm*.
- Baker, H. (1986) The skin as a barrier. In: Rock, A., *Textbook of Dermatology*. Blackwell Scientific Publications: Oxford, 355-365.
- Balaguer, A., Salvador, A., Chisvert, A., Melia, M., Herraiez, M. & Diez, O. (2006) A liquid chromatography-fluorimetric method for the in vitro estimation of the skin penetration of disodium phenyldibenzimidazole tetrasulfonate from sunscreen formulations through human skin. *Analytical and Bioanalytical Chemistry*, 385, 1225-1232.
- Barbero, A.M. & Frasch, H.F. (2009) Pig and guinea pig skin as surrogates for human in vitro penetration studies: A quantitative review. *Toxicology in Vitro*, 23, 1-13.
- Baron, J.M., Holler, D., Schiffer, R., Frankenberg, S., Neis, M., Merk, H.F. & Jugert, F.K. (2001) Expression of multiple cytochrome P450 enzymes and multidrug resistance-associated transport proteins in human skin keratinocytes. *Journal of Investigative Dermatology*, 116, 541-548.
- Barratt, M.D. (1995) Quantitative Structure-Activity Relationships for Skin Permeability. *Toxicology in Vitro*, 9, 27-37.

- Barry, B.W. (1987) Penetration enhancers - Mode of action in humans. *In: Shroot, B. & Schaefer, H., Skin Pharmacokinetics*, 121-137.
- Barry, B.W. (1993) Vehicle Effect: What is an Enhancer? *In: Shah, P.V. & Maibach, H., I., Topical Drug Bioavailability, Bioequivalence and Penetration*. Plenum Press: New York, 261-276.
- Barry, H., Colaizzi, J.L. & Marcus, F. (1972) Value of Repeated Tests in A Percutaneous Absorption Study. *Journal of Pharmaceutical Sciences*, 61, 172-174.
- Bartek, M.J., Labudde, J.A. & Maibach, H.I. (1972) Skin Permeability In-Vivo - Comparison in Rat, Rabbit, Pig and Man. *Journal of Investigative Dermatology*, 58, 114-123.
- BASF SE. (2009) Safety Data Sheet MCPA-2EH-Ester Tech.
- Bätz, F.M., Klipper, W., Korting, H.C., Henkler, F., Landsiedel, R., uch, A., von Fritschen, U., Weindl, Weindl, G. & Schäfer-Korting, M. (2012) Esterase activity in excised and reconstructed human skin - Biotransformation of prednicarbate and the model dye fluorescein diacetate. *Eur J Pharm Biopharm*.
- Baynes, R.E., Brooks, J.D., Barlow, B.M. & Riviere, J.E. (2002) Physicochemical determinants of linear alkylbenzene sulfonate (LAS) disposition in skin exposed to aqueous cutting fluid mixtures. *Toxicology and Industrial Health*, 18, 237-248.
- Beiersdorf Ges mbH & Brand Manager EUCERIN. (2009) Die Epidermis (Oberhaut). URL: <http://www2.eucerin.com/at/ueber-die-haut/alles-ueber-die-haut/die-haut-und-ihre-zellen/die-epidermis-oberhaut> (Status:08.08.2012).
- Beisson, F., Aoubala, M., Marull, S., Moustacas-Gardies, A.M., Voultoury, R., Verger, R. & Arondel, V. (2001) Use of the tape stripping technique for directly quantifying esterase activities in human stratum corneum. *Analytical Biochemistry*, 290, 179-185.
- Belitz, H.-D., Grosch, W. & Schieberle, P. (2008) *Lehrbuch der Lebensmittelchemie*. Springer Verlag: Berlin Heidelberg.
- Blair, A.H. & Vallee, B.L. (1966) Some Catalytic Properties of Human Liver Alcohol Dehydrogenase. *Biochemistry*, 5, 2026-2034.
- Blank, I.H. (1953) Further Observations on Factors Which Influence the Water Content of the Stratum Corneum. *Journal of Investigative Dermatology*, 21, 259-271.
- Blank, I.H. & Mcauliffe, D.J. (1985) Penetration of Benzene Through Human-Skin. *Journal of Investigative Dermatology*, 85, 522-526.
- Blank, I.H. & Scheuplein, R.J. (1967) Mechanism of Percutaneous Absorption .3. Effect of Temperature on Transport of Non-Electrolytes Across Skin. *Journal of Investigative Dermatology*, 49, 582-589.
- Bock, K.W., Josting, D., Lilienblum, W. & Pfeil, H. (1979) Purification of Rat-Liver Microsomal Udp-Glucuronyltransferase - Separation of 2 Enzyme Forms Inducible by 3-Methylcholanthrene Or Phenobarbital. *European Journal of Biochemistry*, 98, 19-26.
- Bodde, H.E., Verhoeven, J. & Vandriel, L.M.J. (1989) The Skin Compliance of Transdermal Drug Delivery Systems. *Critical Reviews in Therapeutic Drug Carrier Systems*, 6, 87-115.
- Boelsma, E., Gibbs, S., Faller, C. & Ponec, M. (2008) Characterization and comparison of reconstructed skin models: Morphological and immunohistochemical evaluation. *Acta Dermato-Venereologica*, 80, 82-88.
- Bos, J.D. & Meinardi, M.M.H.M. (2000) The 500 Dalton rule for the skin penetration of chemical compounds and drugs. *Experimental Dermatology*, 9, 165-169.

- Brain, K.R., James, V.J. & Walters, K.A. (1995) Validation of the integrity of epidermal membranes during assessment of percutaneous penetration. *Prediction of Percutaneous Penetration*.
- Brand, R.M., Charron, A.R., Dutton, L., Gavlik, T.L., Mueller, C., Hamel, F.G., Chakkalakal, D. & Donohue, T.M. (2004) Effects of chronic alcohol consumption on dermal penetration of pesticides in rats. *Journal of Toxicology and Environmental Health-Part A-Current Issues*, 67, 153-161.
- Brandner, J.M. (2010) Tight Junctions: A New Barrier in the Skin? In: Monteiro-Riviere, N.A., *Toxicology of the Skin*. Informa Healthcare: New York, 35-42.
- British Crop Protection Council. (2011) The e-pesticide manual V5.2. British Crop Production Council, Hampshire, UK.
- Bronaugh, R.L. & Franz, T.J. (1986) Vehicle Effects on Percutaneous-Absorption - Invivo and Invitro Comparisons with Human-Skin. *British Journal of Dermatology*, 115, 1-11.
- Bronaugh, R.L. & Stewart, R.F. (1985) Methods for Invitro Percutaneous-Absorption Studies .4. the Flow-Through Diffusion Cell. *Journal of Pharmaceutical Sciences*, 74, 64-67.
- Bronaugh, R.L., Stewart, R.F. & Congdon, E.R. (1983) Differences in Permeability of Rat Skin Related to Sex and Body Site. *Journal of the Society of Cosmetic Chemists*, 34, 127-135.
- Bronaugh, R.L., Stewart, R.F. & Simon, M. (1986) Methods for Invitro Percutaneous-Absorption Studies .7. Use of Excised Human-Skin. *Journal of Pharmaceutical Sciences*, 75, 1094-1097.
- Bucks, D.A.W., Maibach, H.I. & Guy, R.H. (1985) Percutaneous-Absorption of Steroids - Effect of Repeated Application. *Journal of Pharmaceutical Sciences*, 74, 1337-1339.
- Buist, H.E., van de Sandt, J.J.M., van Burgsteden, J.A. & de Heer, C. (2005) Effects of single and repeated exposure to biocidal active substances on the barrier function of the skin in vitro. *Regulatory Toxicology and Pharmacology*, 43, 76-84.
- Bundesamt für Verbraucherschutz und Lebensmittelsicherheit (BVL). (2012a) Pflanzenschutzmittel-Verzeichnis. URL: http://www.bvl.bund.de/DE/04_Pflanzenschutzmittel/01_Aufgaben/02_ZulassungPSM/01_ZugelPSM/05_Verzeichnis/psm_ZugelPSM_Verzeichnis_node.html (State: 15.05.2012).
- Bundesamt für Verbraucherschutz und Lebensmittelsicherheit (BVL). (2012b) Toxikologie und Anwendungssicherheit. URL: http://www.bvl.bund.de/DE/04_Pflanzenschutzmittel/03_Antragsteller/04_Zulassungsverfahren/06_Toxikologie/psm_toxiko_node.html (State: 15.05.2012).
- Burke, M.D., Thompson, S., Elcombe, C.R., Halpert, J., Haaparanta, T. & Mayer, R.T. (1985) Ethoxyphenoxazones, Pentoxyphenoxazones, and Benzyloxyphenoxazones and Homologs - A Series of Substrates to Distinguish Between Different Induced Cytochromes-P-450. *Biochemical Pharmacology*, 34, 3337-3345.
- Burke, M.D., Thompson, S., Weaver, R.J., Wolf, C.R. & Mayer, R.T. (1994) Cytochrome-P450 Specificities of Alkoxyresorufin O-Dealkylation in Human and Rat-Liver. *Biochemical Pharmacology*, 48, 923-936.
- Cessna, A.J. & Grover, R. (1978) Spectrophotometric Determination of Dissociation-Constants of Selected Acidic Herbicides. *Journal of Agricultural and Food Chemistry*, 26, 289-292.
- Challapalli, P.V.N. & Stinchcomb, A.L. (2002) In vitro experiment optimization for measuring tetrahydrocannabinol skin permeation. *International Journal of Pharmaceutics*, 241, 329-339.
- Chilcott, R.P., Dalton, C.H., Emmanuel, A.J., Allen, C.E. & Bradley, S.T. (2002) Transepidermal water loss does not correlate with skin barrier function in vitro. *Journal of Investigative Dermatology*, 118, 871-875.

- Christophers, E. & Kligman, A.M. (1965) Percutaneous absorption in aged skin. *In: Motagna, W., Aging Volume VI Advances in the Biology of the Skin*, 163-175.
- Clark, N.W.E., Scott, R.C., Blain, P.G. & Williams, F.M. (1993) Fate of Fluazifop Butyl in Rat and Human Skin *In Vitro*. *Archives of Toxicology*, 67, 44-48.
- Cleary, G.W. (1993) Transdermal Delivery Systems: A Medical Rationale. *In: Shah, V.P. & Maibach, H.I., Topical Drug Bioavailability, Bioequivalence, and Penetration*. Plenum Press: New York, 17-68.
- Clowes, H.M., Scott, R.C. & Heylings, J.R. (1994) Skin Absorption - Flow-Through Or Static Diffusion Cells. *Toxicology in Vitro*, 8, 827-830.
- Cramer, C.J., Famini, G.R. & Lowrey, A.H. (1993) Use of Calculated Quantum-Chemical Properties As Surrogates for Solvatochromic Parameters in Structure-Activity-Relationships. *Accounts of Chemical Research*, 26, 599-605.
- Crutcher, W. & Maibach, H.I. (1969) Effect of Perfusion Rate on *In Vitro* Percutaneous Penetration. *Journal of Investigative Dermatology*, 53, 264-269.
- Dancik, Y., Thompson, C., Krishnan, G. & Roberts, M.S. (2010) Cutaneous Metabolism and Active Transport in Transdermal Drug Delivery. *In: Monteiro-Riviere, N.A., Toxicology of the Skin*. Informa Healthcare: New York, 69-82.
- Dancik, Y., Miller, M.A., Jaworska, J. & Kasting, G.B. (2013) Design and performance of a spreadsheet-based model for estimating bioavailability of chemicals from dermal exposure. *Advanced Drug Delivery Reviews*, 65, 221-236.
- Davies, D.J., Ward, R.J. & Heylings, J.R. (2004) Multi-species assessment of electrical resistance as a skin integrity marker for *in vitro* percutaneous absorption studies. *Toxicology in Vitro*, 18, 351-358.
- Davis, A.F., Gyurik, R.J., Hadgraft, J., Pellett, M.A. & Walters, K.A. (2002) Formulation Strategies for Modulating Skin Permeation. *In: Walters, K.A., Dermatological and Transdermal Formulations*. Marcel Dekker: New York, 271-317.
- Dearden, J., Cronin, M., Patel, H. & Raevsky, O. (2000) QSAR prediction of human skin permeability coefficients. *Journal of Pharmacy and Pharmacology*, 52, 221.
- Diembeck, W., Beck, H., Benesch-Kieffer, F., Courtellemont, P., Dupuiss, J., Lovell, W., Paye, M., Spengler, J. & Steiling, W. (1999) Test guidelines for *in vitro* assessment of dermal absorption and percutaneous penetration of cosmetic ingredients. *Food and Chemical Toxicology*, 37, 191-205.
- Diez-Sales, O., Perezsayas, E., Martinvillodre, A. & Herraedominguez, M. (1993) The Prediction of Percutaneous-Absorption .1. Influence of the Dermis on *In-Vitro* Permeation Models. *International Journal of Pharmaceutics*, 100, 1-7.
- Dreher, F., Fouchard, F., Patouillet, C., Andrian, M., Simonnet, J.T. & Kieffer, F. (2002) Comparison of cutaneous bioavailability of cosmetic preparations containing caffeine or alpha-tocopherol applied on human skin models or human skin *ex vivo* at finite doses. *Skin Pharmacology and Applied Skin Physiology*, 15, 40-58.
- Dugard, P.H. & Scott, R.C. (1986) A Method of Predicting Percutaneous-Absorption Rates from Vehicle to Vehicle - An Experimental Assessment. *International Journal of Pharmaceutics*, 28, 219-227.
- ECVAM (European Centre for the Validation of Alternative Methods). (2010) Methods Summary - Percutaneous Absorption. URL: <http://ecvam-dbalm.jrc.ec.europa.eu/> (Status 31.01.2011).

- EFSA Panel on Plant Protection Products and their Residues (PPR). (2012) Guidance on Dermal Absorption. *EFSA Journal*, 10.
- Egelrud, T. (1992) Stratum corneum chymotryptic enzyme: Evidence of its location in the stratum corneum intercellular space. *European Journal of Dermatology*, 2, 46-49.
- El Tayar N., Tsai, R.-S., Testa, B., Carrupt, P.-A., Hansch, C. & Leo, A. (1991) Percutaneous Penetration of Drugs A Quantitative Structure-Permeability Relationship Study. *Journal of Pharmaceutical Sciences*, 80, 744-749.
- Elias, P.M. (2005) Stratum corneum defensive functions: An integrated view. *Journal of Investigative Dermatology*, 125, 183-200.
- Elkeeb, R., Hui, X.Y., Chan, H.D., Tian, L.L. & Maibach, H.I. (2010) Correlation of transepidermal water loss with skin barrier properties in vitro: comparison of three evaporimeters. *Skin Research and Technology*, 16, 9-15.
- Elwell, M.R., Stedham, M.A. & Kovatch, R.M. (1990) Skin and Subcutis. In: Boorman, G.A., Eustis, S.L., Elwell, M.R. et al., *Pathology of the Fischer Rat. Reference and Atlas*. Academic Press, Inc.: San Diego, California, 261-277.
- Europäische Arzneibuchkommission. (2008) Chromatographische Trennmethoden. *Europäisches Arzneimittelbuch*, 93-99.
- European Centre for Ecotoxicology and Toxicology of Chemicals. (1993) Monograph No. 20 - Percutaneous Absorption.
- European Centre of the Validation of Alternative Methods ECVAM. (2010) Percutaneous Absorption. URL: <http://ecvam-dbalm.jrc.ec.europa.eu/> (status: 01.05.2012).
- European Chemicals Agency (ECHA). (2008) Guidance in information requirements and chemical safety assessment. Chapter R.7c: Endpoint specific guidance.
- Fang, J.Y. & Leu, Y.L. (2006) Prodrug strategy for enhancing drug delivery via skin. *Current drug discovery technologies*, 3, 211-224.
- Fasano, W.J., Manning, L.A. & Green, J.W. (2002) Rapid integrity assessment of rat and human epidermal membranes for in vitro dermal regulatory testing: correlation of electrical resistance with tritiated water permeability. *Toxicology in Vitro*, 16, 731-740.
- Fitzpatrick, D., Corish, J. & Hayes, B. (2004) Modelling skin permeability in risk assessment - the future. *Chemosphere*, 55, 1309-1314.
- Flynn, G.L. (1990) Physicochemical Determinants of Skin Absorption. In: Gerrity, T.R. & Henry C.J., *Principles of Route-to-Route Extrapolation for Risk Assessment*. Elsevier Science, 93-127.
- Flynn, G.L., Durrheim, H. & Higuchi, W.I. (1981) Permeation of Hairless Mouse Skin .2. Membrane Sectioning Techniques and Influence on Alkanol Permeabilities. *Journal of Pharmaceutical Sciences*, 70, 52-56.
- Flynn, G.L., Yalkowsk, S.H. & Roseman, T.J. (1974) Mass-Transport Phenomena and Models - Theoretical Concepts. *Journal of Pharmaceutical Sciences*, 63, 479-510.
- Frasch, H., Zang, L.Y., Barbero, A.M. & Anderson, S.E. (2010) In Vitro Dermal Penetration of 4-Chloro-3-Methylphenol from Commercial Metal Working Fluid and Aqueous Vehicles. *Journal of Toxicology and Environmental Health-Part A-Current Issues*, 73, 1394-1405.
- Furuse, M., Hata, M., Furuse, K., Yoshida, Y., Haratake, A., Sugitani, Y., Noda, T., Kubo, A. & Tsukita, S. (2002) Claudin-based tight junctions are crucial for the mammalian epidermal barrier: a lesson from claudin-1-deficient mice. *Journal of Cell Biology*, 156, 1099-1111.

- Gabrielli, D., Belisle, E., Severino, D., Kowaltowski, A.J. & Baptista, M.S. (2004) Binding, aggregation and photochemical properties of methylene blue in mitochondrial suspensions. *Photochemistry and Photobiology*, 79, 227-232.
- Geinoz, S., Guy, R.H., Testa, B. & Carrupt, P.A. (2004) Quantitative structure-permeation relationships (QSPeRs) to predict skin permeation: A critical evaluation. *Pharmaceutical Research*, 21, 83-92.
- Ghafourian, T. & Fooladi, S. (2001) The effect of structural QSAR parameters on skin penetration. *International Journal of Pharmaceutics*, 217, 1-11.
- Goetz, C., Pfeiffer, R., Tigges, J., Blatz, V., Jaeckh, C., Freytag, E.M., Fabian, E., Landsiedel, R., Merk, H.F., Krutmann, J., Edwards, R.J., Pease, C., Goebel, C., Hewitt, N. & Fritsche, E. (2012a) Xenobiotic metabolism capacities of human skin in comparison with a 3D epidermis model and keratinocyte-based cell culture as in vitro alternatives for chemical testing: activating enzymes (Phase I). *Experimental Dermatology*, 21, 358-363.
- Goetz, C., Pfeiffer, R., Tigges, J., Ruwiedel, K., Huebenthal, U., Merk, H.F., Krutmann, J., Edwards, R.J., Abel, J., Pease, C., Goebel, C., Hewitt, N. & Fritsche, E. (2012b) Xenobiotic metabolism capacities of human skin in comparison with a 3D-epidermis model and keratinocyte-based cell culture as in vitro alternatives for chemical testing: phase II enzymes. *Experimental Dermatology*, 21, 364-369.
- Gotter, A. (2007) Untersuchungen zu Einflussparametern auf die dermale Permeation in vitro (diploma thesis).
- Gramatica, P. (2007) Principles of QSAR models validation: internal and external. *Qsar & Combinatorial Science*, 26, 694-701.
- Green, K.J. & Jones, J.C.R. (1996) Desmosomes and hemidesmosomes: Structure and function of molecular components. *Faseb Journal*, 10, 871-881.
- Grice, J.E., Zhang, Q. & Roberts, M.S. (2010) Chemical Structure - Skin Transport Relationships. In: Monteiro-Riviere, N.A., *Toxicology of the Skin*. Informa Healthcare: New York, 55-68.
- Guilbault, G.G. & Kramer, D.N. (1964) Fluorometric Determination of Lipase Acylase Alpha-+ Gamma-Chymotrypsin + Inhibitors of These Enzymes. *Analytical Chemistry*, 36, 409-412.
- Guy, R.H. & Potts, R.O. (1992) Structure-Permeability Relationships in Percutaneous Penetration. *Journal of Pharmaceutical Sciences*, 81, 603-604.
- Gysler, A., Kleuser, B., Sippl, W., Lange, K., Korting, H.C., Holtje, H.D. & Schaefer-Korting, M. (1999) Skin penetration and metabolism of topical glucocorticoids in reconstructed epidermis and in excised human skin. *Pharmaceutical Research*, 16, 1386-1391.
- Hansen, S., Henning, A., Naegel, A., Heisig, M., Wittum, G., Neumann, D., Kostka, K.H., Zbytovska, J., Lehr, C.M. & Schaefer, U.F. (2008) In-silico model of skin penetration based on experimentally determined input parameters. Part I: Experimental determination of partition and diffusion coefficients. *European Journal of Pharmaceutics and Biopharmaceutics*, 68, 352-367.
- Harada, K., Murakami, T., Kawasaki, E., Higashi, Y., Yamamoto, S. & Yata, N. (1993) In vitro Permeability to Salicylic-Acid of Human, Rodent, and Shed Snake Skin. *Journal of Pharmacy and Pharmacology*, 45, 414-418.
- Harris, I.R., Siefken, W., Beck-Oldach, K., Brandt, M., Wittern, K.P. & Pollet, D. (2002) Comparison of activities dependent on glutathione S-transferase and cytochrome P-450IA1 in cultured keratinocytes and reconstructed epidermal models. *Skin Pharmacology and Applied Skin Physiology*, 15, 59-67.
- Harrison, S.M., Barry, B.W. & Dugard, P.H. (1984) Effects of Freezing on Human-Skin Permeability. *Journal of Pharmacy and Pharmacology*, 36, 261-262.

- Harville, H.M., Voorman, R. & Prusakiewicz, J.J. (2007) Comparison of paraben stability in human and rat skin. *Drug metabolism letters*, 1, 17-21.
- Hashimoto, K. (1971) Intercellular Spaces of Human Epidermis As Demonstrated with Lanthanum. *Journal of Investigative Dermatology*, 57, 17-8.
- Hautier, A., Sabatier, F., Stellmann, P., Andrac, L., Nouaille De Gorce, Y., Dignat-George, F. & Magalon, G. (2008) Assessment of organ culture for the conservation of human skin allografts. *Cell and Tissue Banking*, 9, 19-29.
- Henkler, F., Luch, A., Schaefer-Korting, M., Weindl, G., Merk, H., Landsiedel, R. & Reisinger, K. (2012) Gemeinsamer Abschlussbericht zum Verbund-Forschungsvorhaben. Ersatzmethoden zum Tierversuch-Charakterisierung der metabolischen Kapazität von in vitro-Hautmodellen zum Zwecke der Identifizierung eines optimalen Modells für die Hauttoxizitätsprüfung sowie zur Expositionsabschätzung von Substanzen mit dermalen Biotransformation. Förderkennzeichen: 0315226A-E.
- Henning, A., Neumann, D., Kostka, K.H., Lehr, C.M. & Schaefer, U.F. (2008) Influence of human skin specimens consisting of different skin layers on the result of in vitro permeation experiments. *Skin Pharmacology and Physiology*, 21, 81-88.
- Hewitt, P.G., Perkins, J. & Hotchkiss, S.A.M. (2000) Metabolism of fluroxypyr, fluroxypyr methyl ester, and the herbicide fluroxypyr methylheptyl ester. I: During percutaneous absorption through fresh rat and human skin in vitro. *Drug Metabolism and Disposition*, 28, 748-754.
- Heylings, J.R., van de Sandt, J.J.M., Gilde, A.J. & Ward, R.J. (2001) Evaluation of SkinEthic human reconstituted epidermis for percutaneous absorption testing. *Toxicology*, 164, 130.
- Hoernicke, E., Westphal, D. & Fachausschuss Anwenderschutz. (1998) Hinweise in der Gebrauchsanleitung zum Schutz von Personen bei Nachfolgearbeiten in mit Pflanzenschutzmitteln behandelten Kulturen (worker re-entry). *Nachrichtenblatt des deutschen Pflanzenschutzdienstes*, 50, 267-268.
- Hohl, D. (1990) Cornified Cell-Envelope. *Dermatologica*, 180, 201-211.
- Hostynek, J.J. & Magee, P.S. (1997) Modelling in vivo human skin absorption. *Quantitative Structure-Activity Relationships*, 16, 473-479.
- Hotchkiss, S.A. (1998) Dermal Metabolism. In: Roberts, M.S. & Walters, K.A., *Dermal Absorption and Toxicity Assessment*. Marcel Dekker: New York, 43-101.
- Hotchkiss, S.A.M., Miller, J.M. & Caldwell, J. (1992) Percutaneous-Absorption of Benzyl Acetate Through Rat Skin In vitro .2. Effect of Vehicle and Occlusion. *Food and Chemical Toxicology*, 30, 145-153.
- Hughes, M.F., Shrivastava, S.P., Fisher, H.L. & Hall, L.L. (1993) Comparative In vitro Percutaneous-Absorption of P-Substituted Phenols Through Rat Skin Using Static and Flow-Through Diffusion-Systems. *Toxicology in Vitro*, 7, 221-227.
- Imhof, R., De Jesus, M., Xiao, P., Ciorte, L., I & Berg, E. (2009) Closed-chamber transepidermal water loss measurement: microclimate, calibration and performance. *International Journal of Cosmetic Science*, 31, 97-118.
- Jacobi, U., Bartoll, J., Sterry, W. & Lademann, J. (2005) Orally administered ethanol: transepidermal pathways and effects on the human skin barrier. *Archives of Dermatological Research*, 296, 332-338.
- Jaekh, C., Blatz, V., Fabian, E., Guth, K., van Ravenzwaay, B., Reisinger, K. & Landsiedel, R. (2011) Characterization of enzyme activities of Cytochrome P450 enzymes, Flavin-dependent monooxygenases, N-acetyltransferases and UDP-glucuronyltransferases in human reconstructed epidermis and full-thickness skin models. *Toxicology in Vitro*, 25, 1209-1214.

- Jaeckh, C., Blatz, V., Guth, K., Noss, A., Reisinger, K., Fabian, E., van Ravenzwaay, B. & Landsiedel, R. (2010a) Characterization of human reconstructed skin models for activities of xenobiotic metabolizing enzymes (conference poster).
- Jaeckh, C., Blatz, V., Guth, K., Reisinger, K., Fabian, E., van Ravenzwaay, B. & Landsiedel, R. (2010b) Analyses of xenobiotic metabolizing enzyme activities in human reconstructed skin equivalents (conference poster).
- Jaeckh, C., Fabian, E., van Ravenzwaay, B. & Landsiedel, R. (2012) Relevance of xenobiotic enzymes in human skin in vitro models to activate pro-sensitizers. *Journal of Immunotoxicology*, 1-13.
- Johnson, P., Gallo, S., Oseroff, A. & Hui, S. (1996) Electroenhanced transdermal transport (ETT) of the photosensitizers methylene blue and delta-amino levulinic acid using surface electrodes on full thickness porcine skin. *Photochemistry and Photobiology*, 63, 91S.
- Jones, C.R. & Lubet, R.A. (1992) Induction of A Pleiotropic Response by Phenobarbital and Related-Compounds - Response in Various Inbred Strains of Rats, Response in Various Species and the Induction of Aldehyde Dehydrogenase in Copenhagen Rats. *Biochemical Pharmacology*, 44, 1651-1660.
- Kahan, V., Andersen, M., Tomimori, J. & Tufik, S. (2009) Stress, immunity and skin collagen integrity: Evidence from animal models and clinical conditions. *Brain Behavior and Immunity*, 23, 1089-1095.
- Kamlet, M.J., Abboud, J.L.M., Abraham, M.H. & Taft, R.W. (1983) Linear Solvation Energy Relationships .23. A Comprehensive Collection of the Solvatochromic Parameters, Pi-Star, Alpha and Beta, and Some Methods for Simplifying the Generalized Solvatochromic Equation. *Journal of Organic Chemistry*, 48, 2877-2887.
- Kansy, M., Senner, F. & Gubernator, K. (1998) Physicochemical high throughput screening: Parallel artificial membrane permeation assay in the description of passive absorption processes. *Journal of Medicinal Chemistry*, 41, 1007-1010.
- Kao, J., Patterson, F.K. & Hall, J. (1985) Skin Penetration and Metabolism of Topically Applied Chemicals in 6 Mammalian-Species, Including Man - An In vitro Study with Benzo[A]pyrene and Testosterone. *Toxicology and Applied Pharmacology*, 81, 502-516.
- Karmazsin, L., Balla, G. & Szollosi, J. (1979) Cellular Esterase-Activity - Estimation by Fluorescein Diacetate Hydrolysis. *Acta Paediatrica Academiae Scientiarum Hungaricae*, 20, 249-253.
- Kawaji, A., Ohara, K. & Takabatake, E. (1993) An Assay of Flavin-Containing Monooxygenase Activity with Benzydamine N-Oxidation. *Analytical Biochemistry*, 214, 409-412.
- Kawakubo, Y., Manabe, S., Yamazoe, Y., Nishikawa, T. & Kato, R. (1988) Properties of Cutaneous Acetyltransferase Catalyzing N-Acetylation and O-Acetylation of Carcinogenic Arylamines and N-Hydroxyarylamines. *Biochemical Pharmacology*, 37, 265-270.
- Kawashima, Y., Someya, Y., Sato, S., Shirato, K., Jinde, M., Ishida, S., Akimoto, S., Kobayashi, K., Sakakibara, Y., Suzuki, Y., Tachiyashiki, K. & Imaizumi, K. (2011) Dietary zinc-deficiency and its recovery responses in rat liver cytosolic alcohol dehydrogenase activities. *Journal of Toxicological Sciences*, 36, 101-108.
- Kielhorn, J. & Melching-Kollmuss, S. (2008) International Perspectives in Dermal Absorption. In: Roberts, M.S. & Walters, K.A., *Dermal Absorption and Toxicity Assessment*. Informa Healthcare: New York, 471-482.
- Kielhorn, J., Melching-Kollmuss, S. & Mangelsdorf, I. (2006) *Dermal absorption, Environmental Health Criteria 235*. World Health Organization.

- Kirchner, L.A., Moody, R.P., Doyle, E., Bose, R., Jeffery, J. & Chu, I. (1997) The prediction of skin permeability by using physicochemical data. *Atla-Alternatives to Laboratory Animals*, 25, 359-370.
- Kirschner, N. (2010) Untersuchung der Expression, Lokalisation und Funktionalität von Tight Junctions in murinen und humanen Modellsystemen mit Barriere-defekten in der Haut.
- Kirschner, N. & Brandner, J.M. (2012) Barriers and more: functions of tight junction proteins in the skin. *Annals of the New York Academy of Sciences*, 1257, 158-166.
- Kirschner, N., Haftek, M., Niessen, C.M., Behne, M.J., Furuse, M., Moll, I. & Brandner, J.M. (2011) CD44 Regulates Tight-Junction Assembly and Barrier Function. *Journal of Investigative Dermatology*, 131, 932-943.
- Krebs, B., Maasfeld, W., Schrader, J., Wolf, R., Hoernicke, E., Nolting, H.G., Backhaus, G.F. & Westphal, D. (2001) Uniform principles for safeguarding the health of workers re-entering crop growing areas after application of plant-protection products. *Worker Exposure to Agrochemicals*, 107-117.
- Kubinyi, H. (1993) Statistical Methods. In: Mannhold, R., Krogsgaard-Larsen, P. & Timmerman, H., *QSAR: Hansch Analysis and Related Approaches*. VCH Verlagsgesellschaft: Weinheim, 91-107.
- Kushner, J., IV, Blankschtein, D. & Langer, R. (2007) Evaluation of the porosity, the tortuosity, and the hindrance factor for the Transdermal delivery of hydrophilic permeants in the context of the aqueous pore pathway hypothesis using dual-radiolabeled permeability experiments. *Journal of Pharmaceutical Sciences*, 96, 3263-3282.
- Land, S.J., Zukowski, K., Lee, M.S., Debiecycchter, M., King, C.M. & Wang, C.Y. (1989) Metabolism of Aromatic-Amines - Relationships of N-Acetylation, O-Acetylation, N,O-Acetyltransfer and Deacetylation in Human-Liver and Urinary-Bladder. *Carcinogenesis*, 10, 727-731.
- Lau, W.M., Ng, K.W., Sakenyte, K. & Heard, C.M. (2012) Distribution of esterase activity in porcine ear skin, and the effects of freezing and heat separation. *International Journal of Pharmaceutics*, 433, 10-15.
- Lawrence, J.N. (1997) Electrical resistance and tritiated water permeability as indicators of barrier integrity of in vitro human skin. *Toxicology in Vitro*, 11, 241-249.
- Ledirac, N., Delescluse, C., deSousa, G., Pralavorio, M., Lesca, P., Amichot, M., Berge, J.B. & Rahmani, R. (1997) Carbaryl induces CYP1A1 gene expression in HepG2 and HaCaT cells but is not a ligand of the human hepatic Ah receptor. *Toxicology and Applied Pharmacology*, 144, 177-182.
- Lee, F.W., Earl, L. & Williams, F.M. (2001) Interindividual variability in the percutaneous penetration of testosterone through human skin in vitro. *Toxicology*, 168, 63.
- Lee, F.W., Minter, H., Pease, C.K.S. & Williams, F.M. (2002) Influence of the skin reservoir on absorption of testosterone through rat skin in vitro and in vivo. *Toxicology*, 178, 40-41.
- Lee, P.H., Conradi, R. & Shanmugasundaram, V. (2010) Development of an in silico model for human skin permeation based on a Franz cell skin permeability assay. *Bioorganic & Medicinal Chemistry Letters*, 20, 69-73.
- Leo, A., Hansch, C. & Elkins, D. (1971) Partition Coefficients and Their Uses. *Chemical Reviews*, 71, 525.
- Leopold, C.S. & Maibach, H.I. (1996) Effect of lipophilic vehicles on in vivo skin penetration of methyl nicotinate in different races. *International Journal of Pharmaceutics*, 139, 161-167.

- Levin, J. & Maibach, H. (2005) The correlation between transepidermal water loss and percutaneous absorption: An overview. *Journal of Controlled Release*, 103, 291-299.
- Li, T.K. (1977) Enzymology of human alcohol metabolism. *Advances in enzymology and related areas of molecular biology*, 45, 427-483.
- Lien, E.J. & Gao, H. (1995) Qsar Analysis of Skin Permeability of Various Drugs in Man As Compared to In-Vivo and In-Vitro Studies in Rodents. *Pharmaceutical Research*, 12, 583-587.
- Lilienblum, W., Walli, A.K. & Bock, K.W. (1982) Differential Induction of Rat-Liver Microsomal Udp-Glucuronosyltransferase Activities by Various Inducing Agents. *Biochemical Pharmacology*, 31, 907-913.
- Lillie, R.D. (2012) Nucleic, Nucleic Acids, General Oversight Stains. *Histopathologic Technic and Practical Histochemistry*. McGraw-Hill: New York, 142-179.
- Lindahl, R. & Evces, S. (1984a) Comparative subcellular distribution of aldehyde dehydrogenase in rat, mouse and rabbit liver. *Biochemical Pharmacology*, 33, 3383-3389.
- Lindahl, R. & Evces, S. (1984b) Rat Liver Aldehyde Dehydrogenase I. Isolation and Characterisation of four high Km normal liver Isozymes. *Journal of Biological Chemistry*, 259, 11986-11990.
- Lipinski, C.A., Lombardo, F., Dominy, B.W. & Feeney, P.J. (1997) Experimental and computational approaches to estimate solubility and permeability in drug discovery and development settings. *Advanced Drug Delivery Reviews*, 23, 3-25.
- Lotte, C., Wester, R.C., Rougier, A. & Maibach, H.I. (1993) Racial-Differences in the Invivo Percutaneous-Absorption of Some Organic-Compounds - A Comparison Between Black, Caucasian and Asian Subjects. *Archives of Dermatological Research*, 284, 456-459.
- Lundehn, J., Westphal, D., Kieczka, H., Krebs, B., Löcher-Bolz, S., Maasfeld, W. & Pick, E. (1992) *Uniform principles for safeguarding the health of applicators of plant protection products (uniform principles for operator protection)*. Biologische Bundesanstalt für Land- und Forstwirtschaft.
- Maibach, H.I., Feldmann, R.J., Milby, T.H. & Serat, W.F. (1971) Regional Variation in Percutaneous Penetration in Man - Pesticides. *Archives of Environmental Health*, 23, 208-211.
- Maid-Kohnert, U. (2001) *Lexikon der Ernährung*. Spektrum Akademischer Verlag: Heidelberg, Berlin.
- Marzulli, F.N. & Brown, D.W.C.M.H.I. (1969) Techniques for studying skin Penetration. *Toxicology and Applied Pharmacology*, 3, 76-83.
- Mccracken, N.W., Blain, P.G. & Williams, F.M. (1993) Nature and Role of Xenobiotic Metabolizing Esterases in Rat-Liver, Lung, Skin and Blood. *Biochemical Pharmacology*, 45, 31-36.
- McKone, T.E. & Howd, R.A. (1992) Estimating Dermal Uptake of Nonionic Organic-Chemicals from Water and Soil .1. Unified Fugacity-Based Models for Risk Assessments. *Risk Analysis*, 12, 543-557.
- Meidan, V.M. & Roper, C.S. (2008) Inter- and intra-individual variability in human skin barrier function: A large scale retrospective study. *Toxicology in Vitro*, 22, 1062-1069.
- Menon, G.K., Lee S.H. & Roberts, M.S. (1998) Ultrastructural Effects of some Solvents and Vehicles on the Stratum Corneum and Other Skin Components: Evidence for an "Extrended Mosaic-Partitioning Model of the Skin Barrier". *Dermal Absorption and Toxicity Assessment*, 727-751.
- Merck. (2006a) Safety Data Sheet Caffeine.
- Merck. (2006b) Sicherheitsdatenblatt Tritriplex(R) II zur Analyse (Ethylendinitrilotetraessigsäure).

- Minchin, R.F., Reeves, P.T., Teitel, C.H., Mcmanus, M.E., Mojarrabi, B., Ilett, K.F. & Kadlubar, F.F. (1992) N-Acetylation and O-Acetylation of Aromatic and Heterocyclic Amine Carcinogens by Human Monomorphic and Polymorphic Acetyltransferases Expressed in Cos-1 Cells. *Biochemical and Biophysical Research Communications*, 185, 839-844.
- Mitragotri, S., Anissimov, Y.G., Bunge, A.L., Frasc, H.F., Guy, R.H., Hadgraft, J., Kasting, G.B., Lane, M.E. & Roberts, M.S. (2011) Mathematical models of skin permeability: An overview. *International Journal of Pharmaceutics*, 418, 115-129.
- Monteiro-Riviere, N.A. (1991) Comparative anatomy, physiology, and biochemistry of mammalian skin. *In: Hobson, D.W., Dermal and Ocular Toxicology: Fundamentals and Methods*. CRC Press: Washington, DC, 3-71.
- Monteiro-Riviere, N.A. (2006) Structure and Function of Skin. *In: Riviere, J.E., Dermal Absorption Models in Toxicology and Pharmacology*. CRC Press: Boca Raton, 1-20.
- Monteiro-Riviere, N.A. (2010) Structure and Function of Skin. *In: Monteiro-Riviere, N.A., Toxicology of the Skin*. Informa Healthcare: New York, 1-18.
- Monteiro-Riviere, N.A., Baynes, R.E. & Riviere, J.E. (2008) Animal Skin Morphology and Dermal Absorption. *In: Roberts, M.S. & Walters, K.A., Dermal Absorption and Toxicity Assessment*, 17-35.
- Monteiro-Riviere, N.A., Inman, A.O., Mak, V., Wertz, P. & Riviere, J.E. (2001) Effect of selective lipid extraction from different body regions on epidermal barrier function. *Pharmaceutical Research*, 18, 992-998.
- Monteiro-Riviere, N.A., Van Miller, J.P., Simon, G., Joiner, R.L., Brooks, J.D. & Riviere, J.E. (2000) Comparative in vitro percutaneous absorption of nonylphenol and nonylphenol ethoxylates (NPE-4 and NPE-9) through human, porcine and rat skin. *Toxicology and Industrial Health*, 16, 49-57.
- Moody, R.P. & MacPherson, H. (2003) Determination of dermal absorption QSAR/QSPRS by brute force regression: Multiparameter model development with Molsuite 2000. *Journal of Toxicology and Environmental Health-Part A*, 66, 1927-1942.
- Moody, R.P., Yip, A. & Chu, I. (2009) Effect of Cold Storage on In Vitro Human Skin Absorption of Six ¹⁴C-Radiolabeled Environmental Contaminants: Benzo[a]Pyrene, Ethylene Glycol, Methyl Parathion, Naphthalene, Nonyl Phenol, and Toluene. *Journal of Toxicology and Environmental Health-Part A-Current Issues*, 72, 505-517.
- Moss, G.P., Dearden, J.C., Patel, H. & Cronin, M.T.D. (2002) Quantitative structure-permeability relationships (QSPRs) for percutaneous absorption. *Toxicology in Vitro*, 16, 299-317.
- Mutschler, E., Geisslinger, G., Kroemer, H.K. & Schaefer-Korting, M. (2001) *Mutschler Arzneimittelwirkungen - Lehrbuch der Pharmakologie und Toxikologie*. Wissenschaftliche Verlagsgesellschaft mbH: Stuttgart.
- Nemes, Z. & Steinert, P.M. (1999) Bricks and mortar of the epidermal barrier. *Experimental and Molecular Medicine*, 31, 5-19.
- Netzaff, F., Lehr, C.M., Wertz, P.W. & Schaefer, U.F. (2005) The human epidermis models EpiSkin (R), SkinEthic (R) and EpiDerm (R): An evaluation of morphology and their suitability for testing phototoxicity, irritancy, corrosivity, and substance transport. *European Journal of Pharmaceutics and Biopharmaceutics*, 60, 167-178.
- Netzaff, F., Kostka, K.H., Lehr, C.M. & Schaefer, U.F. (2006) TEWL measurements as a routine method for evaluating the integrity of epidermis sheets in static Franz type diffusion cells in vitro. Limitations shown by transport data testing. *European Journal of Pharmaceutics and Biopharmaceutics*, 63, 44-50.

- Nitsche, J.M. & Frasc, H. (2011) Dynamics of diffusion with reversible binding in microscopically heterogeneous membranes: General theory and applications to dermal penetration. *Chemical Engineering Science*, 66, 2019-2041.
- Norlen, L. (2008) The Physical Structure of the skin Barrier. *In: Roberts, M.S. & Walters, K.A., Dermal Absorption and Toxicity Assessment*. Informa Healthcare: New York, 37-68.
- OECD. (1995) OECD Guideline for the testing of Chemicals. Water Solubility. Organisation for Economic Co-operation and Development.
- OECD. (2002) OECD Guideline for the testing of chemicals. Acute Dermal Irritation/Corosion - Number 404. Organisation for Economic Co-operation and Development.
- OECD. (2004a) Guidance document for the conduct of skin absorption studies - OECD Series in Testing and assessment - Number 28. Organisation for Economic Co-operation and Development.
- OECD. (2004b) OECD Guideline for the testing of chemicals. Skin absorption: in vitro method 428. Organisation for Economic Co-operation and Development.
- OECD. (2004c) OECD Guideline for the Testing of Chemicals. Skin Absorption: in vivo Method 427. Organisation for Economic Co-operation and Development.
- OECD. (2007) Guidance document on the validation of (quantitative) structure-activity relationships [(Q)SAR] models. Organisation for Economic Co-operation and Development.
- OECD. (2010a) Guidance document for the testing of chemicals. In Vitro Skin Corrosion: Human Skin Model Test. Organisation for Economic Co-operation and Development.
- OECD. (2010b) Guidance document for the testing of chemicals. In Vitro Skin Irritation: Reconstructed Human Epidermis Test Method. Organisation for Economic Co-operation and Development.
- Oesch, F., Fabian, E., Oesch-Bartlomowicz, B., Werner, C. & Landsiedel, R. (2007) Drug-metabolizing enzymes in the skin of man, rat, and pig. *Drug Metabolism Reviews*, 39, 659-698.
- Ohsako, S. & Deguchi, T. (1990) Cloning and Expression of cDNAs for Polymorphic and Monomorphic Arylamine N-Acetyltransferases from Human Liver. *Journal of Biological Chemistry*, 265, 4630-4634.
- Otberg, N., Teichmann, A., Rasuljev, U., Sinkgraven, R., Sterry, W. & Lademann, J. (2007) Follicular penetration of topically applied caffeine via a shampoo formulation. *Skin Pharmacology and Physiology*, 20, 195-198.
- Ottaviani, G., Martel, S. & Carrupt, P.A. (2006) Parallel artificial membrane permeability assay: A new membrane for the fast prediction of passive human skin permeability. *Journal of Medicinal Chemistry*, 49, 3948-3954.
- Peck, K.D., Ghanem, A.H. & Higuchi, W.I. (1994) Hindered Diffusion of Polar-Molecules Through and Effective Pore Radii Estimates of Intact and Ethanol-Treated Human Epidermal Membrane. *Pharmaceutical Research*, 11, 1306-1314.
- Peck, K.D., Ghanem, A.H., Higuchi, W.I. & Srinivasan, V. (1993) Improved Stability of the Human Epidermal Membrane During Successive Permeability Experiments. *International Journal of Pharmaceutics*, 98, 141-147.
- Pendlington, R.U., Sanders, D.J., Bourner, C.E., Saunders, D.R. & Pease, C.K. (2004) Development of a repeat dose in vitro skin penetration model. *In: Brain, K.R. & Walters, K.A., Perspectives in Percutaneous Penetration*. STS Publishing: Cardiff, 79.
- Pendlington, R.U., Sanders, D.J., Cooper, K.J., Howes, D. & Lovell, W. (1997) The use of sucrose as a standard penetrant in in vitro percutaneous penetration experiments.

- PermGear, I. (2005) URL: [http:// www.permegear.com/inline.htm](http://www.permegear.com/inline.htm) (status: 18.05.2012).
- Pion, I. (2012) Skin PAMPA Tutorial Revision 1.1.
- Potts, R.O. & Francoeur, M.L. (1990) Lipid Biophysics of Water-Loss Through the Skin. *Proceedings of the National Academy of Sciences of the United States of America*, 87, 3871-3873.
- Potts, R.O. & Francoeur, M.L. (1991) The Influence of Stratum-Corneum Morphology on Water Permeability. *Journal of Investigative Dermatology*, 96, 495-499.
- Potts, R.O. & Guy, R.H. (1992) Predicting Skin Permeability. *Pharmaceutical Research*, 9, 663-669.
- Pugh, W.J. (2001) Relationship between H-Bonding of Penetrants to Stratum Corneum Lipids and Diffusion. *Journal of Toxicology-Cutaneous and Ocular Toxicology*, 20, 303-317.
- Quan, D., Takayama, K., Mitsuzono, T., Isowa, K. & Nagai, T. (1991) Influence of Novel Percutaneous-Absorption Enhancers, Cyclohexanone and Piperidone Derivatives, on Histopathology of Rat Skin. *International Journal of Pharmaceutics*, 68, 239-253.
- Rasmussen, C., Comer, A., Pirnstill, J., Pirnstill, S., Simon, N. & Ien-Hoffmann, L. (2010a) StrataTest (R) tissue, a novel in vitro alternative for cytotoxicity testing. *Toxicology Letters*, 189, S84.
- Rasmussen, C., Gratz, K., Liebel, F., Southall, M., Garay, M., Bhattacharyya, S., Simon, N., Zanden, M.V., Van Winkle, K., Pirnstill, J., Pirnstill, S., Comer, A. & Ien-Hoffmann, B.L. (2010b) The StrataTest (R) human skin model, a consistent in vitro alternative for toxicological testing. *Toxicology in Vitro*, 24, 2021-2029.
- Rasmussen, C., Liebel, F., Southall, M., Gratz, K., Simon, N., Comer, A. & Allen-Hoffmann, B.L. (2010c) Use of the StrataTest(R) Human Skin Model in Evaluation Environmental Insult-Mediated Damage (conference poster).
- Reifenrath, W.G., Hawkins, G.S. & Kurtz, M.S. (1991) Percutaneous Penetration and Skin Retention of Topically Applied Compounds - An Invitro-Invivo Study. *Journal of Pharmaceutical Sciences*, 80, 526-532.
- Riviere, J.E. & Brooks, J.D. (2005) Predicting skin permeability from complex chemical mixtures. *Toxicology and Applied Pharmacology*, 208, 99-110.
- Riviere, J.E. & Brooks, J.D. (2007) Prediction of dermal absorption from complex chemical mixtures: incorporation of vehicle effects and interactions into a QSPR framework. *Sar and Qsar in Environmental Research*, 18, 31-44.
- Riviere, J.E. (2011a) Absorption. In: Riviere, J.E., *Comparative Pharmacokinetics*. Wiley-Blackwell, 39-71.
- Riviere, J.E. (2011b) Compartmental Models. In: Riviere, J.E., *Comparative Pharmacokinetics*. Wiley-Blackwell, 143-186.
- Riviere, J.E. (2011c) Principles of Drug Movement in the Body. In: Riviere, J.E., *Comparative Pharmacokinetics*. Wiley-Blackwell, 13-25.
- Roberts, M.S. & Cross, S.E. (2002) Skin Transport. In: Walters, K.A., *Dermatological and Transdermal Formulations*. Marcel Dekker, Inc.: New York, 89-195.
- Roberts, M.S., Cross, S.E. & Anissimov, Y.G. (2005) The Skin Reservoir for Topically Applied Solutes. In: Bronaugh, R.L. & Maibach, H., I, *Percutaneous Absorption: Drugs, Cosmetics, Mechanisms, Methodology*. Taylor & Francis: Boca raton, 213-234.
- Roberts, M.S., Gierden, A., Riviere, J.E. & Monteiro-Riviere, N.A. (2008) Solvent and Vehicle Effects on the skin. In: Roberts, M. & Walters, K.A., *Dermal Absorption and Toxicity Assessment*, 433-447.

- Roberts, M.S. & Walker, M. (1993) Water - The Most Natural Penetration Enhancer. In: Walters, K.A. & Hadgraft, J., *Pharmaceutical Skin Penetration Enhancement*. Marcel Dekker: New York, 1-30.
- Roberts, M.S. & Horlock, E. (1978) Effect of Repeated Skin Application on Percutaneous Absorption of Salicylic-Acid. *Journal of Pharmaceutical Sciences*, 67, 1685-1687.
- Rolsted, K., Kissmeyer, A.M., Rist, G.M. & Hansen, S.H. (2008) Evaluation of cytochrome P450 activity in vitro, using dermal and hepatic microsomes from four species and two keratinocyte cell lines in culture. *Archives of Dermatological Research*, 300, 11-18.
- Römpf. (2010) Römpf Online. URL: <http://www.roempp.com> (Status: 30.04.2012), 3.5.
- Roskos, K.V., Maibach, H.I. & Guy, R.H. (1989) The Effect of Aging on Percutaneous-Absorption in Man. *Journal of Pharmacokinetics and Biopharmaceutics*, 17, 617-630.
- Ross, J.H., Fong, H.R., Thongsinthusak, T. & Krieger, R.I. (1992) Experimental method to estimate indoor pesticide exposure to children. In: Guzelian, P.S., Henry, C.J. & Olin, S.S., *Similarities and Differences between Children and Adults: Implications for Risk Assessment*. ILSI Press: Washington, DC, 226-241.
- Rougier, A., Lotte, C., Corcuff, P. & Maibach, H.I. (1988a) Relationship Between Skin Permeability and Corneocyte Size According to Anatomic Site, Age, and Sex in Man. *Journal of the Society of Cosmetic Chemists*, 39, 15-26.
- Rougier, A., Lotte, C. & Maibach, H.I. (1988b) In vivo Relationship Between Trans-Epidermal Water-Loss and Percutaneous-Absorption in Man. *Clinical Research*, 36, A690.
- Rücker, G., Neugebauer, M. & Willems, G.G. (2008) *Instrumentelle pharmazeutische Analytik - Lehrbuch zu spektroskopischen, chromatographischen, elektrochemischen und thermischen Analysemethoden*. Wissenschaftliche Verlagsgesellschaft mbH Stuttgart.
- Ryan, C.A., Gerberick, G.F. & Kern, P.S. (2010) Skin Sensitization. In: Monteiro-Riviere, N.A., *Toxicology of the Skin*. Informa Healthcare: New York, 192-202.
- Safferling, K. (2008) Dermal Permeation in vitro: Einfluss von unterschiedlichen Parametern an Ratten- und Schweinehautmodellen (diploma Thesis).
- Samaras, E.G., Riviere, J.E. & Ghafourian, T. (2012) The effect of formulations and experimental conditions on in vitro human skin permeation-Data from updated EDETOX database. *International Journal of Pharmaceutics*, 434, 280-291.
- Schaefer, H. & Redelmeier, T.E. (1996a) Factors Effecting Percutaneous Absorption. In: Schaefer, H. & Redelmeier, T.E., *Skin Barrier, Principles of Percutaneous Absorption*, 153-212.
- Schaefer, H. & Redelmeier, T.E. (1996b) Prediction and Measurement of Percutaneous Absorption. In: Schaefer, H. & Redelmeier, T.E., *Skin Barrier, Principles of Percutaneous Absorption*, 118-152.
- Schaefer, H. & Redelmeier, T.E. (1996c) *Skin Barrier, Principles of Percutaneous Absorption*.
- Schaefer-Korting, M., Bock, U., Diembeck, W., Duesing, H.J., Gamer, A., Haltner-Ukomadu, E., Hoffmann, C., Kaca, M., Kamp, H., Kersen, S., Kietzmann, M., Korting, H.C., Krachter, H.U., Lehr, C.M., Liebsch, M., Mehling, A., Mueller-Goymann, C., Netzlaff, F., Niedorf, F., Rubbelke, M.K., Schaefer, U., Schmidt, E., Schreiber, S., Spielmann, H., Vuia, A. & Weimer, M. (2008a) The use of reconstructed human epidermis for skin absorption testing: results of the validation study. *Atla-Alternatives to Laboratory Animals*, 36, 161-187.
- Schaefer-Korting, M., Bock, U., Gamer, A., Haberland, A., Haltner-Ukomadu, E., Kaca, M., Kamp, H., Kietzmann, M., Korting, H.C., Krachter, H.U., Lehr, C.M., Liebsch, M., Mehling, A., Netzlaff, F., Niedorf, F., Rubbelke, M.K., Schaefer, U., Schmidt, E., Schreiber, S., Schroder, K.R.,

- Spielmann, H. & Vuia, A. (2006) Reconstructed human epidermis for skin absorption testing: Results of the German prevalidation study. *Atla-Alternatives to Laboratory Animals*, 34, 283-294.
- Schaefer-Korting, M., Mahmoud, A., Borgia, S., Brueggener, B., Kleuser, B., Schreiber, S. & Mehnert, W. (2008b) Reconstructed epidermis and full-thickness skin for absorption testing: Influence of the vehicles used on steroid permeation. *Atla-Alternatives to Laboratory Animals*, 36, 441-452.
- Schaefer-Korting, M. & Schreiber, S. (2008) Use of Skin Equivalents for Dermal Absorption and Toxicity. In: Roberts, M.S. & Walters, K.A., *Dermal Absorption and Toxicity Assessment*. Informa Healthcare: New York, 141-159.
- Scheuplein, R.J. (1972) Properties of the skin as a membrane. *Advances in biology of skin*, 12, 125-152.
- Scheuplein, R.J., Blank, I.H., Brauner, G.J. & Macfarla, D.J. (1969) Percutaneous Absorption of Steroids. *Journal of Investigative Dermatology*, 52, 63-70.
- Schmook, F.P., Meingassner, J.G. & Billich, A. (2001) Comparison of human skin or epidermis models with human and animal skin in in-vitro percutaneous absorption. *International Journal of Pharmaceutics*, 215, 51-56.
- Schmuth, M., Yosipovitch, G., Williams, M.L., Weber, F., Hintner, H., Ortiz-Urda, S., Rappersberger, K., Crumrine, D., Feingold, K.R. & Elias, P.M. (2001) Pathogenesis of the permeability barrier abnormality in epidermolytic hyperkeratosis. *Journal of Investigative Dermatology*, 117, 837-847.
- Schreiber, S., Mahmoud, A., Vuia, A., Rubbelke, M.K., Schmidt, E., Schaller, A., Kandarova, H., Haberland, A., Schaefer, U.F., Bock, U., Korting, H.C., Liebsch, A. & Schaefer-Korting, A. (2005) Reconstructed epidermis versus human and animal skin in skin absorption studies. *Toxicology in Vitro*, 19, 813-822.
- Schrödel, A. (2012) Übersichtsfärbung mit Hämatoxylin und Eosin (H&E). *Biologie in unserer Zeit*, 42, 153.
- Schurer, N.Y. & Elias, P.M. (1991) The Biochemistry and Function of Stratum-Corneum Lipids. *Advances in Lipid Research*, 24, 27-56.
- Schurr, M.J., Foster, K.N., Centanni, J.M., Comer, A.R., Wicks, A., Gibson, A.L., Thomas-Virrig, C.L., Schlosser, S.J., Faucher, L.D., Lokuta, M.A. & Ien-Hoffmann, B.L. (2009) Phase I/II Clinical Evaluation of StrataGraft: A Consistent, Pathogen-Free Human Skin Substitute. *Journal of Trauma-Injury Infection and Critical Care*, 66, 866-873.
- Scientific Committee on Consumer Products (SCCP). (2006) Opinion on Basic Criteria for the in vitro Assessment of dermal Absorption of cosmetic ingredients.
- Scientific Committee on Consumer Safety (SCCS). (2010) Basic criteria for the in vitro assessment of dermal absorption of cosmetic ingredients.
- Scott, R.C., Walker, M. & Dugard, P.H. (1986) A Comparison of the Invitro Permeability Properties of Human and Some Laboratory-Animal Skins. *International Journal of Cosmetic Science*, 8, 189-194.
- Shah, D.K., Khandavilli, S. & Panchagnula, R. (2008) Alteration of Skin Hydration and its Barrier Function by Vehicle and Permeation Enhancers: A Study using TGA, FTIR, TEWL and Drug Permeation as Markers. *Methods and Findings in Experimental and Clinical Pharmacology*, 30, 499-512.
- Shah, P.V., Fisher, H.L., Sumler, M.R. & Hall, L.L. (1988) Dermal absorption and pharmacokinetics of pesticides in rats. In: Wang, R., Franklin, C.A., Honeycutt, R.C. et al., *Biological Monitoring for Pesticides Exposures*. American Chemical Society: Washington, DC, 169-187.

- Siddiqui, O., Roberts, M.S. & Polack, A.E. (1989) Percutaneous-Absorption of Steroids - Relative Contributions of Epidermal Penetration and Dermal Clearance. *Journal of Pharmacokinetics and Biopharmaceutics*, 17, 405-424.
- Sigma-Aldrich. (2006) Sicherheitsdatenblatt Dimethylamin-Lösung.
- Sigma-Aldrich. (2007) Sicherheitsdatenblatt D-Mannitol.
- Sinkó, B., Garrigues, T., Avdeef, A. & Takács-Novák, K. (2011) Skin-PAMPA A new method for fast prediction of skin penetration.
- Sinko, B., Garrigues, T.M., Balogh, G.T., Nagy, Z.K., Tsinman, O., Avdeef, A. & Takacs-Novak, K. (2012) Skin-PAMPA: A new method for fast prediction of skin penetration. *European Journal of Pharmaceutical Sciences*, 45, 698-707.
- Southwell, D. & Barry, B.W. (1983) Penetration Enhancers for Human-Skin - Mode of Action of 2-Pyrrolidone and Dimethylformamide on Partition and Diffusion of Model Compounds Water, Normal-Alcohols, and Caffeine. *Journal of Investigative Dermatology*, 80, 507-514.
- Southwell, D., Barry, B.W. & Woodford, R. (1984) Variations in Permeability of Human-Skin Within and Between Specimens. *International Journal of Pharmaceutics*, 18, 299-309.
- Standing Committee on Biocidal Products. (2008) Assessment Report Cyclohexylhydroxydiazene 1-oxide, potassium salt (K-HDO) Product-type 8 (Wood preservatives).
- Standing Committee on Biocidal Products. (2009) Assessment report Fenpropimorph (PT 8).
- Stratatech Corporation. (2010) StrataTest(R) ST6 Test Tissue. Instructions for Storage and Use.
- Stratatech Corporation. (2012) Press Release: Stratatech Reports Positive Interim Clinical Results for StrataGraft® Skin Substitute. URL: www.stratatechcorp.com (Status 01.06.2012).
- The Commission of the European Communities. (2008) Council regulation (EC) No 440/2008 of 30 May 2008 laying down test methods pursuant to Regulation (EC) No 1907/2006 of the European Parliament and of the Council on the Registration, Evaluation, Authorisation and Restriction of Chemicals (REACH). *Official Journal of the European Union*, L 142, 1.
- The Council of the European Communities. (1976) Council Directive of 27 July 1976 on the approximation of the laws of the Member States relating to cosmetic products (76/768/EEC). *Official Journal of the European Communities*, L 262, 169-200.
- The European Parliament & The Council of the European Union. (2009) Regulation (EC) No 1107/2009. *Official Journal of the European Union*, L309.
- The European Parliament and the Council of the European Union. (2006) Regulation (EC) No 1907/2006 of the European Parliament and of the Council of 18 December 2006 concerning the Registration, Evaluation, Authorisation and Restriction of Chemicals (REACH), establishing a European Chemicals Agency, amending Directive 1999/45/EC and repealing Council Regulation (EEC) No 793/93 and Commission Regulation (EC) No 1488/94 as well as Council Directive 76/769/EEC and Commission Directives 91/155/EEC, 93/67/EEC, 93/105/EC and 2000/21/EC. *Official Journal of the European Union*, L396, 1-849.
- Todeschini, R. & Consonni, V. (2009) *Molecular Descriptors for Chemoinformatics*. Wiley-VCH: Weinheim.
- Toner, F., Garcia, B., Roper, C.S. & Madden, S. (2009) Effect of Repeat Application of [14C]-Caffeine on Percutaneous Absorption Through Human Skin in vitro (conference poster).
- Tsinman, O., Tsinman, K., Sun, N. & Avdeef, A. (2011) Physicochemical Selectivity of the BBB Microenvironment Governing Passive Diffusion-Matching with a Porcine Brain Lipid Extract Artificial Membrane Permeability Model. *Pharmaceutical Research*, 28, 337-363.

- U.S.Department of Health and Human Services.Public Health Service Agency for Toxic Substances and Disease Registry. Toxicological Profile for Polychlorinated Biphenyls.
- United states Environmental Protection agency (EPA). (1996) Health Effects Test Guidelines - OPPTS 870.7600 Dermal Penetration.
- United States Environmental Protection Agency (US-EPA). (2004) Reregistration Eligibility Decision (RED) for MCPA (2-methyl-4-chlorophenoxyacetic acid) List A Case 0017.
- United States Environmental Protection Agency (US-EPA). (2006) Pesticide Fact Sheet - Fenpropimorph.
- United States Environmental Protection Agency (US-EPA). (2011) Pesticide Fact Sheet - Bis-(N-cyclohexyldiazoniumdioxo)-copper.
- Vallet, V., Cruz, C., Josse, D., Bazire, A., Lallement, G. & Boudry, I. (2007) In vitro percutaneous penetration of organophosphorus compounds using full-thickness and split-thickness pig and human skin. *Toxicology in Vitro*, 21, 1182-1190.
- van de Sandt, J.J.M., van Burgsteden, J.A., Cage, S., Carmichael, P.L., Dick, I., Kenyon, S., Korinth, G., Larese, F., Limasset, J.C., Maas, W.J.M., Montomoli, L., Nielsen, J.B., Payan, J.P., Robinson, E., Sartorelli, P., Schaller, K.H., Wilkinson, S.C. & Williams, F.M. (2004) In vitro predictions of skin absorption of caffeine, testosterone, and benzoic acid: a multi-centre comparison study. *Regulatory Toxicology and Pharmacology*, 39, 271-281.
- van Ravenzwaay, B. & Leibold, E. (2004) A comparison between in vitro rat and human and in vivo rat skin absorption studies. *Human & Experimental Toxicology*, 23, 421-430.
- van Ravenzwaay, B., Pigott, G. & Leibold, E. (2004) Absorption, distribution, metabolism and excretion of 4-chloro-2-methylphenoxyacetic acid (MCPA) in rats. *Food and Chemical Toxicology*, 42, 115-125.
- Vecchia, B.E. & Bunge, A.L. (2002) Skin absorption databases and predictive equations. In: Guy, R.H.H.J., *Transdermal Drug Delivery*. Marcel Dekker, 57-141.
- Vecchia, B.E. & Bunge, A.L. (2006) Animal Models: A Comparison of Permeability Coefficients for Excised Skin from Humans and Animals. In: Riviere, J.E., *Dermal Absorption Models in Toxicology and Pharmacology*. CRC Press: Boca Raton, 305-333.
- Vickers, C.F. (1972) Stratum corneum reservoir for drugs. *Advances in biology of skin*, 12, 177-189.
- Vickers, C.F.H. (1963) Existence of Reservoir in Stratum Corneum - Experimental Proof. *Archives of Dermatology*, 88, 20-&.
- Wacker. (2009) Safety Data Sheet Silfoam(R) SRE.
- Walters, K.A., Brain, K.R., Howes, D., James, V.J., Kraus, A.L., Teetsel, N.M., Toulon, M., Watkinson, A.C. & Gettings, S.D. (1997) Percutaneous penetration of octyl salicylate from representative sunscreen formulations through human skin in vitro. *Food and Chemical Toxicology*, 35, 1219-1225.
- Walters, K.A. & Roberts, M.S. (2002) Structure and Function of skin. In: Walters, K.A., *Dermatological and Transdermal Formulations*. Marcel Dekker: New York, 1-39.
- Warner, R.R., Stone, K.J. & Boissy, Y.L. (2003) Hydration disrupts human stratum corneum ultrastructure. *Journal of Investigative Dermatology*, 120, 275-284.
- Waxman, D.J., Lapenson, D.P., Aoyama, T., Gelboin, H.V., Gonzalez, F.J. & Korzekwa, K. (1991) Steroid-Hormone Hydroxylase Specificities of 11 Cdna-Expressed Human Cytochrome-P450S. *Archives of Biochemistry and Biophysics*, 290, 160-166.

- Weiner, J.S. & Hellmann, K. (1960) The Sweat Glands. *Biological Reviews of the Cambridge Philosophical Society*, 35, 141-186.
- Wertz, P.W. (2000) Lipids and barrier function of the skin. *Acta Dermato-Venereologica*, 7-11.
- Wester, R.C., Melendres, J., Sedik, L. & Maibach, H.I. (1994) Percutaneous-Absorption of Azone Following Single and Multiple Doses to Human Volunteers. *Journal of Pharmaceutical Sciences*, 83, 124-125.
- Whitton, J.T. & Everall, J.D. (1973) Thickness of Epidermis. *British Journal of Dermatology*, 89, 467-476.
- Wiechers, J.W. (1989) The Barrier Function of the Skin in Relation to Percutaneous-Absorption of Drugs. *Pharmaceutisch Weekblad-Scientific Edition*, 11, 185-198.
- Wilkinson, S.C., Maas, W.J.M., Nielsen, J.B., Greaves, L.C., van de Sandt, J.J.M. & Williams, F.M. (2006) Interactions of skin thickness and physicochemical properties of test compounds in percutaneous penetration studies. *International Archives of Occupational and Environmental Health*, 79, 405-413.
- Wilkinson, S.C. & Williams, F.M. (2008) Cutaneous Metabolism. In: Roberts, M.S. & Walters, K.A., *Dermal Absorption and Toxicity Assessment*. Informa Healthcare: New York, 89-101.
- Wilschut, A., Tenberge, W.F., Robinson, P.J. & Mckone, T.E. (1995) Estimating Skin Permeation - the Validation of 5 Mathematical Skin Permeation Models. *Chemosphere*, 30, 1275-1296.
- Wishart, G.J. (1978) Demonstration of Functional Heterogeneity of Hepatic Uridine-Diphosphate Glucuronosyltransferase Activities After Administration of 3-Methylcholanthrene and Phenobarbital to Rats. *Biochemical Journal*, 174, 671-672.
- Wold, S., Ruhe, A., Wold, H. & Dunn, W.J. (1984) The Collinearity Problem in Linear-Regression - the Partial Least-Squares (PLS) Approach to Generalized Inverses. *Siam Journal on Scientific and Statistical Computing*, 5, 735-743.
- Wolfe, H.R. (1976) Field exposure to airborne pesticides. In: Lee, R.E., *Air Pollution from Pesticides and Agricultural processes*. CRC Press: Ohio, 137-161.
- Worth, A.P. & Cronin, M.T.D. (2003) The use of discriminant analysis, logistic regression and classification tree analysis in the development of classification models for human health effects. *Journal of Molecular Structure-Theochem*, 622, 97-111.
- Xia, X.R. & Riviere, J.E. (2011) Quantitative Structure-Permeability Relationships. *Comparative Pharmacokinetics*. Wiley-Blackwell, 27-38.
- Yalkowsky, S.H., Valvani, S.C. & Roseman, T.J. (1983) Solubility and Partitioning .6. Octanol Solubility and Octanol-Water Partition-Coefficients. *Journal of Pharmaceutical Sciences*, 72, 866-870.
- Yamazaki, H., Inoue, K., Turvy, C.G., Guengerich, F.P. & Shimada, T. (1997) Effects of freezing, thawing, and storage of human liver samples on the microsomal contents and activities of cytochrome p450 enzymes. *Drug Metabolism and Disposition*, 25, 168-174.
- Yeung, C.K. & Rettie, A.E. (2006) Benzydamine N-oxygenation as a measure of flavin-containing monooxygenase activity. *Methods in molecular biology (Clifton, N.J.)*, 320, 157-162.

10 Publications

Peer-reviewed publication

C. Jaeckh, V. Blatz, E. Fabian, K. Guth, B. van Ravenzwaay, K. Reisinger, R. Landsiedel: Characterization of enzyme activities of Cytochrome P450 enzymes, flavin-dependent monooxygenases, N-acetyltransferases and UDP-glucuronosyltransferases in human reconstructed epidermis and full-thickness skin models. *Toxicology in Vitro*, Vol: 25, Issue: 6, pp. 1209-1214, 2001.

Oral presentation

K. Guth, M. Schaefer-Korting, E. Fabian, B. van Ravenzwaay, R. Landsiedel: Suitability of different skin integrity tests for dermal penetration studies in vitro. 9th International Conference and Workshop on Biological Barriers – in vitro and in silico Tools for Drug Delivery and Nanosafety Research, Saarbrücken, Germany, 2012.

Poster presentations (selected)

K. Guth, M. Schaefer-Korting, E. Fabian, B. van Ravenzwaay, R. Landsiedel: Parameters influencing Dermal Penetration. 51. Jahrestagung der DGPT, Mainz, 2010.

C. Jaeckh, K. Guth, A. Noss, V. Blatz, K. Reisinger, E. Fabian, B. van Ravenzwaay, R. Landsiedel: Characterization of human reconstructed skin models for activities of xenobiotic metabolizing enzymes. *Skin in vitro*, Frankfurt, Germany, 2010.

K. Guth, M. Schaefer-Korting, E. Fabian, B. van Ravenzwaay, R. Landsiedel: Comparative Dermal Penetration Studies in Human Full-thickness and Dermatomed skin. *Skin Forum 12th Annual Meeting. Penetrating the Stratum Corneum – Measurement, Modulation and Modelling*, Frankfurt, Germany, 2011.

K. Guth, M. Schaefer-Korting, E. Fabian, B. van Ravenzwaay, R. Landsiedel: Comparative investigation of different skin integrity tests for dermal penetration studies in vitro. 78. Jahrestagung der Deutschen Gesellschaft für Experimentelle und Klinische Pharmakologie und Toxikologie e. V. (DGPT), Dresden, Germany, 2012.

E. Fabian, C. Goth, K. Guth, A. Mehling, B. van Ravenzwaay, R. Landsiedel: A Screening Method to estimate dermal absorption in vitro. *SOT Annual Meeting & ToxExpoTM*, San Francisco, Ca, USA, 2012.

K. Guth, J. Riviere, J. Brooks, M. Schaefer-Korting, M. Dammann, E. Fabian, B. van Ravenzwaay, R. Landsiedel: In silico models for dermal absorption from complex formulations. 79. Jahrestagung der DGPT, Halle/Saale, 2013.

Publications in preparation

K. Guth, M. Schaefer-Korting, E. Fabian, B. van Ravenzwaay, R. Landsiedel: Suitability of different skin integrity tests for dermal absorption studies in vitro.

K. Guth, J. Brooks, J. E. Riviere, M. Schaefer-Korting, E. Fabian, B. van Ravenzwaay, R. Landsiedel: In silico models to predict dermal absorption from complex pesticide formulations.

K. Guth, C. Rasmussen, L. Allen-Hoffman, M. Schaefer-Korting, E. Fabian, B. van Ravenzwaay, R. Landsiedel: Metabolic characterization of the reconstructed human skin model StrataTest®.

11 Curriculum vitae

For reasons of data protection, the curriculum vitae is not included in the online version.

For reasons of data protection, the curriculum vitae is not included in the online version.

12 Annex

12.1 Abbreviations

1/X	inverse value of parameter X
$\Sigma\alpha_2^H$	overall hydrogen bond acidity
ACN	acetonitrile
AdmeX	property X determined with ABLab feature of ADME Boxes version 4.95
AD	(potentially) absorbable dose = content in skin and receptor fluid
ADH	alcohol dehydrogenase
AI	actual substrate incubation
AIDH	aldehyde dehydrogenase
ApD	applicability domain
$\Sigma\beta_2^H$	overall hydrogen bond basicity
BC	buffer control
BLUE	transepidermal methylene blue absorption
Bq	Becquerel (1 Bq = 60 dpm or disintegrations per minute)
BR(OD)	benzyloxyresorufin(-O-debenzylase)
^{14}C	labeling with isotope ^{14}C
COX	cyclooxygenase
CV	coefficient of variation
CYP	cytochrome P450 isoenzyme
DMS	dermatomed skin
ER(OD)	ethoxyresorufin(-O-deethylase)
FMO	flavin-dependent monooxygenase
FLD	fluorescence detector
FTS	full-thickness skin
GC-MS	gas chromatography with mass spectrometry
GST	glutathione S-transferase
^3H	labeling with isotope ^3H (tritium)
H-bond	hydrogen bond
HBAcc	number of hydrogen bond acceptors
HBDon	number of hydrogen bond donors
HDC	heat-deactivated control
HPLC	high-performance liquid chromatography

H&E	hematoxylin and eosin
ISTD	(transepidermal absorption of an) internal standard
(max)Kp	(maximum) permeability coefficient
LOD	limit of detection
LogX	logarithm of parameter X
LOO	leave-one-out (internal cross-validation procedure)
LMO	leave-many-out (internal cross-validation procedure)
LOQ	limit of quantification
LSC	liquid scintillation counter
MCPA	2-methyl-4-chlorophenoxyacetic acid
MCPA-EHE	2-methyl-4-chlorophenoxyacetyl 2-ethylhexylester
molinspX	parameter X determined with software Molinspiration Property Calculator
MW	molecular weight
NAT	N-acetyltransferase
NAD(P)H	nicotinamide adenine dinucleotide (phosphate)
π_2^H	solute dipolarity/polarizability
PAMPA	Parallel Artificial Membrane Permeability Assay
PC(A)	principle component (analysis)
pKa	acid dissociation constant
P_{ow}	partition coefficient between octanol and water
PR(OD)	pentoxyresorufin(-O-depentylyase)
OECD	Organization for Economic Co-operation and Development
Q ² Ext	external explained variance
Q ² LOO	cross-validated explained variance obtained with leave-one-out procedure
Q ² 25%	cross-validated explained variance obtained with leave-many – (25%) – out procedure
r	Pearson's correlation coefficient
R ²	coefficient of determination
RAD	radio detector
Rf ₂	solute excess molar refractivity
RotB	number of rotatable bonds
S9	S9 fraction (subcellular fraction)
SD	standard deviation
Spl	binary variable 'species indicator' with value 1 for human and 2 for rat experiments

SULT	sulfotransferase
$S_{R/w}$	solubility in receptor fluid / in water
t_0	immediately stopped substrate incubation
TEER	transepidermal electrical resistance to an alternating current (impedance)
TEWL	transepidermal water loss
TJ	tight junction
TWF	transepidermal water flux
TPSA	topological polar surface area
UDP	uridine diphosphate
UGT	UDP-glucuronosyltransferase
UV	ultraviolet (detector)
V_x	McGowan characteristic volume

12.2 Tables

Table 44: Properties of skin samples used for absorption experiments. Given are donor-specific properties and results of integrity tests (TEER, transepidermal electrical resistance; TWF, transepidermal water flux; TEWL, transepidermal water loss; BLUE, transepidermal methylene blue absorption; ISTD, transepidermal absorption of an internal standard) as well as pretreatments with solutions (water, blank (parallel MCPA-DMA-formulation without MCPA), cold (formulation with unlabeled MCPA) or TWF (tritium-labeled water)) or washing procedures (w), whereby the numbers give the number of treatments and washings; 72 h stands for untreated skin samples over 72 h in experimental setup, culture for culture conditions (37°C, 5 % CO₂ and 95 % humidity) in combination with the time period; DMS, dermatomed skin; FTS, full-thickness skin; exp. Date, experimental date; f, female; m, male; a, abdomen; b, back; w, weeks, y, years; n.a. not analyzed, n.d. not determinable. Sample no. corresponds to sample no. in Table 45 and Table 46.

test compound	species	skin type	exp. date	sample no.	thickness [µm]	sex	localization	age	pretreatment	TWF (Kp) [$\times 10^{-5}$ cm/h]	TEER [kOhm]	TEWL [g/(cm ² ·h)]	BLUE - absorption [µg/l]	BLUE - skin coloration	ISTD - AD [%]	ISTD - maxKp [$\times 10^{-5}$ cm/h]	
caffeine	human	DMS	14.-15.10.2009	1	410	f	a	59 y	-	n.a.	8.8	1.6	n.a.	n.a.	n.a.	n.a.	
				2	350	f	a	59 y	-	n.a.	6.2	4.5	n.a.	n.a.	n.a.	n.a.	
				3	360	f	a	59 y	-	n.a.	7.4	3.0	n.a.	n.a.	n.a.	n.a.	
				4	420	f	a	53 y	-	n.a.	4.2	1.8	n.a.	n.a.	n.a.	n.a.	
				5	400	f	a	53 y	-	n.a.	4.2	3.5	n.a.	n.a.	n.a.	n.a.	
			20.-22.01.2010	6	540	f	a	37 y	TWF		306	4.3	8	66	-	13	4
				7	550	f	a	37 y	TWF		168	5.0	3	72	-	15	14
				8	540	f	a	37 y	TWF		161	10.0	8	105	-	8	8
				9	550	f	a	66 y	TWF		229	7.2	9	2056	yes	20	24
				10	580	f	a	66 y	TWF		185	9.9	3	3728	yes	11	16
		24.-25.1.2012	11	380	f	a	51 y	-	n.a.	3.9	4	n.a.	n.a.	n.a.	n.a.	n.a.	
			12	360	f	a	51 y	-	n.a.	4.0	10	n.a.	n.a.	n.a.	n.a.	n.a.	
			13	390	f	a	59 y	-	n.a.	3.9	3	n.a.	n.a.	n.a.	n.a.	n.a.	
			14	400	f	a	59 y	-	n.a.	4.8	2	n.a.	n.a.	n.a.	n.a.	n.a.	
			15	350	f	a	59 y	-	n.a.	3.3	2	n.a.	n.a.	n.a.	n.a.	n.a.	
			16	360	f	a	51 y	-	n.a.	3.6	9	n.a.	n.a.	n.a.	40	104	
			17	360	f	a	51 y	-	n.a.	2.6	8	n.a.	n.a.	n.a.	46	99	
			18	400	f	a	59 y	-	n.a.	3.9	0	n.a.	n.a.	n.a.	36	75	
			19	340	f	a	59 y	-	n.a.	4.0	8	n.a.	n.a.	n.a.	22	48	
			20	390	f	a	59 y	-	n.a.	3.8	2	n.a.	n.a.	n.a.	34	61	
	FTS	20.-22.01.2010	21	1140	f	a	37 y	TWF		244	4.8	9	128	-	42	7	
			22	1160	f	a	37 y	TWF		87	9.6	8	150	-	42	7	
			23	1060	f	a	37 y	TWF		118	10.0	0	133	slight	7	3	
			24	1000	f	a	66 y	TWF		271	5.4	8	267	yes	30	56	
			25	1060	f	a	66 y	TWF		194	1.2	11	239	slight	29	30	
	rat	DMS	22.-23.07.2009	26	305	f	b	8 w	-	n.a.	n.a.	0	n.a.	n.a.	n.a.	n.a.	n.a.
				27	360	f	b	8 w	-	n.a.	n.a.	1.9	n.a.	n.a.	n.a.	n.a.	n.a.
				28	300	f	b	8 w	-	n.a.	n.a.	0	n.a.	n.a.	n.a.	n.a.	n.a.
				29	270	f	b	8 w	-	n.a.	n.a.	3.1	n.a.	n.a.	n.a.	n.a.	n.a.
				30	300	f	b	8 w	-	n.a.	n.a.	0	n.a.	n.a.	n.a.	n.a.	n.a.

Annex

test compound		species	skin type	exp. date	sample no.	thickness [μm]	sex	localization	age	pretreatment	TWF (Kp) [$\cdot 10^{-5}$ cm/h]	TEER [kOhm]	TEWL [g/(cm 2 ·h)]	BLUE - absorption [$\mu\text{g/l}$]	BLUE - skin coloration	ISTD - AD [%]	ISTD - maxKp [$\cdot 10^{-5}$ cm/h]		
caffeine		rat	DMS	22.-23.07.2009	31	280	f	b	8 w	-	n.a.	n.a.	0.5	n.a.	n.a.	n.a.	n.a.		
					32	302	f	b	8 w	-	n.a.	n.a.	1	n.a.	n.a.	n.a.	n.a.	n.a.	
					33	280	f	b	8 w	-	n.a.	n.a.	7.6	n.a.	n.a.	n.a.	n.a.	n.a.	
					34	280	f	b	8 w	-	n.a.	n.a.	8.2	n.a.	n.a.	n.a.	n.a.	n.a.	
					35	280	f	b	8 w	-	n.a.	n.a.	1.8	n.a.	n.a.	n.a.	n.a.	n.a.	
				14.-15.10.2009	36	340	f	b	8 w	-	n.a.	2.5	10.9	n.a.	n.a.	n.a.	n.a.	n.a.	n.a.
					37	350	f	b	8 w	-	n.a.	7.3	9.8	n.a.	n.a.	n.a.	n.a.	n.a.	n.a.
					38	325	f	b	8 w	-	n.a.	5.9	3.1	n.a.	n.a.	n.a.	n.a.	n.a.	n.a.
					39	440	f	b	8 w	-	n.a.	7.0	9.8	n.a.	n.a.	n.a.	n.a.	n.a.	n.a.
					40	435	f	b	8 w	-	n.a.	7.2	0.8	n.a.	n.a.	n.a.	n.a.	n.a.	n.a.
		StrataTest®	FTS	23.-24.8.2011	FTS + membrane	41	115	?	-	-	1d culture	n.a.	1.4	20	n.a.	n.a.	n.a.	n.a.	n.a.
						42	n.d.	?	-	-	1d culture	n.a.	1.5	22	n.a.	n.a.	n.a.	n.a.	n.a.
						43	n.d.	?	-	-	1d culture	n.a.	1.1	22	n.a.	n.a.	n.a.	n.a.	n.a.
						44	n.d.	?	-	-	1d culture	n.a.	2.1	25	n.a.	n.a.	n.a.	n.a.	n.a.
						45	n.d.	?	-	-	1d culture	n.a.	1.2	26	n.a.	n.a.	n.a.	n.a.	n.a.
			FTS + membrane		46	n.d.	?	-	-	1d culture	n.a.	1.2	27	n.a.	n.a.	n.a.	n.a.	n.a.	n.a.
					47	n.d.	?	-	-	1d culture	n.a.	1.9	27	n.a.	n.a.	n.a.	n.a.	n.a.	n.a.
					48	n.d.	?	-	-	1d culture	n.a.	1.3	23	n.a.	n.a.	n.a.	n.a.	n.a.	n.a.
					49	n.d.	?	-	-	1d culture	n.a.	1.4	22	n.a.	n.a.	n.a.	n.a.	n.a.	n.a.
					50	n.d.	?	-	-	1d culture	n.a.	1.5	22	n.a.	n.a.	n.a.	n.a.	n.a.	n.a.
testosterone		human	DMS	24. - 26.11.2009	51	490	f	a	56 y	TWF	142	8.0	2	5	-	12	10		
					52	500	f	a	56 y	TWF	125	8.7	3	10	yes	22	59		
					53	490	f	a	56 y	TWF	916	8.2	11	13	-	21	29		
					54	490	f	a	56 y	TWF	373	2.7	10	5	-	5	11		
					55	495	f	a	56 y	TWF	146	10.6	7	6	-	14	25		
				30.-31.1.2012	56	370	f	a	65	-	n.a.	2.3	10	n.a.	n.a.	n.a.	n.a.	n.a.	
					57	390	f	a	65	-	n.a.	2.4	3	n.a.	n.a.	n.a.	n.a.	n.a.	
					58	380	f	a	65	-	n.a.	2.0	10	n.a.	n.a.	n.a.	n.a.	n.a.	
					59	380	f	a	58	-	n.a.	2.3	9	n.a.	n.a.	n.a.	n.a.	n.a.	
					60	370	f	a	58	-	n.a.	2.0	10	n.a.	n.a.	n.a.	n.a.	n.a.	
		24. - 26.11.2009	61	360	f	a	65	-	n.a.	2.9	2	n.a.	n.a.	62	125				
			62	380	f	a	65	-	n.a.	2.7	9	n.a.	n.a.	75	190				
			63	380	f	a	65	-	n.a.	2.8	8	n.a.	n.a.	70	175				
			64	360	f	a	58	-	n.a.	2.3	9	n.a.	n.a.	86	295				
			65	350	f	a	58	-	n.a.	2.5	9	n.a.	n.a.	83	260				
		FTS	66	935	f	a	56 y	TWF	190	5.7	4	95	-	20	11				
			67	990	f	a	56 y	TWF	78	20.0	2	86	-	10	6				
			68	825	f	a	56 y	TWF	153	8.4	8	53	-	17	15				
			69	935	f	a	56 y	TWF	158	8.8	2	95	-	13	10				
			70	990	f	a	56 y	TWF	115	12.1	2	86	-	13	9				

Annex

test compound	species	skin type	exp. date	sample no.	thickness [μm]	sex	localization	age	pretreatment	TWF (Kp) [$\times 10^{-5}$ cm/h]	TEER [kOhm]	TEWL [g/(cm ² ·h)]	BLUE - absorption [$\mu\text{g/l}$]	BLUE - skin coloration	ISTD - AD [%]	ISTD - maxKp [$\times 10^{-5}$ cm/h]	
testosterone	rat	DMS	29.-30.07.2009	71	330	f	b	8 w	-	n.a.	n.a.	1.4	n.a.	n.a.	n.a.	n.a.	
				72	330	f	b	8 w	-	n.a.	n.a.	0.1	n.a.	n.a.	n.a.	n.a.	n.a.
				73	350	f	b	8 w	-	n.a.	n.a.	0	n.a.	n.a.	n.a.	n.a.	n.a.
				74	350	f	b	8 w	-	n.a.	n.a.	2.6	n.a.	n.a.	n.a.	n.a.	n.a.
				75	350	f	b	8 w	-	n.a.	n.a.	0	n.a.	n.a.	n.a.	n.a.	n.a.
				76	350	f	b	8 w	-	n.a.	n.a.	7.5	n.a.	n.a.	n.a.	n.a.	n.a.
				77	330	f	b	8 w	-	n.a.	n.a.	1.2	n.a.	n.a.	n.a.	n.a.	n.a.
				78	330	f	b	8 w	-	n.a.	n.a.	3	n.a.	n.a.	n.a.	n.a.	n.a.
				79	330	f	b	8 w	-	n.a.	n.a.	1	n.a.	n.a.	n.a.	n.a.	n.a.
				80	330	f	b	8 w	-	n.a.	n.a.	0	n.a.	n.a.	n.a.	n.a.	n.a.
	StrataTest®	FTS + membrane	24.-25.8.2011	81	115	?	-	-	1d culture	n.a.	1.2	20	n.a.	n.a.	n.a.	n.a.	n.a.
				82	n.d.	?	-	-	1d culture	n.a.	2.1	19	n.a.	n.a.	n.a.	n.a.	n.a.
				83	n.d.	?	-	-	1d culture	n.a.	1.5	19	n.a.	n.a.	n.a.	n.a.	n.a.
				84	n.d.	?	-	-	1d culture	n.a.	2.6	17	n.a.	n.a.	n.a.	n.a.	n.a.
				85	n.d.	?	-	-	1d culture	n.a.	2.0	19	n.a.	n.a.	n.a.	n.a.	n.a.
		FTS		86	n.d.	?	-	-	1d culture	n.a.	3.4	24	n.a.	n.a.	n.a.	n.a.	n.a.
				87	n.d.	?	-	-	1d culture	n.a.	2.1	21	n.a.	n.a.	n.a.	n.a.	n.a.
				88	n.d.	?	-	-	1d culture	n.a.	1.9	22	n.a.	n.a.	n.a.	n.a.	n.a.
				89	n.d.	?	-	-	1d culture	n.a.	1.8	13	n.a.	n.a.	n.a.	n.a.	n.a.
				90	n.d.	?	-	-	1d culture	n.a.	1.8	16	n.a.	n.a.	n.a.	n.a.	n.a.
MCPA-EHE	human	DMS	05.-07.10.2010	91	500	f	a	68 y	TWF	282	5.0	7	264	-	19	9	
				92	520	f	a	68 y	TWF	359	3.7	12	197	-	21	4	
				93	550	f	a	68 y	TWF	339	4.0	11	304	-	20	9	
				94	550	f	a	33 y	TWF	390	2.2	12	725	-	38	23	
				95	550	f	a	33 y	TWF	229	4.2	9	5531	yes	33	21	
	FTS			96	1100	f	a	68 y	TWF	234	7.2	13	343	-	23	n.d.	
				97	990	f	a	68 y	TWF	593	2.1	17	124	-	24	4	
				98	1160	f	a	68 y	TWF	517	2.0	11	62	-	15	3	
				99	1300	f	a	33 y	TWF	255	3.7	16	130	-	40	3	
				100	1520	f	a	33 y	TWF	152	7.3	9	180	-	38	1	
MCPA	human	DMS	25.-27.05.2010	101	500	f	a	66 y	TWF	646	2.9	10	366	-	18	18	
				102	500	f	a	66 y	TWF	296	1.9	8	233	-	18	29	
				103	500	f	a	66 y	TWF	294	2.7	8	238	-	15	27	
				104	500	f	a	37 y	TWF	242	2.6	3	115	-	21	11	
				105	500	f	a	37 y	TWF	213	2.8	3	166	-	19	12	
	FTS			106	1050	f	a	66 y	TWF	345	2.9	10	156	-	30	4	
				107	1160	f	a	66 y	TWF	210	4.2	8	289	-	16	3	
				108	1100	f	a	66 y	TWF	491	4.0	10	43	slight	21	5	
				109	1040	f	a	37 y	TWF	372	3.3	7	115	-	24	2	
				110	1040	f	a	37 y	TWF	182	3.7	3	135	-	26	2	

Annex

test compound	species	skin type	exp. date	sample no.	thickness [μm]	sex	localization	age	pretreatment	TWF (Kp) [$\cdot 10^{-5}$ cm/h]	TEER [kOhm]	TEWL [g/(cm ² ·h)]	BLUE - absorption [$\mu\text{g/l}$]	BLUE - skin coloration	ISTD - AD [%]	ISTD - maxKp [$\cdot 10^{-5}$ cm/h]
MCPA	rat	DMS	28.-29.10.2010	111	500	f	b	8 w	-	n.a.	7.7	9	n.a.	n.a.	19	16
				112	495	f	b	8 w	-	n.a.	12.2	9	n.a.	n.a.	14	11
				113	495	f	b	8 w	-	n.a.	5.1	7	n.a.	n.a.	13	13
				114	500	f	b	8 w	-	n.a.	16.7	3	n.a.	n.a.	16	11
				115	495	f	b	8 w	-	n.a.	6.7	8	n.a.	n.a.	27	31
			25.-29.10.2010	116	500	f	b	8 w	72h diff.cell	n.a.	2.1	9	n.a.	n.a.	29	25
				117	495	f	b	8 w	72h diff.cell	n.a.	4.6	4	n.a.	n.a.	29	30
				118	500	f	b	8 w	72h diff.cell	n.a.	3.9	3	n.a.	n.a.	16	16
				119	495	f	b	8 w	72h diff.cell	n.a.	5.4	0	n.a.	n.a.	15	15
				120	493	f	b	8 w	72h diff.cell	n.a.	4.0	1	n.a.	n.a.	29	23
			11.-12.11.2010	121	493	f	b	8 w	-	n.a.	4.1	1	n.a.	n.a.	20	22
				122	440	f	b	8 w	-	n.a.	9.2	0	n.a.	n.a.	16	19
				123	440	f	b	8 w	-	n.a.	31.0	0	n.a.	n.a.	18	25
				124	493	f	b	8 w	-	n.a.	22.9	0	n.a.	n.a.	19	18
				125	495	f	b	8 w	-	n.a.	10.8	1	n.a.	n.a.	22	24
			22.-26.11.2010	126	492	f	b	8 w	3 blank, 3w	n.a.	11.6	49	n.a.	n.a.	72	158
				127	494	f	b	8 w	3 blank, 3w	n.a.	11.3	21	n.a.	n.a.	73	59
				128	490	f	b	8 w	3 blank, 3w	n.a.	19.0	93	n.a.	n.a.	78	193
				129	387	f	b	8 w	3 blank, 3w	n.a.	41.8	9	n.a.	n.a.	41	36
				130	335	f	b	8 w	3 blank, 3w	n.a.	11.4	16	n.a.	n.a.	65	87
				131	493	f	b	8 w	3 cold, 3w	n.a.	8.7	0	n.a.	n.a.	47	63
				132	442	f	b	8 w	3 cold, 3w	n.a.	25.7	48	n.a.	n.a.	81	277
				133	490	f	b	8 w	3 cold, 3w	n.a.	7.9	21	n.a.	n.a.	63	98
				134	390	f	b	8 w	3 cold, 3w	n.a.	14.7	41	n.a.	n.a.	61	128
				135	375	f	b	8 w	3 cold, 3w	n.a.	22.6	0	n.a.	n.a.	42	66
			14.-18.3.2011	136	395	f	b	8 w	3 water, 3w	n.a.	7.9	11	n.a.	n.a.	67	176
				137	440	f	b	8 w	3 water, 3w	n.a.	15.2	21	n.a.	n.a.	60	74
				138	440	f	b	8 w	3 water, 3w	n.a.	20.5	15	n.a.	n.a.	33	47
				139	440	f	b	8 w	3 water, 3w	n.a.	39.0	16	n.a.	n.a.	52	44
				140	440	f	b	8 w	3 water, 3w	n.a.	12.8	51	n.a.	n.a.	56	104
			21.-22.03.11	141	495	f	b	8 w	-	n.a.	8.1	0	n.a.	n.a.	n.a.	n.a.
				142	385	f	b	8 w	-	n.a.	11.7	8	n.a.	n.a.	n.a.	n.a.
				143	495	f	b	8 w	-	n.a.	20.0	11	n.a.	n.a.	n.a.	n.a.
				144	495	f	b	8 w	-	n.a.	6.8	9	n.a.	n.a.	n.a.	n.a.
				145	495	f	b	8 w	-	n.a.	10.8	11	n.a.	n.a.	n.a.	n.a.
02.-06.05.2011	146	440	f	b	8 w	3 water, 1w	n.a.	9.9	15	n.a.	n.a.	38	53			
	147	495	f	b	8 w	3 water, 1w	n.a.	3.8	75	n.a.	n.a.	79	180			
	148	500	f	b	8 w	3 water, 1w	n.a.	12.4	60	n.a.	n.a.	45	58			
	149	490	f	b	8 w	3 water, 1w	n.a.	8.4	49	n.a.	n.a.	54	138			
	150	385	f	b	8 w	3 water, 1w	n.a.	9.0	53	n.a.	n.a.	47	60			

Annex

test compound	species	skin type	exp. date	sample no.	thickness [μm]	sex	localization	age	pretreatment	TWF (Kp) [$\times 10^{-5}$ cm/h]	TEER [kOhm]	TEWL [g/(cm ² ·h)]	BLUE - absorption [$\mu\text{g/l}$]	BLUE - skin coloration	ISTD - AD [%]	ISTD - maxKp [$\times 10^{-5}$ cm/h]			
MCPA	rat	DMS	02.-06.05.2011	151	485	f	b	8 w	3 cold, 1w	n.a.	5.1	37	n.a.	n.a.	53	74			
				152	440	f	b	8 w	3 cold, 1w	n.a.	9.8	42	n.a.	n.a.	77	107			
				153	440	f	b	8 w	3 cold, 1w	n.a.	5.2	19	n.a.	n.a.	49	73			
				154	490	f	b	8 w	3 cold, 1w	n.a.	8.6	53	n.a.	n.a.	85	259			
				155	440	f	b	8 w	3 cold, 1w	n.a.	7.2	45	n.a.	n.a.	70	71			
			156	440	f	b	8 w	3 water, 0w	n.a.	6.3	3	n.a.	n.a.	29	17				
			157	445	f	b	8 w	3 water, 0w	n.a.	17.5	0	n.a.	n.a.	8	9				
			158	445	f	b	8 w	3 water, 0w	n.a.	6.5	9	n.a.	n.a.	25	23				
			159	495	f	b	8 w	3 water, 0w	n.a.	21.1	0	n.a.	n.a.	18	14				
			160	495	f	b	8 w	3 water, 0w	n.a.	19.0	0	n.a.	n.a.	19	19				
			161	495	f	b	8 w	3 blank, 0w	n.a.	3.4	12	n.a.	n.a.	33	33				
			162	495	f	b	8 w	3 blank, 0w	n.a.	48.0	0	n.a.	n.a.	39	30				
			163	490	f	b	8 w	3 blank, 0w	n.a.	11.7	14	n.a.	n.a.	44	44				
			164	335	f	b	8 w	3 blank, 0w	n.a.	9.6	22	n.a.	n.a.	47	54				
			165	480	f	b	8 w	3 blank, 0w	n.a.	18.0	17	n.a.	n.a.	38	29				
			StrataTest®	FTS	15.-16.02.2011	166	100	?	-			4d 8°C, 1d culture	n.a.	1.5	13	n.a.	n.a.	78	391
						167	100	?	-			4d 8°C, 1d culture	n.a.	0.9	13	n.a.	n.a.	87	625
						168	110	?	-			4d 8°C, 1d culture	n.a.	1.4	14	n.a.	n.a.	89	488
						169	105	?	-			4d 8°C, 1d culture	n.a.	1.4	12	n.a.	n.a.	84	260
						170	100	?	-			4d 8°C, 1d culture	n.a.	1.1	15	n.a.	n.a.	85	280
17.-18.02.2011	171	110			?	-			6d culture	n.a.	2.0	10	n.a.	n.a.	69	227			
	172	105			?	-			6d culture	n.a.	2.3	10	n.a.	n.a.	67	235			
	173	105			?	-			6d culture	n.a.	0.5	11	n.a.	n.a.	79	588			
	174	105			?	-			6d culture	n.a.	2.0	11	n.a.	n.a.	72	242			
	175	105			?	-			6d culture	n.a.	2.1	12	n.a.	n.a.	73	250			

Table 45: Experimental conditions of diffusion cell experiments. Skin type: dermatomed skin (DMS), full-thickness skin (FTS), experimental date (exp. date), application area (area), volume (vol), applied test substance concentration (donor conc), applied specific radioactivity (spec.rad.), mode: static (s), flow-through (ft), used internal standard (ISTD): ³H-caffeine: (C), ³H-testosterone (T), ³H-mannitol (M), covering: occluded (occ) or semi-occluded (sem), E:W (1:1): ethanol/water, 1/1, v/v, (tap) water ((T)W), 5% BSA in tap water (BW), 0,7% Texapon® N70 in water (Tex). Sample no. corresponds to sample no in Table 44 and Table 46.

test compound	species	skin type	exp. date	sample no.	mode	area [cm ²]	vol [µl]	donor conc [g/l]	spec.rad. [kBq/cm ²]	vehicle	ISTD	covering	receptor	washing fluid	temperature [°C]
caffeine	human	DMS	14.-15.10.2009	1	s	1	25	4	25	E:W (1:1)	-	occ	TW	E:W (1:1)	32.5
				2	s	1	25	4	25	E:W (1:1)	-	occ	TW	E:W (1:1)	32.5
				3	s	1	25	4	25	E:W (1:1)	-	occ	TW	E:W (1:1)	32.5
				4	s	1	25	4	25	E:W (1:1)	-	occ	TW	E:W (1:1)	32.5
				5	s	1	25	4	25	E:W (1:1)	-	occ	TW	E:W (1:1)	32.5
			20.-22.01.2010	6	s	1	25	4	25	E:W (1:1)	M	occ	TW	E:W (1:1)	32.5
				7	s	1	25	4	25	E:W (1:1)	M	occ	TW	E:W (1:1)	32.5
				8	s	1	25	4	25	E:W (1:1)	M	occ	TW	E:W (1:1)	32.5
				9	s	1	25	4	25	E:W (1:1)	M	occ	TW	E:W (1:1)	32.5
				10	s	1	25	4	25	E:W (1:1)	M	occ	TW	E:W (1:1)	32.5
		24.-25.1.2012	11	s	1	25	4	25	E:W (1:1)	-	occ	TW	E:W (1:1)	32.5	
			12	s	1	25	4	25	E:W (1:1)	-	occ	TW	E:W (1:1)	32.5	
			13	s	1	25	4	25	E:W (1:1)	-	occ	TW	E:W (1:1)	32.5	
			14	s	1	25	4	25	E:W (1:1)	-	occ	TW	E:W (1:1)	32.5	
			15	s	1	25	4	25	E:W (1:1)	-	occ	TW	E:W (1:1)	32.5	
			16	s	1	25	4	25	E:W (1:1)	T	occ	TW	E:W (1:1)	32.5	
			17	s	1	25	4	25	E:W (1:1)	T	occ	TW	E:W (1:1)	32.5	
			18	s	1	25	4	25	E:W (1:1)	T	occ	TW	E:W (1:1)	32.5	
			19	s	1	25	4	25	E:W (1:1)	T	occ	TW	E:W (1:1)	32.5	
			20	s	1	25	4	25	E:W (1:1)	T	occ	TW	E:W (1:1)	32.5	
	FTS	20.-22.01.2010	21	s	1	25	4	25	E:W (1:1)	M	occ	TW	E:W (1:1)	32.5	
			22	s	1	25	4	25	E:W (1:1)	M	occ	TW	E:W (1:1)	32.5	
			23	s	1	25	4	25	E:W (1:1)	M	occ	TW	E:W (1:1)	32.5	
			24	s	1	25	4	25	E:W (1:1)	M	occ	TW	E:W (1:1)	32.5	
			25	s	1	25	4	25	E:W (1:1)	M	occ	TW	E:W (1:1)	32.5	
	DMS	22.-23.07.2009	26	s	1	25	4	25	E:W (1:1)	-	occ	TW	E:W (1:1)	32.5	
			27	s	1	25	4	25	E:W (1:1)	-	occ	TW	E:W (1:1)	32.5	
			28	s	1	25	4	25	E:W (1:1)	-	occ	TW	E:W (1:1)	32.5	
			29	s	1	25	4	25	E:W (1:1)	-	occ	TW	E:W (1:1)	32.5	
			30	s	1	25	4	25	E:W (1:1)	-	occ	TW	E:W (1:1)	32.5	
			31	s	1	25	4	25	E:W (1:1)	-	occ	E:W (1:1)	E:W (1:1)	32.5	
			32	s	1	25	4	25	E:W (1:1)	-	occ	E:W (1:1)	E:W (1:1)	32.5	
			33	s	1	25	4	25	E:W (1:1)	-	occ	E:W (1:1)	E:W (1:1)	32.5	
			34	s	1	25	4	25	E:W (1:1)	-	occ	E:W (1:1)	E:W (1:1)	32.5	
			35	s	1	25	4	25	E:W (1:1)	-	occ	E:W (1:1)	E:W (1:1)	32.5	

Annex

test compound		species	skin type	exp. date	sample no.	mode	area [cm ²]	vol [µl]	donor conc [g/l]	spec.rad. [KBq/cm ²]	vehicle	ISTD	covering	receptor	washing fluid	temperature [°C]	
caffeine		rat	DMS	14.-15.10.2009	36	s	1	25	4	25	E:W (1:1)	-	occ	E:W (1:1)	E:W (1:1)	32.5	
					37	s	1	25	4	25	E:W (1:1)	-	occ	E:W (1:1)	E:W (1:1)	32.5	
					38	s	1	25	4	25	E:W (1:1)	-	occ	E:W (1:1)	E:W (1:1)	32.5	
					39	s	1	25	4	25	E:W (1:1)	-	occ	E:W (1:1)	E:W (1:1)	32.5	
					40	s	1	25	4	25	E:W (1:1)	-	occ	E:W (1:1)	E:W (1:1)	32.5	
		StrataTest®	FTS	23.-24.8.2011	41	s	1	25	4	25	E:W (1:1)	-	occ	TW	E:W (1:1)	32.5	
					42	s	1	25	4	25	E:W (1:1)	-	occ	TW	E:W (1:1)	32.5	
					43	s	1	25	4	25	E:W (1:1)	-	occ	TW	E:W (1:1)	32.5	
					44	s	1	25	4	25	E:W (1:1)	-	occ	TW	E:W (1:1)	32.5	
					45	s	1	25	4	25	E:W (1:1)	-	occ	TW	E:W (1:1)	32.5	
					FTS + membrane	46	s	1	25	4	25	E:W (1:1)	-	occ	TW	E:W (1:1)	32.5
						47	s	1	25	4	25	E:W (1:1)	-	occ	TW	E:W (1:1)	32.5
						48	s	1	25	4	25	E:W (1:1)	-	occ	TW	E:W (1:1)	32.5
						49	s	1	25	4	25	E:W (1:1)	-	occ	TW	E:W (1:1)	32.5
						50	s	1	25	4	25	E:W (1:1)	-	occ	TW	E:W (1:1)	32.5
testosterone		human	DMS	24. - 26.11.2009	51	s	1	25	4	25	E:W (1:1)	M	occ	BW	E:W (1:1)	32.5	
					52	s	1	25	4	25	E:W (1:1)	M	occ	BW	E:W (1:1)	32.5	
					53	s	1	25	4	25	E:W (1:1)	M	occ	BW	E:W (1:1)	32.5	
					54	s	1	25	4	25	E:W (1:1)	M	occ	BW	E:W (1:1)	32.5	
					55	s	1	25	4	25	E:W (1:1)	M	occ	BW	E:W (1:1)	32.5	
				30.-31.1.2012	56	s	1	25	4	25	E:W (1:1)	-	occ	BW	E:W (1:1)	32.5	
					57	s	1	25	4	25	E:W (1:1)	-	occ	BW	E:W (1:1)	32.5	
					58	s	1	25	4	25	E:W (1:1)	-	occ	BW	E:W (1:1)	32.5	
					59	s	1	25	4	25	E:W (1:1)	-	occ	BW	E:W (1:1)	32.5	
					60	s	1	25	4	25	E:W (1:1)	-	occ	BW	E:W (1:1)	32.5	
					61	s	1	25	4	25	E:W (1:1)	C	occ	BW	E:W (1:1)	32.5	
					62	s	1	25	4	25	E:W (1:1)	C	occ	BW	E:W (1:1)	32.5	
					63	s	1	25	4	25	E:W (1:1)	C	occ	BW	E:W (1:1)	32.5	
					64	s	1	25	4	25	E:W (1:1)	C	occ	BW	E:W (1:1)	32.5	
					65	s	1	25	4	25	E:W (1:1)	C	occ	BW	E:W (1:1)	32.5	
		rat	DMS	29.-30.07.2009	71	s	1	25	4	25	E:W (1:1)	-	occ	BW	E:W (1:1)	32.5	
					72	s	1	25	4	25	E:W (1:1)	-	occ	BW	E:W (1:1)	32.5	
					73	s	1	25	4	25	E:W (1:1)	-	occ	BW	E:W (1:1)	32.5	
					74	s	1	25	4	25	E:W (1:1)	-	occ	BW	E:W (1:1)	32.5	
					75	s	1	25	4	25	E:W (1:1)	-	occ	BW	E:W (1:1)	32.5	
human	FTS	24. - 26.11.2009	66	s	1	25	4	25	E:W (1:1)	M	occ	BW	E:W (1:1)	32.5			
			67	s	1	25	4	25	E:W (1:1)	M	occ	BW	E:W (1:1)	32.5			
			68	s	1	25	4	25	E:W (1:1)	M	occ	BW	E:W (1:1)	32.5			
			69	s	1	25	4	25	E:W (1:1)	M	occ	BW	E:W (1:1)	32.5			
			70	s	1	25	4	25	E:W (1:1)	M	occ	BW	E:W (1:1)	32.5			

Annex

test compound	species	skin type	exp. date	sample no.	mode	area [cm ²]	vol [µl]	donor conc [g/l]	spec.rad. [KBq/cm ²]	vehicle	ISTD	covering	receptor	washing fluid	temperature [°C]	
testosterone	rat	DMS	29.-30.07.2009	76	s	1	25	4	25	E:W (1:1)	-	occ	E:W (1:1)	E:W (1:1)	32.5	
				77	s	1	25	4	25	E:W (1:1)	-	occ	E:W (1:1)	E:W (1:1)	32.5	
				78	s	1	25	4	25	E:W (1:1)	-	occ	E:W (1:1)	E:W (1:1)	32.5	
				79	s	1	25	4	25	E:W (1:1)	-	occ	E:W (1:1)	E:W (1:1)	32.5	
				80	s	1	25	4	25	E:W (1:1)	-	occ	E:W (1:1)	E:W (1:1)	32.5	
	StrataTest®	FTS	24.-25.8.2011	81	s	1	25	4	25	E:W (1:1)	-	occ	BW	E:W (1:1)	32.5	
				82	s	1	25	4	25	E:W (1:1)	-	occ	BW	E:W (1:1)	32.5	
				83	s	1	25	4	25	E:W (1:1)	-	occ	BW	E:W (1:1)	32.5	
				84	s	1	25	4	25	E:W (1:1)	-	occ	BW	E:W (1:1)	32.5	
				85	s	1	25	4	25	E:W (1:1)	-	occ	BW	E:W (1:1)	32.5	
				FTS + membrane	86	s	1	25	4	25	E:W (1:1)	-	occ	BW	E:W (1:1)	32.5
					87	s	1	25	4	25	E:W (1:1)	-	occ	BW	E:W (1:1)	32.5
					88	s	1	25	4	25	E:W (1:1)	-	occ	BW	E:W (1:1)	32.5
					89	s	1	25	4	25	E:W (1:1)	-	occ	BW	E:W (1:1)	32.5
					90	s	1	25	4	25	E:W (1:1)	-	occ	BW	E:W (1:1)	32.5
MCPA-EHE	human	DMS	05.-07.10.2010	91	s	1	10	16	37	W	T	sem	W	Tex	32.5	
				92	s	1	10	16	37	W	T	sem	W	Tex	32.5	
				93	s	1	10	16	37	W	T	sem	W	Tex	32.5	
				94	s	1	10	16	37	W	T	sem	W	Tex	32.5	
				95	s	1	10	16	37	W	T	sem	W	Tex	32.5	
	FTS	96	s	1	10	16	37	W	T	sem	W	Tex	32.5			
		97	s	1	10	16	37	W	T	sem	W	Tex	32.5			
		98	s	1	10	16	37	W	T	sem	W	Tex	32.5			
		99	s	1	10	16	37	W	T	sem	W	Tex	32.5			
		100	s	1	10	16	37	W	T	sem	W	Tex	32.5			
MCPA	human	DMS	25.-27.05.2010	101	s	1	10	9	37	W	T	sem	W	Tex	32.5	
				102	s	1	10	9	37	W	T	sem	W	Tex	32.5	
				103	s	1	10	9	37	W	T	sem	W	Tex	32.5	
				104	s	1	10	9	37	W	T	sem	W	Tex	32.5	
				105	s	1	10	9	37	W	T	sem	W	Tex	32.5	
	FTS	106	s	1	10	9	37	W	T	sem	W	Tex	32.5			
		107	s	1	10	9	37	W	T	sem	W	Tex	32.5			
		108	s	1	10	9	37	W	T	sem	W	Tex	32.5			
		109	s	1	10	9	37	W	T	sem	W	Tex	32.5			
		110	s	1	10	9	37	W	T	sem	W	Tex	32.5			

Annex

test compound	species	skin type	exp. date	sample no.	mode	area [cm ²]	vol [µl]	donor conc [g/l]	spec.rad. [KBq/cm ²]	vehicle	ISTD	covering	receptor	washing fluid	temperature [°C]
MCPA	rat	DMS	28.-29.10.2010	111	s	1	10	9	37	W	T	sem	W	Tex	32.5
				112	s	1	10	9	37	W	T	sem	W	Tex	32.5
				113	s	1	10	9	37	W	T	sem	W	Tex	32.5
				114	s	1	10	9	37	W	T	sem	W	Tex	32.5
				115	s	1	10	9	37	W	T	sem	W	Tex	32.5
			25.-29.10.2010	116	s	1	10	9	37	W	T	sem	W	Tex	32.5
				117	s	1	10	9	37	W	T	sem	W	Tex	32.5
				118	s	1	10	9	37	W	T	sem	W	Tex	32.5
				119	s	1	10	9	37	W	T	sem	W	Tex	32.5
				120	s	1	10	9	37	W	T	sem	W	Tex	32.5
			11.-12.11.2010	121	ft	1.1	11	9	37	W	T	sem	W	Tex	32.5
				122	ft	1.1	11	9	37	W	T	sem	W	Tex	32.5
				123	ft	1.1	11	9	37	W	T	sem	W	Tex	32.5
				124	ft	1.1	11	9	37	W	T	sem	W	Tex	32.5
				125	ft	1.1	11	9	37	W	T	sem	W	Tex	32.5
			22.-26.11.2010	126	s	1	10	9	37	W	T	sem	W	Tex	32.5
				127	s	1	10	9	37	W	T	sem	W	Tex	32.5
				128	s	1	10	9	37	W	T	sem	W	Tex	32.5
				129	s	1	10	9	37	W	T	sem	W	Tex	32.5
				130	s	1	10	9	37	W	T	sem	W	Tex	32.5
				131	s	1	10	9	37	W	T	sem	W	Tex	32.5
				132	s	1	10	9	37	W	T	sem	W	Tex	32.5
				133	s	1	10	9	37	W	T	sem	W	Tex	32.5
				134	s	1	10	9	37	W	T	sem	W	Tex	32.5
				135	s	1	10	9	37	W	T	sem	W	Tex	32.5
			14.-18.3.2011	136	s	1	10	9	37	W	T	sem	W	Tex	32.5
				137	s	1	10	9	37	W	T	sem	W	Tex	32.5
				138	s	1	10	9	37	W	T	sem	W	Tex	32.5
				139	s	1	10	9	37	W	T	sem	W	Tex	32.5
				140	s	1	10	9	37	W	T	sem	W	Tex	32.5
21.-22.03.11	141	s	1	10	9	37	W	-	sem	W	Tex	32			
	142	s	1	10	9	37	W	-	sem	W	Tex	32			
	143	s	1	10	9	37	W	-	sem	W	Tex	32			
	144	s	1	10	9	37	W	-	sem	W	Tex	32			
	145	s	1	10	9	37	W	-	sem	W	Tex	32			
02.-06.05.2011	146	s	1	10	9	37	W	T	sem	W	Tex	32.5			
	147	s	1	10	9	37	W	T	sem	W	Tex	32.5			
	148	s	1	10	9	37	W	T	sem	W	Tex	32.5			
	149	s	1	10	9	37	W	T	sem	W	Tex	32.5			
	150	s	1	10	9	37	W	T	sem	W	Tex	32.5			

Annex

test compound															
species	skin type	exp. date	sample no.	mode	area [cm ²]	vol [μl]	donor conc [g/l]	spec.rad. [KBq/cm ²]	vehicle	ISTD	covering	receptor	washing fluid	temperature [°C]	
MCPA	rat	DMS	02.-06.05.2011	151	s	1	10	9	37	W	T	sem	W	Tex	32.5
			152	s	1	10	9	37	W	T	sem	W	Tex	32.5	
			153	s	1	10	9	37	W	T	sem	W	Tex	32.5	
			154	s	1	10	9	37	W	T	sem	W	Tex	32.5	
			155	s	1	10	9	37	W	T	sem	W	Tex	32.5	
		23.-27.05.2011	156	s	1	10	9	37	W	T	sem	W	Tex	32.5	
			157	s	1	10	9	37	W	T	sem	W	Tex	32.5	
			158	s	1	10	9	37	W	T	sem	W	Tex	32.5	
			159	s	1	10	9	37	W	T	sem	W	Tex	32.5	
			160	s	1	10	9	37	W	T	sem	W	Tex	32.5	
	15.-16.02.2011	161	s	1	10	9	37	W	T	sem	W	Tex	32.5		
		162	s	1	10	9	37	W	T	sem	W	Tex	32.5		
		163	s	1	10	9	37	W	T	sem	W	Tex	32.5		
		164	s	1	10	9	37	W	T	sem	W	Tex	32.5		
		165	s	1	10	9	37	W	T	sem	W	Tex	32.5		
	StrataTest®	FTS	15.-16.02.2011	166	s	1	10	9	37	W	T	sem	W	Tex	32.5
				167	s	1	10	9	37	W	T	sem	W	Tex	32.5
				168	s	1	10	9	37	W	T	sem	W	Tex	32.5
				169	s	1	10	9	37	W	T	sem	W	Tex	32.5
				170	s	1	10	9	37	W	T	sem	W	Tex	32.5
17.-18.02.2011		171	s	1	10	9	37	W	T	sem	W	Tex	32.5		
		172	s	1	10	9	37	W	T	sem	W	Tex	32.5		
		173	s	1	10	9	37	W	T	sem	W	Tex	32.5		
		174	s	1	10	9	37	W	T	sem	W	Tex	32.5		
		175	s	1	10	9	37	W	T	sem	W	Tex	32.5		

Table 46: Single cell results of Franz cell experiments. Given are total recovery and recovered dose in washing fluid, tape strips, skin and receptor as well as maxKp, absorption rate (AR) and lag time. The assigned sample no. corresponds to the sample no. in Table 44 and Table 45. +: sample excluded from mean calculation for different reasons (e.g. recovery outside 100 ± 10 %). ^m: content in underlying membrane of StrataTest[®] constructs.

test compound	species	skin type	exp. date	sample no.	recovery [%]	wash [%]	tape strips [%]	skin [%]	receptor [%]	maxKp [^m 10 ⁻⁵ cm/h]	AR [µg/(cm ² *h)]	lag time [h]	remarks
caffeine	human	DMS	14.-15.10.2009	1	97.0	63.1	0.0	0.3	32.2	91.9	3.7	2.2	
				2	86.4	42.2	0.2	8.8	25.1	26.0	1.0	0.9	+
				3	94.7	72.0	0.0	0.7	21.6	65.4	2.6	1.7	
				4	96.3	38.6	0.0	1.5	56.2	179.9	7.2	3.6	
				5	92.5	27.2	0.0	9.9	49.2	113.9	4.6	1.6	
			20.-22.01.2010	6	95.9	33.2	0.3	6.4	46.3	76.8	3.1	5.4	
				7	95.6	59.8	0.3	3.5	31.9	56.6	2.3	6.5	
				8	96.7	50.5	0.6	8.8	36.4	61.5	2.5	7.1	
				9	95.9	27.4	0.0	1.0	66.8	142.7	5.7	3.4	
				10	100.3	62.5	0.0	0.3	33.5	113.1	4.6	2.2	
			24.-25.1.2012	11	101.9	84.3	0.0	0.2	17.3	62.6	2.5	2.2	
				12	100.2	88.1	0.0	0.5	11.3	53.8	2.2	1.5	
				13	102.0	81.3	0.0	0.4	19.5	57.6	2.3	3.6	
				14	103.3	80.4	0.0	0.5	22.3	52.4	2.1	4.2	
				15	98.5	69.7	0.4	0.9	27.5	86.3	3.5	3.8	
				16	97.9	74.9	0.1	0.5	22.1	66.3	2.7	3.5	
				17	108.6	77.5	0.1	1.1	17.1	47.2	1.9	3.0	
				18	103.0	89.2	0.2	0.5	12.8	29.5	1.2	4.2	
				19	102.5	79.2	0.7	0.6	17.3	36.5	1.5	5.2	
				20	104.3	89.8	0.4	0.3	13.5	24.7	1.0	4.4	
	20.-22.01.2010	FTS	21	96.1	52.5	1.2	25.6	16.7	29.6	1.2	10.7		
			22	94.1	32.8	1.7	43.3	16.2	43.7	1.8	15.2		
			23	96.3	66.1	0.5	6.3	23.3	39.7	1.6	9.7		
			24	95.8	44.9	0.0	1.3	49.6	129.8	5.2	2.7		
			25	94.9	40.8	0.1	8.9	45.1	54.0	2.2	3.8		
	22.-23.07.2009	DMS	26	89.6	62.6	0.1	1.1	25.7	135.4	5.4	0.6		
			27	93.4	21.9	1.0	11.0	59.4	262.6	10.6	4.5		
			28	94.2	63.9	0.2	1.2	28.8	104.6	4.2	2.0		
			29	96.0	67.4	0.8	6.4	21.3	144.4	5.8	0.4		
			30	94.9	27.2	2.2	4.6	33.9	125.4	5.0	1.6		
			31	92.6	2.5	0.1	1.3	88.6	492.1	19.8	3.3		
			32	94.7	2.5	0.1	1.4	90.7	419.5	16.9	4.5		
			33	93.0	56.6	0.9	5.0	30.5	182.3	7.3	1.6		
			34	90.0	18.9	1.0	8.1	62.0	331.8	13.3	1.6		
			35	93.0	44.7	0.4	3.7	44.3	218.3	8.8	1.8		

Annex

test compound	species	skin type	exp. date	sample no.	recovery [%]	wash [%]	tape strips [%]	skin [%]	receptor [%]	maxKp [$\times 10^{-5}$ cm/h]	AR [μ g/(cm ² ·h)]	lag time [h]	remarks
caffeine	rat	DMS	14.-15.10.2009	36	100.3	64.6	1.0	9.1	25.4	165.2	6.6	1.3	
				37	97.7	31.8	0.8	10.7	54.3	364.3	14.6	1.6	
				38	99.6	70.8	0.9	7.4	18.8	128.5	5.1	1.0	
				39	97.6	60.5	0.8	10.1	26.3	159.9	6.4	1.5	
				40	97.5	21.1	0.0	3.0	73.1	436.9	17.5	5.8	
	StrataTest®	FTS	23.-24.8.2011	41	95.7	0.3	n.e.	0.5	94.3	1255.4	49.7	0.2	
				42	97.7	0.1	n.e.	0.3	97.3	1646.9	65.2	0.2	
				43	95.6	0.2	n.e.	1.6	93.8	1201.0	47.6	0.2	
				44	97.0	0.1	n.e.	0.8	96.1	993.9	39.4	0.3	
				45	96.6	0.0	n.e.	0.3	96.3	1115.4	44.2	0.2	
		FTS + membrane		46	100.6	0.0	n.e.	0.7	75.2	947.5	37.5	0.3	24.7 ^m
				47	101.2	0.1	n.e.	0.8	76.6	729.6	28.9	0.4	23.6 ^m
				48	100.6	0.1	n.e.	0.6	72.7	607.3	24.0	0.3	27.3 ^m
				49	101.7	0.1	n.e.	0.8	75.9	785.0	31.1	0.4	24.9 ^m
				50	103.2	0.4	n.e.	0.5	79.8	663.1	26.3	0.2	22.5 ^m
testosterone	human	DMS	24. - 26.11.2009	51	98.5	85.6	0.1	0.6	12.0	36.4	1.4	3.0	
				52	99.2	87.2	0.1	0.5	11.5	33.8	1.3	1.6	
				53	93.0	47.6	0.4	23.3	20.5	20.1	0.8	1.6	+
				54	99.2	88.7	0.0	0.3	10.2	33.0	1.3	2.3	
				55	100.0	85.5	0.0	0.7	12.6	37.1	1.5	2.3	
			30.-31.1.2012	56	94.6	61.2	1.5	3.0	28.8	69.3	2.8	6.1	
				57	96.0	81.1	0.6	0.9	13.4	40.8	1.6	3.9	
				58	95.3	76.3	0.8	0.9	17.2	48.1	1.9	3.6	
				59	92.5	47.6	1.0	3.4	40.2	92.3	3.7	5.6	
				60	93.5	69.1	0.6	0.6	22.8	96.2	3.8	2.6	
		61		100.8	91.5	0.5	0.3	7.8	27.9	1.1	2.6		
		62		100.2	84.9	1.1	0.6	13.4	49.1	2.0	2.6		
		63		103.0	95.3	1.2	0.3	5.9	21.1	0.8	1.8		
		64		109.3	65.6	0.3	0.7	42.7	137.6	5.5	2.4		
		65		98.9	80.9	0.6	0.2	17.0	73.3	2.9	2.8		
	FTS	24. - 26.11.2009	66	95.9	72.2	0.2	9.8	13.7	16.5	0.6	6.2		
			67	101.4	90.3	0.1	3.4	7.6	11.7	0.5	5.2		
			68	100.3	77.0	0.2	5.1	18.0	30.5	1.2	5.6		
			69	98.9	75.8	0.1	7.7	15.3	25.1	1.0	6.2		
			70	99.0	81.2	0.1	5.3	12.4	20.5	0.8	6.3		
	rat	DMS	29.-30.07.2009	71	94.0	68.1	0.1	0.8	24.9	89.2	3.5	2.8	
				72	94.8	55.9	0.6	2.4	35.9	109.3	4.2	2.4	
				73	96.2	65.2	0.1	0.9	30.0	79.7	3.1	2.7	
				74	95.9	73.1	0.1	1.5	21.2	50.8	2.0	1.1	
				75	95.2	51.2	0.2	1.6	42.3	81.7	3.2	2.9	

Annex

test compound	species	skin type	exp. date	sample no.	recovery [%]	wash [%]	tape strips [%]	skin [%]	receptor [%]	maxKp [$\cdot 10^{-5}$ cm/h]	AR [μ g/(cm ² ·h)]	lag time [h]	remarks					
testosterone	rat	DMS	29.-30.07.2009	76	91.7	7.7	0.2	4.5	79.3	355.2	13.8	3.2						
				77	91.6	18.5	0.6	2.2	70.3	534.3	20.7	1.6						
				78	92.3	7.6	0.4	3.7	80.7	307.6	11.9	2.3						
				79	93.3	7.1	2.4	3.0	80.7	453.7	17.6	1.7						
				80	91.8	5.9	0.4	4.2	81.3	436.9	17.0	1.6						
	StrataTest®	FTS	24.-25.8.2011	81	89.0	20.9	n.e.	2.6	65.4	427.7	17.2	0.7						
				82	92.3	37.5	n.e.	28.0	22.2	122.8	4.9	0.4						
				83	92.3	29.7	n.e.	2.3	60.3	320.2	12.9	0.4						
				84	87.5	27.0	n.e.	2.2	58.3	283.3	11.4	0.5	+					
				85	87.2	10.1	n.e.	12.8	63.2	805.3	32.4	0.0	+					
				FTS + membrane	86	94.6	13.5	n.e.	2.5	54.5	258.7	10.4	0.8	24.2 ^m				
					87	99.8	24.9	n.e.	4.1	60.2	279.5	11.2	0.6	10.5 ^m				
					88	92.0	7.5	n.e.	7.3	54.0	228.4	9.2	0.8	23.2 ^m				
					89	91.7	59.2	n.e.	3.6	23.3	168.8	6.8	0.8	5.5 ^m				
					90	91.6	37.2	n.e.	3.1	44.2	277.0	11.1	0.8	6.9 ^m				
					MCPA-EHE	human	DMS	05.-07.10.2010	91	110.1	87.7	2.0	4.3	1.0	0.6	0.1	12.9	
									92	93.9	82.0	0.3	0.6	0.4	0.4	0.1	12.9	
									93	89.6	67.7	1.0	0.7	1.6	0.4	0.1	11.2	
									94	100.9	85.2	0.9	1.0	2.8	2.0	0.3	13.3	
95	93.6	85.6	0.4	2.0					3.1	1.4	0.2	13.3						
FTS	96	204.4	186.5	2.3		1.7	0.9		n.d.		+							
	97	94.7	59.2	6.8		1.9	1.4	0.9	0.1	8.8								
	98	97.5	87.1	0.5		1.9	7.0	0.4	0.1	9.2								
	99	94.0	69.8	14.8		3.8	4.9	1.0	0.1	11.2								
	100	93.0	56.1	8.2		6.8	2.8	0.7	0.1	13.3								
MPCA	human	DMS	25.-27.05.2010	101	99.4	84.4	0.0	1.2	13.6	15.1	1.3	4.2						
				102	96.4	83.5	0.0	0.7	12.2	18.4	1.5	4.9						
				103	98.0	86.2	0.0	1.1	10.7	11.1	0.9	4.4						
				104	98.1	86.1	0.5	3.4	7.2	4.9	0.4	7.2						
				105	102.3	87.9	5.1	2.5	6.1	3.9	0.3	7.2						
	FTS	106	95.5	66.8	0.1	3.4	24.9	15.3	1.3	4.3	+							
		107	102.8	87.2	0.1	2.8	12.6	11.0	0.9	5.3								
		108	100.7	83.7	0.0	3.2	13.6	13.6	1.1	6.7								
		109	99.4	74.8	3.9	10.1	10.5	7.6	0.6	9.3								
		110	99.7	80.8	4.5	6.9	7.1	4.9	0.4	9.4								

Annex

test compound	species	skin type	exp. date	sample no.	recovery [%]	wash [%]	tape strips [%]	skin [%]	receptor [%]	maxKp [$\cdot 10^{-5}$ cm/h]	AR [μ g/(cm ² ·h)]	lag time [h]	remarks
MCPA	rat	DMS	28.-29.10.2010	111	104.7	81.3	5.0	5.3	12.8	17.4	1.5	0.6	
				112	104.5	84.0	2.8	3.7	13.7	13.5	1.2	1.2	
				113	99.7	80.4	3.7	3.9	11.4	33.2	2.8	0.4	
				114	116.6	95.6	4.7	5.7	10.5	10.8	0.9	2.8	+
				115	114.3	86.5	3.1	3.5	21.0	35.1	3.0	0.6	+
			25.-29.10.2010	116	101.3	66.4	4.5	8.3	21.8	48.1	4.1	0.5	
				117	106.2	72.7	1.9	6.8	24.3	27.6	2.3	1.1	
				118	101.2	76.5	5.6	5.5	13.3	19.1	1.6	0.7	
				119	100.4	78.6	3.6	5.0	12.5	11.8	1.0	1.0	
				120	103.7	73.5	4.4	0.5	25.0	25.1	2.1	0.4	
			11.-12.11.2010	121	104.1	76.5	7.6	5.5	13.4	50.1	4.3	0.4	
				122	101.4	80.8	6.1	4.2	9.9	17.8	1.5	0.5	
				123	107.1	82.2	10.9	2.2	11.5	10.9	0.9	0.6	
				124	112.0	84.9	9.5	6.4	9.7	12.2	1.0	0.5	+
				125	104.8	83.4	3.4	6.0	11.8	12.6	1.1	0.8	
			22.-26.11.2010	126	108.3	13.2	0.1	3.6	91.2	465.1	39.5	0.0	
				127	108.9	27.3	1.0	8.6	71.8	220.2	18.7	0.2	
				128	104.7	4.7	0.1	5.3	94.6	600.8	51.0	0.0	
				129	105.7	41.3	5.9	9.9	48.2	82.4	7.0	0.3	
				130	104.9	63.5	0.2	3.4	37.6	102.9	8.7	0.0	
				131	111.1	57.3	1.2	5.0	47.4	89.8	7.6	0.2	+
				132	106.0	5.2	0.1	5.2	95.3	1153.7	98.0	0.0	
				133	108.5	51.4	0.1	2.8	54.0	297.9	25.3	0.0	
				134	103.7	12.9	0.0	4.1	86.6	621.6	52.8	0.0	
				135	101.2	49.6	0.3	3.6	47.5	124.4	10.6	0.2	
			14.-18.3.2011	136	85.5	11.3	1.8	6.7	65.6	761.9	68.6	0.0	+
				137	92.2	18.2	2.3	4.4	67.2	181.8	16.4	0.0	
				138	94.9	49.9	2.4	5.7	36.6	103.0	9.3	0.2	
				139	106.0	55.3	3.9	9.4	35.9	79.5	7.2	0.0	
				140	94.4	25.3	3.4	8.1	57.1	326.9	29.4	0.0	
21.-22.03.11	141	102.9	87.1	5.7	1.8	8.1	9.2	0.8	0.7				
	142	102.3	86.0	5.3	1.8	9.2	12.5	1.1	2.7				
	143	105.9	86.9	8.3	6.6	4.0	2.9	0.3	0.7				
	144	104.9	81.0	8.8	1.0	13.7	40.7	3.6	0.7				
	145	97.3	83.2	1.9	0.9	11.1	12.3	1.1	0.8				
02.-06.05.2011	146	98.4	55.4	3.3	5.3	34.2	58.8	5.3	0.3				
	147	94.7	8.4	0.4	5.9	79.8	848.9	76.4	0.0				
	148	104.2	47.7	1.1	5.6	49.1	97.3	8.8	0.2				
	149	82.1	24.0	1.3	5.0	51.7	204.4	18.4	0.0	+			
	150	100.5	44.5	2.0	7.9	45.9	164.9	14.8	0.0				

Annex

test compound	species	skin type	exp. date	sample no.	recovery [%]	wash [%]	tape strips [%]	skin [%]	receptor [%]	maxKp [$\cdot 10^{-5}$ cm/h]	AR [μ g/(cm ² ·h)]	lag time [h]	remarks
MCPA	rat	DMS	02.-06.05.2011	151	99.3	39.8	0.6	3.7	55.0	243.5	21.9	0.5	
				152	101.9	26.0	5.2	14.8	55.6	208.5	18.8	0.0	
				153	102.5	38.2	3.5	4.8	55.9	162.8	14.7	0.1	
				154	108.4	10.6	1.6	4.3	91.4	1007.0	90.6	0.0	
				155	96.8	32.6	1.9	8.1	54.0	167.7	15.1	0.0	
			23.-27.05.2011	156	95.0	78.4	1.0	1.9	13.1	16.2	1.5	-0.2	
				157	97.5	88.6	2.2	1.4	5.0	2.8	0.3	0.0	
				158	99.1	67.9	1.2	4.1	25.7	44.8	4.0	-0.3	
				159	102.5	81.8	3.3	3.8	13.3	6.4	0.6	-1.9	
				160	96.6	75.2	1.5	4.4	14.0	10.9	1.0	0.0	
				161	101.9	54.1	2.0	5.3	40.1	77.5	7.0	-0.4	
				162	93.9	68.9	0.5	2.3	22.0	24.4	2.2	0.0	
				163	92.8	51.8	0.7	2.5	37.7	45.3	4.1	-0.1	
				164	95.3	47.9	0.4	2.1	44.7	86.5	7.8	-0.2	
				165	93.7	65.1	3.0	4.4	20.9	18.6	1.7	-3.0	
	StrataTest®	FTS	15.-16.02.2011	166	94.4	5.3	n.e	0.7	88.2	412.5	37.1	0.1	
				167	97.5	1.9	n.e	0.9	94.6	715.4	64.4	0.0	
				168	97.5	2.8	n.e	1.5	93.1	579.0	52.1	0.3	
				169	99.6	3.2	n.e	1.3	95.0	585.3	52.7	0.5	
				170	98.4	2.7	n.e	0.5	95.0	441.9	39.8	0.2	
			17.-18.02.2011	171	97.3	18.0	n.e	29.4	49.7	86.6	7.8	0.1	
				172	95.1	11.2	n.e	1.4	82.4	364.6	32.8	0.4	
				173	98.0	3.5	n.e	6.5	87.9	1004.0	90.3	0.0	
				174	95.8	11.2	n.e	1.3	83.2	305.8	27.5	0.5	
				175	94.6	8.5	n.e	1.2	84.9	405.1	36.5	0.5	

Table 47: Test substances used to develop in silico prediction models. Shown are common names (or codes) including CAS number if available, molecular weight and logP_{ow} – extracted from Syrres or other sources if indicated – and Abraham descriptors $\Sigma\alpha_2^H$, $\Sigma\beta_2^H$, π_2^H , Rf_2 , V_x – calculated with ADME Boxes version 4.95 – as well as affiliation to training (T) or validation (V) set for substance-specific splitting. No Abraham descriptors were available for substances with unknown structure or for inorganics and polymers which could not be processed in the software.

no.	compound	CAS#	formula	molecular weight [g/mol]	logP _{ow}	$\Sigma\alpha_2^H$	$\Sigma\beta_2^H$	π_2^H	Rf_2	V_x	Set
1	chloridazone	1698-60-8	C ₁₀ H ₈ ClN ₃ O	221.65	1.14	0.21	1.36	1.8	1.8	1.52	V
2	fenpropimorph	67564-91-4	C ₂₀ H ₃₃ NO	303.49	4.93	0	0.95	0.93	1.02	2.74	V
3	pyraclostrobin	175013-18-0	C ₁₉ H ₁₆ ClN ₃ O ₄	387.8 ¹	3.99	0	1.57	2.76	2.52	2.73	T
4	epoxiconazole	106325-08-0(alt); 133855-98-8(new)	C ₁₇ H ₁₃ ClFN ₃ O	329.8	3.44	0	0.91	2.19	2.24	2.22	V
5	zinc oxide	1314-13-2	ZnO	81.4	-	-	-	-	-	-	T
6	dimethomorph	110488-70-5	C ₂₁ H ₂₂ ClNO ₄	387.9	2.68	0	1.56	2.97	2.14	2.85	T
7	dithianon	3347-22-6	C ₁₄ H ₄ N ₂ O ₂ S ₂	296.3	2.84	0	1.48	3.13	2.72	1.93	T
8	fluxapyrad	907204-31-3	C ₁₈ H ₁₂ F ₆ N ₃ O	381.3	3.1 ¹	0.5	0.98	2.31	1.95	2.38	T
9	boscalid	188425-85-6	C ₁₈ H ₁₂ Cl ₂ N ₂ O	343.2	2.96 ¹	0.41	1.13	2.64	2.63	2.39	V
10	trisodium nitrilotriacetate (NTA-Na3)	5064-31-3	C ₆ H ₆ NNa ₃ O ₆	257.1	-10.08 (-2.62 ¹)	1.71	1.52	1.69	0.67	1.28	T
11	kresoxim-methyl	143390-89-0	C ₁₈ H ₁₉ NO ₄	313.4	3.4	0	1.12	1.58	1.51	2.42	T
12	prochloraz	67747-09-5	(C ₁₅ H ₁₆ Cl ₃ N ₃ O ₂) ₄ +CuCl ₂	(376.7) ₄ + 135.5	4.1	0	1.29	2.73	1.95	2.53	T
13	metazachlor	67129-08-2	C ₁₄ H ₁₆ ClN ₃ O	277.8	2.13	0	1.08	2.19	1.78	2.09	V
14	bentazone sodium-salt	50723-80-3 (bentazone)	C ₁₀ H ₁₂ O ₃ N ₂ S	240.3 ²	2.34 ²	0.31	1.26	2.24	1.75	1.67	T
15	ilomastat	142880-36-2	C ₂₀ H ₂₈ N ₄ O ₄	388.5	-	1.39	2.39	3.93	2.39	3.04	T
16	hexabromocyclododecane (HBCD)	25637-99-4	C ₁₂ H ₁₈ Br ₆	641.7	5.63 ³	0	0.42	1.62	2.46	2.74	T
17	N-methylpyrrolidone (NMP)	872-50-4	C ₅ H ₉ NO	99.0	-0.38	0	0.74	0.96	0.61	0.82	T
18	cycloxydim	101205-02-1	C ₁₇ H ₂₇ NO ₃ S	325.5	1.36	0.31	1.25	1.31	1.5	2.60	T

no.	compound	CAS#	formula	molecular weight [g/mol]	logP _{ow}	Σα ₂ ^H	Σβ ₂ ^H	π ₂ ^H	Rf ₂	V _x	Set
19	titanium oxide	13463-67-7	TiO ₂	79.0	-	-	-	-	-	-	T
20	1,1-dicarboxy(2,2-dimethylpropyl)-4,4-diphenylbutadien	363602-15-7	C ₂₈ H ₃₄ O ₄	434.6	-	0	1.13	1.91	1.49	3.64	T
21	Uvinul A Plus	302776-68-7	C ₂₄ H ₃₁ NO ₄	397.5	6.2 ¹	0.13	1.1	2.2	1.82	3.26	T
22	pyrimidinotriazole	214706-53-3	C ₁₇ H ₁₅ ClF ₃ N ₅	381.8	-	0	1.23	1.71	2.1	2.44	T
23	pendimethalin	40487-42-1	C ₁₃ H ₁₉ N ₃ O ₄	281.3	5.18	0.05	0.57	1.59	1.42	2.15	T
24	metaflumizone	139968-49-3	C ₂₄ H ₁₆ F ₆ N ₄ O ₂	506.4	4.56 ¹	0.51	1.25	2.49	1.85	3.23	T
25	(R)-2-(2,4-dichlorophenoxy)propionic acid potassium salt (DPP)	15165-67-0	C ₉ H ₈ Cl ₂ O ₃	235.1	-0.25	0.57	0.61	1.4	1.05	1.52	T
26	RS-dimethenamid P	87674-68-8	C ₁₂ H ₁₈ ClNO ₂ S	275.8	2.15	0	0.91	1.54	1.07	2.06	T
27	styrene	100-42-5	C ₈ H ₈	104.2	2.95	0	0.17	0.7	0.7	0.96	V
28	metconazole	125116-23-6	C ₁₇ H ₂₂ N ₃ OCl	319.8	3.85	0.31	0.94	1.84	1.88	2.44	T
29	flufenoxuron	101463-69-8	C ₂₁ H ₁₁ ClF ₆ N ₂ O ₃	488.8	4	0.6	1.06	2.44	1.8	2.87	T
30	ametoctradin	865318-97-4	C ₁₅ H ₂₅ N ₅	275.4	4.24 ¹	0.21	1.16	1.2	1.54	2.33	T
31	imidazolidin-2-thion	96-45-7	C ₃ H ₆ N ₂ S	102.2	-0.66	0.29	0.82	1	1.04	0.74	T
32	topramezone	210631-68-8	C ₁₆ H ₁₇ N ₃ O ₅ S	363.4	-1.52 ¹	0.13	1.62	2.69	2.27	2.49	V
33	dicamba	1918-00-9	C ₈ H ₆ Cl ₂ O ₃	221.0	2.21 (-1.8) ¹	0.64	0.57	1.35	1.07	1.38	V
34	metiram	9006-42-2	(C ₁₆ H ₂₃ N ₁₁ S ₁₆ Zn ₃) _x	(1088.7) _x	-	-	-	-	-	-	T
35	fluquinconazole	136426-54-5	C ₁₆ H ₆ Cl ₂ FN ₅ O	376.2	3.24	0	1.29	2.85	2.85	2.32	T
36	2'-carboxy-(2-methylpropyl)-2-hydroxy-4-diethylaminobenzophenone	-	C ₂₂ H ₂₇ NO ₄	369.5	-	0.13	1.12	2.17	1.83	2.98	T

no.	compound	CAS#	formula	molecular weight [g/mol]	logP _{ow}	$\Sigma\alpha^H$	$\Sigma\beta^H$	π_2^H	Rf ₂	V _x	Set
37	2'-carboxy-(2-ethylhexyl)-2-hydroxy-4-diethylaminobenzophenone	-	C ₂₆ H ₃₅ NO ₄	425.6	-	0.13	1.14	2.19	1.82	3.55	T
38	hydrocortisterone	50-23-7	C ₂₁ H ₃₀ O ₅	362.5	1.61	0.73	1.9	2.92	2.04	2.80	V
39	2'-carboxyhexyl 2-hydroxy-4-diethylaminobenzophenone	-	C ₂₄ H ₃₁ NO ₄	397.5	-	0.13	1.1	2.2	1.82	3.26	T
40	N-cyclohexyldiazoniumdioxypotassium (K-HDO)	66603-10-9	C ₆ H ₁₁ KN ₂ O ₂	182.3	-0.2 ⁴	0.31	0.81	1.37	0.75	1.12	T
41	bis-(N-cyclohexyldiazoniumdioxycopper (Cu-HDO)	312600-89-8	C ₁₂ H ₂₂ N ₄ O ₄ Cu	349.9	2.6 ⁵	-	-	-	-	-	T
42	dimoxystrobin	149961-52-4	C ₁₉ H ₂₂ N ₂ O ₃	326.4	3.59 ¹	0.26	1.35	1.99	1.78	2.60	T
43	no. 43	-	C ₁₈ H ₁₅ Cl ₂ F ₄ NO ₄	456.2	-	0	1.1	1.87	1.44	2.78	T
44	no.44	-	C ₁₆ H ₁₀ ClF ₄ N ₃ O ₃	403.7	-	0	1.31	2.11	1.99	2.30	T
45	no. 45	-	C ₁₇ H ₁₂ ClF ₄ N ₃ O ₃	417.7	-	0	1.31	2.11	1.99	2.44	T
46	cinidon-ethyl	142891-20-1	C ₁₉ H ₁₇ Cl ₂ NO ₄	394.3	4.51 ⁶	0	1.39	2.36	2.02	2.70	T
47	no. 47	-	C ₂₂ H ₃₅ N ₅ O ₃ Cl ₂	488.5	-	0.68	2.68	3.05	2.47	3.30	V
48	no. 48	-	C ₂₀ H ₃₂ N ₆ O ₂ Cl ₂	459.4	-	0.68	2.75	3.09	2.45	3.06	T
49	no. 49	-	C ₃₀ H ₃₄ N ₄ O ₅	530.6	-	0.64	2.39	3.51	3.27	3.68	T
50	no. 50	-	C ₂₄ H ₃₁ N ₅ O ₄ Cl ₂	524.4	-	1.17	2.77	3.63	2.88	3.47	V
51	no. 51	-	C ₂₃ H ₃₁ N ₆ O ₄	444.5	-	1.17	2.98	3.39	2.56	3.42	T
52	diethylaminobenzoessäurevinylester (DEBV)	-	C ₁₂ H ₁₇ NO ₂	219.3	-	0	0.85	1.33	1	1.83	T
53	no. 53	-	Not known	not known	-	-	-	-	-	-	T
54	1,1-dicarboxyethyl-4,4-diphenylbutadien	-		350.4	-	1.14	1.05	2.1	1.74	2.80	T

no.	compound	CAS#	formula	molecular weight [g/mol]	logP _{ow}	Σα ^H	Σβ ^H	π ₂ ^H	Rf ₂	V _x	Set
55	MCPA-EHE	29450-45-1	C ₁₇ H ₂₅ ClO ₃	312.8	6.8 ⁷	0	0.7	1.26	0.85	2.52	T
56	MCPA (DMA-Salt)	2039-46-5	C ₉ H ₉ ClO ₃	200.6	-0.71 ⁷	0.57	0.65	1.29	0.96	1.39	T
57	testosterone	58-22-0	C ₁₉ H ₂₈ O	288.4	3.32.	0.31	1.01	2.27	1.55	2.38	T
58	caffeine	58-08-2	C ₈ H ₁₀ N ₄ O ₂	194.2	-0.07	0	1.27	1.9	1.48	1.36	T
59	tetrahydrofurane	109-99-9	C ₄ H ₈ O	72.1	0.46	0	0.22	0.42	0.25	0.62	V
60	Disperse Red 60	17418-58-5	C ₂₀ H ₁₃ NO ₄	331.3	4.69	0.38	1.21	2.78	2.99	2.35	T
61	Disperse Yellow 64	10319-14-9	C ₁₈ H ₁₀ BrNO ₃	368.2	-	0.33	1.34	2.78	3.05	2.23	T
62	Disperse Red 17	3179-89-3	C ₁₇ H ₂₀ N ₄ O ₄	344.4	3.69	0.48	1.57	2.07	2.39	2.58	T
63	Disperse Yellow 3	2832-40-8	C ₁₅ H ₁₅ N ₃ O ₂	269.3	3.98	0.91	1.22	1.77	1.96	2.08	T
64	Disperse Blue 165	41642-51-7	C ₁₅ H ₁₅ N ₃ O ₂	405.4	-	0.41	1.63	3.37	2.53	3.03	T
65	no. 65	T2030/76	not known	not known	-	-	-	-	-	-	T
66	carbendazim	10605-21-7	C ₉ H ₉ N ₃ O ₂	191.2	1.52	0.71	0.99	1.86	1.64	1.36	T
67	acifluorfen	50594-66-6	C ₁₄ H ₇ ClF ₃ NO ₅	361.7	3.7	0.57	0.71	2.06	1.45	2.09	T
69	dimethoat	60-51-5	C ₅ H ₁₂ NO ₃ PS ₂	229.3	0.78	0.26	1.32	1.44	1.22	1.58	V
70	fenbutatin-oxide	13356-08-6	C ₆₀ H ₇₈ OSn ₂	1052.7	5.2	0	1.1	2.64	2.93	7.15	T
71	fipronil	120068-37-3	C ₁₂ H ₄ Cl ₂ F ₆ N ₄ OS	437.2	4	0.3	1.32	3.15	1.97	2.25	V
72	flocoumafen	90035-08-8	C ₃₃ H ₂₅ F ₃ O ₄	542.6	4.7	0.31	1.39	2.85	3.07	3.79	T
73	iprodione	36734-19-7	C ₁₃ H ₁₃ Cl ₂ N ₃ O ₃	330.2	3	0.16	1.41	2.06	1.9	2.19	V
74	profoxydim	139001-49-3	C ₂₄ H ₃₂ ClNO ₄ S	466.0	-	0.31	1.57	2.03	2.27	3.53	T
75	prohexadione-calcium	127277-53-6	(C ₁₀ H ₁₀ O ₅) ₂ Ca	(252.3) ₂ +40	-2.9	0.88	1.36	1.96	1.12	1.53	T
76	pyrimethanil	53112-28-0	C ₁₂ H ₁₃ N ₃	199.3	2.84	0.13	0.69	1.39	1.53	1.62	V

no.	compound	CAS#	formula	molecular weight [g/mol]	logP _{ow}	$\Sigma\alpha_2^H$	$\Sigma\beta_2^H$	π_2^H	Rf ₂	V _x	Set
77	tebufenpyrad	119168-77-3	C ₁₈ H ₂₄ ClN ₃ O	333.9	4.61	0.26	1.08	2.09	1.79	2.65	T
78	teflubenzuron	83121-18-0	C ₁₄ H ₆ Cl ₂ F ₄ N ₂ O ₂	381.1	4.56	0.76	0.71	2.16	1.5	2.15	V
79	thiophanate-methyl	23564-05-8	C ₁₂ H ₁₄ N ₄ O ₄ S ₂	342.4	1.4	0.7	1.59	3.22	2.63	2.35	T
80	tridemorph	24602-86-6	C ₁₉ H ₃₉ NO	297.5	6.38	0	0.82	0.64	0.41	2.84	T
81	triticonazole	131983-72-7	C ₁₇ H ₂₀ ClN ₃ O	317.8	3.29	0.31	0.99	1.89	2.01	2.40	T
82	tritosulfuron	142469-14-5	C ₁₃ H ₉ F ₆ N ₅ O ₄ S	445.0	2.85 ¹	0.81	1.54	2.41	1.39	2.43	V
83	vinclozolin	50471-44-8	C ₁₂ H ₉ Cl ₂ NO ₃	286.1	3.1	0	0.92	1.38	1.57	1.84	V
84	cyflumetofen	400882-07-7	C ₂₄ H ₂₄ F ₃ NO ₄	447.5	-	0	1.2	2.31	1.29	3.23	T
85	Uvinul T 150	88122-99-0	C ₄₈ H ₆₆ N ₆ O ₆	823.1	8.1 ¹	0.38	2.31	3.94	3.41	6.74	T
86	mannitol	69-65-8	C ₆ H ₁₄ O ₆	182.2	-3.1	1.62	1.81	1.75	1.23	1.31	T
87	flufenamic acid	530-78-9	C ₁₄ H ₁₀ F ₃ NO ₂	281.2	5.25	0.72	0.59	1.36	1.26	1.83	T
88	nicotin	54-11-5	C ₁₀ H ₁₄ N ₂	162.2	1.17	0	0.91	1.03	1.01	1.37	T
89	clotrimazol	23593-75-1	C ₂₂ H ₁₇ ClN ₂	344.9	6.26	0	0.78	2.37	2.48	2.62	T
90	digoxin	20830-75-5	C ₄₁ H ₆₄ O ₁₄	781.0	1.26	1.58	4.32	4.46	3.67	5.75	T

¹ MSDS, BASF, ² value for bentazone acid, ³ MSDS, Albermarle®, ⁴ Assessment Report (Standing Committee on Biocidal Products 2008) ⁵ Pesticide Fact Sheet (United States Environmental Protection Agency (US-EPA) 2011), ⁶ MSDS, Sigma-Aldrich, ⁷ The Pesticide Manual (British Crop Protection Council 2011)

Table 48: Overview of the final internal database for in silico modeling as defined in chapter 3.7.1. Only experiments with human (h) and rat (r) skin preparations are included. Shown are individual experimental conditions and results in the form of logmaxKp (mean of at least 3 replicates) as well as five example MFs (molinspTPSA, molinspLogHBAcc, AdmeLogHBDOn, AdmeP_{ow} and Adme1/RotB). Compound no. corresponds to no. in Table 47 and each mix no. stands for a special mixture/formulation of the respective compound. Different receptor fluids were combined to seven representative groups ('water', 'water+B', 'water+x', 'PBS, pH4', 'E/W_1', 'E/W_2' and 'E/W_3'; details in chapter 3.7.1) and exposure (expo) and total experimental periods (total) were condensed to periods < 6 h, 6 – 8 h, 8 – 24 h, 24 h, 24 – 48 h and > 48 h. dms: dermatomed skin; epi: epidermis; fts: full-thickness skin; semi: semi-occluded; occ: occluded; fin: finite; inf: infinite.

compound no.	mix no.	species	preparation	receptor	covering	time [h] expo / total	regimen	applied conc [g/l]	molinspTPSA	molinsp LogHBAcc	Adme LogHBDOn	AdmeP _{ow}	Adme1/RotB	LogmaxKp
1	1_1	h	dms	water	semi	6-8 / 24	fin	430	46	0.28	0.28	13	0.43	-7.0
	1_1	r	dms	water	semi	6-8 / 24	fin	430	46	0.28	0.28	13	0.43	-5.5
	1_2	h	dms	water	semi	6-8 / 24	fin	2	29	0.00	0.30	24	0.00	-3.9
	1_2	r	dms	water	semi	6-8 / 24	fin	2	29	0.00	0.30	24	0.00	-3.9
2	2_1	h	epi	E/W_2	none	6-8 / 6-8	fin	312	29	0.21	0.15	12	0.10	-6.3
	2_1	h	epi	E/W_2	none	24 / 24	fin	300	29	0.21	0.15	12	0.10	-5.0
	2_1	r	epi	E/W_2	none	6-8 / 6-8	fin	312	29	0.21	0.15	12	0.10	-4.3
	2_1	r	epi	E/W_2	none	24 / 24	fin	300	29	0.21	0.15	12	0.10	-4.0
	2_2	h	epi	E/W_2	none	6-8 / 6-8	fin	1	29	0.00	0.30	24	0.00	-4.9
	2_2	h	epi	E/W_2	none	24 / 24	fin	1	29	0.00	0.30	24	0.00	-4.3
	2_2	r	epi	E/W_2	none	6-8 / 6-8	fin	1	29	0.00	0.30	24	0.00	-3.8
	2_2	r	epi	E/W_2	none	24 / 24	fin	1	29	0.00	0.30	24	0.00	-3.0
	2_3	h	dms	E/W_2	semi	6-8 / 24	fin	36	40	0.40	0.01	0	0.09	-5.7
	2_4	h	dms	E/W_1	semi	6-8 / 24	fin	3	29	0.00	0.30	24	0.00	-6.9
	2_5	h	epi	E/W_2	none	24 / 24	fin	15	17	0.00	0.00	0	0.00	-2.3
	2_5	r	epi	E/W_2	none	24 / 24	fin	15	17	0.00	0.00	0	0.00	-1.1
	2_6	h	epi	E/W_2	none	24 / 24	fin	5	17	0.00	0.00	0	0.00	-2.3
	2_6	r	epi	E/W_2	none	24 / 24	fin	5	17	0.00	0.00	0	0.00	-1.5
	2_7	h	epi	E/W_2	none	24 / 24	fin	1	17	0.00	0.00	0	0.00	-2.1
2_7	r	epi	E/W_2	none	24 / 24	fin	1	17	0.00	0.00	0	0.00	-1.0	
3	3_1	h	dms	E/W_2	semi	6-8 / 24	fin	41	24	0.21	0.00	0	0.31	-5.6
	3_2	h	dms	E/W_1	semi	6-8 / 24	fin	1	29	0.00	0.29	23	0.01	-4.5
	3_3	h	dms	E/W_1	semi	6-8 / 24	fin	0	29	0.00	0.30	24	0.00	-4.4
	3_4	h	dms	E/W_1	semi	6-8 / 24	fin	2	30	0.01	0.30	24	0.00	-4.5
	3_5	h	dms	E/W_1	semi	6-8 / 24	fin	0	29	0.00	0.30	24	0.00	-3.9
	3_6	h	dms	E/W_1	semi	6-8 / 24	fin	200	39	0.22	0.25	21	0.08	-5.4
	3_7	h	dms	E/W_1	semi	6-8 / 24	fin	5	30	0.01	0.30	24	0.00	-4.8
	3_8	h	dms	E/W_1	semi	6-8 / 24	fin	1	29	0.00	0.30	24	0.00	-4.7
	3_8	r	dms	E/W_1	semi	6-8 / 24	fin	1	29	0.00	0.30	24	0.00	-4.3
	3_9	h	dms	E/W_2	semi	6-8 / 24	fin	203	55	0.45	0.02	0	0.04	-6.2
	3_10	h	dms	E/W_1	semi	6-8 / 24	fin	1	29	0.00	0.30	24	0.00	-5.2
	3_11	h	dms	E/W_1	semi	6-8 / 24	fin	0	29	0.00	0.30	24	0.00	-5.0
	3_12	h	epi	E/W_2	none	24 / 24	fin	38	23	0.13	0.03	0	0.01	-4.4
	3_12	r	epi	E/W_2	none	24 / 24	fin	38	23	0.13	0.03	0	0.01	-3.4
	3_13	h	epi	E/W_2	none	24 / 24	fin	75	22	0.11	0.03	0	0.01	-4.5
	3_13	r	epi	E/W_2	none	24 / 24	fin	75	22	0.11	0.03	0	0.01	-3.4
3_14	h	epi	E/W_2	none	24 / 24	fin	2	22	0.11	0.03	0	0.01	-4.8	
3_14	r	epi	E/W_2	none	24 / 24	fin	2	22	0.11	0.03	0	0.01	-3.2	

Annex

compound no.	mix no.	species	preparation	receptor	covering	time [h] expo / total	regimen	applied conc [g/l]	molinspTPSA	molinsp LogHBAcc	Adime LogHBDon	AdimeP _{ow}	Adime1/RotB	LogmaxKp
4	4_1	h	dms	E/W_2	semi	6-8 / 24	fin	125	60	0.34	0.19	14	0.08	-4.4
	4_1	r	dms	E/W_2	semi	6-8 / 24	fin	125	60	0.34	0.19	14	0.08	-4.5
	4_2	h	dms	E/W_1	semi	6-8 / 24	fin	1	30	0.00	0.30	24	0.00	-4.0
	4_2	r	dms	E/W_1	semi	6-8 / 24	fin	1	30	0.00	0.30	24	0.00	-4.3
	4_3	h	dms	water	semi	6-8 / 24	fin	0	29	0.00	0.30	24	0.00	-4.4
	4_3	r	dms	water	semi	6-8 / 24	fin	0	29	0.00	0.30	24	0.00	-4.3
	4_4	h	dms	water	semi	6-8 / 24	fin	0	29	0.00	0.30	24	0.00	-4.8
	4_5	h	dms	water	semi	6-8 / 24	fin	0	29	0.00	0.30	24	0.00	-4.3
	4_5	r	dms	water	semi	6-8 / 24	fin	0	29	0.00	0.30	24	0.00	-4.2
	4_6	h	dms	water	semi	6-8 / 24	fin	0	29	0.00	0.30	24	0.00	-4.6
	4_7	h	dms	water	semi	6-8 / 24	fin	0	29	0.00	0.30	24	0.00	-4.3
6	6_1	h	dms	E/W_2	semi	6-8 / 24	fin	228	49	0.39	0.22	10	0.14	-4.4
	6_2	h	dms	water	semi	6-8 / 24	fin	2	29	0.00	0.30	24	0.00	-4.2
	6_3	h	dms	water	semi	6-8 / 24	fin	0	29	0.00	0.30	24	0.00	-3.8
	6_4	h	dms	E/W_2	semi	24 / 24	fin	145	22	0.10	0.00	0	0.79	-4.8
	6_4	r	dms	E/W_2	semi	24 / 24	fin	145	22	0.10	0.00	0	0.79	-4.0
	6_5	h	dms	water	semi	24 / 24	fin	2	29	0.00	0.30	24	0.01	-4.9
	6_5	r	dms	water	semi	24 / 24	fin	2	29	0.00	0.30	24	0.01	-4.4
	6_6	h	dms	water	semi	24 / 24	fin	0	29	0.00	0.30	24	0.00	-4.0
	6_6	r	dms	water	semi	24 / 24	fin	0	29	0.00	0.30	24	0.00	-3.8
	6_7	h	dms	water	semi	24 / 24	fin	5	29	0.00	0.30	24	0.00	-5.1
	6_7	r	dms	water	semi	24 / 24	fin	5	29	0.00	0.30	24	0.00	-5.1
7	7_1	h	dms	E/W_2	semi	6-8 / 24	fin	350	55	0.29	0.19	19	0.18	-6.4
	7_1	r	dms	E/W_2	semi	6-8 / 24	fin	350	55	0.29	0.19	19	0.18	-6.4
	7_2	h	dms	E/W_1	semi	6-8 / 24	fin	0	29	0.00	0.30	24	0.00	-5.8
	7_2	r	dms	E/W_1	semi	6-8 / 24	fin	0	29	0.00	0.30	24	0.00	-5.5
8	8_1	h	dms	E/W_1	semi	6-8 / 24	fin	0	29	0.00	0.30	24	0.00	-3.8
	8_1	r	dms	E/W_1	semi	6-8 / 24	fin	0	29	0.00	0.30	24	0.00	-4.3
	8_2	h	dms	E/W_2	none	6-8 / 24	fin	323	43	0.28	0.22	17	0.13	-5.9
	8_3	h	dms	E/W_2	none	6-8 / 24	fin	32	31	0.03	0.29	23	0.01	-5.8
9	9_1	h	dms	E/W_1	semi	6-8 / 24	fin	1	29	0.00	0.30	24	0.00	-5.2
	9_1	h	dms	water	semi	6-8 / 24	fin	1	29	0.00	0.30	24	0.00	-5.0
	9_2	h	epi	water	none	24 / 24	fin	100	32	0.07	0.26	22	0.03	-5.1
	9_2	r	epi	water	none	24 / 24	fin	100	32	0.07	0.26	22	0.03	-4.2
	9_3	h	epi	water	none	24 / 24	fin	10	30	0.01	0.30	24	0.00	-5.3
	9_3	r	epi	water	none	24 / 24	fin	10	30	0.01	0.30	24	0.00	-4.1
	9_4	h	epi	water	none	24 / 24	fin	1	29	0.00	0.30	24	0.00	-4.6
10	10_1	h	dms	water	semi	6-8 / 24	fin	10	30	0.01	0.30	25	0.00	-5.4
11	11_1	h	dms	E/W_1	semi	6-8 / 24	fin	1	29	0.00	0.30	24	0.00	-4.0
	11_2	h	dms	water	semi	6-8 / 24	fin	0	29	0.00	0.30	24	0.00	-4.3

Annex

compound no.	mix no.	species	preparation	receptor	covering	time [h] expo / total	regimen	applied conc [g/l]	molinspTPSA	molinsp LogHBAcc	Adme LogHBDon	AdmeP _{ow}	Adme1/RotB	LogmaxKp
12	12_1	h	dms	E/W_1	semi	6-8 / 24	fin	153	47	0.46	0.00	0	0.22	-5.8
	12_2	h	dms	water	semi	6-8 / 24	fin	2	29	0.00	0.30	24	0.00	-4.9
	12_3	h	dms	water+B	none	6-8 / 24	fin	450	39	0.35	0.11	8	0.19	-6.2
	12_3	r	dms	water+B	none	6-8 / 24	fin	450	39	0.35	0.11	8	0.19	-5.3
	12_4	h	dms	water+B	none	6-8 / 24	fin	2	29	0.00	0.30	24	0.00	-4.9
	12_4	r	dms	water+B	none	6-8 / 24	fin	2	29	0.00	0.30	24	0.00	-4.2
	12_5	h	dms	water	semi	6-8 / 24	fin	1	29	0.00	0.30	24	0.00	-4.7
	12_5	h	dms	water	semi	6-8 / 24	fin	1	29	0.00	0.30	24	0.00	-5.2
13	13_1	h	dms	E/W_1	semi	6-8 / 24	fin	532	39	0.32	0.16	11	0.20	-5.2
	13_1	h	dms	E/W_1	semi	6-8 / 24	fin	504	39	0.32	0.16	11	0.20	-3.7
	13_1	h	dms	E/W_1	?	6-8 / 24	fin	505	39	0.32	0.16	11	0.20	-4.7
	13_2	h	dms	water	semi	6-8 / 24	fin	5	29	0.00	0.30	24	0.00	-3.2
	13_2	h	dms	water	semi	6-8 / 24	fin	5	29	0.00	0.30	24	0.00	-3.8
	13_3	h	dms	water	semi	6-8 / 24	fin	1	29	0.00	0.30	24	0.00	-2.9
	13_4	h	dms	E/W_1	semi	6-8 / 24	fin	488	39	0.32	0.16	11	0.20	-3.9
	13_5	h	dms	E/W_1	semi	6-8 / 24	fin	200	31	0.30	0.01	0	0.41	-5.1
	13_5	h	dms	E/W_1	semi	6-8 / 24	fin	200	31	0.30	0.01	0	0.41	-4.4
	13_6	h	dms	water	semi	6-8 / 24	fin	1	29	0.00	0.30	24	0.00	-3.1
13_6	h	dms	water	semi	6-8 / 24	fin	1	29	0.00	0.30	24	0.00	-3.2	
14	14_1	h	dms	water	semi	6-8 / 24	fin	150	59	0.39	0.20	12	0.17	-6.2
	14_2	h	dms	water	semi	6-8 / 24	fin	2	29	0.00	0.30	24	0.00	-4.4
	14_3	r	dms	water	semi	6-8 / 24	fin	493	45	0.28	0.18	14	0.40	-4.6
	14_4	h	dms	water	semi	6-8 / 24	fin	5	29	0.00	0.30	24	0.00	-5.6
	14_4	r	dms	water	semi	6-8 / 24	fin	5	29	0.00	0.30	24	0.00	-3.8
	14_5	h	dms	water	semi	6-8 / 24	fin	1	29	0.00	0.30	24	0.00	-5.0
	14_5	r	dms	water	semi	6-8 / 24	fin	1	29	0.00	0.30	24	0.00	-3.8
16	16_1	h	dms	water+B	none	6-8 / 24	fin	21	17	0.00	0.00	1	0.00	-6.6
17	17_1	h	dms	water	occ	24 / 24	inf	300	27	0.09	0.21	17	0.00	-3.6
	17_2	h	dms	water	occ	24 / 24	inf	100	28	0.03	0.27	22	0.00	-3.6
	17_2	h	dms	water	occ	6-8 / 6-8	inf	307	27	0.09	0.21	17	0.00	-3.4
	17_3	h	dms	water	occ	24 / 24	inf	30	29	0.01	0.29	23	0.00	-3.5
	17_4	h	dms	water	occ	24 / 24	inf	10	29	0.00	0.30	24	0.00	-3.5
	17_5	h	dms	water	occ	24 / 24	inf	3	29	0.00	0.30	24	0.00	-3.2
	17_6	h	dms	water	occ	24 / 24	inf	1	29	0.00	0.30	24	0.00	-3.5
	17_7	h	dms	water	occ	24 / 24	inf	300	26	0.09	0.21	17	0.00	-3.8
	17_8	h	dms	water	occ	24 / 24	inf	30	29	0.00	0.30	24	0.00	-3.2
17_9	h	dms	water	occ	6-8 / 6-8	inf	1031	20	0.30	0.00	2	0.00	-2.0	
18	18_1	r	dms	water	semi	6-8 / 24	fin	1	30	0.00	0.30	24	0.00	-3.3
	18_2	h	dms	E/W_1	semi	24 / 24	fin	100	30	0.24	0.02	0	0.04	-4.4
	18_2	r	dms	E/W_1	semi	24 / 24	fin	100	30	0.24	0.02	0	0.04	-3.8
	18_3	h	dms	water	semi	24 / 24	fin	2	29	0.00	0.30	24	0.00	-3.4
	18_3	r	dms	water	semi	24 / 24	fin	2	29	0.00	0.30	24	0.00	-3.4
22	22_1	h	dms	E/W_2	none	24 / 24	fin	236	33	0.17	0.22	18	0.13	-5.0
	22_1	r	dms	E/W_2	none	24 / 24	fin	236	33	0.17	0.22	18	0.13	-4.9
	22_2	h	dms	E/W_2	none	24 / 24	fin	59	30	0.04	0.28	22	0.03	-4.7
	22_2	r	dms	E/W_2	none	24 / 24	fin	59	30	0.04	0.28	22	0.03	-4.8
	22_3	h	dms	E/W_2	none	24 / 24	fin	3	29	0.00	0.30	24	0.00	-3.8

Annex

compound no.	mix no.	species	preparation	receptor	covering	time [h] expo / total	regimen	applied conc [g/l]	molinspTPSA	molinsp LogHBACC	Adime LogHBDon	AdimeP _{ow}	Adime1/RotB	LogmaxKp
22	22_3	r	dms	E/W_2	none	24 / 24	fin	3	29	0.00	0.30	24	0.00	-3.7
	22_4	h	dms	E/W_2	semi	24 / 24	fin	202	50	0.35	0.18	14	0.13	-5.1
	22_4	r	dms	E/W_2	semi	24 / 24	fin	202	50	0.35	0.18	14	0.13	-4.5
	22_5	h	dms	E/W_2	semi	24 / 24	fin	1	29	0.00	0.30	24	0.00	-3.4
	22_5	r	dms	E/W_2	semi	24 / 24	fin	1	29	0.00	0.30	24	0.00	-3.3
23	23_1	h	epi	E/W_2	semi	24 / 24	fin	397	42	0.34	0.00	0	0.07	-5.7
	23_1	r	epi	E/W_2	semi	24 / 24	fin	397	42	0.34	0.00	0	0.07	-4.0
	23_2	h	epi	E/W_2	semi	24 / 24	fin	3	29	0.00	0.30	24	0.00	-4.4
	23_2	r	epi	E/W_2	semi	24 / 24	fin	3	29	0.00	0.30	24	0.00	-3.4
24	24_1	h	dms	E/W_2	semi	24 / 24	fin	240	50	0.28	0.27	15	0.08	-5.3
	24_1	r	dms	E/W_2	semi	24 / 24	fin	240	50	0.28	0.27	15	0.08	-5.1
25	25_1	h	epi	water	semi	24 / 24	fin	8	29	0.00	0.30	24	0.00	-4.1
	25_1	r	epi	water	semi	24 / 24	fin	8	29	0.00	0.30	24	0.00	-3.5
26	26_1	h	dms	E/W_2	semi	24 / 24	fin	5	29	0.00	0.30	24	0.00	-2.9
	26_1	r	dms	E/W_2	semi	24 / 24	fin	5	29	0.00	0.30	24	0.00	-2.8
	26_2	h	dms	E/W_2	occ	24 / 24	inf	80	25	0.04	0.13	12	0.02	-2.7
	26_2	r	fts	E/W_2	occ	24 / 24	inf	80	25	0.04	0.13	12	0.02	-3.0
	26_3	h	dms	E/W_2	occ	24 / 24	inf	20	25	0.01	0.14	12	0.00	-2.8
	26_3	r	fts	E/W_2	occ	24 / 24	inf	20	25	0.01	0.14	12	0.00	-2.8
	26_4	h	dms	E/W_2	occ	24 / 24	inf	5	25	0.00	0.15	13	0.00	-2.8
	26_4	r	fts	E/W_2	occ	24 / 24	inf	5	25	0.00	0.15	13	0.00	-2.8
	26_5	h	dms	water+B	occ	24 / 24	inf	80	28	0.06	0.24	19	0.02	-4.0
	26_5	r	fts	water+B	occ	24 / 24	inf	80	28	0.06	0.24	19	0.02	-4.5
	26_5	h	dms	E/W_2	occ	24 / 24	inf	80	28	0.06	0.24	19	0.02	-3.2
	26_5	r	fts	E/W_2	occ	24 / 24	inf	80	28	0.06	0.24	19	0.02	-3.0
	26_6	h	dms	water+B	occ	24 / 24	inf	20	28	0.01	0.27	22	0.00	-3.5
	26_6	r	fts	water+B	occ	24 / 24	inf	20	28	0.01	0.27	22	0.00	-4.2
26_7	h	dms	water+B	occ	24 / 24	inf	5	28	0.00	0.28	23	0.00	-3.0	
26_7	r	fts	water+B	occ	24 / 24	inf	5	28	0.00	0.28	23	0.00	-3.5	
27	27_1	h	dms	water+B	occ	24 / 24	fin	906	0	0.00	0.00	0	1.00	-4.5
28	28_1	h	dms	E/W_2	semi	24 / 24	fin	30	29	0.13	0.15	31	0.09	-4.6
	28_1	r	dms	E/W_2	semi	24 / 24	fin	30	29	0.13	0.15	31	0.09	-4.9
	28_2	h	dms	E/W_2	semi	24 / 24	fin	0	29	0.00	0.30	24	0.00	-2.6
	28_2	r	dms	E/W_2	semi	24 / 24	fin	0	29	0.00	0.30	24	0.00	-2.7
	28_2	h	dms	water	semi	24 / 24	fin	0	29	0.00	0.30	24	0.00	-4.4
	28_2	r	dms	water	semi	24 / 24	fin	0	29	0.00	0.30	24	0.00	-4.3
	28_3	h	dms	E/W_2	semi	24 / 24	fin	60	43	0.42	0.00	0	0.15	-4.7
	28_3	r	dms	E/W_2	semi	24 / 24	fin	60	43	0.42	0.00	0	0.15	-3.5
	28_4	h	dms	E/W_2	semi	24 / 24	fin	0	29	0.00	0.30	24	0.00	-2.6
	28_4	r	dms	E/W_2	semi	24 / 24	fin	0	29	0.00	0.30	24	0.00	-2.4
	28_5	h	dms	water	semi	6-8 / 24	fin	0	29	0.00	0.30	24	0.00	-5.0
	28_6	h	dms	water	semi	6-8 / 24	fin	0	29	0.00	0.30	24	0.00	-4.7
	28_7	h	dms	water	semi	6-8 / 24	fin	0	29	0.00	0.30	24	0.00	-4.4
28_7	r	dms	water	semi	6-8 / 24	fin	0	29	0.00	0.30	24	0.00	-4.7	
28_8	h	dms	E/W_1	semi	6-8 / 24	fin	90	65	0.70	0.10	5	0.13	-5.8	
29	29_1	h	dms	E/W_2	none	24 / 24	fin	100	44	0.38	0.13	2	0.20	-6.4
	29_1	r	dms	E/W_2	none	24 / 24	fin	100	44	0.38	0.13	2	0.20	-5.1
	29_2	h	dms	E/W_2	none	24-48 / 24-48	fin	0	29	0.00	0.30	24	0.00	-5.6
	29_2	r	dms	E/W_2	none	24 / 24	fin	0	29	0.00	0.30	24	0.00	-4.2

Annex

compound no.	mix no.	species	preparation	receptor	covering	time [h] expo / total	regimen	applied conc [g/l]	molinspTPSA	molinsp LogHBAcc	Adme LogHBDon	AdmeP _{ow}	Adme1/RotB	LogmaxKp
30	30_1	h	dms	E/W_1	semi	24 / 24	fin	0	29	0.00	0.30	24	0.00	-4.2
	30_1	r	dms	E/W_1	semi	24 / 24	fin	0	29	0.00	0.30	24	0.00	-4.4
	30_2	h	dms	E/W_2	semi	24 / 24	fin	300	49	0.39	0.22	10	0.14	-5.9
	30_2	r	dms	E/W_2	semi	24 / 24	fin	300	49	0.39	0.22	10	0.14	-5.7
	30_3	h	dms	E/W_1	semi	24 / 24	fin	0	29	0.00	0.30	24	0.00	-4.9
	30_3	r	dms	E/W_1	semi	24 / 24	fin	0	29	0.00	0.30	24	0.00	-5.1
	30_4	h	dms	E/W_2	semi	24 / 24	fin	200	42	0.19	0.28	17	0.09	-5.3
	30_4	r	dms	E/W_2	semi	24 / 24	fin	200	42	0.19	0.28	17	0.09	-5.5
	30_5	h	dms	E/W_1	semi	24 / 24	fin	0	29	0.00	0.30	24	0.00	-4.6
	30_5	r	dms	E/W_1	semi	24 / 24	fin	0	29	0.00	0.30	24	0.00	-4.4
31	31_1	h	dms	water	semi	24 / 24	fin	0	29	0.00	0.30	24	0.00	-4.0
	31_1	r	dms	water	semi	24 / 24	fin	0	29	0.00	0.30	24	0.00	-4.3
	31_2	h	dms	water	semi	24 / 24	fin	1	29	0.00	0.30	24	0.00	-3.9
	31_2	r	dms	water	semi	24 / 24	fin	1	29	0.00	0.30	24	0.00	-4.0
32	32_1	h	dms	E/W_2	semi	24 / 24	fin	32	59	0.32	0.20	15	0.14	-5.6
	32_1	r	dms	E/W_2	semi	24 / 24	fin	32	59	0.32	0.20	15	0.14	-5.0
	32_2	h	dms	E/W_2	semi	24 / 24	fin	0	29	0.00	0.30	24	0.00	-4.6
	32_2	r	dms	E/W_2	semi	24 / 24	fin	0	29	0.00	0.30	24	0.00	-3.5
	32_3	h	dms	E/W_2	semi	24 / 24	fin	0	29	0.00	0.30	24	0.00	-4.4
	32_3	r	dms	E/W_2	semi	24 / 24	fin	0	29	0.00	0.30	24	0.00	-3.8
	32_4	h	dms	E/W_2	semi	24 / 24	fin	0	29	0.00	0.30	24	0.00	-4.5
	32_4	r	dms	E/W_2	semi	24 / 24	fin	0	29	0.00	0.30	24	0.00	-3.6
33	33_1	h	dms	E/W_2	none	24 / 24	fin	419	36	0.18	0.19	15	0.19	-7.3
	33_1	r	dms	E/W_2	none	24 / 24	fin	419	36	0.18	0.19	15	0.19	-4.2
	33_2	h	dms	E/W_2	none	24 / 24	fin	1	29	0.00	0.30	24	0.00	-4.8
	33_2	r	dms	E/W_2	none	24 / 24	fin	1	29	0.00	0.30	24	0.00	-4.1
35	35_1	h	dms	water+B	none	6-8 / 24	fin	54	42	0.38	0.11	4	0.16	-6.1
	35_1	r	dms	water+B	none	6-8 / 24	fin	54	42	0.38	0.11	4	0.16	-5.3
	35_2	h	dms	water+B	none	6-8 / 24	fin	1	29	0.01	0.30	24	0.00	-5.3
	35_2	r	dms	water+B	none	6-8 / 24	fin	1	29	0.01	0.30	24	0.00	-4.6
38	38_1	h	dms	E/W_2	?	24 / 24	fin	5	30	0.00	0.30	24	0.00	-4.8
	38_1	r	fts	E/W_2	?	24 / 24	fin	5	30	0.00	0.30	24	0.00	-3.3
	38_2	h	epi	E/W_2	?	24 / 24	fin	0	29	0.00	0.30	24	0.00	-4.8
	38_2	r	fts	E/W_2	?	24 / 24	fin	0	29	0.00	0.30	24	0.00	-3.6
42	42_1	h	epi	E/W_2	?	24 / 24	fin	30	52	0.31	0.18	13	0.13	-4.9
	42_1	r	epi	E/W_2	?	24 / 24	fin	30	52	0.31	0.18	13	0.13	-3.5
	42_2	h	epi	E/W_2	none	24 / 24	fin	30	52	0.31	0.18	13	0.13	-6.6
	42_2	h	epi	E/W_2	none	24 / 24	fin	30	52	0.31	0.18	13	0.13	-5.5
	42_2	r	epi	E/W_2	none	24 / 24	fin	30	52	0.31	0.18	13	0.13	-4.3
	42_2	r	epi	E/W_2	none	24 / 24	fin	30	52	0.31	0.18	13	0.13	-3.5
	42_3	h	epi	E/W_2	none	24 / 24	fin	6	50	0.29	0.18	13	0.12	-5.0
	42_3	r	epi	E/W_2	none	24 / 24	fin	6	50	0.29	0.18	13	0.12	-3.8
	42_4	h	epi	E/W_2	none	24 / 24	fin	1	51	0.30	0.18	13	0.12	-4.9
	42_4	r	epi	E/W_2	none	24 / 24	fin	1	51	0.30	0.18	13	0.12	-3.6
47	47_1	h	epi	water	occ	6-8 / 6-8	inf	1	40	0.09	0.35	22	0.01	-2.6
48	48_1	h	epi	water	occ	6-8 / 6-8	inf	1	40	0.09	0.35	22	0.02	-3.0
49	49_1	h	epi	water	occ	6-8 / 6-8	inf	1	38	0.08	0.34	22	0.01	-3.1
50	50_1	h	epi	water	occ	6-8 / 6-8	inf	1	39	0.10	0.33	22	0.01	-2.9

Annex

compound no.	mix no.	species	preparation	receptor	covering	time [h] expo / total	regimen	applied conc [g/l]	molinspTPSA	molinsp LogHBAcc	Adime LogHBDon	AdimeP _{ov}	Adime1/RotB	LogmaxKp
55	55_1	h	fts	water	semi	6-8 / 24	fin	17	29	0.01	0.30	24	0.00	-5.1
	55_1	h	dms	water	semi	6-8 / 24	fin	17	29	0.01	0.30	24	0.00	-5.0
56	56_1	r	dms	water	semi	6-8 / 24	fin	9	29	0.00	0.30	24	0.00	-3.6
	56_1	h	fts	water	semi	6-8 / 24	fin	9	29	0.00	0.30	24	0.00	-4.0
	56_1	r	dms	water	semi	6-8 / 24	fin	9	29	0.00	0.30	24	0.00	-3.7
	56_2	r	dms	water	semi	6-8 / 24	fin	9	29	0.00	0.30	24	0.00	-3.8
	56_1	h	dms	water	semi	6-8 / 24	fin	9	29	0.00	0.30	24	0.00	-4.0
57	57_1	h	fts	water+B	occ	24 / 24	fin	4	25	0.00	0.15	13	0.00	-3.7
	57_1	h	dms	water+B	occ	24 / 24	fin	4	25	0.00	0.15	13	0.00	-2.8
	57_1	h	dms	E/W_2	semi	24 / 24	fin	4	25	0.00	0.15	13	0.00	-2.7
	57_1	h	dms	water+B	occ	24 / 24	fin	4	25	0.00	0.15	13	0.00	-3.5
	57_1	r	dms	water+B	occ	24 / 24	fin	4	25	0.00	0.15	13	0.00	-3.1
	57_1	h	dms	E/W_2	occ	24 / 24	fin	4	25	0.00	0.15	13	0.00	-2.5
	57_1	r	dms	E/W_2	occ	24 / 24	fin	4	25	0.00	0.15	13	0.00	-2.4
	57_2	h	dms	E/W_2	?	24 / 24	fin	5	29	0.00	0.30	24	0.00	-2.8
	57_2	r	fts	E/W_2	?	24 / 24	fin	5	29	0.00	0.30	24	0.00	-2.6
58	58_1	h	dms	water	occ	24 / 24	fin	4	25	0.00	0.15	13	0.00	-2.6
	58_1	h	dms	water	occ	24 / 24	fin	4	25	0.00	0.15	13	0.00	-3.0
	58_1	r	dms	water	occ	24 / 24	fin	4	25	0.00	0.15	13	0.00	-2.8
	58_1	h	dms	E/W_2	occ	24 / 24	fin	4	25	0.00	0.15	13	0.00	-2.3
	58_1	r	dms	E/W_2	occ	24 / 24	fin	4	25	0.00	0.15	13	0.00	-2.5
	58_1	r	dms	E/W_2	occ	24 / 24	fin	4	25	0.00	0.15	13	0.00	-2.6
	58_2	h	fts	water	occ	24 / 24	fin	4	25	0.00	0.15	13	0.00	-3.2
	58_2	h	dms	water	occ	24 / 24	fin	4	25	0.00	0.15	13	0.00	-3.1
	58_3	h	dms	E/W_2	semi	24 / 24	fin	100	32	0.08	0.27	22	0.00	-5.0
	58_3	h	dms	E/W_2	semi	24 / 24	fin	10	29	0.01	0.30	24	0.00	-4.0
	58_3	h	dms	E/W_2	semi	24 / 24	fin	1	29	0.00	0.30	24	0.00	-4.1
	58_4	h	epi	water	occ	24 / 24	inf	1	29	0.00	0.30	24	0.00	-4.7
59	59_1	h	dms	PBS,pH4	occ	24-48 / 24-48	inf	890	9	0.00	0.00	0	0.00	-1.6
	59_1	h	dms	PBS,pH4	occ	24-48 / 24-48	inf	890	9	0.00	0.00	0	0.00	-1.0
	59_1	h	dms	water+x	occ	24-48 / 24-48	inf	890	9	0.00	0.00	0	0.00	-1.8
	59_1	h	dms	water+x	occ	24-48 / 24-48	inf	890	9	0.00	0.00	0	0.00	-1.5
	59_2	h	dms	PBS,pH4	occ	8-24 / 24	inf	89	27	0.00	0.27	22	0.00	-1.8
	59_2	h	dms	water+x	occ	24-48 / 24-48	inf	89	27	0.00	0.27	22	0.00	-2.0
	59_3	h	dms	water+x	occ	24-48/ 24-48	inf	223	24	0.00	0.23	18	0.00	-1.6
	59_4	h	dms	water+x	occ	24-48 / 24-48	inf	445	19	0.00	0.15	12	0.00	-1.3
68	68_1	h	epi	E/W_2	?	24 / 24	fin	25	25	0.13	0.03	0	0.01	-4.2
	68_1	r	epi	E/W_2	?	24 / 24	fin	25	25	0.13	0.03	0	0.01	-3.2
	68_2	h	epi	E/W_2	?	24 / 24	fin	5	24	0.12	0.03	0	0.01	-4.7
	68_2	r	epi	E/W_2	?	24 / 24	fin	5	24	0.12	0.03	0	0.01	-3.4
	68_3	h	epi	E/W_2	?	24 / 24	fin	1	24	0.11	0.03	0	0.01	-4.8
	68_3	r	epi	E/W_2	?	24 / 24	fin	1	24	0.11	0.03	0	0.01	-3.3

Annex

compound no.	mix no.	species	preparation	receptor	covering	time [h] expo / total	regimen	applied conc [g/l]	molinspTPSA	molinsp LogHBacc	Adme LogHBDdon	AdmeP _{ow}	Adme1/RotB	LogmaxKp
69	69_1	h	epi	water+B	none	6-8 / 24	fin	399	49	0.33	0.04	0	0.08	-6.5
	69_1	r	epi	water+B	none	6-8 / 24	fin	399	49	0.33	0.04	0	0.08	-4.5
	69_2	h	epi	water+B	none	6-8 / 24	fin	2	29	0.00	0.30	24	0.00	-4.7
	69_2	r	epi	water+B	none	6-8 / 24	fin	2	29	0.00	0.30	24	0.00	-3.3
70	70_1	h	dms	E/W_2	?	6-8 / 24	fin	1	29	0.00	0.30	24	0.00	-4.0
	70_1	r	dms	E/W_2	?	6-8 / 24	fin	1	29	0.00	0.30	24	0.00	-4.8
71	71_1	h	epi	E/W_2	none	24 / 24	fin	50	56	0.28	0.25	16	0.08	-6.0
	71_1	r	epi	E/W_2	none	24 / 24	fin	50	56	0.28	0.25	16	0.08	-4.2
	71_2	h	epi	E/W_2	none	24 / 24	fin	1	30	0.00	0.30	24	0.00	-5.0
	71_2	r	epi	E/W_2	none	24 / 24	fin	1	30	0.00	0.30	24	0.00	-3.6
	71_3	r	dms	E/W_2	none	24 / 24	fin	200	62	0.49	0.17	8	0.09	-4.7
	71_4	r	dms	E/W_2	none	24 / 24	fin	2	30	0.01	0.30	24	0.00	-3.8
	71_5	r	dms	E/W_2	none	24 / 24	fin	0	29	0.00	0.30	24	0.00	-3.3
	71_6	h	epi	E/W_2	none	24 / 24	fin	312	43	0.42	0.33	0	0.07	-6.0
	71_6	r	epi	E/W_2	none	24 / 24	fin	312	43	0.42	0.33	0	0.07	-5.5
	71_7	h	epi	E/W_2	none	24 / 24	fin	6	30	0.01	0.30	23	0.00	-5.2
	71_7	r	epi	E/W_2	none	24 / 24	fin	6	30	0.01	0.30	23	0.00	-4.3
73	73_1	r	epi	E/W_2	none	24 / 24	fin	500	57	0.43	0.15	11	0.30	-4.2
	73_2	h	epi	E/W_2	none	24 / 24	fin	5	30	0.00	0.30	24	0.00	-4.6
	73_2	r	epi	E/W_2	none	24 / 24	fin	5	30	0.00	0.30	24	0.00	-3.3
	73_3	h	epi	E/W_2	none	24 / 24	fin	1	29	0.00	0.30	24	0.00	-4.5
	73_3	r	epi	E/W_2	none	24 / 24	fin	1	29	0.00	0.30	24	0.00	-3.2
74	74_1	h	epi	E/W_2	none	24 / 24	fin	10	14	0.14	0.00	0	0.01	-4.7
	74_1	r	epi	E/W_2	none	24 / 24	fin	10	14	0.14	0.00	0	0.01	-3.7
	74_2	h	epi	E/W_2	none	24 / 24	fin	3	9	0.09	0.00	0	0.01	-4.6
	74_2	r	epi	E/W_2	none	24 / 24	fin	3	9	0.09	0.00	0	0.01	-3.9
	74_3	h	epi	E/W_2	none	24 / 24	fin	1	8	0.08	0.00	0	0.01	-4.4
	74_3	r	epi	E/W_2	none	24 / 24	fin	1	8	0.08	0.00	0	0.01	-3.6
75	75_1	h	dms	water	none	24 / 24	fin	11	30	0.02	0.28	22	0.00	-5.4
	75_1	r	dms	water	none	24 / 24	fin	11	30	0.02	0.28	22	0.00	-4.3
	75_2	h	dms	water	none	24 / 24	fin	0	29	0.00	0.30	24	0.00	-5.0
	75_2	r	dms	water	none	24 / 24	fin	0	29	0.00	0.30	24	0.00	-4.5
76	76_1	h	epi	E/W_2	none	24 / 24	fin	402	38	0.22	0.19	18	0.21	-5.6
	76_1	r	epi	E/W_2	none	24 / 24	fin	402	38	0.22	0.19	18	0.21	-5.3
	76_2	h	epi	E/W_2	none	24 / 24	fin	4	29	0.00	0.30	24	0.00	-3.5
	76_2	r	epi	E/W_2	none	24 / 24	fin	4	29	0.00	0.30	24	0.00	-2.6
77	77_1	h	dms	E/W_2	none	24 / 24	fin	1	29	0.00	0.30	24	0.00	-3.3
	77_1	r	dms	E/W_2	none	24 / 24	fin	1	29	0.00	0.30	24	0.00	-3.7
	77_2	h	dms	E/W_2	none	24 / 24	fin	0	29	0.00	0.30	24	0.00	-3.1
	77_2	r	dms	E/W_2	none	24 / 24	fin	0	29	0.00	0.30	24	0.00	-3.4
78	78_1	h	dms	E/W_2	none	6-8 / 24	fin	152	32	0.11	0.28	18	0.16	-7.0
	78_1	r	dms	E/W_2	none	6-8 / 24	fin	152	32	0.11	0.28	18	0.16	-6.3
	78_2	h	dms	E/W_2	none	6-8 / 24	fin	0	29	0.00	0.30	24	0.00	-7.5
	78_2	r	dms	E/W_2	none	6-8 / 24	fin	0	29	0.00	0.30	24	0.00	-7.5

Annex

compound no.	mix no.	species	preparation	receptor	covering	time [h] expo / total	regimen	applied conc [g/l]	molinspTPSA	molinsp LogHBAcc	Adime LogHBDon	AdimeP _{ow}	Adime1/RotB	LogmaxKp
79	79_1	h	dms	E/W_2	?	24 / 24	fin	508	64	0.44	0.41	12	0.14	-4.9
	79_1	r	fts	E/W_2	?	24 / 24	fin	508	64	0.44	0.41	12	0.14	-4.4
	79_2	h	dms	E/W_2	?	24 / 24	fin	5	30	0.01	0.30	24	0.00	-4.3
	79_2	r	fts	E/W_2	?	24 / 24	fin	5	30	0.01	0.30	24	0.00	-3.6
	79_3	h	dms	E/W_2	?	24 / 24	fin	1	29	0.00	0.30	24	0.00	-4.1
	79_3	r	fts	E/W_2	?	24 / 24	fin	1	29	0.00	0.30	24	0.00	-3.4
81	81_1	h	epi	E/W_2	?	24 / 24	fin	297	39	0.23	0.21	15	0.14	-5.7
	81_1	r	fts	E/W_2	?	24 / 24	fin	297	39	0.23	0.21	15	0.14	-5.8
	81_2	h	epi	E/W_2	?	24 / 24	fin	15	30	0.01	0.30	24	0.01	-5.5
	81_2	r	fts	E/W_2	?	24 / 24	fin	15	30	0.01	0.30	24	0.01	-5.0
82	82_3	r	epi	E/W_2	none	24 / 24	fin	2	45	0.13	0.30	32	0.01	-4.6
	82_1	h	epi	E/W_2	none	24 / 24	fin	143	58	0.28	0.30	27	0.04	-6.2
	82_1	r	epi	E/W_2	none	24 / 24	fin	143	58	0.28	0.30	27	0.04	-5.7
	82_2	h	epi	E/W_2	none	24 / 24	fin	19	46	0.15	0.30	32	0.01	-5.8
	82_2	r	epi	E/W_2	none	24 / 24	fin	19	46	0.15	0.30	32	0.01	-5.3
	82_3	h	epi	E/W_2	none	24 / 24	fin	2	45	0.13	0.30	32	0.01	-5.0
83	83_1	h	epi	E/W_2	?	24 / 24	fin	6	25	0.00	0.15	13	0.00	-3.8
	83_1	h	epi	E/W_2	?	24 / 24	fin	6	25	0.00	0.15	13	0.00	-3.4
83	83_1	r	epi	E/W_2	?	24 / 24	fin	6	25	0.00	0.15	13	0.00	-2.8
	83_1	r	epi	E/W_2	?	24 / 24	fin	6	25	0.00	0.15	13	0.00	-2.6
	83_2	h	epi	E/W_2	?	24 / 24	fin	0	25	0.00	0.15	13	0.00	-2.6
	83_2	h	epi	E/W_2	?	24 / 24	fin	0	25	0.00	0.15	13	0.00	-2.6
	83_2	r	epi	E/W_2	?	24 / 24	fin	0	25	0.00	0.15	13	0.00	-2.0
	83_2	r	epi	E/W_2	?	24 / 24	fin	0	25	0.00	0.15	13	0.00	-2.3
84	84_1	h	dms	water	occ	6-8 / 24	fin	200	37	0.18	0.00	1	0.02	-4.9
	84_2	h	dms	water	occ	6-8 / 24	fin	0	24	0.00	0.00	2	0.00	-4.8
87	87_1	h	epi	water	?	24 / 24	inf	1	29	0.00	0.30	24	0.00	-2.3

12.3 Statement of authorship

I, Katharina Guth, confirm that the work presented in the current report has been performed and presented solely by myself except where explicitly identified to the contrary.

Berlin, _____